Predator-prey dynamics in a rotifer-algal microcosm and the emergence of defensive traits in the prey

Catharina Broch

Master Thesis

Section for Aquatic Biology and Toxicology

Department of Biosciences

UNIVERSITY OF OSLO

2015

Predator-prey dynamics in a rotifer-algal microcosm and the emergence of defensive traits in the prey

2015

Predator-prey dynamics in a rotifer-algal microcosm
and the emergence of defensive traits in the prey

http://www.duo.uio.no/

Print: Reprosentralen, University of Oslo

ACKNOWLEDGEMENTS

The master project has posed many challenges and innumerable insights from the early onset until the very end, and I can say unconditionally that all my achievements have only been possible thanks to all the excellent people who have influenced my work.

I want to express the deepest gratitude to my main supervisor, Professor Tom Andersen, who more than anyone else has made this project feasible. Your infinite knowledge in all natural sciences, ceaseless interest and inspiration to seek deeper understanding have been invaluable throughout the entire process.

I am also very grateful to my co-supervisor, Professor Dag O. Hessen, for your enlightening insights and generous recommendations which made it possible for me to visit the research group that my project was so heavily inspired by.

Heartfelt thanks to Per-Johan Færøvig, the unsurpassable handy man who has been a momentous help in all practical aspects of the project. My heartfelt thanks also go to Jan-Erik Thrane for sharing so willingly your own findings, for the numerous clarifying discussions and for your contagious R skills.

I thank Professor Nelson G. Hairston Jr., Brooks Miner and Lindsay Schaffner at Cornell University for their unlimited hospitality during my visit and that they so readily shared their experience and results.

I am thankful to Professor Dag Klaveness whose expertise in algal culturing has been a source of great help and learning. Thank you Berit Kaasa for the many hours you spent analysing my samples. Thank you also Ola Tobias Hafslund for all the guidance when I made my first insecure steps in the lab, and thank you Thomas Taskoudis for being such cheerful lab co-worker. Huge thanks to Lars Petter Onsrud and Ken Conte who miraculously resurrected the instrument that my project was so dependent on.

To my fellow students and the PhDs at AQUA, thank you for all the fun, caring and shared excitement for biology during my master's work.

Lastly, I also want to thank my tiny study creatures for their cooperation and for uncovering their little wonders. You have made it evident that if one "look closely, one will notice the grand within the small"[1].

[1] "Se nøie, skal du øine/ det Store i det Smaa" from the poem *Egebladene* (1840) by Henrik Wergeland.

ABSTRACT

Predator-prey interactions are prevalent in all natural ecosystems and are regarded as a fundamental force in ecological as well as in evolutionary processes. A series of studies have investigated predator-prey dynamics using a combined approach of laboratory experiments and theoretical modelling of a rotifer-algal microcosm. The results from these studies have demonstrated that evolution of defensive traits in the algal prey can happen so rapidly that it alters the trajectory of ecological dynamics (termed eco-evolutionary dynamics). The overarching goal with this master project was to reproduce some of the previous findings from the rotifer-algal microcosm and, specifically, to generate two qualitatively different population dynamics (steady state vs. persisting population cycles) based on a mathematical model of the system. Additionally, a goal for this project was to investigate the mechanism for the defensive trait in the algal prey and its effects on the population dynamics.

Two sets of preliminary experiments were conducted in order to compose a suitable growth medium and to estimate algal growth parameters specific to the experimental conditions. Next, eight continuous cultures of the freshwater rotifer *Brachionus calyciflorus* and the algae *Chlamydomonas reinhardtii* were established where all cultures were diluted by a rate of 0.3 /day, while four cultures were supplied medium with a nitrogen concentration of 50 µmol/l and the other four 250 µmol/l. The choice of dilution rate and nitrogen concentration was determined prior to the experiment by an analysis of the set of ordinary differential equations that describe the *Chlamydomonas-Brachionus* predator-prey system. The eight continuous cultures were maintained for 11 weeks and the density of rotifers and algae, distribution of algal size and concentration of dissolved nutrients in the cultures were estimated every other day in this period.

The four rotifer-algal cultures that were supplied medium with a low nitrogen concentration were expected to develop into a steady state, but the rotifer population went extinct in three of the four cultures after approximately 40 days. Two of the high nutrient cultures exhibited large-amplitude and regular population cycles, while the cycles in other two cultures were small and irregular. A comparison of the model predictions and the experimental results revealed several aspects of the model that were ill-defined for the current rotifer-algal system. The phenotypic change in *C. reinhardtii* that is associated with predator defence (formation of cell clusters called palmelloids) were observed in all high nutrient cultures, but were absent from the low nutrient ones. Whether this phenotypic change in *C.*

reinhardtii is incited by rapid evolution caused by predation pressure is disputable as *C. reinhardtii* is reported to induce formation of palmelloid cell clusters under several other conditions. Alternative views on the palmella formation in *C. reinhardtii* are discussed in relation to its evolutionary kinship to multicellular species, and it is proposed that this could serve as a case for genetic accommodation. It is also addressed whether the rotifer-algal system can demonstrate the significance of predation as an evolutionary force.

PREFACE

The format of this master thesis differs from most theses published at the Department of Biosciences. Rather than presenting the work as a comprehensive article, I have attempted to structure the thesis as a monograph. The main reason for this decision is because it allowed me to present the project as an unfolding narrative which reflected the scientific approach of my studies. Of equal importance, I choose this format because I believe it would enhance the readability and thus facilitate the evaluation of my arguments and findings. A large part of the thesis includes appendixes that supplement methods and results which are not crucial for the assessment, but which could strengthen the perception and increase the transparency of my work.

CONTENTS

INTRODUCTION

An essential feature of the natural world is its dynamical structure. Since the origin of life more than 3.8 billion years ago, the diversity of life has been expanding and ever-changing. Life as we know today has emerged from an interplay between abiotic and biotic factors over billions of years, and each species carries with it a vast evolutionary history. In ecology, the leading aim is to understand the interactions that structure ecological systems of the present as well as ecosystems of the past. It is a scientific discipline that studies patterns in nature, why some organisms are found in large numbers in some areas or time points whilst they are non-existent in other (Kingsland 1985). The population is a fundamental unit in both ecological and evolutionary studies. The structuring forces behind the rise and fall of populations has been a lasting fascination among biologists and a recurrent theme in population ecology (Bjørnstad & Grenfell 2001).

The interactions between populations and the environment is the main viewpoint in population ecology (Kingsland 1985). These interactions unite the inanimate world to the living and link populations in intricate systems through modes of predation, competition and cooperation. Fluctuations in population densities, and maybe cyclic populations in particular, have for more than a century been studied by population ecologists, followed by prolonged debates over the relative importance of biotic vs. abiotic control of the observed fluctuations (Bjørnstad & Grenfell 2001). Undoubtedly, the most prominent case study in population ecology is the time series of the Canadian lynx and snowshoe hare. It frequently serves as the grand example of predator-prey cycles in the wild. Although influences of seasonality and space are not dismissed, the consensus is that the hare-lynx dynamics is dominated by the interaction between the predator and prey (Bjørnstad & Grenfell 2001).

Predation is a fundamental mechanism in all natural systems. The large majority of organisms on earth either face the risk of being eaten or not obtaining enough food for survival. Indeed, the distinguished G. E. Hutchinson asserted that “in any study of evolutionary ecology, food relations appear as one of the most important aspects of the system of animate nature” (Hutchinson 1959, p. 147). Hutchinson wrote these words in his celebrated article *Homage to Santa Rosalia or why are there so many kinds of animals?* The selective force of predation is indisputable and is considered to have played a major role in the evolution of life (Abrams 2000; Bengtson 2002). It is associated with the major transitions in evolution; at the base of the tree, the origin of the eukaryotic cell is viewed as a symbiotic

or predatory event, and throughout evolution, the rises of multicellularity and increasing complexity are linked to strong predation pressures (Bengtson 2002; Parfrey & Lahr 2013).

Acknowledging predation as an evolutionary force has evoked questions about its effects on community stability (Abrams 2000). From one perspective, predation can be viewed as a driver for increased species diversity, which is associated with enhanced community stability. In conclusion to the contemplations of *why there are so many kinds of animals*, Hutchinson (1959) writes that one answer to why there is such a great diversity of life is because complex communities are more stable than simple ones, and he assigns, in part, the observed cyclic oscillations of arctic and boreal populations to the lesser complexity of these ecosystems. From another perspective, it has been questioned whether evolution of predation-related traits can produce cycles in otherwise stable systems (Abrams 2000). Evolution of defensive traits in the prey can be a source of instability if it gives rise to a cycling time lag between the changes in predator density and prey vulnerability, i.e. if it generates a positive feedback between the predator amplitude and the selection for defensive traits in the prey (Abrams 2000).

To elucidate the mechanisms of predator-prey dynamics, laboratory microcosms have proven to be a powerful approach. Particularly, continuous cultures of rotifers, small multicellular zooplankton, and green algae have been a favoured model system to investigate predator-prey interactions. Studies of long term interactions between rotifer and algae stems back to M. E. Boraas (1980) who presented a method for continuous culturing of the freshwater rotifer *Brachionus calyciflorus* and the green algae *Chlorella vulgaris,* taking after studies of bacterial-protozoan systems. His results served promising prospects for the model system, reporting stable dynamics and, intriguingly, predator-prey oscillations that did not behave according to the expectation.

Two decades later, a revived interest in rotifer-algae systems has produced a series of studies that have revealed novel aspects of predator-prey dynamics. A group of scientists revolving around the freshwater ecologist N. G. Hairston Jr. and the mathematician S. P. Ellner adopted Boraas' *Brachionus – Chlorella* system and have for more than a decade produced compelling results from rotifer-algal systems. In 2000 they published results showing that they could induce qualitative changes in the rotifer-algal dynamics by adjusting an experimental parameter in accordance with a mathematical model of the system (Fussmann *et al.* 2000). A continuation of this study revealed that rapid evolution of a defensive trait in the prey can have a marked effect on the behaviour of oscillating rotifer-algae populations; an

effect that significantly alter the classical pattern of predator-prey cycles (Yoshida *et al.* 2003). Later on, they replaced *Chlorella vulgaris* for another green algae, *Chlamydomonas reinhardtii,* and demonstrated that the rotifer-algal dynamics also were significantly altered in this system where the algal species exhibited a different defensive trait, while additionally linking the population dynamics to gene expression levels in the algae (Becks *et al.* 2010; 2012).

The predator-prey dynamics that emerge when evolution happens so rapidly that it alters ecological interactions have been termed eco-evolutionary dynamics (Fussmann *et al.* 2007; Ellner & Becks 2010). This finding is of major significance because it implies a convergence of ecological and evolutionary time (Hairston *et al.* 2005). Conventionally, ecological and evolutionary processes are thought of as processes that happen on very different time scales. However, the results from the rotifer-algal microcosms have been used as evidence that genetically based phenotypic changes can happen so rapidly that it alters trajectories of ecological dynamics (Hairston *et al.* 2005). Nevertheless, rapid changes in phenotypes can also be assigned to a different mechanism than evolution. Phenotypic plasticity is widely recognized as a mechanism that can induce adaptive phenotypes in response to altered environmental conditions (Price *et al.* 2003). This has been the viewpoint of a different group of scientists studying rotifer and algal dynamics. Using the green algae *Scenedesmus oliquus,* which is known to induce phenotypic changes in presence of zooplankton grazers, these scientists have investigated the effects of phenotypic plasticity on trophic structures (Verschoor *et al.* 2004b; Vos *et al.* 2004b).

Microalgae may be thought of as primitive forms of life, drifting aimlessly in water bodies without any sophisticated abilities to cope with challenges posed by the environment they inhabit. But their evolutionary history is as long as any other living organism of today. They are the descendants of organisms that have been facing environmental challenges for billions of years. So although their appearance is primitive compared to “higher organisms”, their facets are not simplistic. It is well known that microalgae are responsive to changes in ambient nutrient, light and temperature conditions, and that some algal species exhibit structures or toxins that protect them from zooplankton grazers. However, that single algal species can exhibit transient resistance to grazers is an insight that was presented quite recently. In 1993, Hessen and van Donk published results showing that *Scenedesmus subspicatus,* a species of green algae, formed large colonies in presence of the zooplankton grazer *Daphnia magna.* Induced defences in phytoplankton have since then been found in

many different taxa (Van Donk *et al.* 2010), and the plastic responses are also found to be highly variable within strains of the same species (Verschoor *et al.* 2004a).

In essence, there are two mechanisms that can be the source to phenotypic variation within species. Variation could be assigned to phenotypic plasticity, as in the case of colony formation in the *Scenedesmus,* or it could be due to heritable variations that origins in fixed differences in the nucleotide sequences of individuals' genomes. However, one can also argue that there exists a third mechanism for phenotypic variation within species, a mechanism which is somewhat intermediate between the other two. Epigenetic inheritance is basically the transmission of a distinct plastic phenotype across generations, and it is found to be a source of variation in both unicellular and multicellular organisms (Jablonka 2013).

In the rotifer-algal studies presented by the group of scientists associated with Hairston Jr., the phenotypic variation observed in the algal populations was assigned to heritable differences in the genetic code. For the prey species *Chlorella vulgaris* it was identified an evolutionary trade-off between the algae's competitive ability and defence against predation, which was associated the algal nutrient content (Yoshida *et al.* 2004). The other algal species used as prey in the studies by Hairston and colleagues, *Chlamydomonas reinhardtii,* exhibited a similar evolutionary trade-off between competitive ability and defence against rotifer grazing, only now the grazing resistance was associated with the formation of cell clusters (Becks *et al.* 2010).

C. reinhardtii is a species of flagellated single celled algae, but can also be observed in multicellular non-motile clusters encapsulated in a gelatinous substance. These multicellular aggregates resemble the algae *Palmella* in the order Tetrasporales and have thus been denoted a *palmelloid* state of *C. reinhardtii* (Harris 2009). Palmella formation in *C. reinhardtii* has been interpreted as a defensive trait against herbivore grazers because it is found to occur when the algae is cultured together with rotifers (Lürling & Beekman 2006; Becks *et al.* 2010; Fischer *et al.* 2014). Nonetheless, *C. reinhardtii* has also been found to form palmelloids under a wide range of other conditions, including the presence of organic acids (Iwasa & Murakami 1968), calcium deficiency (Iwasa & Murakami 1969), high chemostat dilution rates (Olsen *et al.* 1983) and after strong selection for large aggregate size (Ratcliff *et al.* 2013).

Different mechanisms are reported to give rise to palmella formation in *C. reinhardtii*. In some studies it is reported as an induced character (Iwasa & Murakami 1968; 1969; Olsen *et al.* 1983; Lürling & Beekman 2006), while in other studies arguments are made asserting it

is caused by evolved genetic alterations (Becks *et al.* 2010; Ratcliff *et al.* 2013). The evolutionary relationships of *C. reinhardtii* may however elucidate our understanding of palmella formation in this species. The order Chlamydomonadales includes species with morphologies ranging from unicelled flagellates, e.g. *C. reinhardtii*, to various colonial and multicellular forms, e.g. *Gonium pectorale* and *Volvox carteri*, and representatives from this algal order have thus served as a model system for the evolution of multicellularity (Leliaert *et al.* 2012). Hence, colonies are a frequent display among the relatives of *C. reinhardtii*.

The overarching goal for this master project was to set up a system of continuous cultures with the freshwater rotifer *Brachionus calyciflorus* and the algae *Chlamydomonas reinhardtii* in order to reproduce some of the results presented by the studies of Hairston Jr. and colleagues. A fundament for my study of rotifer-algal dynamics is the mathematical model of the *Chlamydomonas* - *Brachionus* system presented in Becks *et al.* (2010). A simplified block diagram of the model is given below (Diagram 1), while a detailed description is presented in Appendix C. This model describes how the dynamics between the rotifers, algae and the concentration of nitrogen are expected to change depending on two experimental parameters. In continuous cultures, the culture's dilution rate and the nutrient concentration of the supplied medium are two key parameters that regulate the abundance of

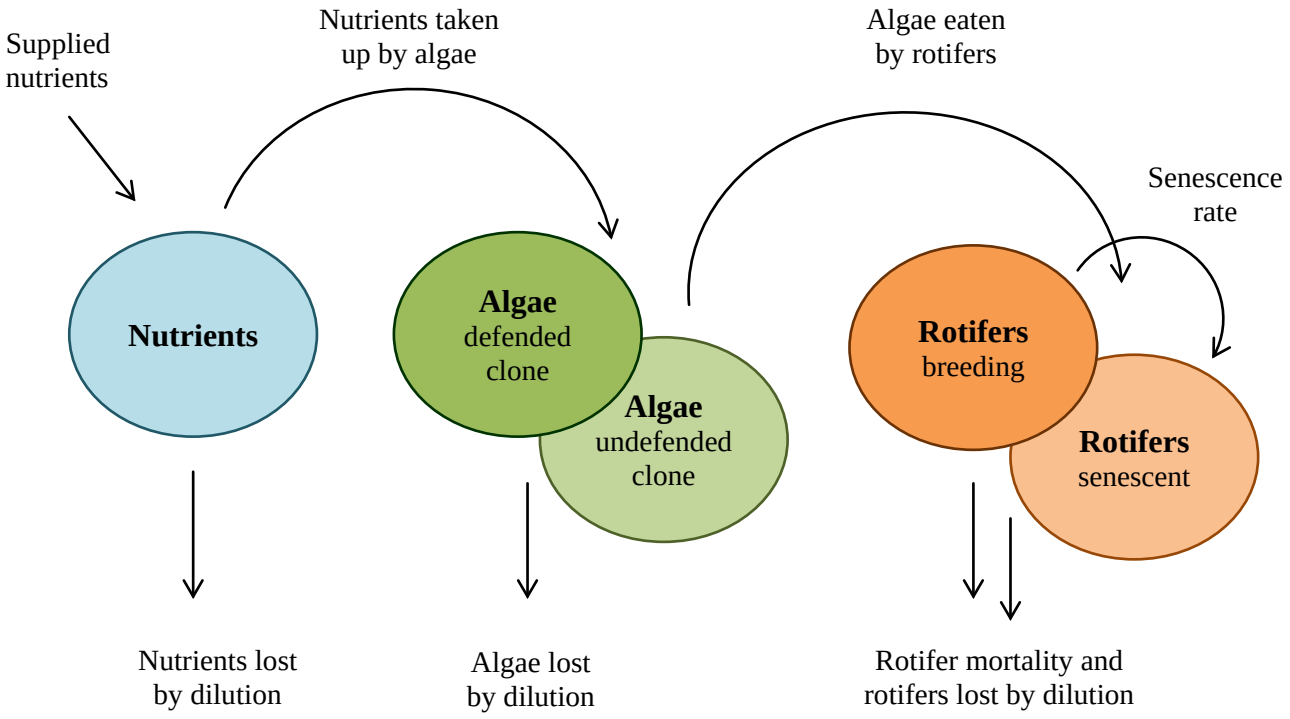

Diagram 1. A simplified block diagram of the *Brachionus – Chlamydomonas* model by Becks *et al.* (2010), which is an essential part of this rotifer-algal project.

organisms and, as demonstrated by the studies of Fussmann *et al.* (2010) and Becks *et al.* (2010), that structure the rotifer-algal dynamics. The nutrient concentration of the supplied medium determines the level for maximum algal density which, at the next level, sets the maximum density of rotifers, while the dilution rate governs the washout rate of organisms and the rate of nutrient enrichment to the system. The *Chlamydomonas – Brachionus* model describes a system where the algal population consists of two algal clones with contrasting levels of competitive ability and defence against rotifer predation. This is an important aspect of the model with a major effect on the predator-prey dynamics and will be described in greater detail later in the thesis.

The specific goal for the master project was twofold:

I. The principal aim was to generate two qualitatively different predator-prey dynamics by adjusting the nutrient concentration of the medium supplied to the microcosms.

Based on an analysis of the *Chlamydomonas – Brachionus* model, I wanted to establish two sets of microcosms which would be supplied medium of either low or high nutrient concentrations. The expectation was that the low nutrient system would generate a steady state population development, while the high nutrient system would generate persisting population cycles.

II. The second aspect of the predator-prey dynamics that I wished to investigate was the mechanism for palmella formation in *C. reinhardtii* and its effects on the predator-prey dynamics.

I expected that palmelloids would arise in the rotifer and algal cultures, and since the literature suggests that the palmelloids are inferior competitors for nutrients compared the single celled flagellates, I expected that the palmella formation would be strongest in the high nutrient microcosms. Further, if a significant palmella formation would occur in the high nutrient systems, I expected that it would have a stabilizing effect on the population cycles.

To reach these goals, it was necessary to conduct two preliminary experiments and to make a thorough analysis of the *Chlamydomonas – Brachionus* model in order to select values for the

system’s experimental parameters. The two preliminary experiments are presented in the first part of the thesis’ midsection. The purpose of these experiments was to compose a suitable growth medium and to estimate algal growth parameters specific to my experimental conditions. In the second part, I present the investigations of my *Chlamydomonas* – *Brachionus* system; first the results of the theoretical analysis and then the experimental results. I close the thesis with a synthesis of the most interesting aspects of this rotifer-algal system.

PART 1
Preliminary experiments and analyses

1.1 Medium test

Composing a suitable medium for the culturing of phytoplankton has been a laborious task. One important early effort was by Pringsheim, who in the early nineteen hundreds found that adding extracts from soil and peat enhanced the growth of algae in purely mineral media (Preisig & Andersen 2005). Soil extracts have been in wide use since then, with an understanding that it adds important micronutrients and humic compounds with chelating properties (Sunda *et al.* 2005). Despite its advantages can the use of soil extracts introduce variability between experiments and thus give poor reproducibility (Sunda *et al.* 2005). This has led to the development of fully defined medium, which there now exists many types of.

One defined freshwater medium that is commonly used to grow phytoplankton is the WC medium (Kilham *et al.* 1998). This medium is credited Robert R. L. Guillard who combined and modified the famous Chu #10 medium (Chu 1942) with the vitamins and a shortened list of the trace metals from a medium published in Wright (1964) (Andersen *et al.* 2005). The WC medium is composed of six major elements, seven micronutrients and three vitamins. The exact composition is given in Guillard & Lorenzen (1972) and is for later comparisons listed in Appendix A.

Preceding this master project, there had been conducted experiments with *C. reinhardtii* at the department using a medium based on water from a hard water lake, with the rationale being that this water has a natural high content of bicarbonate (HCO_3). A high content of bicarbonate is expected to increase the water's buffer capacity (high alkalinity) and also make it less susceptible to carbon limitation through the mechanisms governed by the carbon dioxide – bicarbonate system (Brönmark & Hansson 2005). In growing algal cultures, the rate of photosynthesis will exceed the respiration rate, which thus leads to a net uptake of carbon dioxide. Bicarbonate can in such circumstances serve as a carbon source, as described by the reaction: $HCO_3^- + H^+ \rightarrow H_2O + CO_2$ (Brönmark & Hansson 2005).

Following the practice of the preceding work, I chose to use a modified WC medium with lake water as a basis for the planned rotifer-algal experiments. But since the experiments would demand a large amount of water, it would be convenient if the lake water could be diluted with distilled water without deteriorating in quality as growth medium. The aim with this first experiment was then to compare the growth of *C. reinhardtii* cultured in a WC medium that had pure lake water as basis against a medium where the basis was a mix between lake water and distilled water. The expectation was that the lake water could be

diluted without deteriorating in quality as a growth medium. In addition, media with tap water as basis was included in the comparison.

MATERIALS AND METHODS

Water

The lake water was collected from Gullerudtjern, a small lake situated approximately 35 km northwest of Oslo, Norway. This lake was chosen because it is located in an area with calcareous bedrock, and the water body is thus expected to be rich in bicarbonate. Pervious chemical analysis of this lake water has shown that it has an alkalinity of 2.05 mmol/l (J. E. Thrane, *personal communication*), which signifies that it has a high content of dissolved inorganic carbon, such as bicarbonate. 80 litres of the lake water were collected in late autumn 2013 and subsequently filtrated with glass microfiber filters of pore size 1.2 µm (Whatman GF/C). Upon filtration, the water was aerated for six months and then stored dark and cold until prepared for use as medium.

The tap water at the department of Biosciences has its source from a lake in Oslo (Maridalsvannet) and has upon distribution been purified and disinfected by UV radiation (Enander 2008). This water is classified as soft water (hardness of 2.4 - 3.0 ºdH) and has a relatively low alkalinity (0.60 – 0.80 mmol/l) (VAV 2014).

The distilled water used in the experiment is made by distillation of the tap water. The approximate concentration of dissolved inorganic carbon in distilled water can be calculated using the volume fraction of carbon dioxide in dry atmosphere (397 ppmv) and Henry's law constant for the solubility of carbon dioxide in liquid water (29.4 liter atm/mol) (Tom Andersen, *personal communication*). This gives an estimated concentration of 0.015 mmol/l dissolved inorganic carbon in distilled water.

Samples of lake water were taken out for analysis of total organic carbon, total nitrogen, nitrate and total phosphorus content. Concentrations of total organic carbon and total nitrogen were determined with a total organic carbon analyser (TOC-V CHP, Shimadzu, Tokyo, Japan), while nitrate and total phosphorus concentrations were determined with an autoanalyzer (AutoAnalyzer 3, SPX Process Equipment, Bran + Luebbe, Norderstedt, Germany). The samples for analysis of total phosphorus were digested with persulfate and then analysed according to the AutoAnalyser application method G-297-03. The nitrate contents were analysed as described in the AutoAnalyser application method G-172-96. Prior to analysis, the lake samples were sterile filtered through a polyethersulfone (PES) membrane

with a pore size of 0.22 µm (Corning). All chemical analyses were conducted by the laboratory engineer Berit Kaasa

The algae

The strain of *Chlamydomonas reinhardtii* used in the experiment (CC-1690 wild type mt+ [Sager 21 gr]) was obtained from Chlamydomonas Resource Center and is a wild type strain that grows on nitrate (Chlamydomonas Resource Center 2015).

Experimental setup

To compare the growth of *C. reinhardtii* in media with different water as basis, lake water, tap water and distilled water were combined in different ways to produce five distinct mixtures that contained:

A. 100% distilled water
B. 70% distilled and 30% lake water
C. 100% lake water
D. 30% lake water and 70% tap water
E. 100% tap water

Table 1.1. Concentration of chemicals that were added to all five medium types.

Chemical component concentration in µmol/l		JET medium
Major elements	$NaNO_3$	1000
	K_2HPO_4	50
Algal trace elements	$Na_2EDTA \cdot 2H_2O$	11.700
	$FeCl_3 \cdot 6H_2O$	11.650
	$CuSO_4 \cdot 5H_2O$	0.040
	$ZnSO_4 \cdot 7H_2O$	0.077
	$CoCl_2 \cdot 6H_2O$	0.042
	$MnCl_2 \cdot 4H_2O$	0.910
	$Na_2MoO_4 \cdot 2H_2O$	0.025
	H_3BO_3	16.000
Vitamins	Vitamin B12	0.0004
	Biotin (H)	0.0020
	Vitamin B1	0.3000

Extra nutrients were added in equal amounts to all five water mixtures according to a recipe of a modified WC medium (Table 1.1.). This modification of Guillard's WC medium was made by the PhD candidate Jan-Erik Thrane for his experiments with *C. reinhardtii* using lake water from Gullerudtjern as a basis, and I will in the following refer to it as the JET medium. The JET medium is equal to the WC medium in chemical composition, except for the major elements. The list of six major elements in WC is reduced to two in JET, where JET still includes the two important plant nutrients nitrate and phosphate (see Appendix A for a full comparison).

The media containing lake water were sterilized with a polyethersulfone (PES) membrane filter of pore size of 0.22 µm (Corning) before the inoculation of algae. An advantage of this sterilization method is that one avoids the possible precipitation of minerals that can be an issue when autoclaving media.

Three batch cultures of *C. reinhardtii* were initiated for each of the five medium types, each culture holding a starting a volume of 30 ml and an initial algal concentration of approximately 1300 cells/ml. The cultures were kept in small tissue flasks (Nunclon Delta flasks with filter caps) and grown at 19°C with a 14/10 hours light/dark cycle and a light intensity of approximately 80 µE /m^2 /s. White fluorescent light were used as a light source. For the ten days the experiment lasted, a sample of the cultures was taken out daily in order to estimate the population densities of algae. The algal counts were made using a particle counter (CASY TT; Shärfe, Reutlingen, Germany).

Statistical analysis

The daily algal counts were analysed using nonlinear mixed-effects modelling in order to investigate potential differences in the growth trajectory of *C. reinhardtii* in the five medium types. The details of the analysis are presented in Appendix B. All analysis and plotting were done in the R programming environment (R Core Team 2015), and the appendix was put together with R Markdown.

RESULTS

Lake water chemistry

According to the chemical analysis of Gullerudtjern does the lake water contain approximately 550 µmol/l dissolved organic carbon (DOC) and 95 µmol/l nitrogen species, where about 30% of the nitrogen is in the form of nitrate (Table 1.2). The level of total phosphorus was estimated to 0.6 µmol/l. Medium type B and D, that contains 30% of this lake water, would then get a contribution of about 8 µmol/l nitrate and about 0.18 µmol/l of total phosphorus from the lake water.

Table 1.2. Results of the chemical analysis of the Gullerudtjern lake water. The lake water was stored in three containers and water samples from all three were analysed.

Container	DOC µmol/l	Total Nitrogen µmol/l	Nitrate (NO_3^-) µmol/l	Total Phosphorus µmol/l
1	551	102	26	0.3
2	552	92	29	0.8
3	544	89	25	0.7
Mean	549	94	27	0.6

Algal growth trajectories

The growth of *C. reinhardtii* was similar for the medium types that contained lake water and tap water, while it was markedly different for the medium with only distilled water as basis (Figure 1.1). The cultures that contained lake water as basis (B and C) could seem to yield a slightly higher asymptotic algal density than the cultures that contained tap water (D and E). However, the statistical analysis could not identify significant differences in the asymptotic densities between these four medium types (see Appendix B for details). A single model was thus appropriate to describe the growth in the B, C, D and E medium types. The solid curves in Figure 1.1 depict the fit of the resulting model to the growth in the B, C, D and E cultures. The data from the A cultures were left out of the analysis because the growth in this medium obviously differed from the other media. According to the final model does the JET media support an asymptotic algal concentration of 661 000 cells/ml (see Appendix B). This would imply, given an initial nitrate concentration of approximately 1000 µmol/l, that *C. reinhardtii* had a conversion factor of $0.000661 \cdot 10^9$ cells/ µmol N in these media.

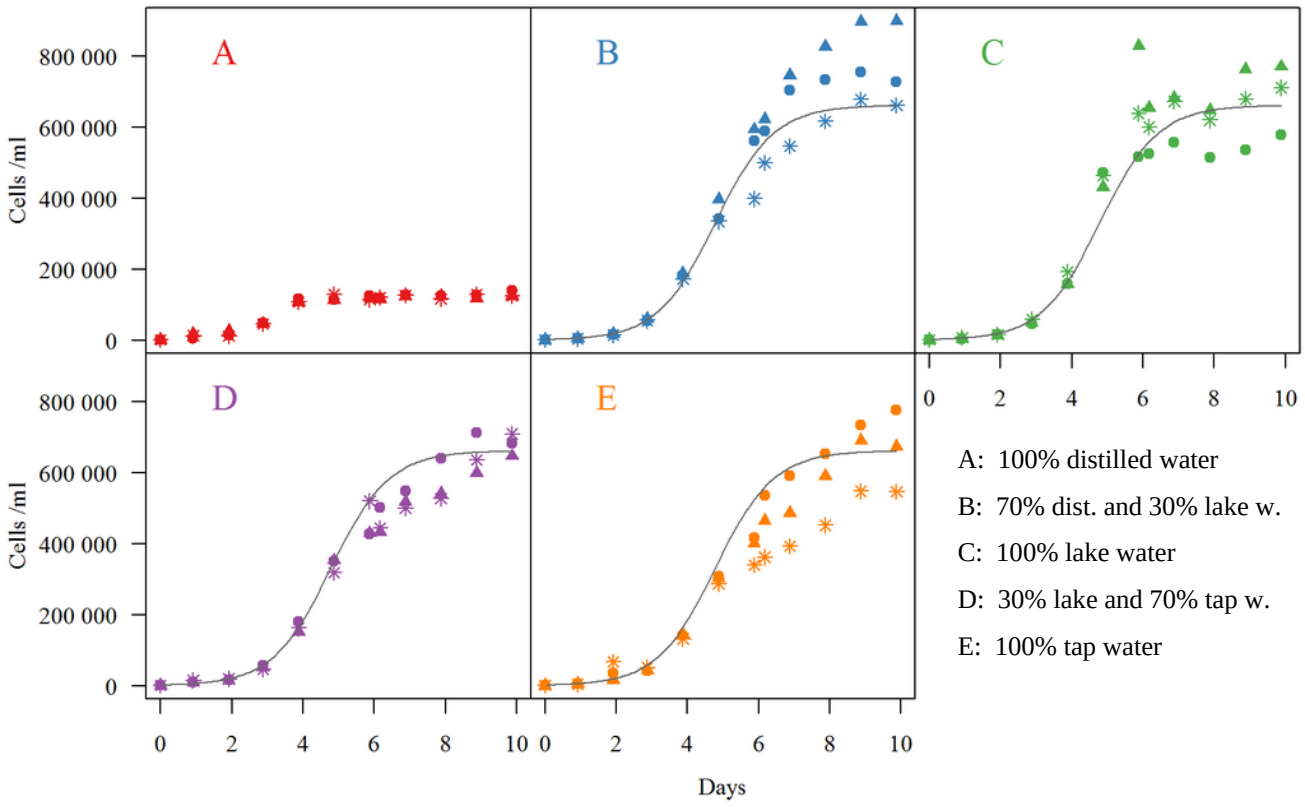

Figure 1.1. The daily algal counts for each medium type and the model with the best fit to the data (solid curve). The different point characters represent the three replicates for each of the medium types. A second algal count was made at day six, because the first population density estimates for one of the C replicates (triangle) was unexpectedly high.

DISCUSSION AND OUTCOME

The medium test proved that the lake water could be diluted with distilled water without deteriorating in quality as growth medium for *C. reinhardtii*. The growth of *C. reinhardtii* in the JET medium that contained only lake water showed no significant differences compared to the medium that contained lake water diluted with distilled water, and also no significant difference compared to the media that contained tap water. In contrast, distilled water proved to be unsuitable as the sole basis for the JET medium, as it gave an asymptotic algal concentration that was more than three times lower than for the other medium types.

The poor growth in the medium containing only distilled water could not be ascribed to nitrate or phosphate limitation, since these macronutrients were added in equal amounts to all treatments. However, the alkalinity and the contents of carbon and other nutrients are expected to be different. The distillation process removes minerals from the water and the alkalinity and carbon content would thus be lowered to a minimum. Using alkalinity as a proxy for inorganic carbon content implies that the inorganic carbon contents of the lake and tap water are substantially higher than that of distilled water (0.015 mmol/l vs. about 2.05 mmol/l in lake water and 0.70 mmol/l in the tap water).

According to the chemical analysis of the lake water does this water contribute with a substantial amount of dissolved organic carbon to the medium. This carbon is largely constituted by humic substances which are known to have chelating properties. Although it is possible that chelating humic substances or additional micronutrients supplemented by the lake or tap water could explain the superior growth in the media containing these water sources, it is more likely that the enhanced growth is associated with the inorganic carbon contents. Hence, the poor growth in the medium with distilled water as basis was probably caused by an early limitation of carbon dioxide.

Compared to Guillard's WC medium does the JET medium's chemical list lack four major elements: carbon (sodium bicarbonate), calcium, magnesium and silicon (see Appendix A). Silicon is a key element in the cell wall of diatoms (Brönmark & Hansson 2005), while carbon is a bulk constituent of all algae (and all life) and is consequently required in large quantities. The rationale for not keeping sodium bicarbonate on the chemical list of the JET medium was because it would be replaced by the high bicarbonate content of the lake water. Considering the results of the medium test, it seems like the bicarbonate fulfilled this role. Also the demand for calcium and magnesium, elements that are important components of the

algal cell membrane and chlorophyll (Brönmark & Hansson 2005), is likely met through the supplements of the lake water, as hard waters often are high in these elements (Cronan 2009).

However, the medium test cannot disentangle whether it was the availability of inorganic carbon or other nutrients that in the end determined the asymptotic algal concentration in the cultures with lake and tap water. The lake water's higher alkalinity and likely higher contents of carbon, calcium and magnesium would give an expectation of higher asymptotic algal densities compared to the tap water, but the statistical analysis did not reveal any significant differences between the two water types. The results cannot therefore give an definite answer to whether it was carbon or other elements that was the limiting substrate in the cultures. Anyways, for the purpose of the experiment do the results give a clear answer; the lake water can be diluted without losing quality as growth medium.

Although the lake water could introduce unaccounted effects due to the fact the chemical properties of the water are not fully defined, I chose to use the JET medium with the B-mix (30% lake water and 70% distilled water) for the rotifer-algal experiments. However, the experiment has ignored to address an important question; that is whether this medium also is suitable for culturing rotifers. The WC medium was developed for freshwater algae (Guillard & Lorenzen 1972) and the JET medium specifically for *C. reinhardtii.* There exist several freshwater media specific to the culturing zooplankton, e.g. Keating's MS (1985) and Elendt & Bias' M4 medium (1990), and also media that is suitable for both algae and zooplankton. One such media in wide use is COMBO, which is, a little simplified, a WC medium with an additional five animal trace elements (Kilham *et al.* 1998). The necessity of these additional trace elements for rotifers is however ambiguous as all zooplankton media above were assessed using daphnids. Boraas (1980) successfully used a modification of Chu #10 as medium in his rotifer-algae experiments with an extra addition of vitamin B_{12}, as he found that *Brachionus calyciflorus* would not reproduce without this vitamin. Since the JET medium includes vitamin B_{12} and the lake water likely contributes with some additional trace elements, it is likely not a problem that animal trace elements are absent from the JET medium's chemical list.

Another important question in this context is how the growth conditions in my rotifer-algal experiment are compared to the conditions at the Hairston lab. Since my experiment was designed using the rotifer-algal model by Becks *et al.* (2010), it was crucial that the model parameters describing algal growth were representative for algal growth under my experimental conditions. All rotifer-algal experiments at the Hairston lab (Fussmann *et al.*

2000; Yoshida *et al.* 2003; Becks *et al.* 2010) were conducted using a medium quite different from the JET medium (see Appendix A for comparison). When the aim is to reproduce results from the Hairston lab, one can argue that this is severe weakness of the setup. On the other hand, if the results could be reproduced also under slightly different conditions, it would give additional support to the robustness of their findings.

In the model by Becks *et al*. (2010) the algal conversion factor was set to $0.0027 \cdot 10^9$ cells/ µmol N for *C. reinhardtii* (Appendix C). In stark difference do the results from the medium test suggest that the conversion factor is $0.000661 \cdot 10^9$ cells/ µmol N under the current conditions. This accentuates principally two things: that the growth very unlikely was nitrogen limited and the necessity to re-estimate the algal parameters in the model to ensure representative values under the planned experimental conditions. The next experiment had this as its main purpose.

1.2 Algal growth parameters

Microalgae is a large and very diverse group of organisms found basically everywhere on Earth (Radmer 1996; Falkowski *et al.* 2004). While the individual microalgae are invisible to the naked eye, it is estimated that the aquatic members of this group perform almost half of the planet's annual primary production (Field *et al.* 1998). Among many things, this signifies an impressive vitality, and the genus *Chlamydomonas* is a typical algal genus in this sense. Representatives are distributed in places ranging from the tropics to the poles, from sewage ponds to great lakes, and from soils to a petri dish exposed one minute to the outside air from an airplane flying at 1100 m altitude (Harris 2009). The diversity of habitats entails a substantial flexibility of growth, a feature that is also characteristic for *C. reinhardtii.*

Although originally isolated from soil, the dominant laboratory strains of *C. reinhardtii* can be grown in liquid culture or on agar (Harris 2009). Its modes of growth are likewise adaptable. Depending on the conditions, *C. reinhardtii* can switch between phototrophic, heterotrophic or mixotrophic growth (Boyle & Morgan 2009). Furthermore, the cell cycle is responsive to environmental conditions. *C. reinhardtii* divides by multiple fission, which means that it has a prolonged growth phase (G1) followed by successive rounds of alternating phases of DNA synthesis and mitosis that produce 2^n daughter cells (Cross & Umen 2015). The size of the mother cell determines the number of daughter cells, which can be up to 32, but more typically 2, 4 or 8 cells (Cross & Umen 2015). Variability in light and temperature have been shown to influence cell cycle progression, but the exact mechanism determining the number of daughter cells seems to be unresolved (Oldenhof *et al.* 2006; Oldenhof *et al.* 2007; Cross & Umen 2015).

An essential environmental factor for the growth of microalgae is the ambient nutrient supply. Microalgae, as all organisms, require a varied set of elements to sustain life. Some elements are required in large quantities (e.g. carbon and nitrogen) whereas others only in traces (e.g. zinc and cobalt). The pattern of elemental compositions in organisms is the central theme in the field of ecological stoichiometry (Sterner & Elser 2002). Since Alfred Redfield's seminal paper from 1958, postulating an average carbon : nitrogen : phosphorus ratio of 106:16:1 in phytoplankton, stoichiometric variability is increasingly recognized, and the flexibility of plankton stoichiometry has now become one of the fundamentals in ecological stoichiometry (Klausmeier *et al.* 2008). *C. reinhardtii* is found to conform to this pattern. Nitrogen deprivation has been shown to produce a large change in gene expression compared to nutrient replete cells, coupled with an increase in the cellular carbon : nitrogen ratio from 6

to about 15 (Park *et al.* 2015). Such changes in cellular contents of elements may have a significant impact on the organisms preying on the algae because it could decrease the nutritional value and possibly also lead to production of toxic compounds (Van de Waal *et al.* 2014). Experiments by Felpeto & Hairston (2013) indicate that both effects are relevant when *B. calyciflorus* preys on nutrient limited *C. reinhardtii*. Compared to the *C. reinhardtii* that was grown in nutrient sufficient conditions, phosphorus limitation lowered the food quality of the algae while nitrogen limitation had an effect on *B. calyciflorus* that suggested formation of toxic compounds (Felpeto & Hairston 2013).

Modelling of phytoplankton growth dates back to the works by Caperon (1967) and Dugdale (1967) who described nitrogen uptake by algal cells as a function of ambient nitrogen concentration, using Michaelis-Menten kinetics much in the same manner as Monod had done earlier for bacterial populations (Haney & Jackson 1996). Nutrient uptake rate by cells as a function of nutrient concentration is almost always formulated using a hyperbolic relationship, and since nitrogen is most often considered to limit phytoplankton growth, it is the common choice as model currency (Haney & Jackson 1996). The representation of algal growth in the *Chlamydomonas - Brachionus* model is true to this tradition (see Appendix C).

The results from the medium test indicated that it was necessary to re-estimate the algal parameters in the *Chlamydomonas - Brachionus* model by Becks *et al.* (2010). This is further emphasized when considering all the factors that have the potential to influence the growth of *C. reinhardtii*. My rotifer-algal experiment and the one by Becks and colleagues will not only differ in the composition of the growth medium, but will also differ in the temperature and light conditions. The main goal with the current experiment was therefore to estimate two growth parameters of *C. reinhardtii* under my experimental conditions. These two parameters are the algal conversion parameter (10^9 cells /µmol N) and the maximum algal per capita recruitment (/day), which together also derive the maximum algal nutrient uptake (µmol N /10^9 cells /day). An additional motive for the experiment was to compare algal growth data obtained using different methods.

MATERIALS AND METHODS

Isolation of a single algal clone

The stock culture of *C. reinhardtii* used in the medium test was bought from the *Chlamydomonas* Resource Center in 2013 and has been kept under variable and largely undocumented conditions since purchasing. Previous rotifer-algal studies have shown that

clonal variation in the algal population can have a significant effect on the population dynamics (Yoshida *et al.* 2003; Becks *et al.* 2010). Although the allocated stock of *C. reinhardtii* originally contained a single clone, it could not be guaranteed that this was still the case. I therefore deemed it necessary to establish a new single clone culture of *C. reinhardtii* for the current experiment.

The single clone of *C. reinhardtii* was isolated by the following procedure. A drop from the stock culture was streaked out on an agar plate made for growing phytoplankton (provided by Professor Dag Klaveness). After 11 days of growth on agar, five well separated colonies were picked and transferred to separate culture flasks containing JET medium. Subsequent growth and microscopic inspection of the five single clone cultures indicated no apparent differences between them, such that the clone used in the current experiment was chosen arbitrarily among these five.

Experimental setup

Media of five different nutrient concentrations were prepared to estimate algal growth parameters. All media were made with diluted lake water as basis, same as the B-mix in the medium test, and nutrients were added as in the JET medium except for the major elements, nitrogen and phosphorus. These two elements were added to the media to produce the five concentration levels listed in Table 1.3. Since the results of the previous chemical analysis revealed a considerable amount of nitrate in the lake water (see Table 1.2), its expected contribution of nitrate to the medium was taken into account (approximately 8 µmol/l). The contribution of phosphate from the lake water was considered to be negligible and thus ignored. The media were sterilized with a polyethersulfone (PES) membrane filter of pore size of 0.22 µm (Corning).

Table 1.3. Nitrate and phosphate concentrations of the five media used in the experiment.

Medium	Nitrate µmol /l	Phosphate µmol /l
F	20	2/3
G	40	1 1/3
H	80	2 2/3
I	160	5 1/3
J	320	10 2/3

The rotifer-algal experiment is based on a model that does not account for the possibility that algal stoichiometry could change in parallel with the depletion of ambient nutrients. Because the results by Felpeto & Hairston (2013) indicated significant differences between the growth of *B. calyciflorus* that is fed nutrient replete or nutrient limited *C. reinhardtii*, the nitrogen to phosphorus ratio of the medium needed to be considered. Recent

experiments by Jan-Erik Thrane, a PhD candidate in my group, have shown that *C. reinhardtii* has optimal growth when the N:P ratio is close to 30:1, and I therefore used this ratio in my experiments (Table 1.3).

For the experiment were three batch cultures established for each of the five nutrient levels, all with an initial volume of 200 ml medium and an initial algal concentration of approximately 800 cells/ml. The cultures were inoculated with algae from the single clone culture described above. The cultures were bubbled with a continuous flow of sterile air since the medium test suggested that the algae were carbon limited, and because the final rotifer-algal cultures are to be turbulently mixed. Air bubbling is known to prevent limitation of carbon dioxide and to enhance mixing. An illustration and photos of the experimental setup are presented in Appendix D. The light regime and temperature conditions were chosen to match the conditions of the final rotifer-algal experiment. The cultures were continuously illuminated using a grow light panel with red and blue LED lights (25-35 µE /m^2 /s) and kept at 17.5-19.0°C.

The cultures were sampled daily the first 10 days of the experiment and then once at day 13. The samples were used for pH measurements and to collect data on algal abundance by two different methods. Estimates of cell density and cell sizes were obtained with a particle counter (CASY TT; Shärfe, Reutlingen, Germany), while chlorophyll *a* content was estimated using an extraction protocol established by Jan-Erik Thrane. The protocol is as follows. 250 µl subsamples from each culture were transferred to a 96-microwell plate and then stored in a freezer. Later, these samples were freeze dried using a vacuum pump (Trivac D10E, Leybold, Eschborn/Taunus, Germany) until all water had sublimated. The dried remainders were extracted for 4 hours with 96% ethanol, 300 µl in each well. Relative chlorophyll *a* concentrations were estimated with a fluorescence microplate reader (Synergy MX, BioTek Instruments, Winooski, USA) using an excitation wavelength of 425 nm and an emission wavelength of 675 nm. The amount of chlorophyll *a* is assumed to be proportional to the fluorescence signal.

Statistical analysis

In order to estimate algal population parameters, the daily cell counts were analysed using nonlinear mix-effect modelling. The details of modelling and the calculation of the algal growth parameters are presented in Appendix E. All analysis and plotting were done in the R programming environment (R Core Team 2015) and the appendix was put together with R Markdown.

RESULTS

Algal growth parameters

The results of the algal counts for all cultures are plotted together with the fitted growth model in Figure 1.2 (top). According to the statistical model is the maximum algal per-capita recruitment 1.34 /day (with 95% confidence interval of 1.23 – 1.46), while the asymptotic cell density for each nutrient level is as listed in Table 1.4. The linear fit between the asymptotic cell densities and the medium's initial nutrient concentration (R^2 = 0.99) gives an algal conversion factor of $0.0035 \cdot 10^9$ cells /µmol N. Together the two growth parameters give a maximum nutrient uptake rate of 387 µmol N /10^9 cells /day. See Appendix E for details of these results.

Table 1.4. The asymptotic cell densities for the five nutrient levels estimated by the fitted growth model.

Medium	Initial N conc. (µmol N/ l)	Asymptotic cell density (cells/ml)	95% confidence interval of density estimate
F	20	49 599	42 048 - 57 151
G	40	96 986	82 916 - 111 055
H	80	216 234	194 340 - 238 129
I	160	440 207	406 260 - 474 153
J	320	1 086 622	1 023 917 - 1 149 329

Additional aspects of growth

The results for the fluorescence of extracted chlorophyll *a* were scaled with the cell counts in order to find the amount of fluorescence per cell for each day of the experiment. This conveyed a distinct increase in the amount fluorescence per cell over the first four days, followed by similar decrease over the next three days (see bottom plot of Figure 1.2). A compilation of the cell counts, data on algal fluorescence and distribution of cell size is presented in Appendix F. The plots in the appendix show that the culture fluorescence (fluorescence per ml) was at its highest at day 3 for the F cultures, day 4 for the G cultures, day 4-5 for the H cultures and at day 5 for the I and J cultures, and show further that the peaks in fluorescence come close after the estimated time point for the maximum rate of increase (xmid).

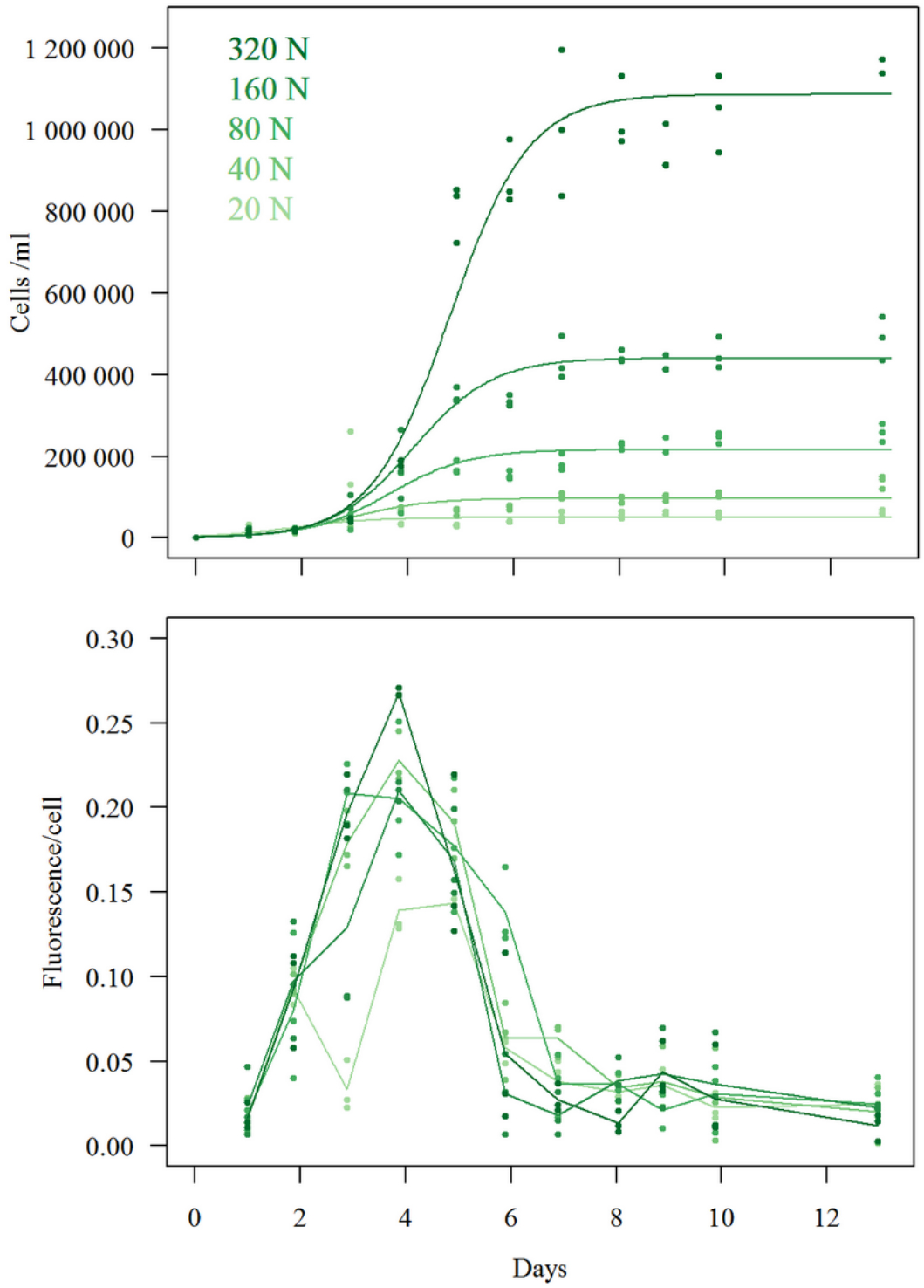

Figure 1.2. The top plot shows the results for the cell density estimates (points) and the fitted model (line) for each of the five nutrient levels (shades of green). The three replicates of each nutrient level are plotted with the same point character. **The bottom plot** shows the estimates of fluorescence per cell for the five nutrient levels (shades of green). The points indicate the value for each of the replicates and the line draws the average value within each nutrient level. The cell counts for the F cultures at day 3 are unexplainably high, which also is reflected in the low fluorescence/cell estimate for this day.

The distribution of cell sizes changed during the course of growth (Appendix F). Initially, during the exponential phase, the algal populations consisted predominantly of small cells with a cell diameter of about 4 µm. Then, about the same time or shortly after the fluorescence values were at its peak value, the cell sizes increased and the populations were dominated by cells with a diameter of about 6 µm and 7 µm.

The pH of the cultures were for most days between 6.6 and 7.6 (mean 7.06 and standard deviation 0.19), but a higher pH was measured on day 5 and 6 for the J cultures (Table 1.5).

Table 1.5. High pH measurements of the algal cultures.

Culture	Day	pH
J.1	5	7.87
J.2	5	8.24
J.3	5	8.21
J.2	6	7.90
J.3	6	8.26

DISCUSSION AND OUTCOME

The parameters estimated from the current experiment suggest a more vigorous growth of *C. reinhardtii* compared to the parameter values used in Becks *et al.* (2010). The maximum growth rate is almost the double of what Becks and colleagues reported (0.72 vs. 1.34 /day) and the 95% confidence interval for my estimate is far from including Becks' value (1.21 – 1.46). Also the estimated algal conversion factor suggests that each µmol N yields more cells of *C. reinhardtii* than what Becks assumed (0.0027 vs. $0.0035 \cdot 10^9$ cells /µmol N), as well as the estimated maximum nutrient uptake was found to be significantly higher (270 vs. 387 µmol N /10^9 cells /day).

Temperature and light are recognized environmental factors affecting growth of phytoplankton. Dissimilarities of the estimated parameter values were therefore not unexpected since these factors differed between the current experiment and the ones by Becks and colleagues. The algae in Becks' experiments were kept at 25°C and a light intensity of 120 µE /m^2 /s (white light), while the algae in the current experiment were cultured at 17.5-19°C and a light intensity of 25-35 µE /m^2 /s (red and blue LED lights). The photoperiods were equal among the experiments. However, based on the environmental differences one would expect the growth in the current experiment to be less vigorous than the growth in Becks'. Growth rates of phytoplankton are typically positively correlated with temperature and light intensity (e.g. Eppley & Sloan 1966; Rhee & Gotham 1981), whereas here the experiment with lowest temperature and lowest light intensity yielded the highest growth rate. This seemingly counterintuitive result could be caused by different ways of estimating the

parameter values (see Appendix C for Becks' method) and thus be more a methodological artefact than actual differences. Or it could suggest that *C. reinhardtii* has a growth optimum at temperatures below 25°C or that red and blue LED lights serve a high quality light source.

The maximum growth rate of *C. reinhardtii* in the five nutrient treatments were equal according to the selected growth model, while the asymptotic cell density and the time point for the maximum rate of increase were positively correlated with the initial nutrient concentration of the medium. The uniformity of the maximum growth rate is reasonable since the temperature and light conditions were equal for all treatments. The strong linear relationship between the asymptotic cell density and the initial nutrient concentration of the medium is also as anticipated, as the initial concentration of the limiting nutrient determines the system's carrying capacity.

In contrast to the medium test experiment, it does not seem like carbon limitation was an issue in the current experiment. The pH values were relatively low for all cultures throughout the growth period, except for the J cultures at day 5 and 6. These were the cultures which reached the highest algal densities and their elevated pH values occurred jointly with the peak in fluorescence per ml. This suggests that the continuous flow of air was not sufficient to completely cover the demand for carbon dioxide when the algal cultures of this density had high rates of photosynthesis, but that it was sufficient otherwise.

The results of the current experiment display significant changes in the cell sizes and the amount of fluorescence per cell during the course of growth. The algal populations were dominated by cells of smaller sizes during the early growth phase and larger sizes thereafter. A similar change is cell sizes was observed in study by Oldenhof *et al.* (2007). This study conveys that the small cells of *C. reinhardtii* are the recently released daughter cells after cell division, while the larger cells are the maturing and replicating cells. From their experiments, Oldenhof *et al.* (2007) also calculated the relationship between mother cell size and the number of daughter cells released. According to their results, mother cells with a size of about 200 μm^3 produce two daughter cells, while those of about 400 μm^3 produce four daughter cells. When assuming a spherical shape of the cell, these cell volumes correspond to diameters of approximately 7.3 µm and 9.3 µm. Since the largest cell sizes measured in the current experiment had diameters of about 7 µm, it is likely that these are cells that divide after the first round of DNA replication, releasing two daughter cells.

Another distinct result in the current experiment was the markedly change in the chlorophyll *a* content during algal growth. Quite unequivocally do the highest chlorophyll *a*

contents occur in the period of maximum growth, and then decrease sharply when the populations approach the carrying capacity. In this case, approaching the carrying capacity likely corresponds to the onset of nitrogen limitation, and this is known to produce adverse responses in *C. reinhardtii*. Park *et al.* (2015) investigated the effects of nitrogen deprivation on the growth of *C. reinhardtii* and found that nitrogen deprivation almost immediately initiates great changes in gene expressions levels. One group of genes that is found to be activated are those involved in the repartitioning of internal nitrogen sources, which seemingly allows for one extra cell doubling after the onset of deprivation (Park *et al.* 2015). The utilization of internal nitrogen pools for further growth explains the substantial difference in C:N ratios between nitrogen sufficient and nitrogen limited cells, and it might also explain the marked change in chlorophyll *a* contents. Since the chlorophyll *a* molecule contains nitrogen, it is not unreasonable to suppose that these pigments can serve as a nitrogen source.

Although the results seem to indicate that the algae were nitrogen limited, this finding is disputable. A nitrogen to phosphorus ratio of 30:1 is quite high, and the results of the final rotifer-algal experiment indicated that the phosphorus sources were depleted in all cultures at high algal densities while the nitrogen sources were not. However, the results from the rotifer-algal system may not be representative for the algal monocultures, as the rotifers would be expected to regenerate nutrients from the ingested algal biomass. Anyway, the results from the algal growth experiment provide an estimate for the amount of algae each µmol nitrogen would support under the specific conditions, regardless of whether nitrogen was the limiting substance or not.

In the rotifer-algal experiment was the algal populations monitored using an imaging cytometer instead of the two methods applied here. The main reason for this is because the cell clustering of *C. reinhardtii* reported in earlier rotifer-algal studies precluded the use of the more custom particle counter. Initially, the current experiment was set out with an expectation that it also would assess the quality of data generated by the imaging cytometer by comparing the results to the other two methods applied here. But due to some technical problems, the imaging cytometer could not be utilized in the current experiment.

Studies of *C. reinhardtii* have shown that its morphology and physiology is highly shaped by the ambient environmental conditions. The current experiment has emphasized the variability in morphology within the cell cycle of this species and that this may serve as indicators for the physiological state of the algal population. The experiment has also revealed a significant difference between the re-estimated algal parameters and the values used in the

Chlamydomonas – Brachionus model by Becks and colleagues. Although the cause for this difference is not obvious, the quality of results from the current experiment gives confidence to use the re-estimated algal parameters to describe the growth of *C. reinhardtii* in the final rotifer-algal experiment.

The results have conveyed a distinct change in the chlorophyll *a* contents of the cells during the different phases of growth, a change that likely is correlated with a change in algal stoichiometry. The experiments by Felpeto & Hairston (2013), among multitude of others, have shown that the elemental composition of algae is decisive for its quality as food for zooplankton. The relevance of integrating changes in food quality, together with food quantity, in predator-prey models is elucidated in the literature (see Andersen *et al.* 2004), but the likely change in algal stoichiometry is nevertheless an absent aspect of the *Chlamydomonas - Brachionus* model by Becks *et al.* (2010). However, an aspect which is related to algal quality and which *is* present in the *Chlamydomonas - Brachionus* model is what they denote the algal palatability. The effects of this quality parameter on the rotifer-algal dynamics will be considered in the next section.

PART 2
Rotifer-algal-nutrient dynamics

2.1 The theoretical dynamics

In the 20th century, scientists have aspired to transform ecology to an exact science, taking after the disciplines physics and chemistry (Kingsland 1985). Earlier, the methodologies of ecology were largely descriptive and this kept its esteem quite low in beginning of the century, but the extensive development of theoretical population biology in the 50s and 60s started to change this conception (Kingsland 1985; Palladino 1991). However, it was not until the rise of the environmental movement, stirred by Rachel Carson's *Silent Spring* from 1962, that the regard for ecology increased significantly (Palladino 1991). Today ecological insights and models of ecosystem functions receive large attention, both in public and in scientific communities. Knowledge about ecological mechanisms is for example crucial in global climate models, in sustainable harvest management and in pest control.

Two renowned names in theoretical population biology are Alfred J. Lotka and Vito Volterra. Independently, in the mid-1920s, they used their background in mathematics, physics and chemistry to describe the interaction between predators and prey as a set of differential equations (Kingsland 1985). Although these scientists usually are remembered in association with the predator-prey oscillations that their basic equations produce, their contributions were larger. The predator-prey equations occupy only a few pages of Lotka's book *Elements of Physical Biology*, which in its entirety was a study of the dynamic processes of nature (Kingsland 1985). The ecosystem perspective is also explicit in Volterra's publication. He connected the analysis of the simple predator-prey interaction to the interactions between natural populations and portrayed how these fundamental dynamics could lead to an understanding of the entire ecological community, and in the end, lead to a mathematical theory of evolution (Kingsland 1985).

Mathematical models in ecology might sometimes seem to be introduced without an explicit idea of what purpose it is serving. For the fisheries manager, the purpose of a model for sustainable harvest is of course obvious. The model is a description of a harvestable population and is utilized as a tool for exploiting it in a sustainable way. However, the purpose of laboratory-scale predator-prey models, like the *Brachionus – Chlamydomonas* model, is more ambiguous. The *Brachionus – Chlamydomonas* microcosm have little resemblance to the real world and one could question to what degree it can serve relevant insights about nature outside the laboratory.

Models are made for different purposes. Some models are made to create an image of a phenomenon, to aid our understanding of it, whereas others are made for their power to

predict future events. Some models are created for exploratory purposes, as a tool for investigation. Models of the latter type often aim to reveal fundamental mechanisms of the object that is examined. The complexity of ecological systems makes it to a large extent impossible to study the system in its entirety. In fact, models covering dynamics beyond three-four species are uncommon and often immensely complex. Compromises are therefore often made in order to be able to study ecological systems at all.

Richard Levins presented what now has become a renowned classification of ecological models in his article *The strategy of model building in population biology* (1966) (Palladino 1991). There he classifies ecological models according to how they balance three model requirements, "generality", "precision" and "realism", and argues that not all requirements can be met at the same time. Although this claim can be questioned (see e.g. Palladino 1991), it nevertheless points to some intrinsic problems in modelling of ecological systems. Levins himself, and other ecologists with him, regarded the exploratory aspect of ecological models to be the most important; models should be representations of fundamental mechanisms of complex ecological phenomena, and potential mismatches between the model and phenomenon serve to point out the direction for continued investigations (Palladino 1991). The series of rotifer-algal studies from the Hairston lab seems partly to have been motivated by such a mismatch been model and experimental results, which will be described in the following.

The paper by Fussmann *et al.* (2000) presents the first study in the series of rotifer-algal experiments at the Hairston lab. In this paper they demonstrated that the predator-prey dynamics could be perturbed from a stable equilibrium to population cycles by changing the dilution rate of the system (Figure 2.1). Although the mathematical model quite accurately predicted when the system would oscillate, the cycles had a different pattern than the model predicted. The cycles did not look like classical consumer-resource cycles where the peak of

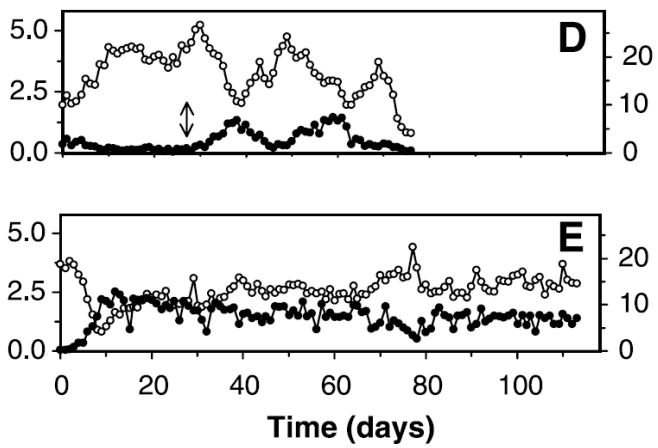

Figure 2.1. The figure is taken from Fussmann *et al.* (2000) and shows two of their experimental results. **D)** Transition from equilibrium to cycles; Dilution rate (D)=1.15 per day on the left side of the arrow, D = 0.95 on the right side of the arrow. **E)** Equilibrium at high D (1.24 per day). Ni was set to 80 µmol/l. Open circles *C. vulgaris*; filled circles *B. calyciflorus.* The y-axis on the left gives the algal density (10^6 cells/ml) and the one on the right gives the density of rotifers (females/ml).

the predator population lags a quarter of a cycle behind the peak in prey. Instead, their observed rotifer-algal cycles had a long period and an antiphase pattern where the peak of the predator coincided with the trough of the prey (see plot D in Figure 2.1).

This unexpected behaviour of the predator-prey system spurred further investigations to reveal the cause for the antiphase dynamics. The results of these studies are presented in Shertzer *et al.* (2002), Yoshida *et al.* (2003) and Yoshida *et al.* (2004). In the first paper they describe how they tested four candidate hypotheses by making extensions to the original mathematical model of the rotifer-algal system. The theoretical analyses suggested that clonal, phenotypic variability in the prey could be a causal factor for the observed antiphase cycles, which implied that their original algal stock consisted of multiple clones with variable phenotypic traits. To test this hypothesis they ran replicated experiments of the rotifer-algal system with an algal stock that now were ascertained to consist of only a single clone. Two results from the replicated experiment are shown in Figure 2.2. The population cycles in this system now exhibited classical consumer-resource cycles with the peak in predators lagging approximately a quarter of a cycle behind the peak in prey. These results, they concluded, supported the hypothesis that the antiphase cycles observed in the experiments presented in Fussmann *et al.* (2000) were caused by rapid evolution in the algal population because it held multiple algal clones with variable phenotypes (Yoshida *et al.* 2003).

Next they investigated the phenotypic traits that were under selective pressure in the algal population that consisted of multiple clones, and the results detected a trade-off between the algae's competitive ability and defence against rotifer grazing (Yoshida *et al.* 2004). Algae that had a high defence against rotifer grazing were the individuals with the lowest competitive ability, while those with low defence against grazing had the highest competitive ability. For the algal species in these experiments, *Chlorella vulgaris*, the defence against rotifer grazing was associated with the algae's nutritional value, with the rationale being that

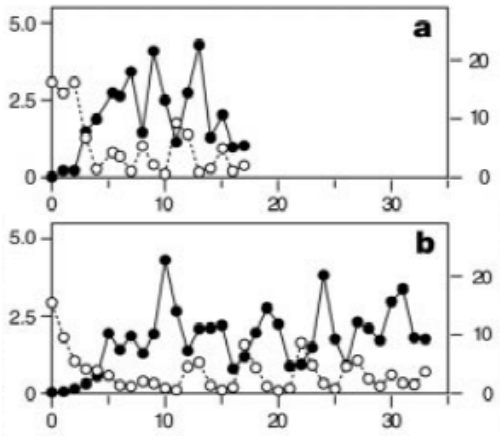

Figure 2.2. The figure shows two of the results from the single algal clone cultures of Yoshida *et al.* (2003). **a)** D=0.57 **b)** D=0.65, Ni was in both cases 80 µmol/l. Open circles *C. vulgaris*; filled circles *B. calyciflorus*. The y-axis on the left gives the algal density (10^6 cells/ml) and the one on the right the density of rotifers (females/ml). The x-axis is in days.

algae with low nutrient contents would support a weaker rotifer recruitment compared to algae with high nutrient contents (Yoshida *et al.* 2004). Hence, the algae with low nutrient contents have a higher defence against grazing compared to the algae of high nutritional value.

Shertzer *et al.* (2002) argue that the antiphase pattern of the rotifer-algal system is caused by a shift in fitness between the different algal clones during the population cycles. In times of high rotifer density would the algae with low food value have the highest fitness and thus increase in proportion, while the algae with the highest competitive ability would be favoured in times when the rotifer population is low and the competition for nutrients is the strongest selection pressure. It is this change in frequencies of different algal clones which is termed eco-evolutionary dynamics and which is believed to cause the antiphase cycles in the rotifer-algal system in Fussmann *et al.* (2000) and later in Becks *et al.* (2010). An illustration of how the *Chlamydomonas – Brachionus* model predicts eco-evolutionary dynamics is presented on page 133 in Appendix G.

In the continuation of rotifer-algal studies at the Hairston lab was *C. vulgaris* replaced by *Chlamydomonas reinhardtii* which is known to exhibit a more explicit response to grazing. When cultured together with *B. calyciflorus*, the single celled flagellate *C. reinhardtii* is found to form clusters of cells called palmelloids (Lürling & Beekman 2006; Becks *et al.* 2010). The ingestion rate of *B. calyciflorus* is observed to decrease when the palmelloids consist of eight cells or more, and the size of the palmelloids is thus the trait that is assumed to determine the degree of defence against rotifer grazing (Becks *et al.* 2010). Likewise to *C. vulgaris*, it is assumed that the defensive trait in *C. reinhardtii* lower the competitive ability because the cell clusters and the gelatinous matrix surrounding the palmelloids would reduce the efficiency of nutrient uptake (Becks *et al.* 2010). Hence, the individuals with a high defence against rotifer grazing (low palatability) are the individuals with low competitive ability.

In the *Chlamydomonas – Brachionus* experiments by Becks *et al.* (2010) they investigated how the initial degree of defence in the algal population would influence the rotifer-algal dynamics, and their results clearly indicated that the initial degree of palmella formation determines the system's behaviour. Hence, not only are the dynamics of the rotifer-algal system governed the experimental parameters (dilution rate and nitrogen concentration of the supplied medium) as shown in Fussmann *et al.* (2000), also the initial palatability of the prey population plays a major structuring force. For the design of the planned rotifer-algal

experiment, it was therefore necessary to analyse the effects of prey palatability together with the effects of the experimental parameters.

This part of the thesis presents the theoretical analysis of how the *Chlamydomonas – Brachionus* system is expected to behave for different values of the experimental parameters and for varying degree of algal palatability. The algal parameters describing the growth of *C. reinhardtii* in the original *Chlamydomonas – Brachionus* model are replaced by the parameters that were estimated in the algal growth experiment (part 1.2), but otherwise is the model identical to the one described in the supporting material in Becks *et al.* (2010) (and Appendix C). The goal with this part of the project was to identify values for the experimental parameters in the final rotifer-algal experiment that would generate a steady state population development and persisting population cycles.

METHODS

The analysis of the *Chlamydomonas – Brachionus* model of differential equations was done with the aid of the *deSolve* package written for the R programming environment by Soetaert *et al.* (2010). This package serves functions for solving ordinary differential equations and does this by means of numerical methods. Based on the solver from the *deSolve* package, time series, bifurcation diagrams and parameter planes of the model were constructed in R (R Core Team 2015). A bifurcation diagram is a plot that shows how the qualitative behaviour of the system changes as a function of one specific model parameter, while a parameter plane is a plot that shows the behaviour as a function of two model parameters.

The two central model parameters that were investigated for their effects on the system were the experimental parameters Ni and D, the nitrate concentration of the supplied medium and the culture's dilution rate. Additionally, I investigated how the palatability of the defended algal clone, p_1, affected the population dynamics. The palatability parameter ranges from 0 to 1, where 0 denotes algae with the lowest palatability and maximum defence and 1 denotes algae with the highest palatability and no defence (single celled algae). The model assumes that there is a linear trade-off curve between the algal palatability (p_1) and the competitive ability. The competitive ability is represented by the algal half-saturation constant ($K_{c,1}$) in the *Chlamydomonas – Brachionus* model (Appendix C).

A detailed presentation of the model analysis of the *Chlamydomonas – Brachionus* system is given in Appendix G, which additionally provides the code for the results below. The appendix was put together with R Markdown.

RESULTS

The set of parameter planes presented in Figure 2.3 shows that the expected behaviour of the *Chlamydomonas – Brachionus* system is dependent on both experimental parameters (D and Ni) and the palatability of the defended algal clone (p_1). The parameter combinations of D and Ni that are expected to produce a stable equilibrium (light and dark green areas) change depending on the p_1 parameter, but all plots depict stable equilibriums when D is in the range 0.2 – 0.8 /day and Ni is between 40-100 µmol/l. The undefended algal clone is expected to dominate the algal population for this area on the parameter map (light green areas). Figure 2.4 shows how the model typically predicts a development of a stable equilibrium over time, here when D=0.3 /day and Ni=50 µmol/l.

Two of the parameter planes in Figure 2.3 indicate that the defended algal clone will dominate the stable equilibriums (dark green areas) when the supplied nitrate concentration is above about 100 µmol/l (p_1=0.25 and p_1=0.50). The bifurcation diagram in Figure 2.5 depicts similarly how the dominance of algal clones, together with qualitative behaviour of the system, changes with increasing values of Ni. The system is expected to be in a stable equilibrium for Ni-values below 450 µmol/l and to oscillate for Ni-values above 450 µmol/l.

The model predicts population cycles for a range of combinations of Ni and D values (blue areas) and also that this behaviour depends on the value for the p_1 parameter. Roughly, all parameter planes depict that stable cycles are expected when D is in the range 0.2 – 1.0 /day and Ni is in the range 100 – 300 µmol/l. I have indicated in the parameter planes two specific combinations of D and Ni (stars). One is where D=0.3 /day and Ni=50 µmol/l and is a combination that predicts stable equilibrium for all values of p_1 (as in Figure 2.4). The other parameter combination is where D=0.3 /day and Ni=250 µmol/l. Figure 2.6 depicts four time series plots for this parameter combination. The predicted behaviour is here dependent on the palatability of the defended algal clone. The model predicts stable cycles with both clones present (eco-evolutionary dynamics) when p_1=0.05, dampened oscillations when p_1=0.25, stable cycles with a shift in dominance of algal clones when p_1=0.75, and a stable cycle with dominance of the undefended algal clone when p_1=0.90. The cycles in the systems with a defended algal clone with a low degree of defence (p_1=0.75 and p_1=0.90) are in essence classical consumer-resource cycles.

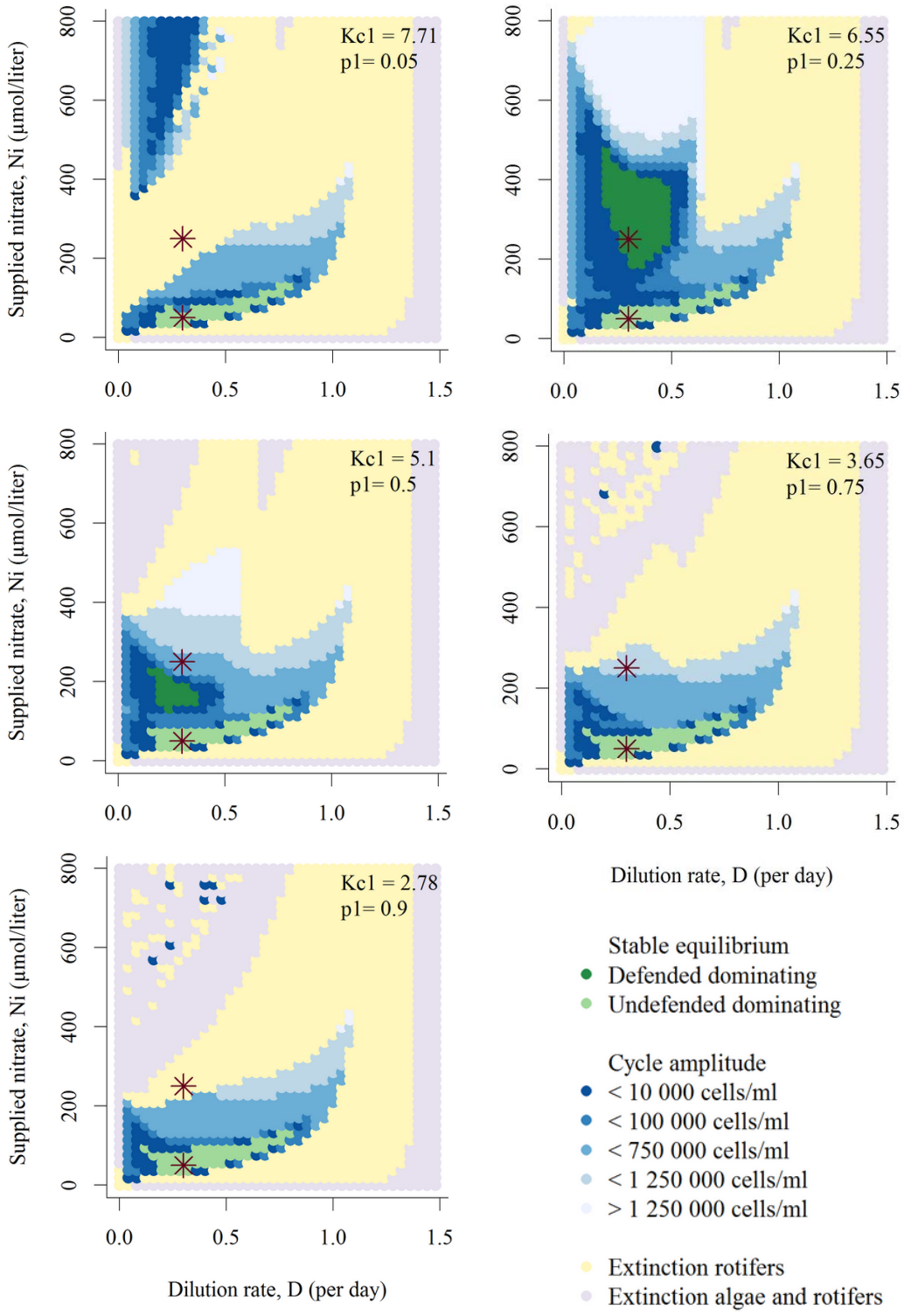

Figure 2.3. Parameter planes for the *Chlamydomonas – Brachionus* model for different values of palatability of the defended algal clone (p_1), p_1=0 for algae with maximum defence and p=1 for algae with no defence. $K_{c,1}$ represents the algal half-saturation constant. Each parameter plane shows the behaviour of the model system as a function of the experimental parameters Ni and D. The size of the cycle amplitude is given in concentration of algal cells, and the stars are placed where D=0.3 /day and Ni either equals 50 or 250 µmol/l.

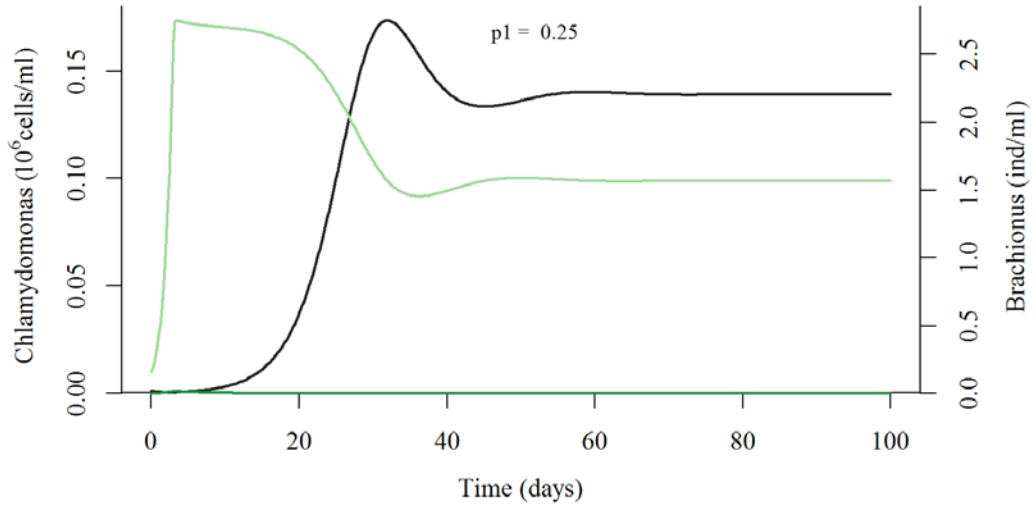

Figure 2.4. Time series plot of the *Chlamydomonas – Brachionus* system when D=0.3, Ni=50 and p_1=0.25. After an initial peak in the population densities, the system is expected to stabilize in stable equilibrium with only the undefended algal clone present.

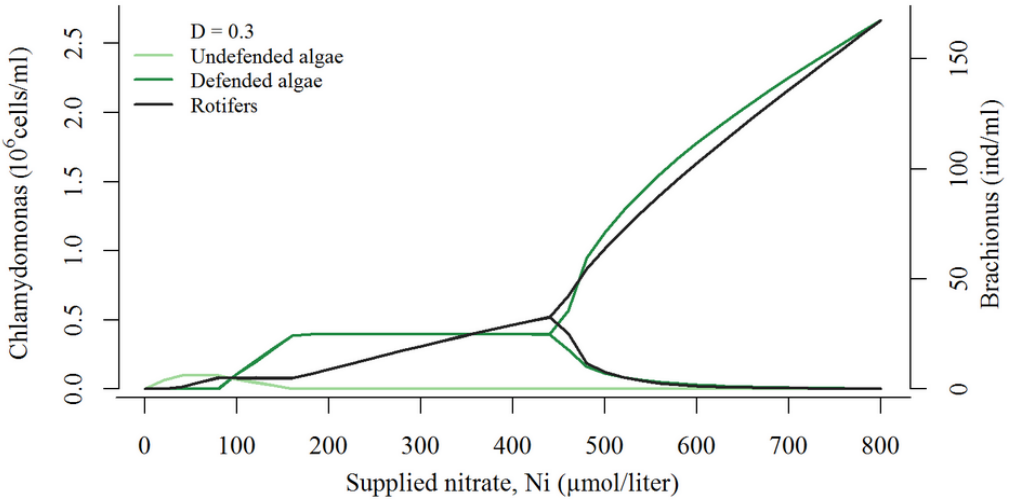

Figure 2.5. Bifurcation diagram of the *Chlamydomonas – Brachionus* system with Ni as the bifurcation parameter. The dilution rate (D) is set to 0.3 and the palatability of the defended algal clone (p_1) is set to 0.25.

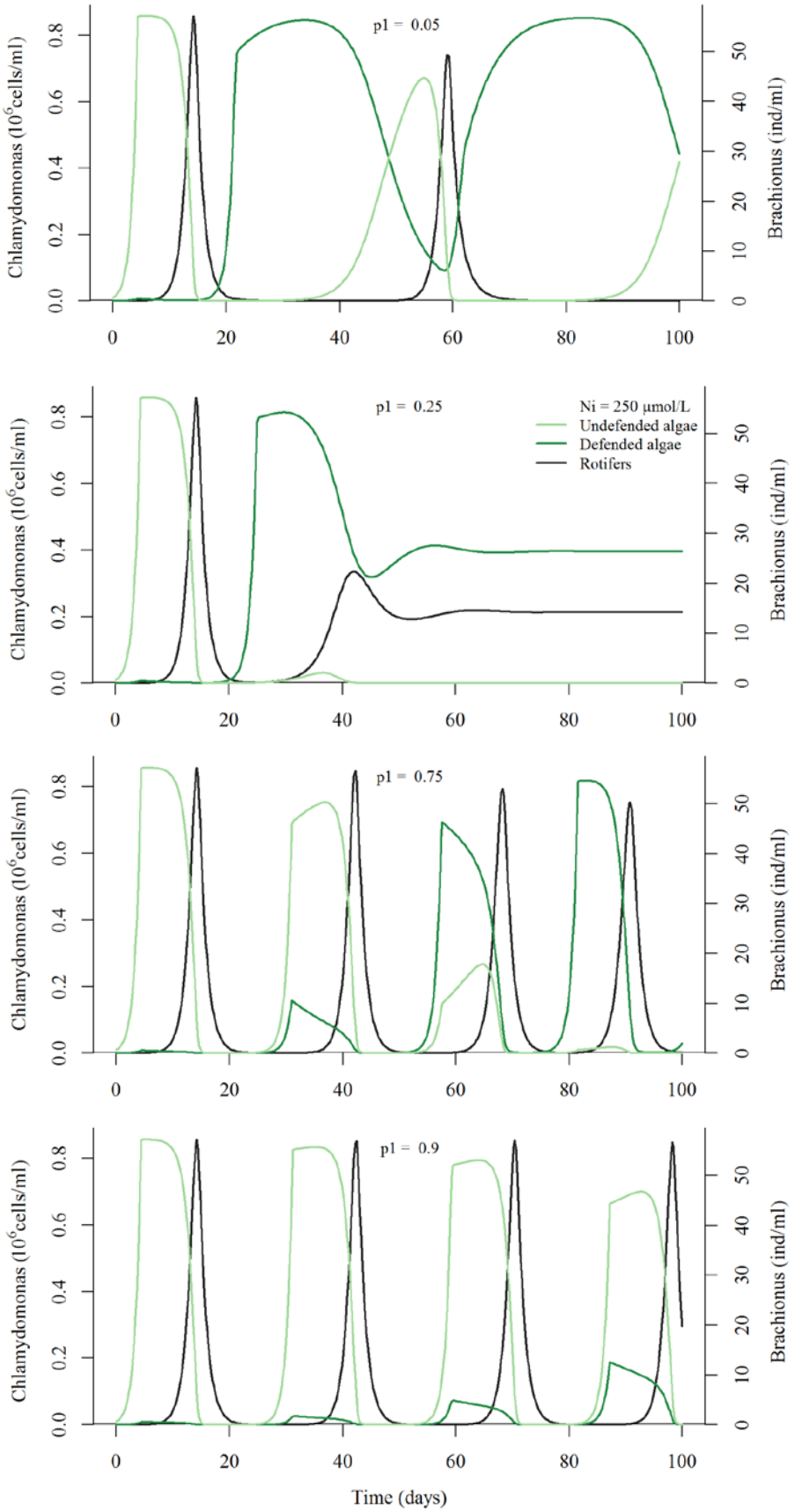

Figure 2.6. The expected behaviour of the *Chlamydomonas – Brachionus* system for different values of the palatability of the defended algal clone (p_1) when D=0.3 and Ni=250.

DISCUSSION AND OUTCOME

The analysis of the *Chlamydomonas – Brachionus* model displays several interesting aspects of the dynamics in this rotifer-algal-nutrient system. One apparent aspect is that enrichment destabilizes the system. This is a phenomenon well-known under the term *paradox of enrichment* after the article by Rosenzweig (1971) who described the phenomenon mathematically. The *Chlamydomonas – Brachionus* system is in general expected to oscillate when the nitrate concentration of the supplied medium exceeds 100 µmol/l. The amplitude of the oscillation is further expected to increase with increasing nitrate concentrations, until the oscillations are so large that they result in extinction of the predator or both predator and prey. Regardless of the palatability of the defended algal clone, a nitrate concentration of 50 µmol/l for the supplied medium supports a stable equilibrium of the rotifer-algal system, while a concentration of 250 µmol/l could lead to several distinct dynamics depending on the palatability of the defended algal clone.

For two of the palatability values, p_1=0.05 and p_1=0.90, the parameter planes portray that Ni=250 µmol/l would lead to extinction of the predator, while the time series plots in Figure 2.6 depict stable cycles. The disagreement between the figures is a result of how the threshold for rotifer extinction was set in the parameter planes. The threshold was set to 5 breeding individuals per 500 ml (0.01 ind/ml), because the risk of stochastic extinction was considered to be high if the rotifer abundances were lower. A cycle amplitude of about 55 rotifers/ml, as predicted for Ni=250 µmol/l, is quite large but not unrealistic. Becks *et al.* (2010) measured once a rotifer density of about 60 ind/ml in their *Chlamydomonas – Brachionus* experiments (Ni=160 µmol/l), however their rotifer densities were most often between 20 and 40 ind/ml.

Another apparent aspect of the *Chlamydomonas – Brachionus* system is that the palatability of the defended algal clone has a strong effect on the system's dynamics. In general, larger areas of stable equilibriums and stable cycles are found in the parameter planes that have a defended algal clone with a high degree of defence (low palatability). Such effects of variable prey palatability in the *Chlamydomonas – Brachionus* system was the focal point in the study by Becks *et al.* (2010). Their theoretical and experimental analyses indicated that the initial variance in algal palatability would determine whether the system developed into a stable equilibrium, standard consumer resource cycles or eco-evolutionary cycles. Similarly, it has been shown for a *Chlorella – Brachionus* system that the predator-prey dynamics are

structured by the initial algal genetic variance in traits associated with a trade-off in competitive ability and defence against predators (Kasada *et al.* 2014).

The long antiphase cycles observed in the studies by Fussmann *et al.* (2000), Becks *et al.* (2010) and also Kasada *et al.* (2014) are ascribed to a feedback between ecological and evolutionary processes, hence the term eco-evolutionary cycles. Evolution is the change in heritable traits or, more broadly, the change in frequencies of genotypes in populations across generations (Futuyma 2009, p. 2). Thus a premise for the eco-evolutionary dynamics is that the variance in adaptive traits in the algal population is based on fixed genetic differences. The *Chlamydomonas – Brachionus* model illustrates how eco-evolutionary dynamics might appear in systems when the prey population consist of two genetically different clones with contrasting fitness traits (see page 133 in Appendix G).

Nevertheless, the genetic basis for the different phenotypes of the algal prey is not evident. The previous section (algal growth parameters) emphasized the plasticity of algal morphology and physiology to changes in the abiotic environment. Additionally, biotic cues are found to induce phenotypic changes, such as colony formation, in several algal species (Van Donk *et al.* 2010). Becks *et al.* (2010) argued that palmella formation in their stock of *C. reinhardtii* was caused by fixed genetic differences since separate experiments had showed that grazed algae continued to form palmelloids for nine generations in the absence of *B. calyciflorus.* It is however questionable whether this is enough to dismiss the possibility that the trait is plastic.

One motivation for exploring how predator-prey systems are affected by variance in fitness traits has been to elucidate whether evolution, or the presence of genetic variation, can have a stabilizing effect on ecological systems (Fussmann *et al.* 2007; Becks *et al.* 2010). For similar reasons have the effects of inducible defences also been investigated in predator-prey systems. Theoretical analyses indicate that inducible defences in prey promotes stability in population communities (Vos *et al.* 2004a; Yamamichi *et al.* 2011), a finding that is also supported by experimental results (Verschoor *et al.* 2004b). Using a rotifer-algal system, Verschoor *et al.* (2004b) tested the predictions by Vos *et al.* (2004a) and observed a significant difference between enriched food chains that contained algae with inducible defences (*Scenedesmus obliquus*) compared to those that contained algae without induced defences (*Desmodesmus bicellularis*). The typical fluctuations of enriched food chains were absent from the systems with algae exhibiting inducible defences, while the fluctuations were observed in the systems with undefended algae.

Whether caused by rapid evolution or phenotypic plasticity, rapid adaptation of prey species seems to stabilize population dynamics (Yamamichi *et al.* 2011). The crucial point is that all mechanisms that cause an increase in the mortality of the predator will have a stabilizing effect on oscillating predator-prey systems (Vos *et al.* 2004a). However, the speed of adaptation is not trivial. Yamamichi *et al.* (2011) compared the effects of the two mechanisms and found that phenotypic plasticity tends to stabilize predator-prey dynamics more strongly than rapid evolution, primarily because phenotypic plasticity promotes faster changes. But this finding presupposes that the variance in fitness traits is equal for the two mechanisms. The range of the phenotype is a crucial factor in adaptation, and it is unclear whether inter-individual fixed differences or intra-individual phenotypic plasticity offer the broader range in natural populations (Yamamichi *et al.* 2011).

For my rotifer-algal experiment, I inoculated the systems with unicellular *C. reinhardtii* that had no recent history of rotifer grazing. The decision of values for the experimental parameter was complicated by the uncertainties concerning the palatability of my algal stock. Even though the rotifer-algal system would commence in a state where the palatability of the entire algal population was high (low defence), this would change as soon as palmelloids would start to occur. In the study by Becks *et al.* (2010) did the systems that were inoculated with unicellular *C. reinhardtii* stabilize in a steady state after some initial fluctuations when the dilution rate was set to 0.3 /day and the supplied nitrate concentration was 160 µmol/l. I chose to set the dilution rate equal to Becks *et al.* (2010) in my rotifer-algal experiment, while I chose a nitrate concentration of 250 µmol/l for the high nutrient treatment in order to the increase the likelihood of persisting population cycles. For the low nutrient treatment, I chose a nitrate concentration of 50 µmol/l for the supplied medium since it is predicted that this concentration generates a steady state population development across the range of palatability values investigated.

2.2 The experimental dynamics

Stephen A. Forbes, an early pioneer in limnology, portrayed a single body of water on land as "[…] a little world within itself, - a microcosm within which all the elemental forces are at work and the play of life goes on in full, but on so small a scale as to bring it easily within the mental grasp" (Forbes 1887, p. 77). The microcosm that Forbes described resembles the concept of an ecosystem, which is a term that was introduced first 48 years after Forbes' publication (Lewis 2009). Another landmark in ecology came with Raymond Lindeman's publication *The Trophic-Dynamic Aspect of Ecology* (1942), which was a product of an analysis of all the feeding relationships among organisms in Cedar Bog Lake, Minnesota, USA (Lewis 2009). Hence, there is a strong research tradition among limnologists to study population and community structure using freshwater microcosms.

Phytoplankton and zooplankton constitute two of the fundamental trophic levels in lake ecosystems, the primary and secondary producers. Although zooplankton is found on several trophic levels, feeding on organisms ranging from bacteria to other zooplankton, it is their role as herbivores that has been especially well studied (Sterner 2009). Herbivorous zooplankton are often considered to be key players in lake systems because of their high impact as grazers on the algal community (Sterner 2009). Rotifers are the smallest representatives of the multicellular zooplankton, mostly ranging in size between 200-500 µm, and their importance as grazers in lake systems is usually considered to be inferior to the cladocerans and copepods (Sterner 2009). However, their high reproductive rates makes them capable of reaching high population numbers in zooplankton communities (Wallace & Smith 2009).

The rapid reproduction of the freshwater rotifer *Brachionus calyciflorus* has contributed to its role as a model organism in aquatic research. Similarly to the daphnids, *B. calyciflorus* reproduce by cyclic parthenogenesis, which means that they can alternate between sexual and asexual reproduction. The dominant reproductive mode is asexual where females produce diploid, clonal daughters. In the sexual mode females produce haploid eggs that have two possible fates. If the haploid eggs are left unfertilized they develop into males, whereas if fertilized they develop into resting eggs that give rise to sexually produced females (Gilbert 2004). Sexual reproduction in *B. calyciflorus* is found to be triggered by high population densities of conspecifics (Gilbert 2004). However, the propensity to reproduce sexually has been shown to vary within different strains of *B. calyciflorus* (Gilbert 2004). This does not primarily point to intraspecific genetic variation, but rather that *B. calyciflorus* is a

cryptic species complex (Gilbert & Walsh 2005). Furthermore, *B. calyciflorus* has been found to lose its ability to reproduce sexually after prolonged selection for asexual reproduction (Fussmann *et al.* 2003; Stelzer *et al.* 2010).

The primary producers in the pelagic zone face several challenges. Their subsistence is dependent on the availability of light and nutrients, on competition and parasitism, and not the least on the grazing pressure exerted by herbivores. These structuring forces on the phytoplankton community are however not constant throughout the water column or across seasons. Thus a wide variety of adaptive strategies exist in the phytoplankton to meet the challenges of a variable environment. This is apparent both by the large diversity of species in phytoplankton communities and by the extensive variability in morphological features. Freshwater environments hold especially large and diverse assemblies of green algae (Leliaert *et al.* 2012). The Chlamydomonadales, which *Chlamydomonas reinhardtii* belongs to, is large taxa of green algae that contain species with highly diverse morphologies, including unicells, filaments, colonies and multicellular forms (Leliaert *et al.* 2012). *C. reinhardtii* is usually a single celled flagellate, but is also observed in a palmelloid state where non-motile cells are clustered together and embedded in a gelatinous substance.

Becks and colleagues (2010) argued that there is fixed genetic basis for the formation of palmelloids in their stock of *C. reinhardtii* and assumed that the palmelloids have a lower competitive ability compared single cells because the cell clusters and gelatinous matrix would reduce the nutrient uptake rates of the cell. One of the main findings in the study by Becks *et al.* (2010) was that the initial variance in unicelled and palmelloid algae in the prey population (i.e. initial variance in prey defence) determines the behaviour of the rotifer-algal dynamics. Figure 2.7 shows an example of their experimental results and illustrate the difference between systems that were inoculated with only single celled *C. reinhardtii* (plot e and f, “ungrazed algae” i.e. algae that have no recent history of grazer presence) and systems that were inoculated with an algae population consisting of both unicells and palmelloids (plot c and d, “grazed algae” i.e. algae that have a recent history of grazer presence). The systems with low initial prey defence (ungrazed) displayed dampened oscillations towards a stable equilibrium, while the systems with high initial prey defence (grazed) displayed antiphase eco-evolutionary cycles. Recall introduction in part 2.1 for a description of eco-evolutionary cycles.

Becks *et al.* (2010) argue that palmella formation in their stock of *C. reinhardtii* is a heritable trait that arose due to strong selection by rotifer grazing. However, palmelloids have

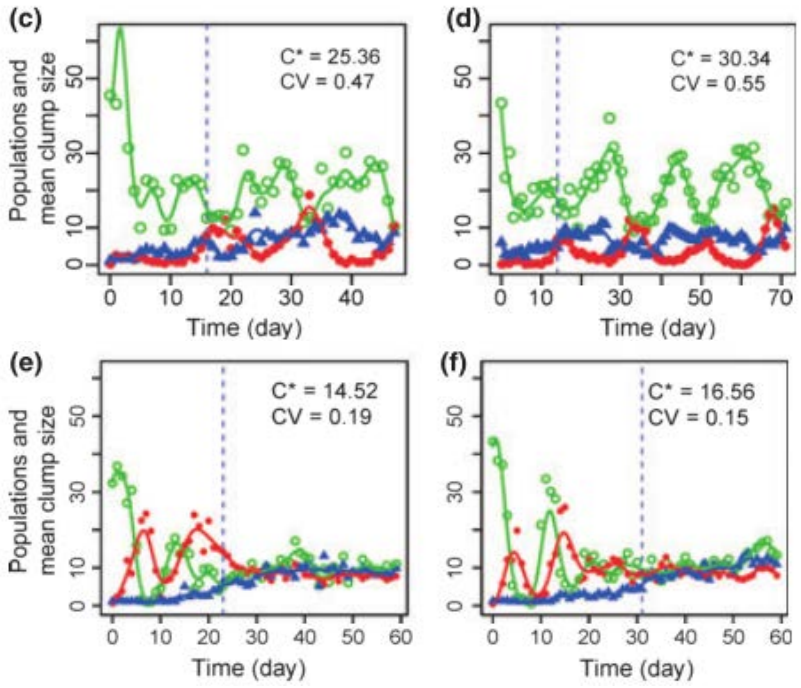

Figure 2.7. The figures are taken from Becks *et al.* (2010) and show the contrasting dynamics between cultures that are initiated with "grazed" *C. reinhardtii*, i.e. that have a recent history of rotifer grazing (c and d) and ungrazed *C. reinhardtii* (e and f). Open circles and green curves represent the algal density (10^4 cells/ml), solid circles and red curves represents the population density of *B. calyciflorus* (females/ml), and the triangles and blue curves describe the mean clump size of the algal palmelloids (cells per colony). The dilution rate was set to 0.3 /day and the supplied nitrate concentration to 160 µmol/l.

been shown to occur in cultures of *C. reinhardtii* under other conditions as well. In a short term rotifer-algal assay, Lürling & Beekman (2006) report that populations of *C. reinhardtii* cultured for one day together with *B. calyciflorus* showed a significant higher proportion of colonies (65 ± 9 % unicells in control vs. 30 ± 12 % unicells in rotifer treatment) and conclude that palmella formation is an inducible trait. Iwasa and Murakami (1968; 1969) observed that palmella formation can be induced by organic acids and that calcium deficiency impede the dissociation of dividing cells. Further, palmelloids have been found to appear in monocultures of *C. reinhardtii* after three days of high chemostat dilution rates (Olsen *et al.* 1983) and after approximately 140 days of strong selection for cells with the fastest sedimentation rates (Ratcliff *et al.* 2013). Hence, the environmental factors and response patterns explaining the palmella formation in *C. reinhardtii* are unclear.

The main goal with this final part of the master project was to establish a set of rotifer-algal-nutrient microcosms and see if it was possible to generate two qualitatively different population dynamics by varying the nutrient load. Based on the analysis the *Chlamydomonas – Brachionus* model by Becks and colleagues (part 2.1), I identified conditions that I expected would generate either steady state population development or persisting population cycles. A second ambition I had for this part of the project was to elucidate the mechanism behind palmella formation in *C. reinhardtii* and the effects it has on the rotifer-algal dynamics. Based on previous studies, I expected that palmelloids would arise and that they would have a

stabilizing effect on the predator-prey system. Additionally, resting on the assumption that palmelloids have higher fitness in high nutrient environments, I expected that the degree of palmella formation would be higher in the high nutrient microcosms.

MATERIALS AND METHODS

The organisms

The stock of *C. reinhardtii* used for the present study was the same as the isolated single clone culture in the algal growth experiment (part 1.2). *B. calyciflorus* was obtained from Pentair Aquatic Eco-Systems as resting eggs and were hatched four weeks prior to the onset of the experiment. Because the resting eggs came without information about how they were isolated and because *B. calyciflorus* is found to be a cryptic species complex, one female rotifer was chosen to establish a single clone population of *B. calyciflorus.* This rotifer population was fed *C. reinhardtii* from the same stock as described above and reared in darkness to prevent algal growth.

Experimental setup

Eight continuous cultures holding a volume of 550 ml were established as depicted in Appendix H. The dilution rate was set to 0.3 /day for all eight cultures, whereas four cultures received a supplied nitrate concentration of 50 µmol/l and the other four a concentration of 250 µmol/l. The composition of the medium is identical to the medium used in the algal growth experiment, i.e. a JET medium with diluted lake water as basis and a nitrate to phosphate ratio of 30:1. The medium was sterilized by filtration through a polyethersulfone (PES) membrane filter of pore size of 0.22 µm (Corning).

Before the onset of the experiment, ethanol (70 %) was pumped through the culture systems followed by distilled water and then the assigned medium. At the day of inoculation, 40 female rotifers were added to each culture flask and algae were added to give an initial concentration of approximately 1100 cells/ml. The cultures were bubbled continuously with sterile air to enhance mixing and to prevent limitation of carbon dioxide. Red and blue LED lights (25-35 µE /m^2 /s) provided a constant source of light and the room temperature was between 17.5-19.0°C.

The state of the rotifer-algal-nutrient systems was recorded every second day for a duration of 11 weeks. Samples from each culture were obtained by collecting the culture volume that was washed out by the dilution process over a 4-5 hour period. This gave approximately 20 ml sample from each culture. The samples were used to obtain data on algal

and rotifer abundances, and additionally used for pH and temperature measurements and for analysis of the culture medium's contents of nitrogen, nitrate and phosphorus. The dilution rate of the systems was also recorded every other day.

Data on algal abundance and size was obtained with an imaging cytometer (iCys Research Imaging Cytometer, CompuCyte, Massachusetts, USA). This instrument use lasers and photomultiplier detectors to measure properties of cells based on fluorescence. For the current objective the cells were made fluorescent by exciting the chlorophyll *a* with a 488nm argon ion laser. Depending on the concentration of algal cells, between 2 – 200 µl of the culture sample was transferred to a 96-microwell plate (F96 MicroWell Plate, Polystyrene, Nunclon Delta Surface). Distilled water was added to the wells in addition to the algal sample such that each well held a total volume of 200 µl. To enhance the precision of the estimates for algal abundance and size, six technical replicates were made for each culture. The culture samples taken out for the six technical replicates were of two different volumes, three small and three larger volumes depending on the algal densities.

The iCys cytometer collects data on multiple sets of cell samples by an automated scanning procedure. A requirement for this procedure is that the cells are stationary and lie at the same focal level. The flagellated cells of *C. reinhardtii* were made motionless by heating the samples in the microwell plate to approximately 55°C. This was sufficient to kill the algae and the rotifers. The microwell plate was next centrifuged in order to settle the cells on the bottom of the plate. The iCys scanning protocol for 96-well plates collects data on cell properties from each well by scanning an area of 0.77 mm^2. The settings of the iCys instrument were adjusted based on tests prior to the experiment. The same scanning protocol was used throughout the entire experiment.

Estimates of rotifer abundance were obtained by manual counts under a dissecting microscope. In most cases were the estimates based on a 20 ml culture sample, but sometimes less. Four different categories were used for the rotifer counts: females with eggs, females without eggs, dead females and males.

After I had collected data on pH, temperature and organism abundance, the 20 ml culture samples were filtered through a glass microfiber filter with a pore size of 1.2 µm (Whatman GF/C). The filtrates were stored in scintillation vials and frozen for subsequent chemical analysis, which included analyses of nitrogen, nitrate and phosphate concentrations. Concentrations of dissolved total nitrogen were determined with a total organic carbon analyser (TOC-V CHP, Shimadzu, Tokyo, Japan), while contents of dissolved nitrate and

phosphate were determined with an autoanalyzer (AutoAnalyzer 3, SPX Process Equipment, Bran + Luebbe, Norderstedt, Germany) as described in the AutoAnalyser application methods G-172-96 and G-297-03, respectively. The chemical analyses were performed by the laboratory engineer Berit Kaasa.

Data analysis

The mean value of the algal counts from the six technical replicates was used as an estimate for the algal densities, whereas the data from the six technical replicates were combined to produce summary statistics of the distribution of cell or cell aggregate sizes.

Relationships between algal and rotifer density at different time lags were investigated by computing cross-correlation functions (Venables & Ripley 2002). The rotifer counts were also used to make estimates of the rotifer maximum per capita recruitment and the rotifer conversion factor. These analyses were only performed on the results from the high nutrient cultures due to low densities and eventual extinction of the rotifers in the low nutrient ones. All analyses and plotting were done using R (R Core Team 2015).

RESULTS

Experimental conditions

The measured dilution rates of the eight continuous cultures were close 0.3 /day throughout the experimental period. However, the measurements suggest that the dilution rate differed slightly between the cultures and also that the rate decreased slightly during the course of the experiment. Details of these results are presented in Appendix I together with the results for temperature and pH measurements. The cultures' temperatures were stable around 18.5 °C and the pH were relatively low ranging between 6.7 – 7.3 in the low nutrient cultures and between 6.9 – 8.0 in the high nutrient cultures.

Population dynamics

Contrasting population dynamics was observed in the two sets of rotifer-algal systems (Figure 2.8 and 2.9). In the low nutrient systems (Figure 2.8), the algal population reached a peak density of about 60 000 cells/ml at day 6 followed by a peak in rotifer densities 6-10 days later. After the peak in rotifers, the concentration of rotifers and algae dropped and very few organisms were detected in the following two weeks. At day 42, I increased the nutrient concentration of the supplied medium from 50 to 150 µmol nitrate/l and from 1.66 to 5 µmol phosphate/l. The first algae were detected again 5 days after the nutrient increase in L1, and

then consecutively for the other replicates: after 7 days in L2, 9 days in L3 and 11 days in L4. However, the rotifer population had gone extinct in all but one of the replicates (culture L2). The results for the nutrient dynamics of the systems are presented in Appendix J. Initially the nitrate and phosphate concentrations drop as the concentration of algae increases. During the two weeks' time when the concentration of organisms was very low, the nitrate concentration stabilized at 50 µmol/l (the concentration of the supplied medium), while the phosphate levels were low.

The model expectation for the low nutrient systems was that they would develop into a stable equilibrium with both organisms present. A comparison between the predicted and observed population dynamics is presented in Appendix K. In addition to the obvious contrasting steady states of the expected and observed systems (viable populations vs. extinction), the predicted maximum algal density was more than three times higher than the observed and the predicted rotifer maximum density was more than five times higher.

The population development in the high nutrient systems showed strong fluctuations, with algal densities ranging between 0 to over 2 000 000 cells/ml and rotifer densities ranging between 0 to 20 females/ml (Figure 2.9). Initially, the population development was almost identical between the four replicates; at day 8 the algal populations had reached a peak

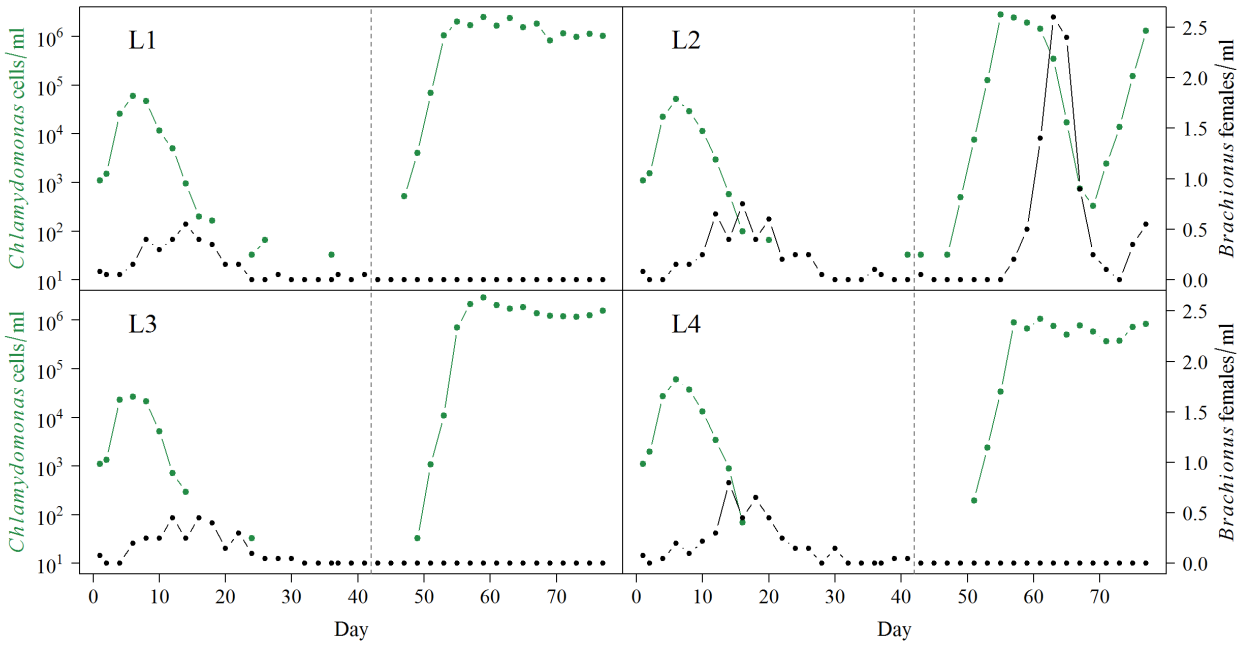

Figure 2.8. Population dynamics in the four low nutrient systems. The green curves represent the algal population densities and black curves represent the density of live rotifer females. At day 42 (vertical line), the nitrate concentration of the supplied medium was increased from 50 to 150 µmol/l.

concentration of about 1 000 000 cells/ml and the peak in rotifers (< 5 females/ml) followed 4 to 6 days later in the four systems. However, the subsequent population development varied considerably between the four replicates. In two of the systems (M1 and M4), the population fluctuations were relatively small and irregular, whereas for the two other systems (M2 and M3) the fluctuations were large and regular. Nevertheless, also the regular fluctuations differed between the M2 and M3 systems. In M2, algal fluctuations started to dampen at around day 40 while the peaks in rotifer abundance started to increase at the same time. A similar dampening of the algal fluctuations occurred in M3 at about day 60. Interestingly in M1, after approximately 20 days of irregular and small population fluctuations, the populations started to oscillate in a fashion that resembles the dynamics of the M2 and M3 cultures.

The results for the nutrient dynamics in the high nutrient systems are presented in Appendix J. In these systems, there is an evident positive correlation between the dissolved macronutrient concentrations and also an evident negative correlation between algal densities and nutrient levels. The dissolved total nitrogen levels were never below 50 µmol/l, while the minimum levels of dissolved phosphate (orthophosphate) were below the detection limit. The measurements of total nitrogen represent the total amount of nitrogen species dissolved in the medium (i.e. not in the organisms) and would include nitrate, ammonium and dissolved

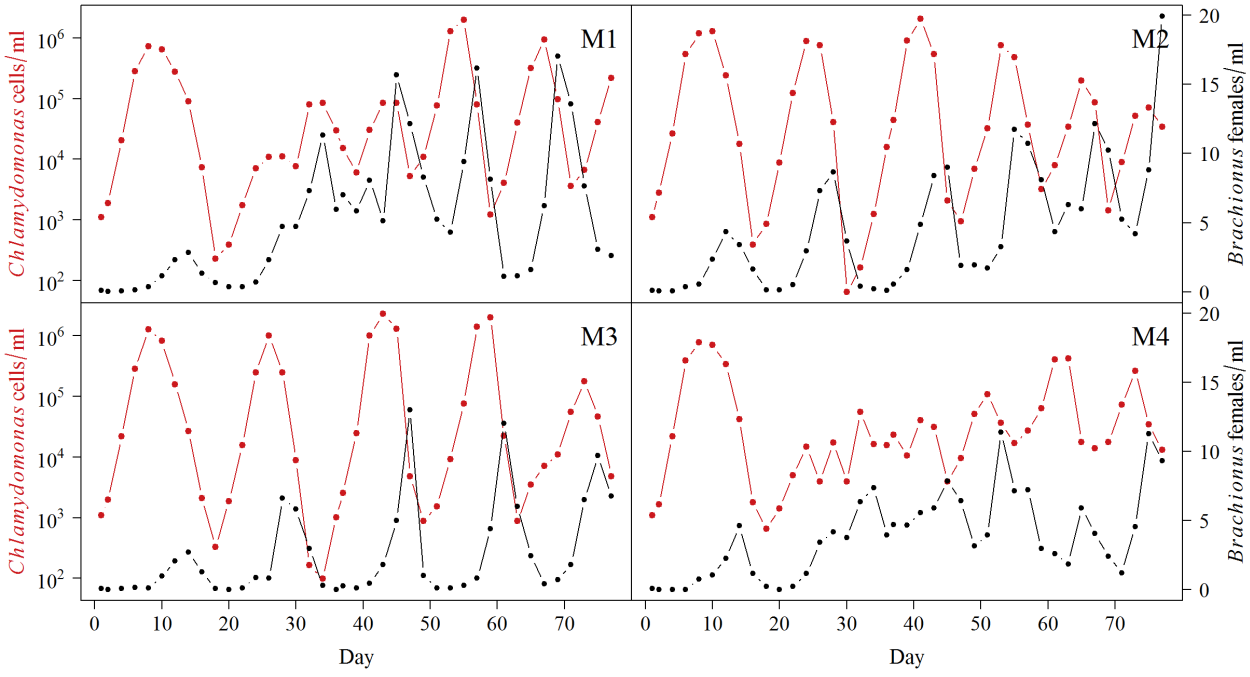

Figure 2.9. Population dynamics in the four high nutrient systems. The red curves represent the algal population densities and black curves represent the density of live rotifer females.

organic nitrogen such as free amino acids and other macromolecules. For the first 41 days, the nitrate levels were measured to be consistently lower than the level of total nitrogen, whereas the levels were closer for the remaining days.

The mathematical model predicted large and persisting population cycles for the high nutrient system. Although two of the experimental systems did show stable cycles, there are considerable discrepancies between the prediction and the observations (see Appendix K). For the direct comparison of the predicted and experimental results, I chose the model with a defended algal clone with a low degree of defense (p_1=0.9) because this model seemed to have the closest fit to the observations. The comparison shows that the predicted cycle period is much longer than the observed (25 days vs. about 17 days) and that the observed maximum rotifer density is three times lower than predicted. The initial peaks in algal abundances were close to the prediction, whereas for some of the subsequent peaks the algal abundances were almost two times higher than the predicted maximum density. For the nitrogen dynamics,

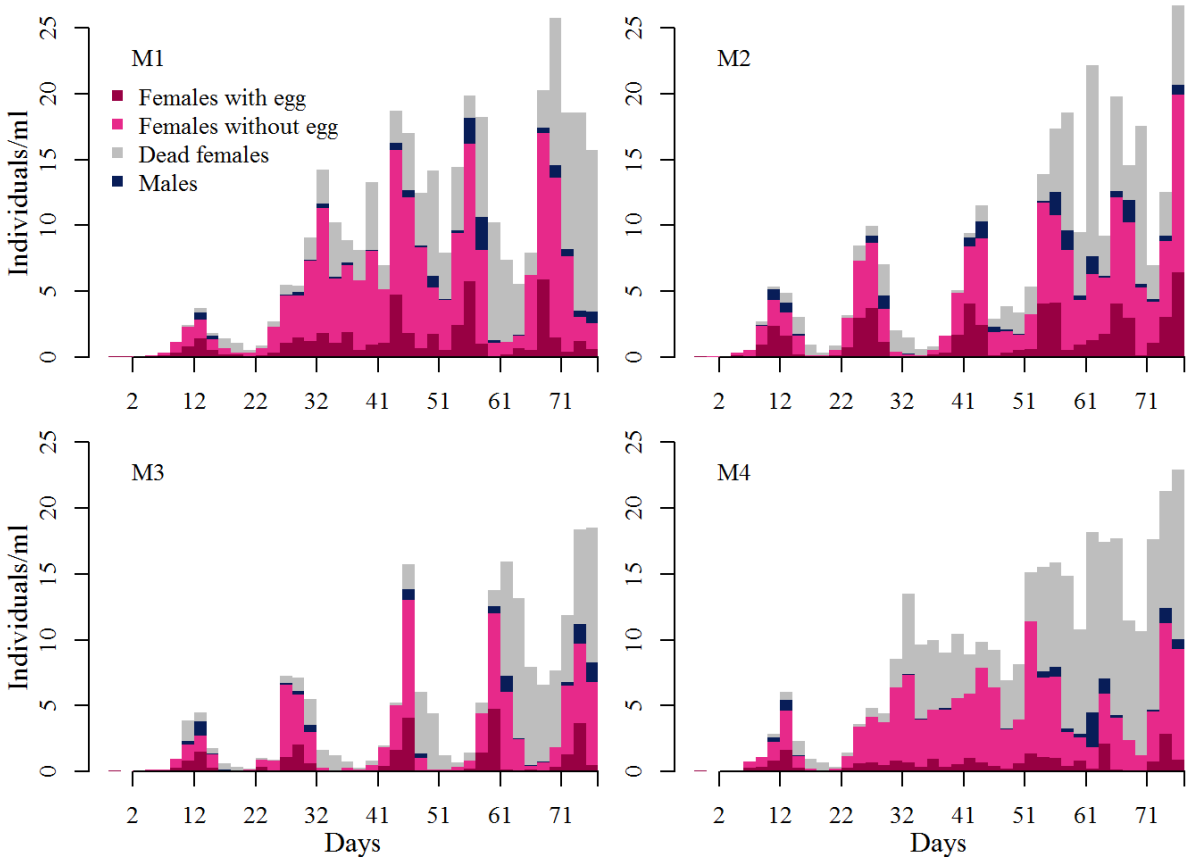

Figure 2.10. The stacked bars plots present the demographic structure of the rotifer population in the four high nutrient systems. The dark pink bars represent the counts of females with egg (per ml), the brighter pink bars represent females without eggs, the dark blue bars represent males and the grey bars represent dead females.

there is a clear discrepancy in the minimum levels; the model predicts total depletion of nitrogen sources when the algal densities are high, whereas the measurement of total dissolved nitrogen in the cultures did not drop below 50 µmol/l.

Rotifer demography

Only counts of live females were included in the plots depicting the rotifer-algal dynamics (Figure 2.8 and 2.9). Details of the rotifer population structure in the high nutrient cultures are presented in Figure 2.10. Male rotifers were observed regularly in all four cultures but in relatively low numbers compared to females. No males were observed in the low nutrient cultures (except for the L2 culture after the nutrient level was increased). The density of females is significantly correlated with the densities of males two days later and at the same time point (lag 0). Figure 2.11 shows the same data as the stacked bar plot before (Figure 2.10), only now the four categories of the rotifer population are presented as fractions of the total population size. The plots depict a strong correlation between algal density and fractions

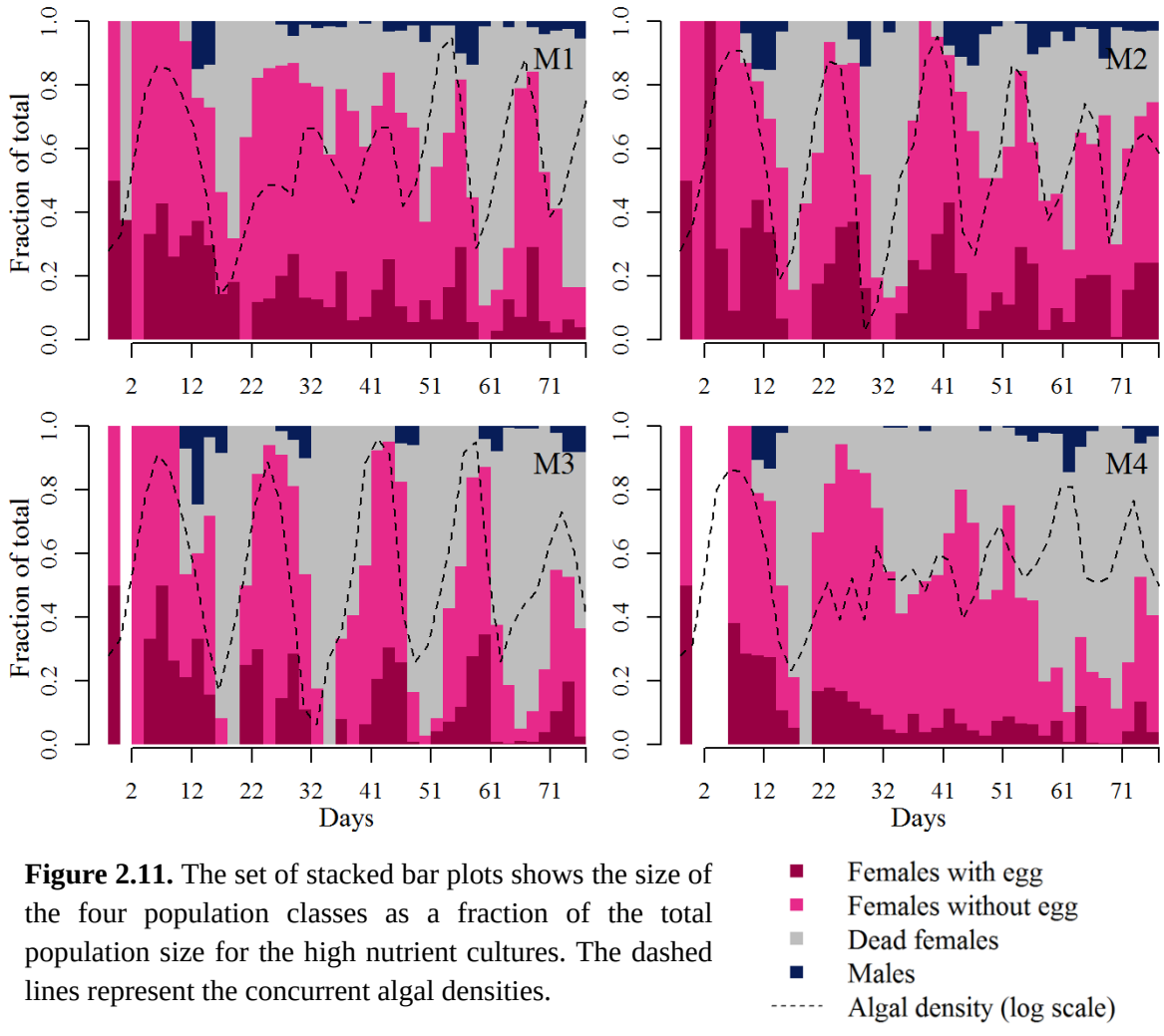

Figure 2.11. The set of stacked bar plots shows the size of the four population classes as a fraction of the total population size for the high nutrient cultures. The dashed lines represent the concurrent algal densities.

of dead and live females. Correlation analysis affirms that there is a strong negative correlation between algal abundance and the fraction of dead females two days later (Appendix L).

Analysis of the rotifer growth in the M2 and M3 high nutrient cultures gave an estimate for the net specific growth rate that equals 0.81 /day (Appendix M). This value for the rotifer recruitment would equal to $e^{0.81} = 2.24$ if converted to the growth factor used in discrete time models. The slope of the observed relationship between algal densities and densities of rotifers two days later suggests that the rotifer conversion factor is 202 rotifers/ 10^6 *Chlamydomonas* cells (Appendix M).

Emergence of palmelloids

Palmelloids of *C. reinhardtii* emerged in all of the four high nutrient cultures. However, the time of emergence and the degree of presence differed between the replicates. The first unmistakable observation of palmelloids was in culture M2 at day 37, and from that day the presence of palmelloids persisted, and increased, until the termination of the experiment. In the other cultures some signs of palmelloids were observed at day 51 in M1, day 59 in M3 and day 61 in M4, while a strong presence was observed from day 63 and onwards in M1 and from day 67 in M3. Some scan images from the iCys instrument that depict the size distribution of the algal populations are presented in Appendix N. When the presence of palmelloids was high in the cultures, wall growth was observed in addition to a substantial sedimentation of algae at the bottom of the culture flask. Photos of this are also included in Appendix N.

Palmelloids were not observed in the low nutrient cultures. A summary statistic of the distribution of cell or cell aggregate size in each culture during the entire experimental period (77 days) is listed in Table 2.1. The coefficient of variation in size is consistently lower for the low nutrient cultures than for the high nutrient cultures, and thus confirms that the emergence of palmelloids in the high nutrient cultures increased the variation in cell sizes.

Table 2.1. Coefficient of variation (σ/μ) for the size distribution of cells or cell aggregates.

Culture	CV*
L1	0.86
L2	0.70
L3	0.80
L4	0.65
M1	1.15
M2	1.50
M3	1.08
M4	1.37

*the five largest observations in each group were left out of the calculation.

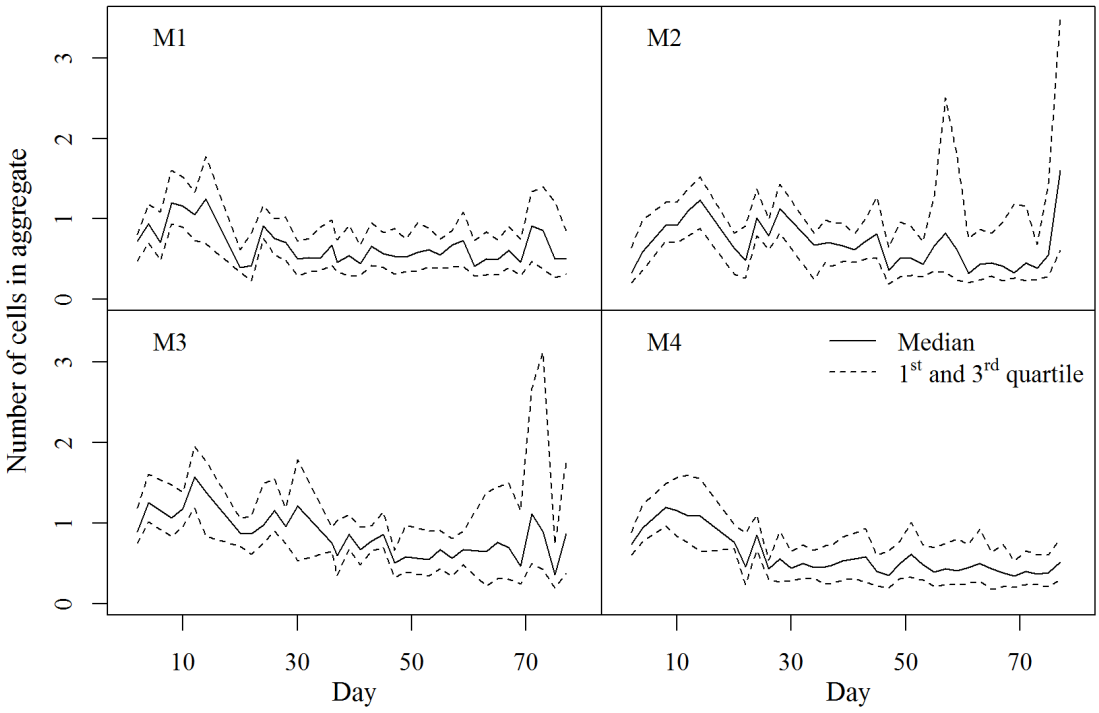

Figure 2.12. Median and interquartile ranges of the algal aggregate sizes in the high nutrient cultures. The cell sizes are estimated from detected fluorescence of chlorophyll *a* and scaled relative to the average size of single cells during the first 14 days of the experiment.

The iCys imaging cytometer estimates the size of each detected cell by calculating the area (µm^2) from which it receives a signal of fluorescence. The raw data for the distribution of cell sizes for all cultures during the course of time are shown in Appendix O, while Figure 2.12 shows a condensed summary of the distribution of cell sizes in the high nutrient cultures. In this figure, the cell sizes are scaled to the average size of the cells during the first 14 days of the experiment (the algal populations consisted only of single cells during this time), and the scaled algal sizes thus give an estimate of the number of cells in palmelloids when they were detected. Assuming a circular shape of the cells, the average diameter of single cells during the first 14 days was measured to 16 µm (Appendix O). After the first 14 days, the estimated median cell sizes seem to decrease in all four cultures, whereas the third quartile show a marked increase in culture M2 at day 57 and 77, and in culture M3 at day 71 and 73. The largest values for the third quartile in M2 and M3 are estimated to represent palmelloids that consist of three cells.

DISCUSSION

Observed population dynamics

The two sets of rotifer-algal microcosms generated contrasting population dynamics as expected, however the dynamics differed from the model predictions. First, the low nutrient systems did not support a stable equilibrium with viable predator and prey populations. Instead both populations seemed to have gone extinct after the initial peaks in population numbers. For more than two weeks after the drop in rotifer densities, no algae were observed in the low nutrient cultures. This was quite puzzling as one would expect that the algal population would increase as soon as the nutrient levels increased and the grazing pressure was released.

The results from the nutrient analysis seem to indicate that the low nutrient systems were phosphate limited although the picture is not clear. In all four cultures, the phosphate levels dropped to zero in parallel with the increase in algal numbers, and for three of the cultures the phosphate levels remained low despite the seemingly absence of algae. Since the algal numbers increased after the nutrient levels were raised at day 42, the algae had not gone extinct. Thus, the initial nutrient level was sufficient to sustain a (small) population of algae, but not to let it increase in numbers. It could be that a substantial amount of heterotrophic bacteria emerged with the decay of algae and rotifers and that these bacteria in some way drained the medium for phosphate and hence impeded algal growth.

The population development in the high nutrient cultures was closer to the expectation, displaying large population fluctuations as predicted by the model. Nevertheless, after an almost identical initial population development, the four systems diverged considerably. Two systems developed into a state of large and regular population fluctuations, whereas in the other two the fluctuations were smaller and more irregular. The cause for this divergence is disputable. It could have been caused by some external factor, although the monitoring of the dilution rate, temperature and pH does not give any indications of variation in these variables that can explain the divergence. However, the differing time points of the rise in algal numbers in the low nutrient cultures (5, 7, 9 and 11 days after the increase in nutrient levels) match the slightly differing dilution rates that were measured for these systems. The diverging population dynamics in the high nutrient cultures could also suggest that there is an inherent instability or chaotic element in the system that makes it sensitive to stochastic variation in the population development of predator and prey.

Another expectation for the experimental system was that *C. reinhardtii* would form palmelloids in presence of rotifers and that this would have a stabilizing effect on the rotifer-algal dynamics. Differential palmella formation could potentially have been a factor explaining the diverging population dynamics in the four high nutrient systems. However, palmelloids of *C. reinhardtii* were not observed in the high nutrient cultures at this early stage of the population development, making it unlikely that this factor played a role in the divergence of the systems. Although the observations seem to rule out an effect of palmella formation during the early stage of the population development, the results strongly indicate that formation of palmelloids had a substantial effect on the dynamics when it occurred at a later stage. In the two systems that displayed large and regular population oscillations (M2 and M3), a considerable dampening of the algal cycle co-occurred with the emergence of palmelloids; there was a strong presence of palmelloids from day 37 and onwards in the M2 culture and an apparent cycle dampening from day 40, and likewise, a strong presence of palmelloids were observed in M3 from day 63 and cycle dampening from day 60.

Worth addressing in this context is the accuracy of the algal counts in times of high palmella formation. Since the iCys imaging cytometer cannot distinguish cells packed closely together, a palmelloid consisting of four cells would be recorded as a single object. Thus the size of the algal population would be underestimated when there is a high frequency of palmelloids. I had the possibility to account for this inaccuracy by adjusting the cell counts against the recorded cell sizes obtained by the iCys instrument. However, I considered that this likely would not be decisive for the interpretation of the results since the cycle dampening was not only manifested in decreasing values of the peak algal densities, but also in increasing values for the minimum population densities. Two arguably more important factors associated with the formation of palmelloids were the increasing algal wall growth and sedimentation. This increased the spatial heterogeneity of the system and also most likely decreased the algal washout loss rate (mortality caused by dilution) significantly.

The nearly complete clearance of algae that was observed initially in the M2 and M3 cultures during peak rotifer densities seems to have been impeded in subsequent peaks by the emergence of palmelloids. The compelling question here is *what* it was that hindered the rotifers from grazing down the algal population. Becks *et al.* (2010) claim that *B. calyciflorus* are more able to ingest single cells and small clusters (< about eight cells) and thus argue that the degree of grazer resistance is associated with the size of the clusters. That size is a determinant for prey vulnerability to predation is widely recognized as many predators are

restricted by a limited gape size. However, whether the palmelloids were sufficiently large to impede rotifer grazing is questionable. In contrast to many other zooplankton, rotifers are found to not be inhibited by filamentous cyanobacteria (Walz 1995). Although the cause for this is likely manifold, one factor could be that rotifers feeding apparatus make them capable of feeding on food particles that are larger than their gape size. One study reports that *B. calyciflorus* is observed "nibbling" at the ends of filamentous cyanobacteria (Dumont 1977 in Walz 1995). Nevertheless, clearance rates in rotifers are found to be affected by particle size. A study of three species of *Brachionus,* including *B. calyciflorus*, demonstrated that the optimal spectrum for food size was 12 µm or smaller depending on the size of the rotifer (Rothhaupt 1990a). *B. calyciflorus* had the highest clearance rate for the largest particle size (12 µm) tested in Rothhaupt's study.

The results from the iCys imaging cytometer convey that the average diameter of single celled *C. reinhardtii* ranged between 12-16 µm, which is considerably larger than what was recorded for *C. reinhardtii* in the algal growth experiment (part 1.2) using a particle counter (CASY). According to the results from the algal growth experiment, the diameter of single celled *C. reinhardtii* range between 4-8 µm depending on the phase of growth. The size estimate from the particle counter is unquestionably the most accurate and also in accordance with estimates presented in publications (e.g. Rothhaupt 1990b; Oldenhof *et al.* 2007). The size estimates from the iCys cytometer are probably inflated because the fluorescence halo surrounding the cells is included in the size estimates.

However, on a relative scale, the results from the iCys cytometer provide information about the size distribution of the algal population. Figure 2.12 depicts that despite of an observed strong presence of palmelloids in the M2 and M3 cultures, 50 per cent of the detected algae are through all times single cells. Also the third quartiles do for the most time stay within the range of a single cell, with a few marked exceptions where the third quartile corresponds to a particle size of about three single cells. So although the scan images from iCys depict a strong presence of palmelloids in M2 and M3 at several time points, the algal populations seems to have been dominated by single cells.

With this in mind, it does not seem very likely that the rotifers were impeded from efficient grazing solely because the algal population were protected by larger particle size. If the palmelloids were protected by their increased size, one would expect that the algal size distribution would have shifted more strongly to larger particle sizes. Additionally, one would expect to see signs of reduced rotifer recruitment if the palatability of the algal population

decreased. There seems to be no signs of this, but rather the contrary in the M2 culture (the peak in rotifer abundance seemed to increase). Another possibility is that the changed phenotype of the palmelloid algae changed the encounter rates between the predator and prey. A significant wall growth and sedimentation of algae was observed in parallel with the emergence of palmelloids in the M2 and M3 cultures. This altered spatial distribution of the algae could have served as a refuge both from predators and from the continuous washout caused by the dilution process. Following this reasoning, algae occupying the more protected areas in the microcosm could have contributed to the dampening of the algal cycle by enhancing the algal recovery rate between periods of high rotifer grazing.

Comparison between predicted and observed dynamics

The foundation and starting point for this study of rotifer-algal dynamics is the *Chlamydomonas – Brachionus* model developed by Becks and colleagues (2010). Despite the model's apparent sensitivity to the algal palatability parameter, the preconception was that this relatively complex model would adequately describe the relatively simple experimental system of predator and prey. However, the discrepancies between the model and observations were substantial. The observed cycle period is considerably shorter and the maximum rotifer densities much lower than the model predicts. Moreover, the observed dynamics differs markedly from the experimental results of Becks *et al.* (2010) who observed a rapid cycle dampening or antiphase eco-evolutionary dynamics depending on the grazer history of the algal population (Figure 2.7). The oscillations in the M2 and M3 systems show a closer fit to classical consumer-resource cycles with the peak in predators lagging the peak of prey by a quarter of a cycle period.

There are likely several factors that contribute to the lack of fit between the model and my observations. The algal populations in my experimental systems seemed to have been limited by phosphate, while nitrate was the limiting nutrient in the model as well as the experimental systems of Becks *et al.* (2010). However, it seems improbable that this alone could account for the observed discrepancies. Boraas (1980) reports that in his *Chlorella – Brachionus* system the observed oscillations had a shorter period than predicted by the model and further that a shortening of the cycle period could be achieved by including internal cycling of ammonia in the model. Although the concentrations of both total nitrogen and nitrate were measured in my rotifer-algal systems, the seemingly inaccurate nitrate measurements (Appendix J) make it unsuitable to draw any conclusions from these data about Boraas' proposed effects of internal nitrogen cycling.

The comparison of the dynamics in the high nutrient cultures and the predictions of the *Chlamydomonas – Brachionus* model (Appendix K) depicts that the model performs worst in describing the development of the rotifer population. The initial development of algae shows an almost perfect fit to the model, but the rotifer population reaches its peak densities and graze down the algal population much earlier than the model predicts. Also the maximum rotifer densities are several orders of magnitude lower than the prediction. Hence, it seems evident that the discrepancy between model and observations is due to some critical factor involving the description of the rotifer growth that is not described correctly in the model.

Rotifers depend on higher food concentrations for survival than other zooplankton, e.g. cladocerans, because most rotifers have a limited ability to make energy reserves and because rotifers use a disproportionate amount of energy on locomotion compared to other zooplankton (Epp & Lewis 1984; Walz 1995). The experimental results indicate that rotifer mortality is strongly correlated with food abundance, whereas the model defines the mortality rate to be constant. An associated factor to food concentration is the food quality, which also is known to have a significant effect on rotifer growth (Walz 1995; Hessen *et al.* 2007). The quality of the prey in the oscillating rotifer-algal systems is likely to change with the biomass-specific nutrient availability for the algae. However, the results from the nutrient analyses seem to indicate that the nitrate sources were never fully depleted in the systems and that the phosphate sources was only depleted for a short period of time when the algal density was at its maximum (Appendix J). This could imply that the nutrient content of *C. reinhardtii* did not change substantially during the population cycles.

Another aspect of the rotifer growth in the *Chlamydomonas – Brachionus* model that does not seem to fit my results is the reproductive period. Becks *et al.* (2010) set the senescence rate to 0.4 /day, which corresponds to an average reproductive period of 1 / 0.4 = 2.5 days, while there are reports of *B. calyciflorus* breeding for more than 9 days (Kauler & Enesco 2011). However, the 9-day reproductive period of *B. calyciflorus* were observed for individuals that were kept at 16°C, whereas the period was substantially shorter for individuals that were reared at higher temperatures (about 5 days at 22°C and 3 days at 29°C) (Kauler & Enesco 2011). The rotifer-algal cultures in the study of Becks *et al.* (2010) were kept at 25°C and the short reproductive period is thus not unlikely for their system. But since my cultures held an average temperature of 18.5°C, the rotifers probably reproduced at ages beyond 2.5 days.

The maximum per capita rotifer recruitment in the *Chlamydomonas – Brachionus* model by Becks *et al.* (2010) was set to 1.9 /day. This is in stark contrast to the results from my experiment where the maximum net specific growth rate was estimated to 0.81 /day. A study comparing the growth rates of *B. calyciflorus* fed different algal species (at 20°C) reports of maximum growth rates ranging between 0.42 – 1.02 /day depending on the algal quality and particle size (Rothhaupt 1990b). Since rotifer growth is shown to be strongly dependent on the temperature conditions (Ma *et al.* 2010; Kauler & Enesco 2011), it could have been plausible that the high growth estimate of Becks *et al.* (2010) is explained by the higher temperatures of their system. However, a later study at the Hairston lab (Felpeto & Hairston 2013) that investigated the growth of *B. calyciflorus* fed *C. reinhardtii* of varying food quality, but otherwise under equal culture conditions as in Becks *et al.* (2010), reports of significantly lower growth rates than 1.9 /day. In this study, Hairston & Felpeto found that the maximum growth *factor* for *B. calyciflorus* was 3.31 when fed nutrient sufficient algae, 1.97 for nitrogen limited and 1.57 for phosphorus limited *C. reinhardtii*. Converting these values to the estimate for the maximum per capita recruitment (intrinsic rate of increase), will yield the values 1.20 /day, 0.68 /day and 0.45 /day, respectively. Hence, it might seem like Becks *et al.* (2010) used the growth factor instead of the intrinsic rate of increase in their *Chlamydomonas – Brachionus* population model.

Sexual reproduction in *B. calyciflorus* is found to be induced at population densities of about four females/ml by a density dependent chemical cue released by the females (Gilbert 2003; Stelzer & Snell 2003). However, the ability to reproduce sexually has been found to be permanently lost in many strains of *B. calyciflorus* (Stelzer *et al.* 2010), including the strain used in the rotifer studies at the Hairston lab (Fussmann *et al.* 2003). Recent investigations have revealed that the transition to obligate asexual reproduction in *B. calyciflorus* is controlled by a single locus, where obligate parthenogens are homozygous for a recessive allele (Stelzer *et al.* 2010). The obligate parthenogens are also found to be about half the size of the wild type clones (Stelzer *et al.* 2010). This could be of significance for the observed discrepancies between the rotifer growth described in the population model by Becks *et al.* (2010) and the rotifer growth in my experiments where male rotifers were observed in all high nutrient cultures at female densities down to about two individuals per ml.

In retrospect it is obvious that there would not be a close fit between the model predictions and my experimental results. The comparisons have clearly demonstrated several aspects of the *Chlamydomonas – Brachionus* model by Becks *et al.* (2010) that are ill-defined

for my rotifer-algal system. The last aspect of this specific predator-prey system that I will review is the mechanism for palmella formation in *C. reinhardtii.*

Formation of palmelloids in *C. reinhardtii*

The formation of palmelloids in *C. reinhardtii* has been described as both a fixed genetic trait that arise due to strong selection pressure (Becks *et al.* 2010; Ratcliff *et al.* 2013) and as an character that is induced by a range of environmental factors (Iwasa & Murakami 1968; 1969; Olsen *et al.* 1983; Lürling & Beekman 2006; Fischer *et al.* 2014). In my experiment, palmelloids were observed in all high nutrient algal-rotifer systems, while they were absent from the cultures receiving a low nutrient supply. Since it is assumed that palmelloids have higher fitness in high nutrient environments, because of a lower surface to volume ratios and decreased efficiency of nutrient uptake through the gelatinous extracellular matrix, there was an expectation that there would be a higher degree of palmella formation in the high nutrient system. However, due to the extinction of the predator in all but one of the low nutrient systems, it cannot be resolved whether the absence of palmelloids in these cultures was caused by low nutrient availability or low predator densities.

The first unmistakeable observation of palmelloids in my systems was in culture M2 at day 37, while they appeared two-three weeks later in the other cultures. This timing of palmelloid emergence is markedly different from the results of Becks *et al.* (2010) who report of increased mean algal clump size around day 10 for all six cultures that were inoculated with ungrazed unicelled *C. reinhardtii* (recall Figure 2.7, but the timing of the first emergence of palmelloids is more clear in the other replicates in the study). Becks *et al.* (2010) argue that palmella formation is an evolved heritable trait because independent experiments had shown that previously grazed *C. reinhardtii* continues to form palmelloids for more than nine generations in absence of rotifers. An aspect of the palmella formation which they do not express explicitly, however, is that if the trait purely is based on genetic differences, this would imply that the transition to a palmelloids state evolved independently, and at a rapid and similar pace, in all six rotifer-algal cultures that were inoculated with unicelled algae.

If the emergence of palmelloids is an evolved heritable trait, it would entail that the transition was caused by random mutations. It is maybe not be unreasonable to believe that there would emerge individuals that carry a beneficial mutation in a microcosm that at the most inhabits an algal population of more than half a million individuals/ml. But it does not seem very likely that it would occur in parallel in several separate systems. Moreover, estimates of the mutation rate in *C. reinhardtii* indicate that it is among the lowest recorded

for eukaryotes (Ness *et al.* 2012). However, the strongest argument against that the palmelloid state in *C. reinhardtii* is an evolved heritable trait is all the instances were palmelloids are shown to be induced.

Lürling & Beekman (2006) argue that palmelloids in *C. reinhardtii* is an induced character they exhibit to prevent grazing. In their study they observed a substantial increase in multi-celled algae after one day of culturing with *B. calyciflorus.* Yet, a crucial aspect of their experiment is that their control populations of *C. reinhardtii*, cultured in the absence of rotifers, also included a substantial amount of multi-celled algae (about 35%). Thus, in their system palmelloids do not occur solely in the presence of rotifers, but increase in proportions. One can argue that a similar increase in proportions could be caused by selective grazing by the rotifers and not primarily by an induction of increased palmella formation. Lürling & Beekman (2006) consider this possibility, but argue that the growth rate of *C. reinhardtii* is too high and the rotifer grazing rate too low for it to be a likely explanation.

The timing of the emergence of multi-celled *C. reinhardtii* differs markedly between the results of Lürling & Beekman (2006), Becks *et al.* (2010) and my experiment. The first observes multi-celled algae at the onset of the experiment, the other after approximately 10 days and I observed the first multi-celled algae at day 37. Significant variation in induction of colony formation has been demonstrated among strains of the green algae *Scenedesmus obliquus* in response to *B. calyciflorus* (Verschoor *et al.* 2004a), and recently a study has shown a similar variation in palmella formation for *C. reinhardtii* (Fischer *et al.* 2014). The ambition of Fischer *et al.* (2014) was to investigate how strains of *C. reinhardtii* with different propensity for palmella formation and different growth rates would respond to the presence of *B. calyciflorus* by comparing gene expression. Their results show that the gene expression differed strongly between the strains in absence of rotifers and also that the presence of rotifers induced changes, both in morphology and gene expression, which varied among the algal strains. Collectively, these results indicate that the propensity to form palmelloids is a variable character among strains of *C. reinhardtii*, i.e. there is an aspect of heritability in the induced response.

Several studies have demonstrated the co-occurrence of palmelloids in *C. reinhardtii* and the grazer *B. calyciflorus,* and the changed morphology of the algae has thus been interpreted as a trait for predator defence. But *C. reinhardtii* is found to form palmelloids under other conditions as well. Olsen *et al.* (1983) observed palmelloids after three days in their continuous cultures of *C. reinhardtii* with high dilution rates (> 0.16 / hour), while it was

absent in the cultures with lower dilution rates. Earlier, Iwasa & Murakami (1968; 1969) had found that certain organic acids induce palmelloids in *C. reinhardtii* and also that calcium deficiency seems to hinder dissociation of the palmelloids. Interestingly, what Iwasa & Murakami (1969) observed was that palmelloids were induced in medium deficient in calcium or medium that contained EDTA (chelating agent) equivalent to the calcium concentrations. Further they report that since phosphate combines with calcium, excess phosphate had the same effect on *C. reinhardtii* as calcium deficiency. This raises the question whether calcium deficiency could have played a role in the formation of palmelloids in the rotifer-algal systems. The medium used by Becks *et al.* (2010) seems to have had low concentrations of calcium compared to phosphate (15 vs. likely 200 µmol/l), whereas the medium used in my experiment likely had high concentrations of calcium relative to the low concentrations of phosphate (the lake water is high in calcium).

Although there is ample evidence that palmelloids of *C. reinhardtii* increases when cultured together with *B. calyciflorus*, the causal factor for the response is not resolved. It is established that chemical cues from herbivore zooplankton can induce defences in phytoplankton, but the exact mechanism and correlated factors have seldom been investigated (Van Donk *et al.* 2010). In the case of palmella formation in *C. reinhardtii*, Iwasa & Murakami (1968) states that "it is well known that in an aged culture of *Chlamydomonas* (Volvocales), there are bodies which consist of four to sixteen cells" (p. 1224). Recall also that multi-celled bodies in powers of 2^n have been investigated in *C. reinhardtii* as a result of altered cell cycle progression associated with variable light and temperature conditions (introduction in part 1.2). Thus, multi-celled individuals are described as a common feature of *C. reinhardtii*, which adds to the complex picture of the diverse set of factors that is associated with the formation of cell clusters in this species.

Upon the survey of the specific *Chlamydomonas – Brachionus* predator-prey system, one is inclined to reflect on whether "these facts and ideas derived from a study of our aquatic microcosm [have] any general application to a higher plane" (Forbes 1887, p. 87). Stephen A. Forbes addressed this question in his renowned article *The Lake as a Microcosm,* and I will next consider whether the facts and ideas derived from the study of my aquatic microcosm can add to the understanding of ecological and evolutionary processes.

SYNTHESIS

Oscillating natural populations

The underlying motive for studying oscillating population dynamics under controlled laboratory conditions is to reveal why natural populations can display such a striking numerical variability (McCauley & Murdoch 1987). The growth and decline of populations is arguably a major factor in governing the diversity of life as it is the fundamental outcome of the struggle for existence (Darwin 1859). Several natural systems are renowned for their regular fluctuations, such as the oscillations of the Canadian lynx and snowshoe hare or those of voles and lemmings (Bjørnstad & Grenfell 2001). Moreover, other systems are renowned for their fluctuations that are associated with seasonal events, such as the spring bloom in aquatic systems (McCauley & Murdoch 1987). These examples illustrate a fundamental question in the studies of population fluctuations, namely the relative importance of abiotic vs. biotic control of natural populations.

In aquatic systems, the greatest source of variation in population numbers is usually associated with changes in temperature and nutrient availability which follow seasonal forcings (McCauley & Murdoch 1987). However, internally generated oscillations in phytoplankton and zooplankton communities have also been found to be common. McCauley & Murdoch (1987) analysed a large set of studies that addressed the seasonal dynamics between *Daphnia* and algal abundances in freshwater lakes, and their findings indicated that *Daphnia* and algal populations display cycles that seems to be internally driven (i.e. fluctuations not associated with seasonal forcings). These observations, among others, provides support for the appropriateness to use simple consumer-resource theory as a starting point to investigate population dynamics in the field (McCauley *et al.* 1999).

The fundamental cause for oscillating predator-prey cycles in laboratory systems is well understood. In addition to the extensive literature on rotifer-algal predator-prey dynamics, there are also comprehensive reports of experimental studies with daphnids as predators (see McCauley & Murdoch 1990; McCauley *et al.* 1999; McCauley *et al.* 2008). As predicted by simple predator-prey models, these aquatic experimental studies have demonstrated that the oscillating population dynamics is caused by the depression of predator growth due to their exhaustion of food sources. However, the studies have also demonstrated a substantial variability in the dynamics between predator and prey. In my high nutrient systems, two of the replicate systems showed regular large-amplitude fluctuations while the

other two showed fluctuations that were irregular and with small amplitudes. McCauley *et al.* (1999) report of similar results in their daphnid-algal system and suggest that it is an indication of coexisting attractors.

Although simple consumer-resource theory can serve as an explanation to why some natural population fluctuates, results from zooplankton-algal dynamics in laboratory systems have shown that the mechanisms that structure even simple predator-prey interactions are not clear-cut. Only within the *Chlamydomonas-Brachionus* system, the dynamics are reported to be influenced by both evolutionary and plastic responses to predation (Lürling & Beekman 2006; Becks *et al.* 2010; Fischer *et al.* 2014), and further, studies of similar systems of *Brachionus* and other algal species have demonstrated that the predator-prey dynamics can be significantly influenced by rapid prey evolution (Yoshida *et al.* 2003) and phenotypic plasticity (Verschoor *et al.* 2004b). Using a somewhat different approach, McCauley *et al.* (1999) have demonstrated that the dynamics between a population of *Daphnia* and a community of several algal species is strongly affected by the diversity of algal species. *Daphnia*-algal systems that only contained easily edible algal species displayed large-amplitude cycles in enriched systems, whereas systems that contained a mix of edible and inedible algal species displayed small-amplitude cycles (McCauley *et al.* 1999). The stabilizing effect of inedible species is presumably caused by the intensified competition for resources that would lower of the effective carrying capacity of the edible algae (Scheffer & Boer 1995; McCauley *et al.* 1999).

The common finding for the laboratory studies of zooplankton-algal dynamics appears to be that phenotypic variability in the prey population stabilizes predator-prey dynamics, and also, that this phenotypic variability is associated with the prey's competition for resources and vulnerability to predation. Although the phenotypic variability was associated with different units in the daphnid-algal and the rotifer-algal systems (different algal species vs. different algal clones or induced morphotypes), the stabilizing mechanism is essentially the same. The demonstrations of how different levels of prey variability can stabilize enriched systems are relevant to natural systems because it can indicate the forces that are at play and structure communities in the wild. The extensive study by McCauley & Murdoch (1987) revealed that natural populations of *Daphnia* and algae display internally driven population cycles, however, in contrast to theory, the observed cycles had small amplitudes (Scheffer & Boer 1995; McCauley *et al.* 1999). The presence of inedible algae has been posed as factor that explains the relative stable natural populations of daphnids, which, with an even broader

viewpoint, can be associated with Hutchinsons' (partial) answer to why there are so many animals: "because communities of many diversified organisms are better able to persist than are communities of fewer less diversified organisms" (Hutchinson 1959, p. 150).

Although species diversity is recognized as a factor that enhances stability, there are also posed other factors that can contribute to community stability. One of these factors, which seemed relevant in my predator-prey system, is spatial heterogeneity. Scheffer & Boer (1995) argue that the small amplitude cycles of natural populations of *Daphnia* and algae, like those reported by McCauley & Murdoch (1987), also can be explained by a simple predator-prey model that incorporates spatial structure. In Scheffer & Boer's model, *Daphnia* occupies only a part of the total space, while the algae can diffuse between the compartment where the predator is present and the compartment where it is not. Simulation of this model demonstrated that oscillating predator-prey systems would display smaller cycles when the prey are partially protected from predators by the spatial structure of the system. This finding has not been considered in any of the studies on rotifer-algal dynamics. However, my results from the *Chlamydomonas – Brachionus* experiment seems to indicate that one important reason why the emergence of palmelloids dampened the oscillating population dynamics was that the palmelloid cell clusters occupied areas of the culture flask (walls and floor) which served as refuges from predation (and the continuous dilution process).

Predation as an evolutionary force

The subsistence of natural populations is governed by a range of both abiotic and biotic factors. Predation is regarded as a major biotic factor as most organisms either face the risk of being eaten or not obtaining enough food for survival. The selection pressure for predator avoidance is therefore often considered to be substantial. The rotifer-algal studies from the Hairston lab (Yoshida *et al.* 2003; Yoshida *et al.* 2004; Becks *et al.* 2010) have largely taken this viewpoint when they argue that rapid evolution of the algal phenotype is caused by a strong predation pressure by the rotifer grazer.

Before I continue to discuss the implications of the findings of Hairston and colleagues, it is necessary to clarify some important details of their experimental results. In their first rotifer-algal experiments, they used *Chlorella vulgaris* as the algal prey and found that the *initial* clonal variability in a heritable trait associated with predator defence had a significant effect on the pattern of the predator-prey cycles (recall introduction in part 2.1). Instead of observing typical consumer-resource cycles where the peak in predator lags behind the peak in prey by a quarter of a cycle period, they observed long-period cycles where the

peaks in prey and predator were out of phase (recall Figure 2.1 D). Based on mathematical modelling they argued that the altered antiphase cycles of the *Chlorella-Brachionus* system was caused by the rapid change in the *frequencies* of the different algal clones in the population, and thus, since evolution in its most basic sense can be regarded as the change in allele frequencies from one generation to the next, Hairston and colleagues argue that the results provided evidence for how rapid evolution can alter ecological dynamics (hence the term eco-evolutionary dynamics).

For the next experiments at the Hairston lab, they used *Chlamydomonas reinhardtii* as the algal prey (Becks *et al.* 2010) and argued that the formation of palmelloids was a heritable defensive trait that emerged due to strong predation pressure (recall introduction in part 2.2). Their results demonstrated again that the systems which contained an algal population with an initial clonal variability in the defensive trait showed antiphase eco-evolutionary dynamics (recall Figure 2.7 c and d). However, their systems that were inoculated with an algal population that only consisted of single cells (i.e. no recent history of rotifer presence) also displayed a presence of palmelloids after about 10 days.

This, together with all the other factors that have been shown to induce palmella formation in *C. reinhardtii,* makes it questionable whether the eco-evolutionary dynamics observed in Becks *et al.* (2010) simply was caused by heritable variation in the prey. In this context, I will also point out that there were no signs of antiphase eco-evolutionary dynamics in my high nutrient rotifer-algal system with a considerable presence of palmelloids (recall culture M2 in Figure 2.9). However, this alone does not necessarily disapprove the findings of Becks *et al.* (2010) since the analysis of the *Chlamydomonas-Brachionus* model predicted that classical consumer-resource cycles would occur if the palatability of the defended algal clone was high or, equally, if its defence against predation was low (recall Figure 2.6). Nevertheless, it seems questionable whether the premise for the eco-evolutionary dynamics is true for the *Chlamydomonas-Brachionus* system of Becks and colleagues (2010); the formation of palmelloids is unlikely simply a fixed genetic trait that differs among clones.

The reason why I have focused so much attention on these details is because the results from the rotifer-algal systems has been presented as evidence for the significance of rapid evolution in ecological processes or, more explicitly, that evolution can happen so rapidly that it can alter the trajectory of ecological processes. This finding has received considerable attention because these are processes that conventionally are believed to happen on very different time scales; the finding has, in its broadest sense, implied a convergence of

ecological and evolutionary time (Hairston *et al.* 2005). I do not intend to disprove that rapid evolution can have the potential to alter ecological dynamics, but I inquire whether rapid evolution in algal defensive traits really is a relevant factor for the dynamics in the specific *Chlamydomonas-Brachionus* system as well as in aquatic ecosystems in the wild.

The formation of palmelloids in *C. reinhardtii* has been interpreted to be caused by a strong predation pressure by rotifer grazers. However, it is questioned whether predation in today's aquatic environments would select for multicellular prey since such individuals would be subjected to predation by larger predators and to competition from other multicellular species (Boraas *et al.* 1998). There is a selective advantage of being large if the predator is small, but reversely also a selective advantage of being small if the predator is large (Beardall *et al.* 2009). Moreover, the selective advantages or disadvantages for different algal size is not only associated with vulnerability to grazing, but also associated with important selective factors such as the efficiency of intracellular transport, diffusion rates for nutrients through the boundary layer, and vertical movement in the water column which can be of crucial importance because it influences access to light and nutrients (Beardall *et al.* 2009). Hence, the selective pressure on phytoplankton in today's aquatic environments involves several other important forces apart from predation by small zooplankton grazers. These selective forces often work in opposite directions, which also could imply that phenotypic flexibility could be a favourable trait among phytoplankton.

It has been posed that a major challenge for eco-evolutionary theory is to establish the importance of rapid evolution in natural populations and communities (Fussmann 2010). Studies of rotifer-algal systems have argued that both rapid evolution and induced changes of the prey phenotype can have a stabilizing effect on predator-prey dynamics (Yamamichi *et al.* 2011), but its relevancy in natural systems is not that evident. The interspecies diversity in phenotypes is likely a larger contributing factor to community stability than the phenotypic diversity exhibited within species. Nevertheless, the numerous reports of observed responses in phytoplankton to predator presence (Van Donk *et al.* 2010) indicate that predation has been a strong force in phytoplankton evolution. Several of the major transitions in the evolution of life, e.g. transitions to multicellular life forms, have been associated to the selective forces of predation (Bengtson 2002), which further emphasize its role in the evolution of natural communities.

Phenotypic plasticity as a driver for evolutionary change

Evolution is the heritable change in phenotypes of individuals in biological populations. Commonly are these heritable changes associated with mutations in the DNA sequence (including point mutations, deletion and duplication events), but it has become increasingly recognized that also fixed changes in epigenetic traits can be driven by natural selection (Klironomos *et al.* 2013). Epigenetic modifications and phenotypic plasticity are related mechanisms that can cause changes in the phenotype without changes in the DNA sequence (Schlichting & Wund 2014). The main distinction between the two mechanisms is that phenotypic plasticity is associated with the phenotypic change of an individual, usually mediated by changes in transcription factors, in direct response to external environmental stimuli, while epigenetics is associated with phenotypic changes that are mediated by changes in patterns of DNA methylation and histone modification (Klironomos *et al.* 2013; Schlichting & Wund 2014). Epigenetic modifications are an essential mechanism in cell differentiation and have recently also been recognized as a mode that allows for the phenotype of the mother to affect the phenotype of her offspring, often termed epigenetic inheritance or maternal effects (Räsänen & Kruuk 2007; Jablonka 2013) .

There are several reports of phenotypic plasticity in phytoplankton in response to grazers (Van Donk *et al.* 2010), and phenotypic plasticity in other traits is also found to be common in a wide range of taxa (Price *et al.* 2003). I am not aware of any reports of epigenetic inheritance in phytoplankton, but recent studies indicate that it is widespread among multicellular organisms and also demonstrated for unicellular organisms such as ciliates and the yeast *Saccharomyces cerevisiae* (Räsänen & Kruuk 2007; Jablonka 2013).

Together with the accumulated observations of phenotypic plasticity and epigenetic inheritance, it has been posed several hypotheses for their adaptive value. Klironomos (2013) argue that epigenetic changes are more likely to be beneficial than genetic mutations because they share properties with adaptive phenotypic plasticity, and Räsänen & Kruuk (2007) argue along similar lines that epigenetic inheritance provides one of the strongest cases for adaptive plasticity because it could amplify any response to selection. Moreover, phenotypic plasticity *per se*, i.e. the phenotypic change of an individual in response to external stimuli, has been hypothesised to be favoured in unstable or heterogeneous environments, while genetic variation for a fixed phenotype is favoured in stable environments (Svanbäck *et al.* 2009).

The reports of the morphological variability in *Chlamydomonas reinhardtii* indicate that the phenotype is responsive to external environmental factors and possibly also that the

transition from unicellular flagellates to multicellular palmelloids could be amplified by epigenetic inheritance. Epigenetics could potentially explain the disagreement between the results of Lürling & Beekman (2006), who concluded that palmella formation was an induced response to rotifer presence, and those of Becks *et al.* (2010), who concluded that it was a heritable trait. I would argue that epigenetic inheritance could be an explanation for why Becks *et al.* (2010) observed that *C. reinhardtii* continued to form palmelloids for nine generations in the absence of *B. calyciflorus* and thus concluded that it was a heritable trait.

The increasing recognition of the adaptive effects of phenotypic plasticity and epigenetic inheritance has posed question about their roles in evolutionary processes. On the one hand, these mechanisms can influence the course of genetic evolution by permitting survival in changed environments or by exposing cryptic genetic variation (Price *et al.* 2003; Schlichting & Wund 2014). One the other hand, it has been posed that these mechanisms also can serve as drivers for evolutionary change through the process of genetic accommodation (Price *et al.* 2003; Schlichting & Wund 2014). Genetic accommodation or, equally, genetic assimilation was famously demonstrated experimentally by Waddington (1953; 1959) and is defined as "a process by which phenotypic variants that are initially strictly environmentally induced are selected to become genetically determined (i.e. heritable)" (Schlichting & Wund 2014, p. 657). Direct field-based evidence for the role of genetic accommodation in adaptive evolution is difficult to demonstrate, but it is for instance believed to have played a role in the osmoregulatory adaptation of threespine sticklebacks to freshwater environments (Schlichting & Wund 2014).

As a substitute for direct evidence of genetic accommodation in natural systems, phylogenetic inference is considered to be a valuable tool in addressing the role of phenotypic plasticity as a driving force in evolutionary change (Schlichting & Wund 2014). The idea is that if the patterns of phenotypic plasticity within a species reflect the patterns of phenotypic divergence among the species in its lineage, this could be an indication that phenotypic plasticity drove the evolutionary branching (Schlichting & Wund 2014). With this in mind, I would argue that the palmella formation in *C. reinhardtii* could provide an interesting view on the evolutionary history of the Chlamydomonadales.

The order that *C. reinhardtii* belongs to include a great variety of both colonial (e.g. *Basichlamys, Gonium* and *Volvulina*) and multicellular forms (e.g. *Volvox cartieri*), and the order has thus frequently been used as a model system for the evolution of multicellularity (Herron & Michod 2008; Leliaert *et al.* 2012). In phylogenetic studies of the

Chlamydomonadales, *C. reinhardtii* is described as a single celled flagellate and a representative for the ancestral form of the lineage (Herron & Michod 2008), while the reports of induced palmella formation in *C. reinhardtii* does not seem to be considered. Although the mechanism for palmella formation in *C. reinhardtii* is unresolved, it is compelling that the palmella formation in this species reflects the pattern of phenotypic divergence in its lineage. Several of the colonial species in this lineage are held together by an extracellular matrix that resembles the gelatinous matrix observed in palmelloids of *C. reinhardtii.*

The emergence of palmelloids in *C. reinhardtii* has been posed as experimental evidence for that "multicellularity can evolve rapidly in an organism that has never had a multicellular ancestor" (Ratcliff *et al.* 2013, p. 5). Although there probably is an aspect of heritability in the palmella formation of *C. reinhardtii,* I would argue that the reports of induced palmella formation and the species' relatedness to colonial forms makes it unlikely that palmelloids in *C. reinhardtii* is an evolutionary "novelty" brought by genetic mutations. In my view, the reports of palmella formation of *C. reinhardtii* raise a set of very interesting questions: Do *C. reinhardtii* and its related species serve as an example of genetic accommodation? Can the inducing agents of palmelloids in *C. reinhardtii* reveal something about the selective forces that led to the branching from unicellular to multicellular species in this lineage? Do the rotifer-algal experiments indicate that predation was such a selective force? To what degree is epigenetic variation heritable in unicellular organisms, and can it have an adaptive value in phytoplankton populations?

The often presumed simplicity of unicellular organisms such as *C. reinhardtii* or small zooplankton such as *B. calyciflorus* might make experimentalists and theoreticians inclined to make simple deductions about the responses they observe. This study, I believe, has shown that the behaviour of even such simple organisms is difficult to elucidate, and it has made me appreciate the significance of the vast evolutionary history that is harboured in even the simplest organisms as well as in all other organisms of today – "in each cell is the ancient ocean closed within us"[2].

[2] "i hver celle er selve urhavet stengt inn i oss" from the poem *Hvor mye smerte* in the collection *Nattmaskin* (1998) by Stein Mehren.

Conclusion

The overarching goal of this master project was to reproduce results from the rotifer-algal studies by Hairston Jr. and colleagues. Based on their mathematical model of the rotifer-algal system, I specifically aimed at identifying experimental conditions that would generate two qualitatively different predator-prey dynamics and test whether the theoretical predictions could be achieved experimentally. The two sets of rotifer-algal microcosms in my study clearly exhibited qualitatively different predator-prey dynamics, but the results differed considerably from the model predictions. Two reasons for this could be that my systems seemed to have been limited by phosphorus rather than nitrogen and potentially also that a presence of bacteria might have introduced unaccounted effects. But more importantly, the results revealed several aspects of the mathematical model that were ill-defined for my rotifer-algal system. This finding raises questions about the generality and precision of the model and also brings doubt to the validity of the inferences that have been made from the rotifer-algal microcosms.

The other specific goal I had for this project was to investigate the mechanism for palmella formation in *C. reinhardtii* and its effect on the predator-prey dynamics. Due to the extinction of rotifers in the low nutrient systems, my results could not elucidate whether nutrient concentration is a relevant factor in the formation of palmelloids, and the relative low number of replicates in my set of high nutrient systems makes it difficult to draw any solid conclusions about the effects of palmella formation on rotifer-algal dynamics. However, my results question whether the larger size of the cell clusters in itself has protective function and suggest that the spatial heterogeneity that arose with the palmelloids also could have played an important role. My review of the literature on palmella formation in *C. reinhardtii* suggests that it is a relatively unspecific response and it has additionally portrayed an interesting view on the evolution of multi-celled bodies within the Chlamydomonadales.

This project has demonstrated that mathematical models are a powerful tool for investigating biological systems, but also that one must take care when making inferences about the causal relationships that govern the biological responses. From a series of rotifer-algal studies, it was advocated a story which portrayed how rapid evolution of the prey phenotype can radically alter ecological population dynamics. My study has on the other hand portrayed a more complex picture of the factors that can cause changes in the algal phenotype and its potential effects on predator-prey dynamics.

Bibliography

Abrams, P. A. (2000). The evolution of predator-prey interactions: theory and evidence. *Annual Review of Ecology, Evolution, and Systematics*, **31**: 79-105.

Andersen, R. A., J. A. Berges, P. J. Harrison & M. M. Watnabe (2005). Appendix A - Recipies for freshwater and seawater media. In: *Algal Culturing Techniques*. Edited by R. A. Andersen. Elsevier Academice Press, p. 429-532.

Andersen, T., J. J. Elser & D. O. Hessen (2004). Stoichiometry and population dynamics. *Ecology Letters*, **7**(9): 884-900.

Beardall, J., D. Allen, J. Bragg, Z. V. Finkel, K. J. Flynn, A. Quigg, T. A. V. Rees, A. Richardson & J. A. Raven (2009). Allometry and stoichiometry of unicellular, colonial and multicellular phytoplankton. *New Phytologist*, **181**(2): 295-309.

Becks, L., S. P. Ellner, L. E. Jones & N. G. Hairston (2010). Reduction of adaptive genetic diversity radically alters eco-evolutionary community dynamics. *Ecology Letters*, **13**(8): 989-997.

Becks, L., S. P. Ellner, L. E. Jones & N. G. Hairston (2012). The functional genomics of an eco-evolutionary feedback loop: linking gene expression, trait evolution, and community dynamics. *Ecology Letters*, **15**(5): 492-501.

Bengtson, S. (2002). Origins and early evolution of predation. *Paleontological Society Papers*, **8**: 289-317.

Bjørnstad, O. N. & B. T. Grenfell (2001). Noisy clockwork: time series analysis of population fluctuations in animals. *Science*, **293**(5530): 638-643.

Boraas, M. E. (1980). A chemostat system for the study of rotifer-algal-nitrate interactions. In: *Evolution and ecology of zooplankton communities. Special symposium volume 3, American society of Limnology and Oceanography*. Edited by W. C. Kerfoot. University Press of New England, Hanover, New Hampshire and London, p. 173-182.

Boraas, M. E., D. B. Seale & J. E. Boxhorn (1998). Phagotrophy by a flagellate selects for colonial prey: A possible origin of multicellularity. *Evolutionary Ecology*, **12**(2): 153-164.

Boyle, N. R. & J. A. Morgan (2009) Flux balance analysis of primary metabolism in Chlamydomonas reinhardtii. *BMC Systems Biology*, **3**(4), doi: 10.1186/1752-0509-3-4.

Brönmark, C. & L.-A. Hansson (2005). *The Biology of Lakes and Ponds.* Oxford University Press Inc., New York, Second, p. 285.

Caperon, J. (1967). Population growth in micro-organisms limited by food supply. *Ecology*, **48**(5): 715-722.

Chlamydomonas Resource Center, The University of Minnesota (2015). CC-1690 wild type mt+ [Sager 21 gr]. Retrieved 4. June 2015, from http://chlamycollection.org/strain/cc-1690-wild-type-mt-sager-21-gr/.

Chu, S. P. (1942). The influence of the mineral composition of the medium on the growth of planktonic algae Part 1. Methods and culture media. *Journal of Ecology*, **30**: 284-325.

Cronan, C. S. (2009). Major cations (Ca, Mg, Na, K, Al). In: *Encyclopedia of Inland waters*. Edited by G. E. Likens. Elsevier, p. 45-51.

Cross, F. R. & J. G. Umen (2015). The Chlamydomonas cell cycle. *Plant Journal*, **82**(3): 370-392.

Darwin, C. R. (1859). *On the origin of species by means of natural selection, or the preservation of favoured races in the struggle for life.* John Murray, London, First edition, p. 502.

Dugdale, R. C. (1967). Nutrient limitation in the sea: Dynamics, identification, and significance. *Limnology and Oceanography*, **12**(2): 685-695.

Dumont, H. J. (1977). Biotic factors in the population dynamics of rotifers. *Ergebnisse der Limnologie*, **8**: 98-122.

Elendt, B. P. & W. R. Bias (1990). Trace nutrient deficiency in Daphnia magna cultured in standard medium for toxicity testing - effects of the optimization of culture conditions on life history parameters of Daphnia magna. *Water Research*, **24**(9): 1157-1167.

Ellner, S. P. & L. Becks (2010). Rapid prey evolution and the dynamics of two-predator food webs. *Theoretical Ecology*, **4**(2): 133-152.

Enander, L., (2008). Nye Oset vannbehandlingsanlegg. Retrieved 9. July 2015, from http://www.sweco.no/no/Norway/Nyheter/2008/Kategori/Nye-Oset-vannbehandlingsanlegg/.

Epp, R. W. & W. M. Lewis (1984). Cost and speed of locomotion for rotifers. *Oecologia*, **61**(3): 289-292.

Eppley, R. W. & P. R. Sloan (1966). Growth rates of marine phytoplankton: correlation with light absorption by cell chlorophyll a. *Physiologia Plantarum*, **19**(1): 47-59.

Falkowski, P. G., M. E. Katz, A. H. Knoll, A. Quigg, J. A. Raven, O. Schofield & F. J. R. Taylor (2004). The evolution of modern eukaryotic phytoplankton. *Science*, **305**(5682): 354-360.

Felpeto, A. B. & N. G. Hairston (2013). Indirect bottom-up control of consumer–resource dynamics: Resource-driven algal quality alters grazer numerical response. *Limnology and Oceanography*, **58**(3): 827-838.

Field, C. B., M. J. Behrenfeld, J. T. Randerson & P. Falkowski (1998). Primary production of the biosphere: Integrating terrestrial and oceanic components. *Science*, **281**(5374): 237-240.

Fischer, B. B., M. Kwiatkowski, M. Ackermann, J. Krismer, S. Roffler, M. J. F. Suter, R. I. L. Eggen & B. Matthews (2014). Phenotypic plasticity influences the eco-evolutionary dynamics of a predator-prey system. *Ecology*, **95**(11): 3080-3092.

Forbes, S. A. (1887). The lake as a microcosm. *Bulletin of the Scientific Association (Peoria Illinois)*: 77-87.

Fussmann, G. F. (2010). Rotifers: excellent subjects for the study of macro- and microevolutionary change. *Hydrobiologia*, **662**(1): 11-18.

Fussmann, G. F., S. P. Ellner & N. G. Hairston, Jr. (2003). Evolution as a critical component of plankton dynamics. *Proceedings of the Royal Society B*, **270**(1519): 1015-1022.

Fussmann, G. F., S. P. Ellner, K. W. Shertzer & N. G. Hairston Jr. (2000). Crossing the hopf bifurcation in a live predator-prey system. *Science*, **260**: 1358-1360.

Fussmann, G. F., M. Loreau & P. A. Abrams (2007). Eco-evolutionary dynamics of communities and ecosystems. *Functional Ecology*, **21**(3): 465-477.

Futuyma, D. J. (2009). *Evolution.* Sinauer Associates Inc., Sunderland, Massachusetts, USA, Second edition, p. 633.

Gilbert, J. J. (2003). Specificity of crowding response that induces sexuality in the rotifer Brachionus. *Limnology and Oceanography*, **48**(3): 1297-1303.

Gilbert, J. J. (2004). Population density, sexual reproduction and diapause in monogonont rotifers: new data for Brachionus and a review. *Journal of Limnology*, **63**(1): 32-36.

Gilbert, J. J. & E. J. Walsh (2005). Brachionus calyciflorus is a species complex: Mating behavior and genetic differentiation among four geographically isolated strains. In: *Rotifera X*. Edited by A. Herzig, R. D. Gulati, C. D. Jersabek and L. May. Springer Netherlands, p. 257-265.

Guillard, R. R. L. & C. J. Lorenzen (1972). Yellow-green algae with chlorophyllide c. *Journal of Phycology*, **8**(1): 10-14.

Hairston, N. G., S. P. Ellner, M. A. Geber, T. Yoshida & J. A. Fox (2005). Rapid evolution and the convergence of ecological and evolutionary time. *Ecology Letters*, **8**(10): 1114-1127.

Haney, J. D. & G. A. Jackson (1996). Modeling phytoplankton growth rates. *Journal of Plankton Research*, **18**(1): 63-85.

Harris, E. H. (2009). *The Chlamydomonas Sourcebook.* Academic Press, Amsterdam, 2nd, p. 444.

Herron, M. D. & R. E. Michod (2008). Evolution of complexity in the volvocine algae: transitions in individuality through Darwin's eye. *Evolution*, **62**(2): 436-451.

Hessen, D. O., T. C. Jensen, M. Kyle & J. J. Elser (2007). RNA responses to N- and P-limitation; reciprocal regulation of stoichiometry and growth rate in Brachionus. *Functional Ecology*, **21**(5): 956-962.

Hessen, D. O. & E. Van Donk (1993). Morphological-changes in Scenedesmus induced by substances released from Daphnia. *Archiv Fur Hydrobiologie*, **127**(2): 129-140.

Hutchinson, G. E. (1959). Homage to Santa Rosalia or why are there so many kinds of animals? *American Naturalist*, **93**(870): 145-159.

Iwasa, K. & S. Murakami (1968). Palmelloid formation of Chlamydomonas. I. Palmelloid induction by organic acids. *Physiologia Plantarum*, **21**(6): 1224-1233.

Iwasa, K. & S. Murakami (1969). Palmelloid formation of Chlamydomonas II. Mechanism of palmelloid formation by organic acids. *Physiologia Plantarum*, **22**(1): 43-50.

Jablonka, E. (2013). Epigenetic inheritance and plasticity: The responsive germline. *Progress in Biophysics and Molecular Biology*, **111**(2-3): 99-107.

Kasada, M., M. Yamamichi & T. Yoshida (2014). Form of an evolutionary tradeoff affects eco-evolutionary dynamics in a predator-prey system. *Proceedings of the National Academy of Sciences of the United States of America*, **111**(45): 16035-16040.

Kauler, P. & H. E. Enesco (2011). The effect of temperature on life history parameters and cost of reproduction in the rotifer Brachionus calyciflorus. *Journal of Freshwater Ecology*, **26**(3): 399-408.

Keating, K. I. (1985). A system of defined (sensu strictu) media for daphnid (Cladocera) culture. *Water Research*, **19**: 73-78.

Kilham, S. S., D. A. Kreeger, S. G. Lynn, C. E. Goulden & L. Herrera (1998). COMBO: a defined freshwater culture medium for algae and zooplankton. *Hydrobiologia*, **377**: 147-159.

Kingsland, S. E. (1985). *Modeling Nature: Episodes in the History of Population Ecology.* The University of Chicago Press, Chicago and London, p. 264.

Klausmeier, C. A., E. Litchman, T. Daufresne & S. A. Levin (2008). Phytoplankton stoichiometry. *Ecological Research*, **23**(3): 479-485.

Klironomos, F. D., J. Berg & S. Collins (2013). How epigenetic mutations can affect genetic evolution: Model and mechanism. *Bioessays*, **35**(6): 571-578.

Leliaert, F., D. R. Smith, H. Moreau, M. D. Herron, H. Verbruggen, C. F. Delwiche & O. D. Clerck (2012). Phylogeny and molecular evolution of the green algae. *Critical Reviews in Plant Sciences*, **31**: 1-46.

Levins, R. (1966). The strategy of model builing in population biology. *American Scientist,* **54**: 421-431.

Lewis, W. M. (2009). Lakes as Ecosystems. In: *Encyclopedia of Inland waters*. Edited by G. E. Likens. Elsevier, p. 431-440.

Lindeman, R. L. (1942). The Trophic-Dynamic Aspect of Ecology. *Ecology*, **23**(4): 399-417.

Lürling, M. & W. Beekman (2006). Palmelloids formation in Chlamydomonas reinhardtii : defence against rotifer predators? *Annales de Limnologie - International Journal of Limnology*, **42**(2): 65-72.

Ma, Q., Y.-L. Xi, J.-Y. Zhang, X.-L. Wen & X.-L. Xiang (2010). Differences in life table demography among eight geographic populations of Brachionus calyciflorus (Rotifera) from China. *Limnologica*, **40**(1): 16-22.

McCauley, E. & W. W. Murdoch (1987). Cyclic and stable populations - plankton as paradigm. *American Naturalist*, **129**(1): 97-121.

McCauley, E. & W. W. Murdoch (1990). Predator prey dynamics in environments rich and poor in nutrients. *Nature*, **343**(6257): 455-457.

McCauley, E., W. A. Nelson & R. M. Nisbet (2008). Small-amplitude cycles emerge from stage-structured interactions in Daphnia-algal systems. *Nature*, **455**(7217): 1240-1243.

McCauley, E., R. M. Nisbet, W. W. Murdoch, A. M. de Roos & W. S. C. Gurney (1999). Large-amplitude cycles of Daphnia and its algal prey in enriched environments. *Nature*, **402**(6762): 653-656.

Ness, R. W., A. D. Morgan, N. Colegrave & P. D. Keightley (2012). Estimate of the spontaneous mutation rate in Chlamydomonas reinhardtii. *Genetics*, **192**(4): 1447-1454.

Oldenhof, H., V. Zachleder & H. Van den Ende (2006). Blue- and red-light regulation of the cell cycle in Chlamydomonas reinhardtii (Chlorophyta). *European Journal of Phycology*, **41**(3): 313-320.

Oldenhof, H., V. Zachleder & H. van den Ende (2007). The cell cycle of Chlamydomonas reinhardtii: the role of the commitment point. *Folia Microbiologica*, **52**(1): 53-60.

Olsen, Y., G. Knutsen & T. Lien (1983). Characteristics of phosphorus limitation in *Chlamydomonas reinhardtii* (Chlorophyceae) and its palmelloids. *Journal of Phycology*, **19**: 313-319.

Palladino, P. (1991). Defining ecology: Ecological theories, mathematical models, and applied biology in the 1960s and 1970s. *Journal of the History of Biology*, **24**(2): 223-243.

Parfrey, L. W. & D. J. G. Lahr (2013). Multicellularity arose several times in the evolution of eukaryotes. *Bioessays*, **35**(4): 339-347.

Park, J. J., H. Wang, M. Gargouri, R. R. Deshpande, J. N. Skepper, F. O. Holguin, M. T. Juergens, Y. Shachar-Hill, L. M. Hicks & D. R. Gang (2015). The response of Chlamydomonas reinhardtii to nitrogen deprivation: a systems biology analysis. *The Plant Journal*, **81**(4): 611-624.

Preisig, H. & R. A. Andersen (2005). Historical review of algal culturing techniques. In: *Algal Culturing Techniques*. Edited by R. A. Andersen. Elsevier Academic Press, p. 1-12.

Price, T. D., A. Qvarnström & D. E. Irwin (2003). The role of phenotypic plasticity in driving genetic evolution. *Proceedings of the Royal Society B: Biological Sciences*, **270**(1523): 1433-1440.

Radmer, R. J. (1996). Algal diversity and commercial algal products. *Bioscience*, **46**(4): 263-270.

Ratcliff, W. C., M. D. Herron, K. Howell, J. T. Pentz, F. Rosenzweig & M. Travisano (2013). Experimental evolution of an alternating uni- and multicellular life cycle in Chlamydomonas reinhardtii. *Nature Communications*, **4**: 2742.

Rhee, G. Y. & I. J. Gotham (1981). The effect of environmental factors on phytoplankton growth: Temperature and the interactions of temperature with nutrient limitation. *Limnology and Oceanography*, **26**(4): 635-648.

Rosenzweig, M. L. (1971). Paradox of enrichment: destabilization of exploitation ecosystems in ecological time. *Science*, **171**(3969): 385-387.

Rothhaupt, K. O. (1990a). Differences in particle size-dependent feeding efficiencies of closely related rotifer species. *Limnology and Oceanography*, **35**(1): 16-23.

Rothhaupt, K. O. (1990b). Population growth rates of two closely related rotifer species: effects of food quantity, particle size, and nutritional quality. *Freshwater Biology*, **23**(3): 561-570.

Räsänen, K. & L. E. B. Kruuk (2007). Maternal effects and evolution at ecological time-scales. *Functional Ecology*, **21**(3): 408-421.

Scheffer, M. & R. J. D. Boer (1995). Implications of spatial heterogeneity for the paradox of enrichment. *Ecology*, **76**(7): 2270-2277.

Schlichting, C. D. & M. A. Wund (2014). Phenotypic plasticity and epigenetic marking: an assessment of evidence for genetic accomodation. *Evolution*, **68**(3): 656-672.

Shertzer, K. W., S. P. Ellner, G. F. Fussmann & N. G. Hairston (2002). Predator-prey cycles in an aquatic microcosm: testing hypotheses of mechanism. *Journal of Animal Ecology*, **71**(5): 802-815.

Soetaert, K., T. Petzoldt & R. W. Setzer (2010). Solving differential equations in R: package deSolve. *Journal of Statistical Software*, **33**(9): 1-25.

Stelzer, C.-P., J. Schmidt, A. Wiedlroither & S. Riss (2010). Loss of sexual reproduction and dwarfing in a small metazoan. *Plos One*, **5**(9): e12854.

Stelzer, C. P. & T. W. Snell (2003). Induction of sexual reproduction in Brachionus plicatilis (Monogononta, Rotifera) by a density-dependent chemical cue. *Limnology and Oceanography*, **48**(2): 939-943.

Sterner, R. W. (2009). The role of zooplankton in aquatic ecosystems. In: *Encyclopedia of Inland waters*. Edited by G. E. Likens. Elsevier, p. 678-688.

Sterner, R. W. & J. J. Elser (2002). *Ecological Stoichiometry. The biology of elements from molecules to the biosphere.* Princeton University Press, p. 464.

Sunda, W., N. Price & F. Morel (2005). Trace metal ion buffers and their use in culture studies. In: *Algal Culturing Techniques*. Edited by R. A. Andersen. Elsevier Academic Press, p. 35-64.

Svanbäck, R., M. Pineda-Krch & M. Doebeli (2009). Fluctuating population dynamics promotes the evolution of phenotypic plasticity. *American Naturalist*, **174**(2): 176-189.

R Core Team (2015). R: A language and environment for statistical computing. R Foundation for Statistical Computing, Vienna, Austria. http://www.R-project.org/

Van de Waal, D. B., V. H. Smith, S. A. J. Declerck, E. C. M. Stam & J. J. Elser (2014). Stoichiometric regulation of phytoplankton toxins. *Ecology Letters*, **17**(6): 736-742.

Van Donk, E., A. Ianora & M. Vos (2010). Induced defences in marine and freshwater phytoplankton: a review. *Hydrobiologia*, **668**(1): 3-19.

VAV, Oslo vann- og avløpsetat (2014). Drikkevannkvalitet. Retrieved 9. July 2015, from https://www.oslo.kommune.no/vann-og-avlop/drikkevannkvalitet/.

Venables, W. N. & B. D. Ripley (2002). *Modern Applied Statistics with S.* Springer-Verlag, New York, p. 498.

Verschoor, A. M., I. van der Stap, N. R. Helmsing, M. Lurling & E. van Donk (2004a). Inducible colony formation within the Scenedesmaceae: Adaptive responses to infochemicals from two different herbivore taxa. *Journal of Phycology*, **40**(5): 808-814.

Verschoor, A. M., M. Vos & I. van der Stap (2004b). Inducible defences prevent strong population fluctuations in bi- and tritrophic food chains. *Ecology Letters*, **7**(12): 1143-1148.

Vos, M., B. W. Kooi, D. L. DeAngelis & W. M. Mooij (2004a). Inducible defences and the paradox of enrichment. *Oikos*, **105**(3): 471-480.

Vos, M., A. M. Verschoor, B. W. Kooi, F. L. Wackers, D. L. DeAngelis & W. M. Mooij (2004b). Inducible defenses and trophic structure. *Ecology*, **85**(10): 2783-2794.

Waddington, C. H. (1953). Genetic assimilation of an aquired character. *Evolution*, **7**(2): 118-126.

Waddington, C. H. (1959). Canalization of development and genetic assimilation of aquired characters. *Nature*, **183**(4676): 1654-1655.

Wallace, R. L. & H. A. Smith (2009). Rotifera. In: *Encyclopedia of Inland Waters*. Edited by E. Likens Gene. Elsevier, p. 689-703.

Walz, N. (1995). Rotifer populations in plankton communities: Energetics and life history strategies. *Experientia*, **51**(5): 437-453.

Wright, R. T. (1964). Dynamics of a phytoplankton community in an ice-covered lake. *Limnology and Oceanography*, **9**(2): 163-178.

Yamamichi, M., T. Yoshida & A. Sasaki (2011). Comparing the effects of rapid evolution and phenotypic plasticity on predator-prey dynamics. *The American Naturalist*, **178**(3): 287-304.

Yoshida, T., N. G. Hairston & S. P. Ellner (2004). Evolutionary trade-off between defence against grazing and competitive ability in a simple unicellular alga, Chlorella vulgaris. *Proceedings of the Royal Society B-Biological Sciences*, **271**(1551): 1947-1953.

Yoshida, T., L. E. Jones, S. P. Ellner, G. F. Fussmann & N. G. Hairston (2003). Rapid evolution drives ecological dynamics in a predator-prey system. *Nature*, **424**(6946): 303-306.

APPENDIXES

TABLE OF APPENDIXES

APPENDIX A

Comparison of medium types

Chemical component concentration in µmol/l		WC medium	JET medium	Cool medium
Major elements	$NaNO_3$	1000	1000	-
	KNO_3	-	-	160*
	K_2HPO_4	50	50	200*
	$CaCl_2 \cdot 2H_2O$	250	-	15
	$MgSO_4 \cdot 7H_2O$	150	-	81
	$NaHCO_3$	150	-	-
	$Na_2SiO_3 \cdot 9H_2O$	100	-	-
Algal trace elements	$Na_2EDTA \cdot 2H_2O$	11.700	11.700	-
	$FeCl_3 \cdot 6H_2O$	11.700	11.650	-
	Fe-EDTA	-	-	10.079
	$CuSO_4 \cdot 5H_2O$	0.040	0.040	0.004
	$ZnSO_4 \cdot 7H_2O$	0.080	0.077	0.076
	$CoCl_2 \cdot 6H_2O$	0.050	0.042	0.042
	$MnCl_2 \cdot 4H_2O$	0.900	0.910	0.900
	$Na_2MoO_4 \cdot 2H_2O$	0.030	0.025	0.025
	Na_3VO_4	-	-	0.003
	H_3BO_3	16.000	16.000	24.800
Vitamins	Cyanocobalmin (B12)	0.0004	0.0004	0.0006
	Biotin (H)	0.0020	0.0020	0.0025
	Thiamin (B1)	0.3000	0.3000	0.2965
Animal trace elements	LiCl	-	-	3.600
	RbCl	-	-	0.297
	$SrCl_2 \cdot 6H_2O$	-	-	0.285
	NaBr	-	-	0.078
	Kl	-	-	0.012
	H_2SeO_3	-	-	0.008

* The concentration used in the N-limited experiments of Felpeto & Hairston (2013). The nitrate concentration was also set to 160 µmol/l in the experiments of Becks *et al.* (2010), while the concentration of phosphate is not reported.

The recipe for the WC medium is taken from Guillard and Lorenzen (1972), and the composition of Cool Medium is given in Felpeto & Hairston (2013). This Cool medium is the medium used for the rotifer-algal experiments at the Hairston lab (Fussmann *et al.* 2000; Yoshida *et al.* 2003 and Becks *et al.* 2010).

Appendix B

Analysis of growth curves using nonlinear mixed-effects modelling (medium test)

The appendix presents the analyses that support the conclusions made about the different medium types in part **1.1**. The analyses have been made with the guidance of Pinheiro and Bates's *Mixed-Effects Models in S and S-PLUS* (2000), in particular chapter 5 (Extending the Basic Linear Mixed-Effects Model) and 8 (Fitting Nonlinear Mixed-Effects Models).

Mixed effects models is a tool for the analysis of grouped data (Pinheiro & Bates 2000) and offer the possibilty to test for the inclusion of covariates explaining the response in interest. In the case of the medium test, a possible covariate is *medium type*, and the main goal with the following analysis is to consider whether *medium type* should be included as a covariate or not. This would signify whether the growth of *Chlamydomonas reinhardtii* differs in the five medium types.

A nonlinear model is relevant in this case as the growth trajectory of algae is nonlinear in batch cultures. The logistic function is a common model used to describe population growth, and it is the nonlinear model that will be fitted to the data from the medium test. It is often decribed in the following form:

$$y_{(x)} = \frac{K}{1 + (\frac{K - y_0}{y_0})(e^{-rx})}$$

where the constant **K** is the system's carrying capacity (asymptote), **r** the population growth rate and y_0 the initial population size. $y_{(x)}$ then gives the size of the population at time **x**.

In Pinheiro and Bates's package for nonlinear mixed effects models (nlme), this equation has been parameterized to:

$$y_{(x)} = \frac{Asym}{1 + e^{-(\frac{x - xmid}{scal})}}$$

where **Asym** denote the carrying capacity, **xmid** the x-value for the inflection point of the curve and where **scal** is inversely proportional to the population growth rate (**scal=1/r**) (ibid.; Tom Andersen *personal communication*).

The term "mixed" in mixed effects models denotes that this are models that include both fixed and random effects. The fixed effects represent the parameters associated with the entire population and the random effects the parameters associated with the individual experimental units drawn at random from the population (ibid.). Said differently, the random effects represent the individual group's deviation from the fixed effects, which might be caused by unexplained variation between groups or by differences in covariate values among them (ibid.).

As an example, if the medium test data indicate that the asymptote differs in the five treatments, while the two other growth parameters are equal for all, the model would have five fixed effects for the asymptote (one for each medium type), while one fixed effect for the other two. And if the scal parameter estimated for each culture indidividually deviates from the fixed effect for some unexplained reason, this would be classified as a random effect.

Required packages

```
library(nlme) # Pinheiro and Bates's accompanying R package
library(RColorBrewer) # colour palettes for plotting
library(knitr) # for nicer looking tables
```

Reading the data file

```
mediumtest1 <- read.table("Mediumtest.nlme.txt", header=TRUE)
medium.grouped <- groupedData(cells~hours | replicate, mediumtest1, order.groups=F)
# a later function requires that the data is organized as a grouped data object
```

Plot of the data (code hidden)

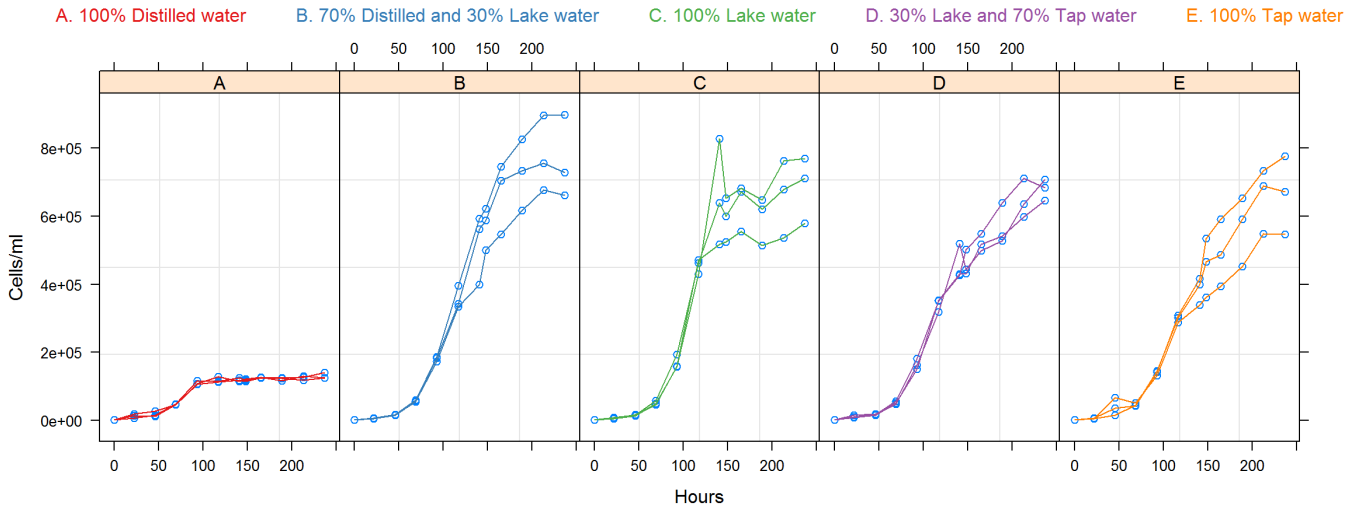

Medium type A stands out from the other types and is clearly a bad choice for medium. I choose to remove it from the analysis as it would have a dominant effect on the model (which I am not interested in).

```
mediumtest <- read.table("Mediumtest.nlme.txt", header=TRUE)[-(1:36),] # remove A
cultures
medium.grouped <- groupedData(cells~hours | replicate, mediumtest, order.groups=F)
```

Starting the NLME-fit

Separate fits by replicate

Following Pinheiro & Bates's example, I use the self starting logistic function SSlogis and start by making separate fits for each of the 12 replicates. The authors recommend to make plots of these separate fits, as it could suggest a structure of the future model's fixed and random effects.

```
medium.lis <- nlsList(SSlogis, medium.grouped)

plot(intervals(medium.lis), layout=c(3,1))
pairs(medium.lis, id=0.01)
```

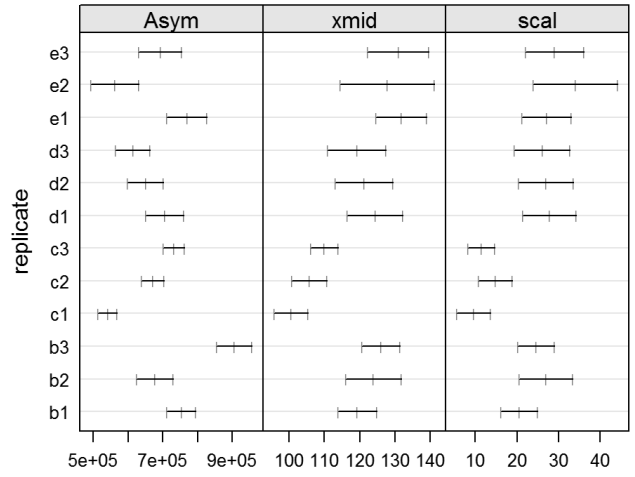

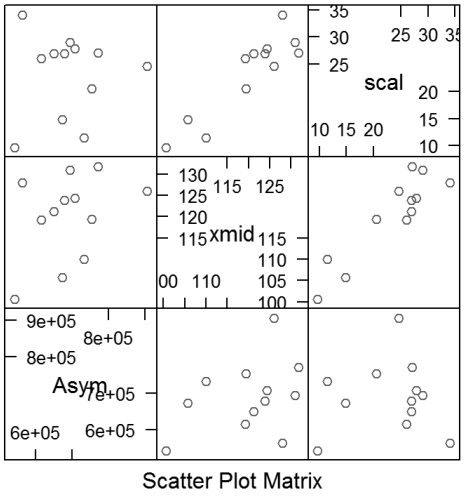

The first plot (left) shows the 95% confidence intervals of the parameters found by making separate fits to each of the cultures. Within each medium type, the variability of parameter estimates is highest for the Asym parameter (not all confidence intervals overlap). According to Pinheiro & Bates, this might suggest that the Asym parameter require random effects to account for the within-group variation. The within-group variability for the xmid and scal parameters are in contrast low.

The second plot gives a view of the random effects covariance structure. There is positive correlation between the xmid and scal estimates, while the Asym parameter is not strongly correlated with any of the two. That there is a correlation between the parameters is probably explained by how the logistic function is parameterized in the nlme-package (Tom Andersen *personal communication*). Instead of using the value for the initial population (y_0) and two parameters (the carrying capacity and the growth rate) to fit the logitic function, the nlme-package uses the three parameters Asym, xmid and scal. From the two ways of parameterizing the logistic function, it can be deduced that:

$$xmid = scal \cdot \log(\frac{Asym - y_0}{y_0})$$

which explains why the xmid and scal parameters could be positively correlated (Tom Andersen *personal communication*).

The id argument in pairs() is specified in order to identify outliers. No outliers were found in the dataset.

Combined fit to a single nlme model

The nlsList object, medium.lis, provides starting estimates for the nlme-model. The plot of the augPred function (next page) shows the predictions augumented with the observed values. The dashed curve draws the separate model fits for each culture, while the blue curve draws the prediction of the combined fit of all cultures.

```
medium.nlme <- nlme(medium.lis)
plot(augPred(medium.nlme, level=0:1), layout=c(3,4), lty=1:2, ylab="Cells/ml", xla
b="Hours")
```

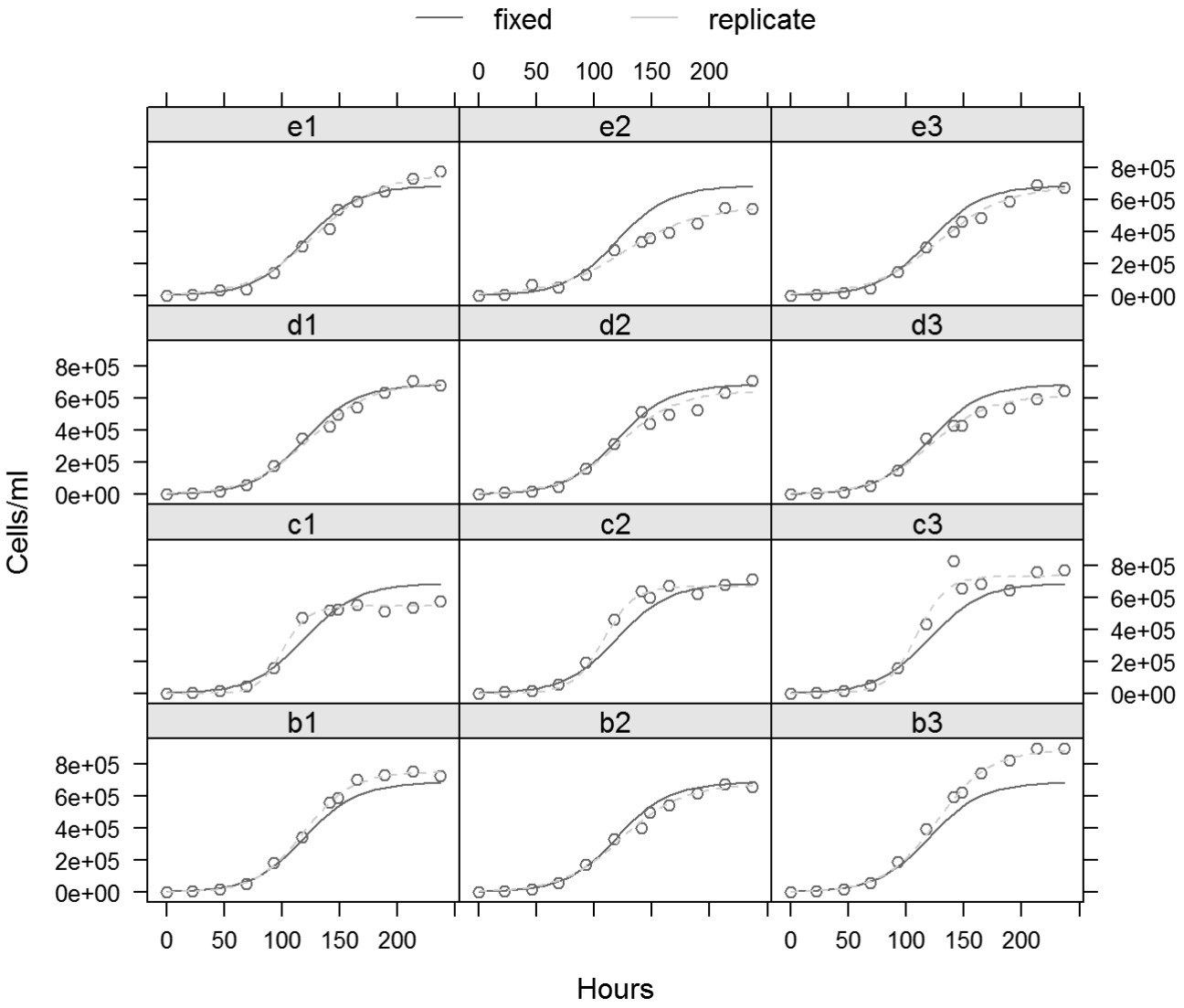

The combined fit seems to do quite well in predicting the algal growth in all four medium types. Before I analyse whether it is appropriate to include a covariate structure, I need to assess the model assumptions.

Model assumptions

The nlme model rest on two basic assumptions (ibid.):

1. the errors within each group are independent and indentically normally distributed, with mean zero and variance σ^2, and they are independent of random effects.
2. the random effects are normally distributed, with mean zero and covariance matrix not depending on group, and are independent for different groups.

Diagnostic plots to assess the model assumptions

```
plot(medium.nlme, resid(., type="n") ~ hours, abline = 0, cex=0.8)
qqnorm(medium.nlme, abline=c(0,1), cex=0.8)
```

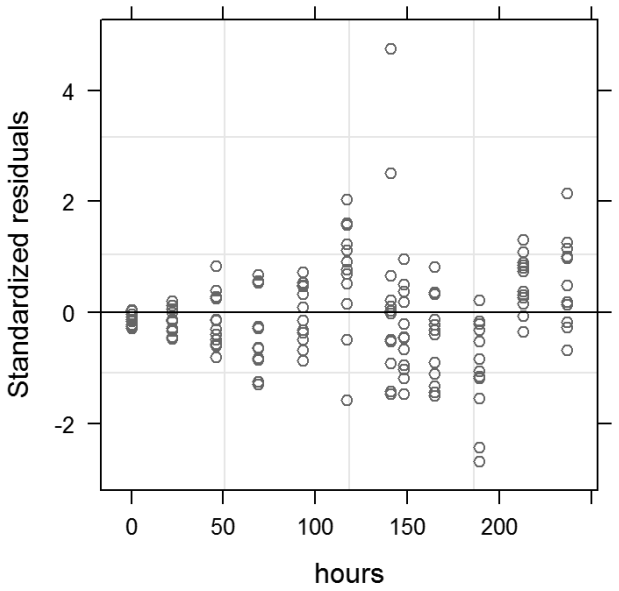

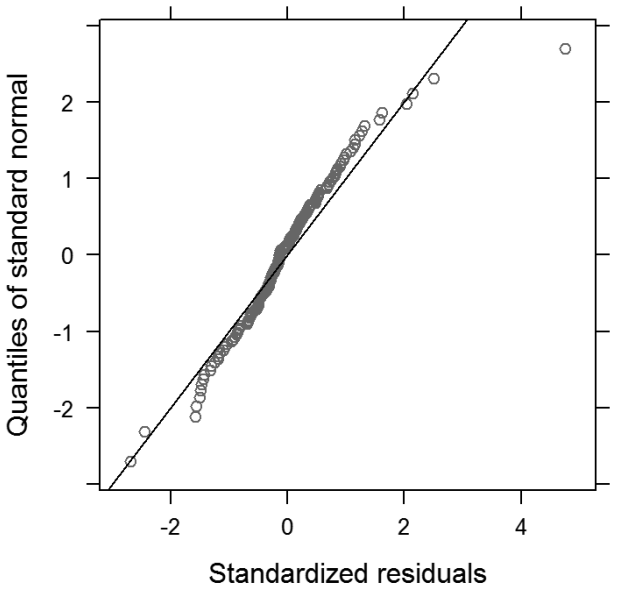

The first plot clearly depict that the residuals are heteroscedastic; the within-group variance increases with the concentration of cells. The plots also show signs of autocorrelation; the residuals are more similar to the residals at consecutive time points than would be expected if the errors were fully independent.

Fixing heteroscedasticity

I need to include a variance function to account for the heteroscedastic residuals. The variance functions in nlme are used to model the variance structure of the within-group errors using covariates (ibid.). The nlme library provides a set of different variance functions (see ?varClasses).

varPower - one parameter variance function

This variance function is described as a power of the absolute value of the variance covariate. It is one of the simplest variance functions and it seems to be the preferred choice by Pinheiro & Bates.

```
medium.nlme.var1 <- update(medium.nlme, weights = varPower())
kable(anova(medium.nlme, medium.nlme.var1)[,-1])
```

	Model	df	AIC	BIC	logLik	Test	L.Ratio	p-value
medium.nlme	1	10	3487.548	3517.246	-1733.774		NA	NA
medium.nlme.var1	2	11	3437.179	3469.847	-1707.589	1 vs 2	52.36929	0

The model quality measures (AIC/BIC) are significantly lower for the the model with variance function and thus indicate that the model with variance function is better than the one without.

```
plot(medium.nlme.var1, resid(., type="n") ~ hours, abline = 0, cex=0.8)
plot(medium.nlme.var1, resid(., type="n") ~ hours | medium, abline = 0, cex=0.8)
```

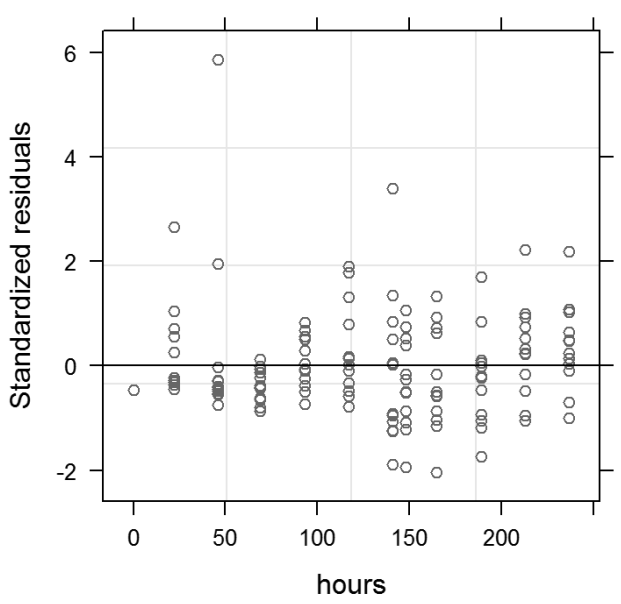

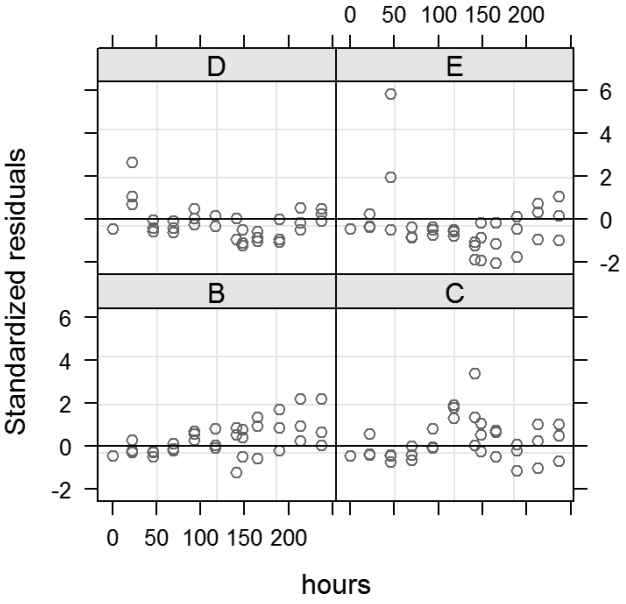

Including the variance function with one parameter seems to account for the heteroscedasticity in the data adequately, and I therefore keep this variance function in the model.

Correlation structures

The plots above suggest that the residuals are correlated (i.e. violating the assumption of independence). The nlme library includes an empirical autocorrelation function (ACF) which can be used to investigate correlation structures. The argument *resType* control what type of residuals that are plotted. I choose to plot the normalized residuals, i.e. the standardized residuals premultiplied by the inverse square root factor of the estimated error correlation matrix (ibid.)

```
plot(ACF(medium.nlme.var1, maxLag=8, resType="normalized"), alpha = 0.05)
```

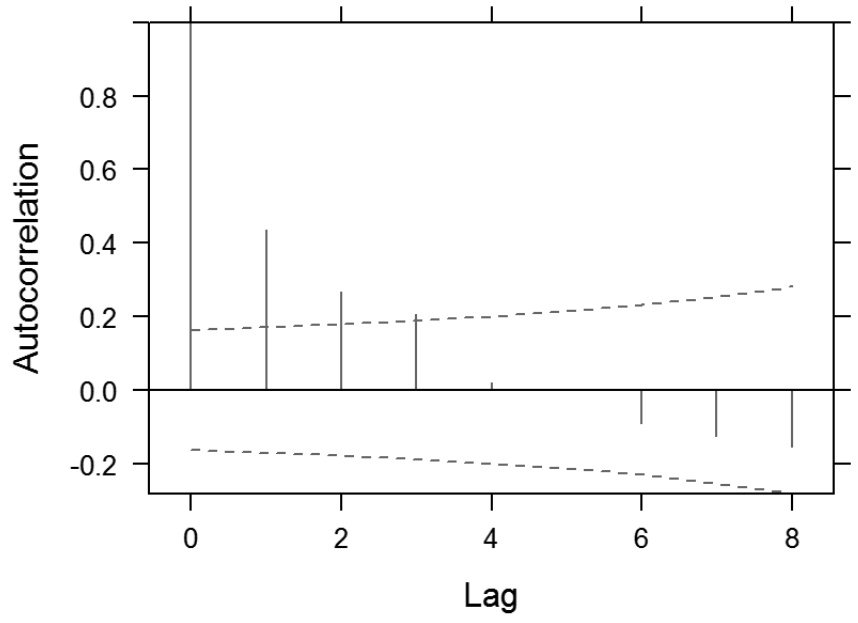

The plot indicates significant autocorrelations at lag 1 and 2 (and possibly lag 3). The necessity of incorporating a correlation structure is thus evident.

The nlme library provides a set of both serial and spatial correlation functions for modelling dependence among within-group errors (see ?corClasses). I tried three serial correlation functions in the nlme-library:
- the corCAR1, continuous autoregressive models of order 1.
- the corARMA(p=0, q=2), moving average models.
- the corARMA(p=1, q=1), a combination of autoregressive and moving average models.

All models with a correlation structure are better than the one without (script not included). Among these models did the moving average model perform the worst, while there was no significant difference between the autoregressive model (corCAR1) and the mixed autoregressive-moving average model (corARMA(p=1,q=1)). Since the corCAR1 is the simplest one of the two, I choose to include this correlation function in the model.

corCAR1 - continuous autoregressive model of order 1

Autoregressive models capture the correlation in serial observations by expressing the current observation as a linear function of previous observations in addition to a homoscedastic noise term (ibid.). The *order* of the autoregressive model denotes the number of previous observations that are considered in the linear function (ibid.). Autoregressive models of order 1 have a correlation function that decreases in absolute value exponentially, and the authors state that such models are one of the most useful autoregressive models. The correlation parameter estimated by the function is called **phi** and represents the lag-1 correlation (ibid.).

```
medium.nlme.var1.CAR1 <- update(medium.nlme.var1, correlation=corCAR1())
kable(anova(medium.nlme.var1, medium.nlme.var1.CAR1)[,-1])
```

	Model	df	AIC	BIC	logLik	Test	L.Ratio	p-value
medium.nlme.var1	1	11	3437.179	3469.847	-1707.589		NA	NA
medium.nlme.var1.CAR1	2	12	3398.507	3434.145	-1687.254	1 vs 2	40.67141	0

```
plot(ACF(medium.nlme.var1.CAR1, maxLag=8, resType="normalized"), alpha = 0.05, mai
n="CAR1")
```

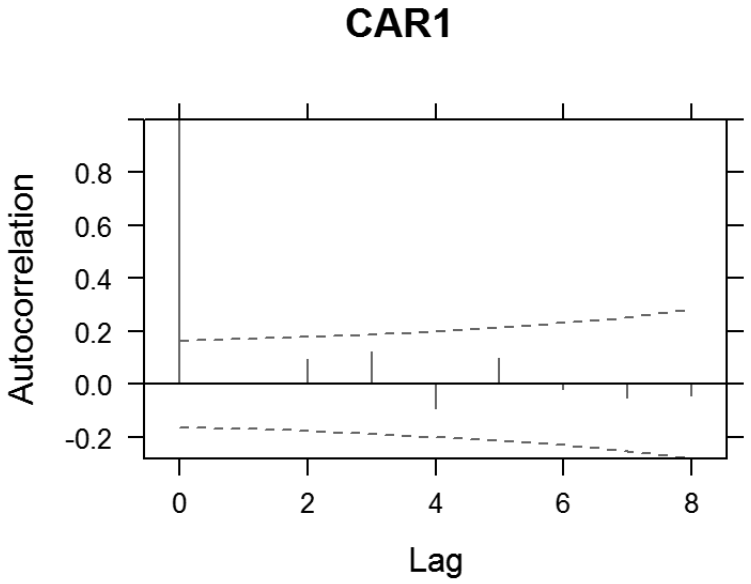

As reported on the previous side, the model comparisons indicate that the corCAR1-function gives a significantly better representation of the within-group correlation. The updated plot of the empirical autocorrelation function shows that the corCAR1 function removed the correlation structure in the data.

Random effects

The last aspect that needs to be evaluated before I can test for the inclusion of covariates, is whether the random effects structure is over-parameterized. A previous plot indicated that Asym was the only parameter that required random effects to account for the variation within groups (recall the plot of the 95% confidence intervals of the parameters estimated for the separate fits). To assess the random effects of the current model, I use the ranef() function to extract the random effects estimates and then plot the results.

```
medium.nlme.var1.CAR1.RE <- ranef(medium.nlme.var1.CAR1, augFrame=T)
plot(medium.nlme.var1.CAR1.RE, form=~medium,, layout=c(3,1))
pairs(medium.nlme.var1.CAR1.RE[1:3])
```

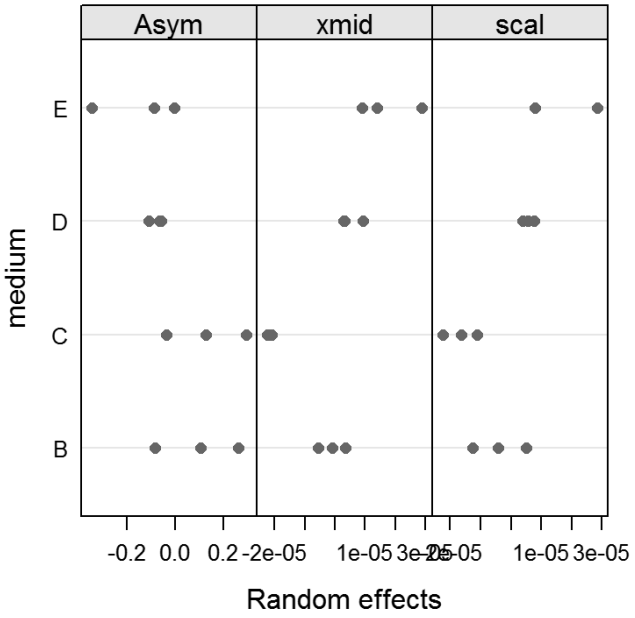

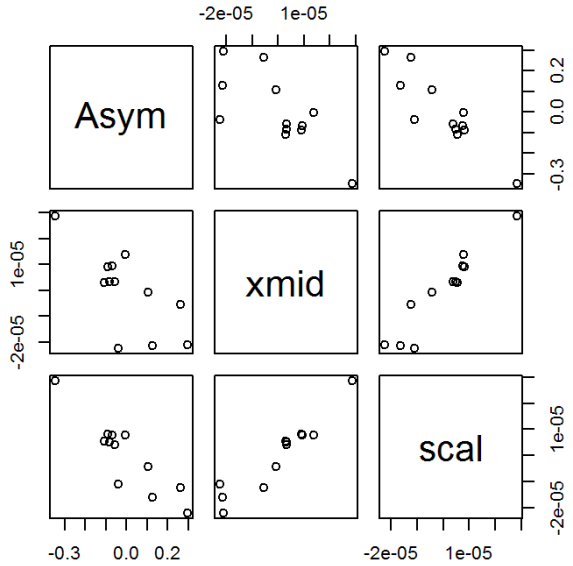

The correlation between xmid and scal is still strong, and Asym's correlation between the other parameters are stronger than it was initially. A high correlation between the parameter's random effects are, according to Pinheiro & Bates, an indication of over-parameterization. As before, the variation within medium types seems to be largest for the Asym parameter estimates. I therefore choose to keep the random effects for Asym, while I remove it from scal and xmid.

Remove scal and xmid random effects

```
medium.nlme.rsx <- update(medium.nlme.var1.CAR1, random=Asym ~ 1)
kable(anova(medium.nlme.var1.CAR1, medium.nlme.rsx)[,-1])
```

	Model	df	AIC	BIC	logLik	Test	L.Ratio	p-value
medium.nlme.var1.CAR1	1	12	3398.507	3434.145	-1687.254		NA	NA
medium.nlme.rsx	2	7	3388.508	3409.296	-1687.254	1 vs 2	0.0002227	1

There is no significant difference in the fits between the model with random effects for scal and xmid and the model without these random effects, and I therefore keep the simpler model without fewer random effects parameters.

Covariate structure

The main goal with this nonlinear mixed effect modelling was to investigate whether the growth of *C. reinhardtii* differs in the five medium types. The growth in the A cultures obviously differed from the other types, whereas the variation observed between the B, C, D and E cultures was more vague. To test whether some of this variation could be explained by the different medium types, I will next include medium type as a covariate in the model.

Asym ~ medium

If there is a difference in the growth trajectories between the medium types, it seems natural to expect that this difference would be in the carrying capacity/asymptote. The model is however not significantly improved by including medium type as a covariate to explain the variation observed between the groups' asymptotic values.

```
medium.nlme.c1 <- update(medium.nlme.rsx, fixed = list(Asym ~ medium, scal + xmid ~
1), start = c(660793, 0, 0, 0, 20,115)) # model with covariate structure for Asym
kable(anova(medium.nlme.c1))
```

	numDF	denDF	F-value	p-value
Asym.(Intercept)	1	127	47.2113589	0.0000000
Asym.medium	3	127	0.1202059	0.9480718
scal	1	127	135.8834862	0.0000000
xmid	1	127	3021.1534635	0.0000000

```
kable(anova(medium.nlme.rsx,medium.nlme.c1)[,-1])
```

	Model	df	AIC	BIC	logLik	Test	L.Ratio	p-value
medium.nlme.rsx	1	7	3388.508	3409.296	-1687.254		NA	NA
medium.nlme.c1	2	10	3385.958	3415.656	-1682.979	1 vs 2	8.549981	0.035913

The individual Asym parameters estimated for each medium type are not significantly different from each other. The comparison between this model to the one without a covariate structure indicates that the covariate do not improve the model (medium.nlme.c1 has lower AIC but higher BIC, and the p-value is close to the common 0.05 significance cut-off).

Including separate scal and xmid parameters for each medium type (scal~medium and xmid~medium) did not improve the model either (code not shown).

Conclusion: The data do not support the inclusion of medium type as covariate in the model, and hence the variation observed in the growth trajectories of the B, C, D and E cultures could not be separated from stochastic variation.

The final growth model for the B, C, D and E cultures

```
## Nonlinear mixed-effects model fit by maximum likelihood
##   Model: cells ~ SSlogis(hours, Asym, xmid, scal)
##   Data: medium.grouped
##   Log-likelihood: -1687.254
##   Fixed: list(Asym ~ 1, xmid ~ 1, scal ~ 1)
##         Asym         xmid         scal
## 660793.41504    114.66722     19.63784
##
## Random effects:
##  Formula: Asym ~ 1 | replicate
##             Asym Residual
## StdDev: 75.81344 35.86188
##
## Correlation Structure: Continuous AR(1)
##  Formula: ~1 | replicate
##  Parameter estimate(s):
##       Phi
## 0.5855951
## Variance function:
##  Structure: Power of variance covariate
##  Formula: ~fitted(.)
##  Parameter estimates:
##     power
## 0.5849752
## Number of Observations: 144
## Number of Groups: 12
```

Extracting model coefficients and making curve for plotting

```
mediumcoef <- medium.nlme.rsx$coef
mediumfix <- mediumcoef$fixed

logist <- function(x, Asym, xmid, scal) Asym/(1 + exp(-(x-xmid)/scal))
mediumfunc <- logist(1:237, mediumfix[1], mediumfix[2], mediumfix[3])
```

Code rendering Figure 1.1.

```
# Make a plot function

mediumplot <- function(rep1, rep2, rep3, name, plotcol){
plot(mediumtest1[1:12,3],rep1, pch=19, col=brewer.pal(5,"Set1")[plotcol],
xlab="", ylab="", ylim=c(0,900000), yaxt="n", xaxt="n", xlim=c(0,240))
points(mediumtest[1:12,3],rep2, pch=8, col=brewer.pal(5,"Set1")[plotcol])
points(mediumtest[1:12,3],rep3, pch=17, col=brewer.pal(5,"Set1")[plotcol])
legend("topleft", legend=name, bty="n", cex=1.5, text.col=brewer.pal(5,"Set1")[plotco
l])
}
```

```
par(mfrow=c(2,3), oma = c(5,5,1,5) + 0.1, mar = c(0,0,0,0), family="serif", cex=1)

# Data from A cultures
mediumplot(mediumtest1[1:12,4],mediumtest1[13:24,4],mediumtest1[25:36,4],"A",1)

axis(2, at=seq(0,900000,200000), labels=format(seq(0,900000,200000), big.mark=" ", sc
ientific=FALSE), las=1); mtext(2, text="Cells /ml", line=4, col="black")

# Data from B cultures
mediumplot(mediumtest1[37:48,4],mediumtest1[49:60,4],mediumtest1[61:72,4],"B",2)
points(1:237,mediumfunc, type="l", col="dimgray") # the growth model

# Data from C cultures
mediumplot(mediumtest1[73:84,4],mediumtest1[85:96,4],mediumtest1[97:108,4],"C",3)
points(1:237,mediumfunc, type="l", col="dimgray") # the growth model

axis(1, seq(0,240,48), labels=seq(0,10,2))

# Data from D cultures
mediumplot(mediumtest1[109:120,4],mediumtest1[121:132,4],mediumtest1[133:14
4,4],"D",4)
points(1:237,mediumfunc, type="l", col="dimgray") # the growth model

axis(2, at=seq(0,900000,200000), labels=format(seq(0,900000,200000), big.mark=" ", sc
ientific=FALSE), las=1)
mtext(2, text="Cells /ml", line=4, col="black"); axis(1, seq(0,240,48), labels=se
q(0,10,2))

# Data from E cultures
mediumplot(mediumtest1[145:156,4],mediumtest1[157:168,4],mediumtest1[169:18
0,4],"E",5)
points(1:237,mediumfunc, type="l",col="dimgray" ) # the growth model

axis(1, seq(0,240,48), labels=seq(0,10,2)); mtext(1, text="Days", line=2.5)
```

APPENDIX C

Model and parameter values for the *Chlamydomonas - Brachionus* system of continuous cultures

The model equations and the parameter values for the *Chlamydomonas - Brachionus* system that are described in Becks *et al*. (2010) are published as supporting information accompanying the journal article. This model has four state variables

- ***N*** that denotes the concentration of the limiting substrate (Nitrogen, µmol/l)
- $\boldsymbol{C_j}$ that denotes the concentration of algal cells (10^6 cells/ml), and where j=1,2 indicates the two algal clones
- ***B*** that denotes the concentration of breeding rotifers (individuals/ml)
- ***S*** that denotes the concentration of senescent rotifers (individuals/ml)

And the model is as follows:

$$\frac{dN}{dt} = \delta(N_i - N) - \frac{\rho C_1 N}{K_{c,1} + N} - \frac{\rho C_2 N}{K_{c,2} + N}$$

$$\frac{dC_j}{dt} = C_j \left[\frac{X_C \rho N}{K_{c,j} + N} - \frac{p_j G(B+S)}{K_B + \max(Q, Q^*)} - \delta\right], \quad j = 1,2$$

$$\frac{dB}{dt} = B\left[\frac{X_B G Q}{K_B + \max(Q, Q^*)} - (\delta + m + \lambda)\right]$$

$$\frac{dS}{dt} = \lambda B - (\delta + m)S$$

Where $\boldsymbol{Q}$ is the sum of the total prey available for the predator, $\boldsymbol{Q = p_1 C_1 + p_2 C_2}$, i.e. the sum of the concentration of the algal clones ($\boldsymbol{C_1}$, $\boldsymbol{C_2}$) scaled by their estimated palatability ($\boldsymbol{p_1}$, $\boldsymbol{p_2}$). The other parameter values and a description of them are given below in table C.1.

Table C.1. Parameter values as listed in the supporting information of Becks *et al*. (2010) (with a few amendments).

Parameter	Description	Value	Source
Experimental parameters			
N_i	Concentration of limiting nutrient	160 µmol N/l	
δ	Culture dilution rate	0.1 - 0.5 / day	
V	Culture volume	330 ml	
Algal parameters			
X_C	Algal conversion	$0.0027 \cdot 10^9$ cells/ µmol N	Becks
B_C	Maximum algal per-capita recruitment	0.72 / day	Becks
ρ	Maximum nutrient uptake rate (B_C/ X_C)	270 µmol N/ 10^9 cells/ day	-
$K_{c,1}$	Half saturation constant, defended algae	dependent on p_1	Becks*
$K_{c,2}$	Half saturation constant, undefended algae	2.2 µmol N/l	Becks
p_1	Algal palatability, defended algae	variable (from 1 to 0)	Becks*
p_2	Algal palatability, undefended algae	1 ($\geq$ 0.95)	Becks*
Rotifer parameters			
m	Rotifer mortality	0.055 / day	F&Y
λ	Rotifer senescence rate	0.4 / day	F&Y
Q^*	Critical prey density for rotifer clearance	$0.05 \cdot 10^6$ algal cells/ml	Felpeto
B_B	Maximum rotifer per-capita recruitment	1.9 /day	F&Y/Fitted
X_B	Rotifer conversion	170 rotifers /10^6 algal cells	Fitted
K_B	Rotifer half-saturation constant	$0.15 \cdot 10^6$ algal cells/ml	Fitted
G	Rotifer grazing rate parameter = B_B/ X_B	0.011 ml/rotifer/day	-

The parameters with Becks* as source were originally not listed in the table, but described in the text. When cultured together with rotifers, *Chlamydomonas reinhardtii* has been observed to form clusters of cells (palmelloids), and Becks and colleagues (2010) assume that this change in morphology would increase the algal half saturation constant ($\boldsymbol{K_c}$) because it reduces the cell surface area in direct contact with the growth medium. They have assumed a linear tradeoff curve between the half saturation constant ($\boldsymbol{K_c}$) and the algal palatability ($\boldsymbol{p}$), with $\boldsymbol{K_{c,2}}$ = 2.2 µmol N/l for the undefended algae ($\boldsymbol{p}$ = 1), and $\boldsymbol{K_{c,1}}$ = 8 µmol N/l for the algae with maximum defence ($\boldsymbol{p}$ = 0).

The other algal parameters have Becks and colleagues estimated from batch culture experiments with *C. reinhardtii* and initial nitrate concentration of 4, 80, 160 and 400 µmol N/l. To estimate the parameter values from these data, they write that they used nonlinear

least squares trajectory-matching of the model with rotifers absent, a single algal clone and the dilution rate set to 0.

The rotifer parameters of mortality (***m***), senescent rate (***λ***) and maximum per capita recruitment ($\boldsymbol{B_B}$) were determined during the course of the previous rotifer-algal studies at the Hairston lab (Fussmann *et al.* 2000; Yoshida *et al.* 2003). Counts of dead rotifers from continuous cultures were used to estimate rotifer mortality, and counts of subitaneous eggs per rotifer were used to estimate the senescence rate (Fussmann *et al*. 2000). Fussmann and colleagues extracted the value for the maximum rotifer per capita recruitment ($\boldsymbol{B_B}$) from exponentially growing *Brachionus calyciflorus* under high algal density (*Chlorella vulgaris*) and determined it to be 2.25 per day (Fussmann *et al*. 2000). Yoshida and colleagues (2003) later estimated $\boldsymbol{B_B}$ to be 1.9 per day (fed *C. vulgaris*), a value which Becks *et al*. (2010) argue is close to the observed recruitment by *B. calyciflorus* feeding on *C. reinhardtii*.

The value for the critical prey density for rotifer clearance (***Q****) was estimated from batch culture experiments at the Hairston lab by Aldo Barreiro Felpeto. Becks and colleagues estimated the value for the rotifer conversion factor ($\boldsymbol{X_B}$) and the rotifer half saturation constant ($\boldsymbol{K_B}$) by probe matching to features of the initial phase from the data in the rotifer-algal experiment with ungrazed algae. Those features of the initial phase were the rotifer density at the initial rotifer peak, the minimum algal density following the rotifer peak, and the time between the rotifer peak and the next algal peak.

Intrinsic to the *Chlamydomonas* - *Brachionus* model are the organisms' functional and numerical responses. Becks and colleagues (2010) report that batch culture experiments with *B. calyciflorus* feeding on *C. reinhardtii* indicate that the rotifer functional response is linear (type I) at low food abundance (below *Q**), while it follows a type II response at high food abundances (see figure D.1). This is an observation that also Yoshida and colleagues (2003) did in experiments with *B. calyciflorus* feeding on *C. vulgaris.* The numerical response of *B. calyciflorus* feeding on *C. reinhardtii* is plotted in figure D.2.

The algal functional response is described as a Holling's type II for both the undefended and defended clone (figure D.3). As described above, it is assumed that the formation of palmelloids in the defended clone decreases its nutrient intake rate, and this is accounted for by the half saturation constant ($\boldsymbol{K_c}$). The value for the half saturation constant in the defended clone is dependent on the degree of palmella formation. In the plots below (D.3 and D.4), I have chosen a half saturation constant of 4.4 µmol N/l for the defended clone, i.e. a clone with an intermediate degree of defence (***p***=0.62).

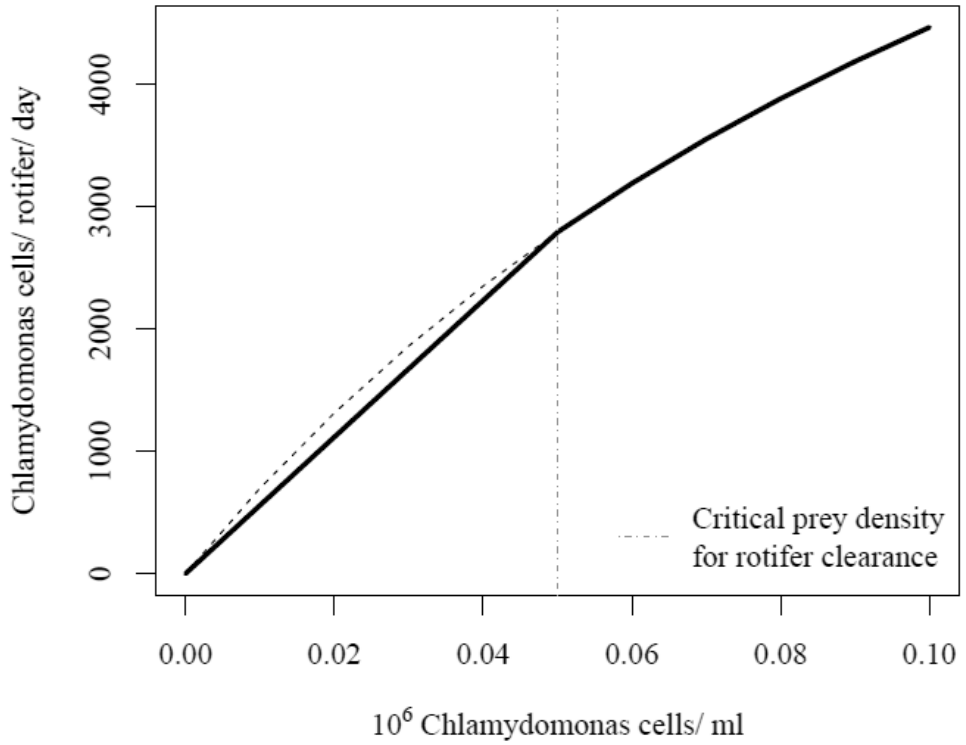

Figure C.1. The intake rate of *B. calyciflorus* as a function of algal density (functional response, Holling's type I ½). The dashed line shows the trajectory of a type II response.

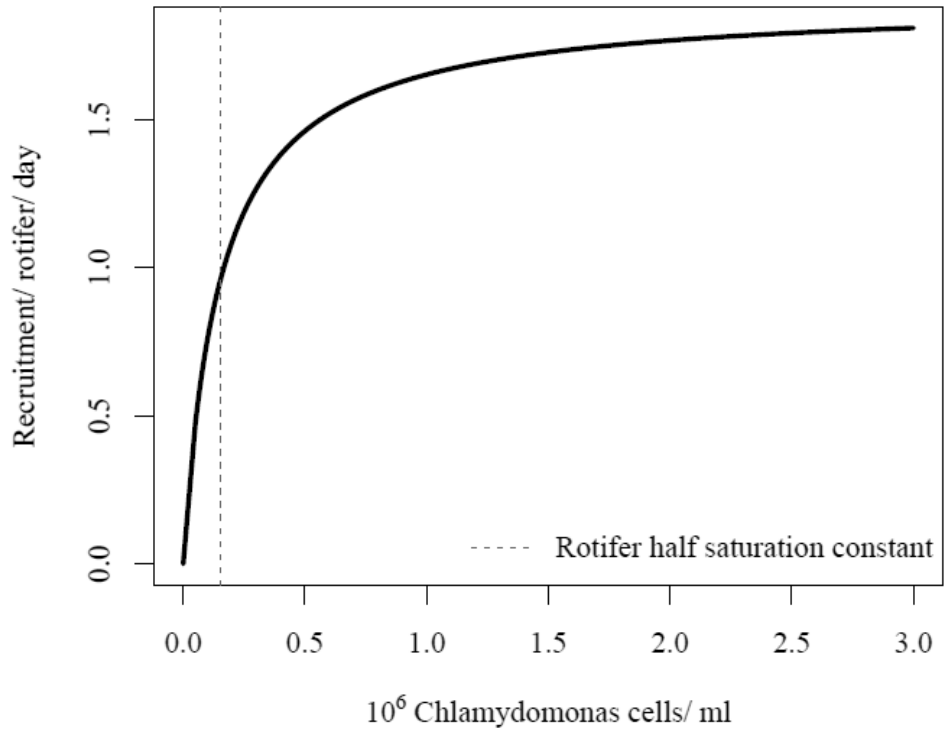

Figure C.2. The reproduction rate of *B. calyciflorus* as a function of algal density (numerical response).

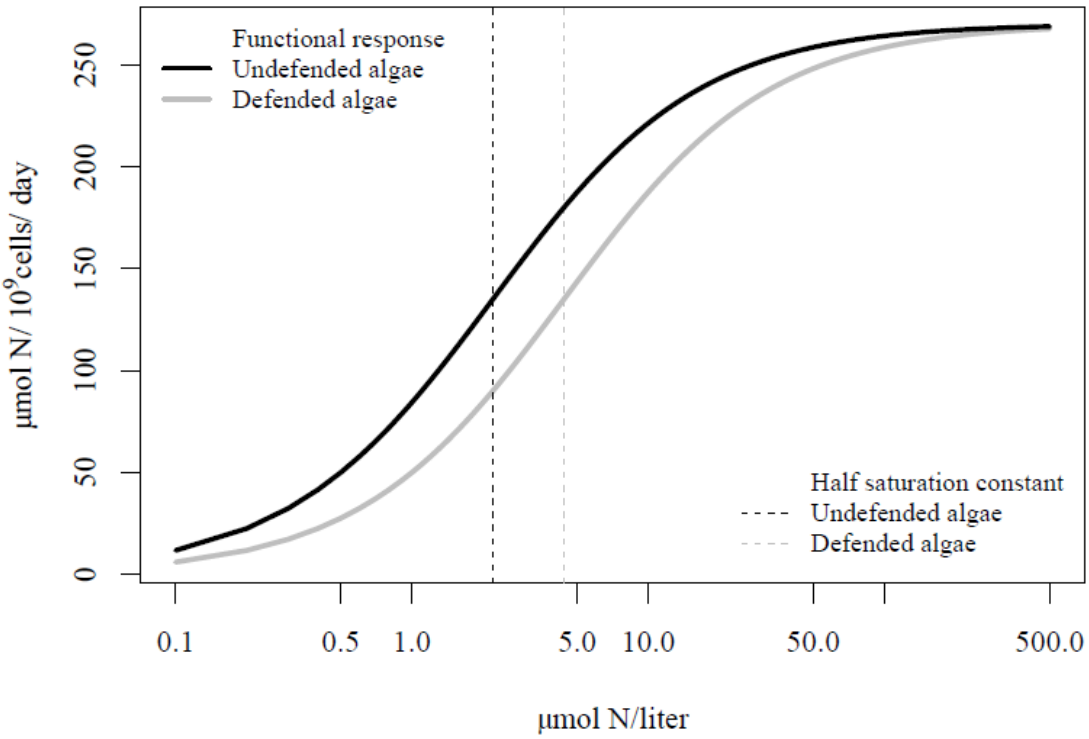

Figure C.3. The nutrient intake rate of two clones of *C. reinhardtii* as a function of nutrient concentration (Holling's type II). The function looks like a type III response because the x-axis is log scaled.

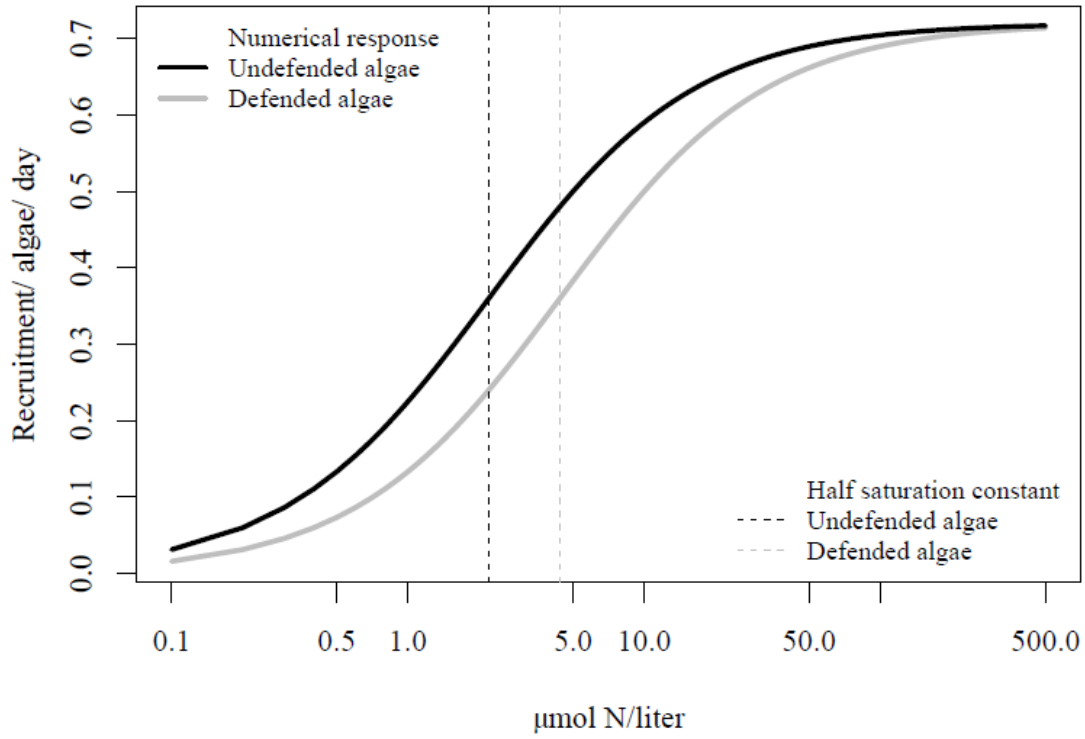

Figure C.4. The growth rate of two clones of *C. reinhardtii* as a function of nutrient concentration.

APPENDIX D

Schematic drawing and pictures of the algal growth experiment

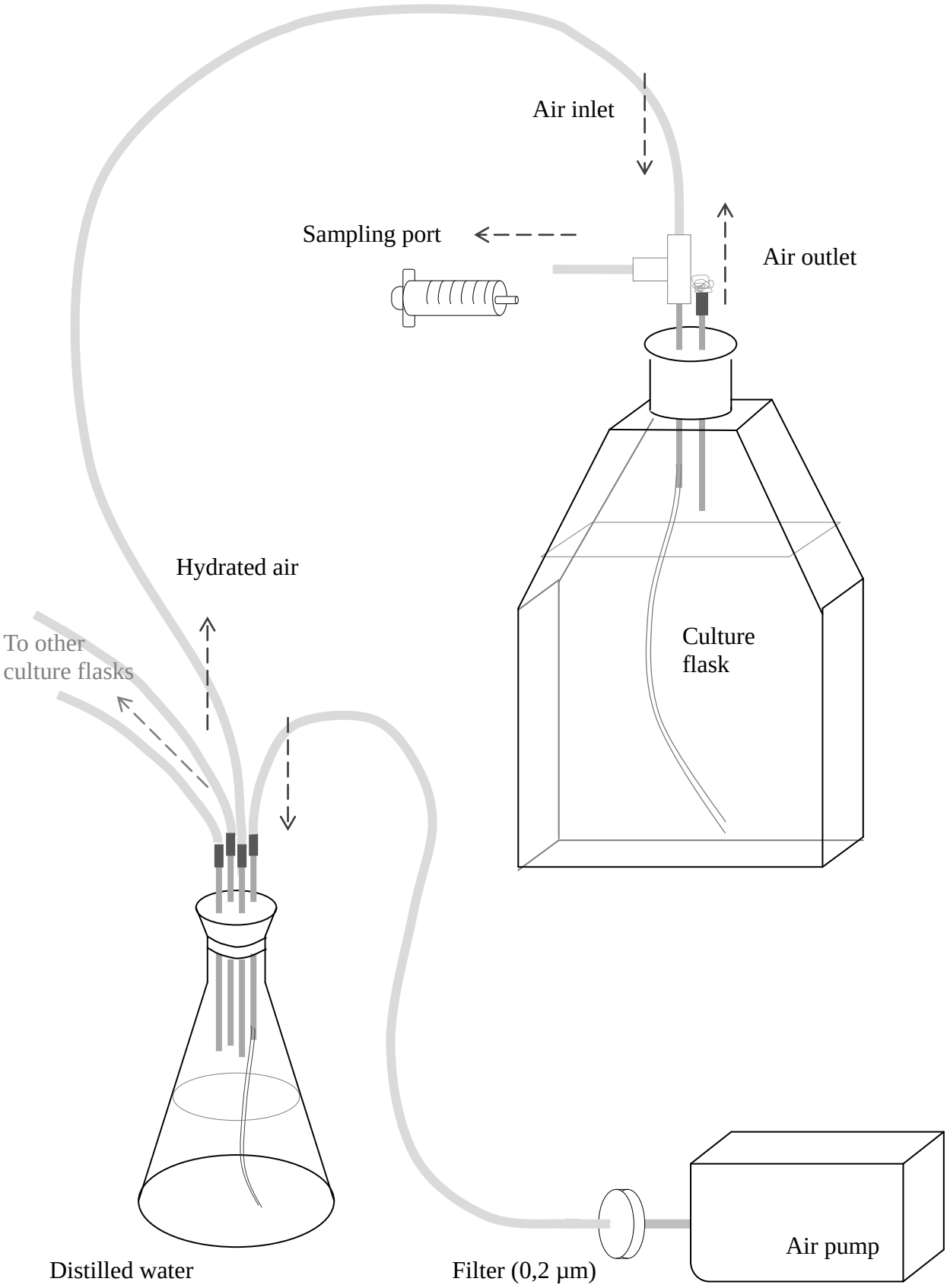

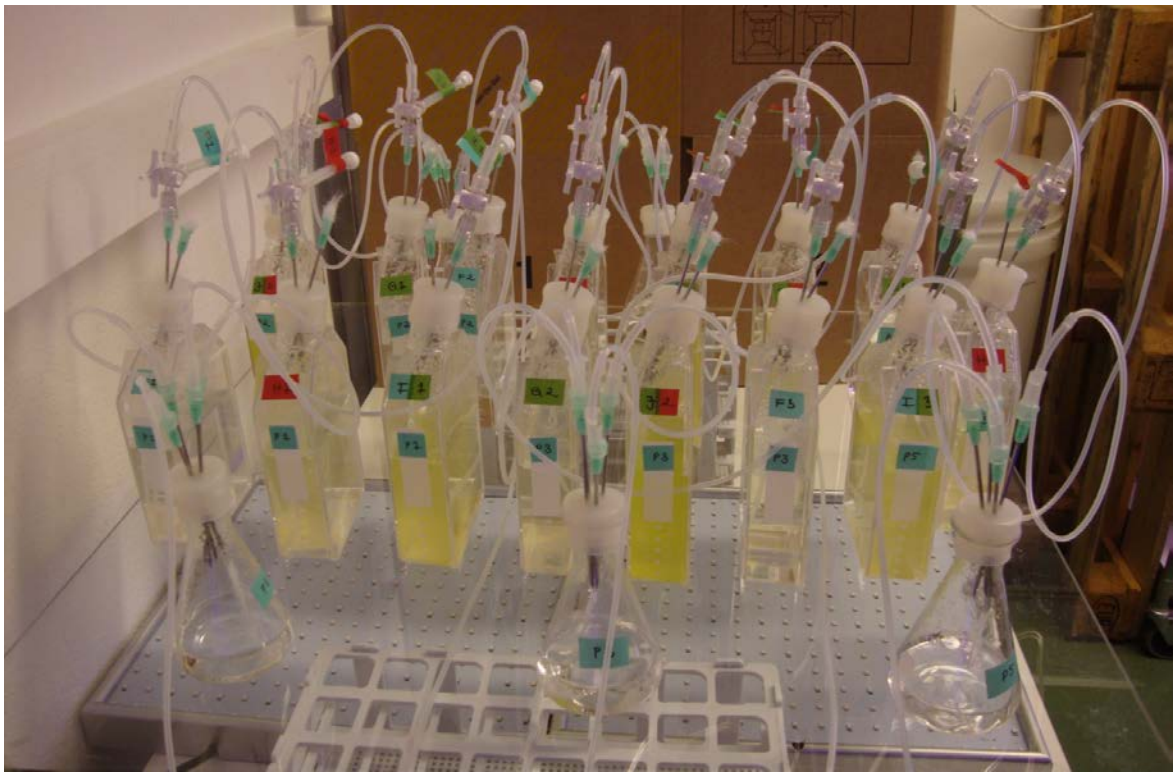

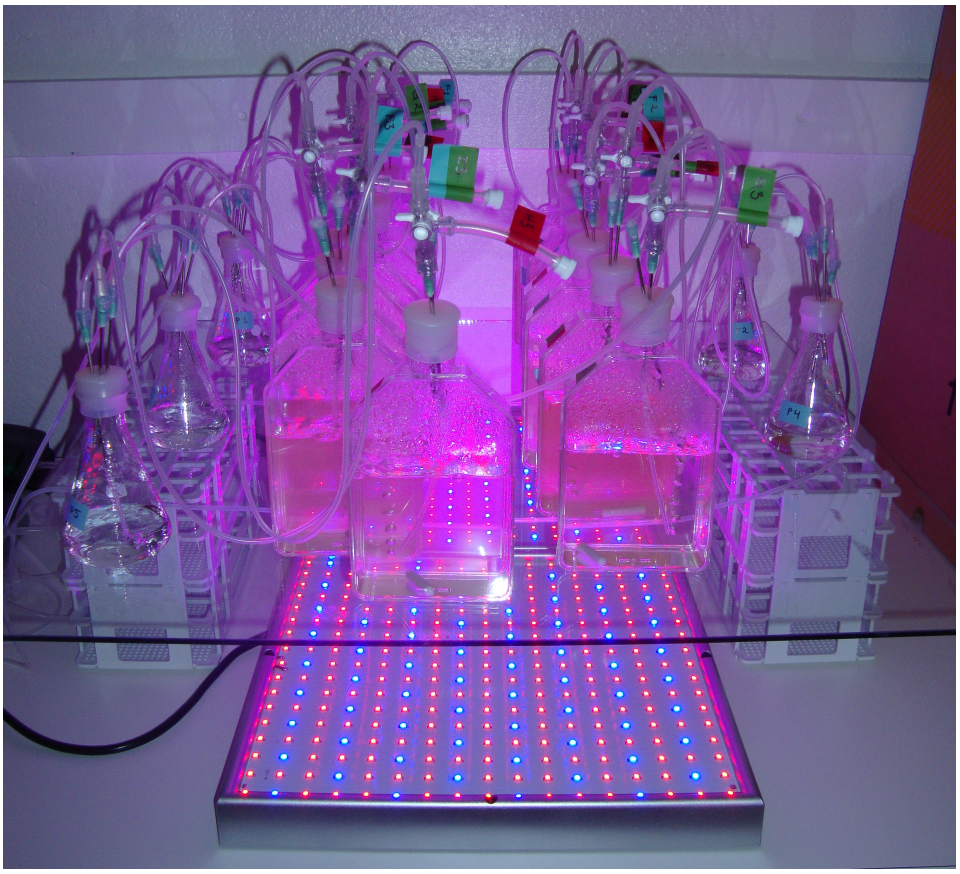

Pictures from the 10th day of the experiment.

Appendix E

Analysis of growth curves and calculation of growth parameters

This appendix serves the analysis and calculations supporting the results in part **1.2**. The goal with this analysis is to extract information from the growth curves of *C. reinhardtii* and use these to calculate the algal parameters for the *Chlamydomonas - Brachionus* model.

A large part of the appendix shows the nonlinear mixed-effects modelling of the results from the algal growth experiment, and this was, as in the medium test, done with the the guidance of Pinheiro and Bates's *Mixed-Effects Models in S and S-PLUS* (2000). The introduction to nlme given in the appendix for the medium test (appendix B), and most of the reasonings given along that analysis, apply for the current nlme analysis too. However, for the sake of simplicity, it will only be repeated briefly.

As in the medium test, the logistic function will be fitted to the data. The logistic function is a mechanistic model, meaning that it is based on a model of the mechanism producing the response, and the parameters have therefore a biological interpretation (Pinheiro & Bates 2000).

Recall the parameterization of the logistic equation in the nlme package:

$$y_{(x)} = \frac{Asym}{1 + e^{-(\frac{x - xmid}{scal})}}$$

where **Asym** denote the carrying capacity, **xmid** the x-value for the inflection point of the curve, and where **scal** is inversely proportional to the population growth rate (**scal=1/r**) (ibid.; Tom Andersen *personal communication*).

The parameters of particular interest in this analysis are **Asym** and **scal**, which will be used to make estimations of algal conversion parameter (X_c) and the parameter for the maximum algal per capita reqruitment (B_c).

Analysis of growth curves using nonlinear mixed-effects modelling

Required packages

```
library(nlme) # Pinheiro and Bates's accompanying R package
library(RColorBrewer) # colour palettes for plotting
library(knitr) # for nicer looking tables
```

Reading the data file

```
algaegrowth1 <-read.table("Algevekst.nlme.txt", header=TRUE)
algaegrowth.grouped <- groupedData(cells~hours | replicate, algaegrowth1, order.group
s=F)
```

Plot of the data (code hidden)

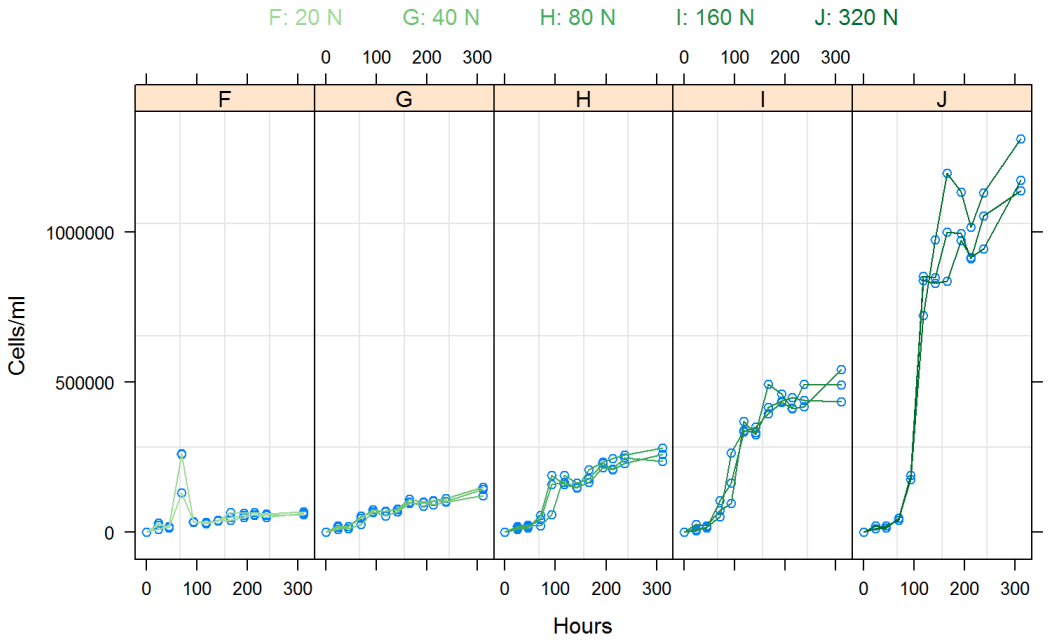

The counts for the F-cultures at 70 hours are much higher than expected. I am not aware of any contamination, but it cannot be the correct count. As these datapoints also cause problems for the nlme model fitting, I exclude them from the analysis.

```
algaegrowth <- algaegrowth1[-c(4,16,28),]
algaegrowth.grouped <- groupedData(cells~hours | replicate, algaegrowth, order.group
s=F)
```

Starting the NLME-fit

Separate fits by replicate

The self starting logistic function SSlogis makes separate fits for each of the 15 replicates.

```
growth.lis <- nlsList(SSlogis, algaegrowth.grouped)

plot(intervals(growth.lis), layout=c(3,1))
pairs(growth.lis, id=0.1)
```

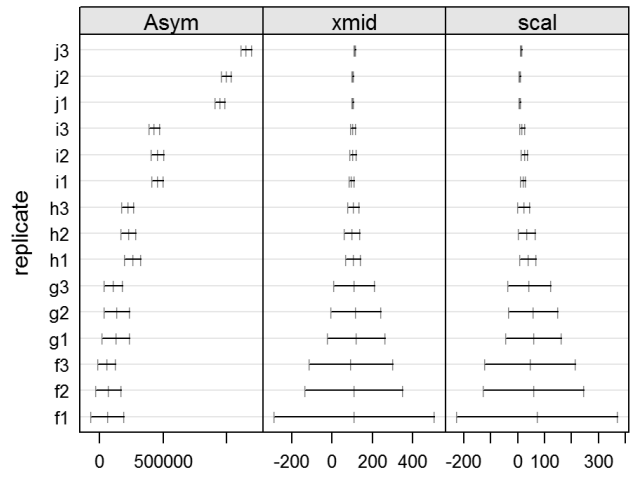

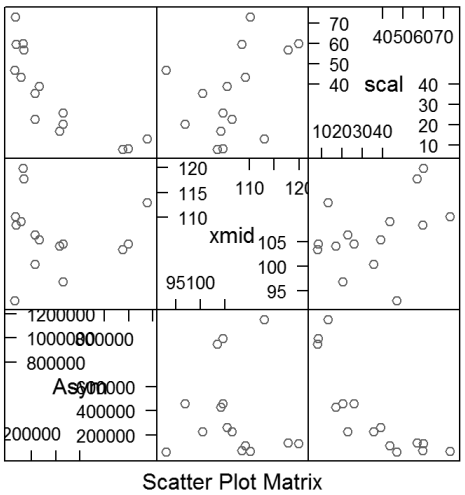

The variability of the Asym estimates is small within each medium type compared to the variation between the medium types. This is as expected; increasing the nutrient level should increase the system's carrying capacity. It is thus obvious that *medium type* should be included as a covariate explaining the variability in the Asym estimates.

The pattern is less obvious for the scal and xmid estimates. Here the variability is small for the cultures with high nutrient levels and large for the cultures with low. This is probably a symptom of the inadequacy current model, as this changes when important covariates are included in the model.

Combined fit to a single nlme model

I make a combined fit and add medium type as a covariate in the model to explain the variation observed in the Asym estimates.

```
agrowth.nlme <- nlme(growth.lis) # the combined nlme fit

agrowth.nlme.Asym <- update(agrowth.nlme, fixed = list(Asym ~ medium, scal + xmid ~
1), start = c(377748, 0, 0, 0, 0, 25,101)) # add covariate structure to explain Asym
variation
```

Diagnostic plots to assess the model assumptions

```
plot(agrowth.nlme.Asym, resid(., type="n") ~ hours | medium, abline = 0, cex=0.8)
qqnorm(agrowth.nlme.Asym, abline=c(0,1), cex=0.8)
```

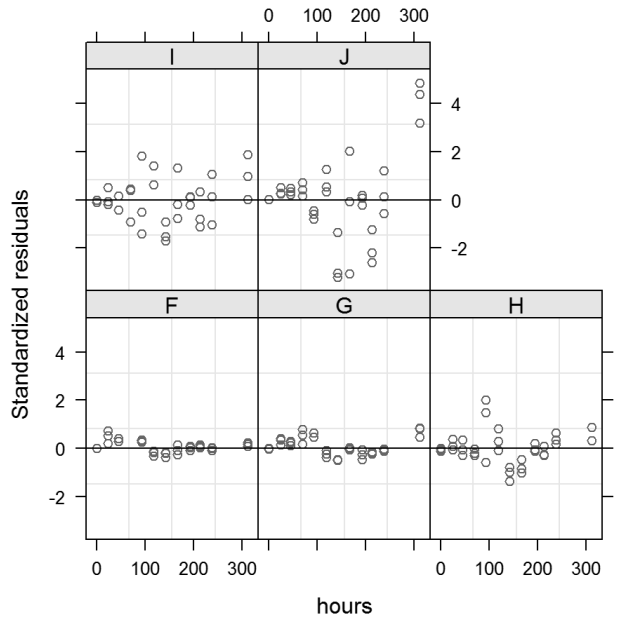

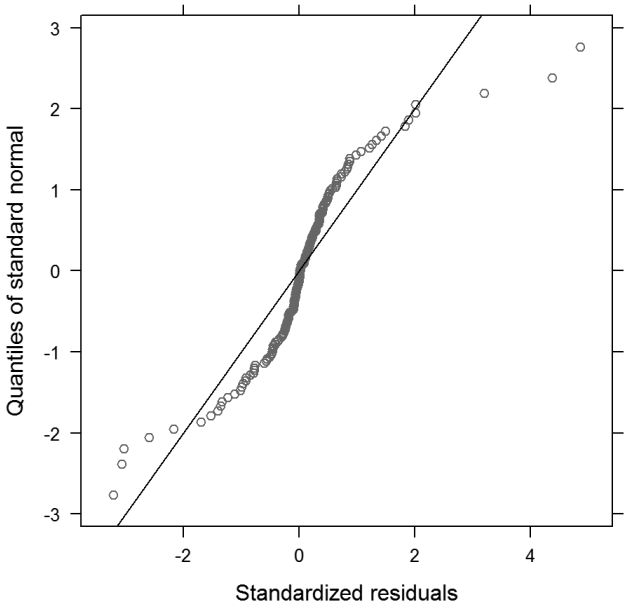

The diagnostic plots show that the residuals are heteroscedastic and possibly also autocorrelated. It is thus necessary to test for the inclusion of variance and correlation functions.

Fixing heteroscedasticity

varPower - one parameter variance function

```
agrowth.nlme.Asym.var1 <- update(agrowth.nlme.Asym, weights = varPower())
kable(anova(agrowth.nlme.Asym, agrowth.nlme.Asym.var1)[,-1])
```

	Model	df	AIC	BIC	logLik	Test	L.Ratio	p-value
agrowth.nlme.Asym	1	14	4341.892	4386.358	-2156.946		NA	NA
agrowth.nlme.Asym.var1	2	15	4147.624	4195.266	-2058.812	1 vs 2	196.2677	0

```
plot(agrowth.nlme.Asym.var1, resid(., type="n") ~ hours | medium, abline = 0, ce
x=0.8)
qqnorm(agrowth.nlme.Asym.var1, abline=c(0,1), cex=0.8)
```

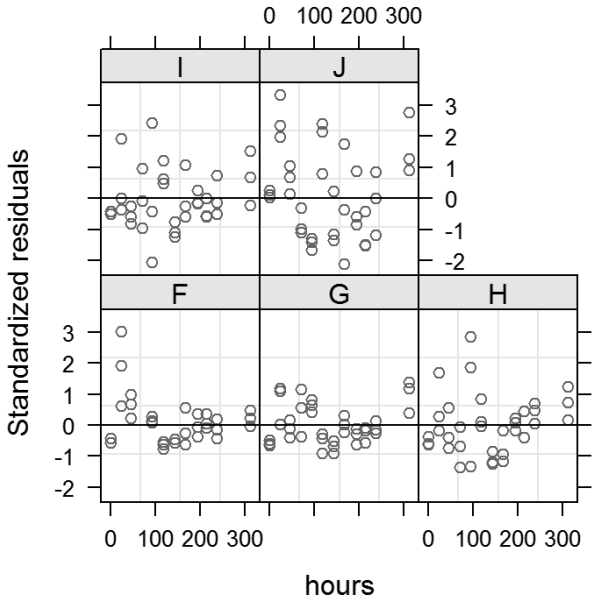

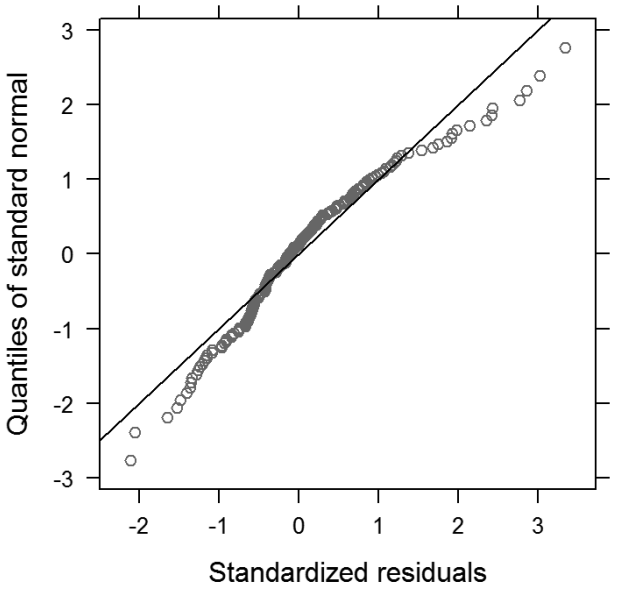

The model with variance function has a significantly better fit than the model without, and I thus keep it in the model. Including the variance function have rendered the variance more constant (left figure), and possibly also removed some signs of autocorrelation (right figure).

Correlation structures

```
plot(ACF(agrowth.nlme.Asym.var1, maxLag=8, resType="normalized"), alpha = 0.05)
```

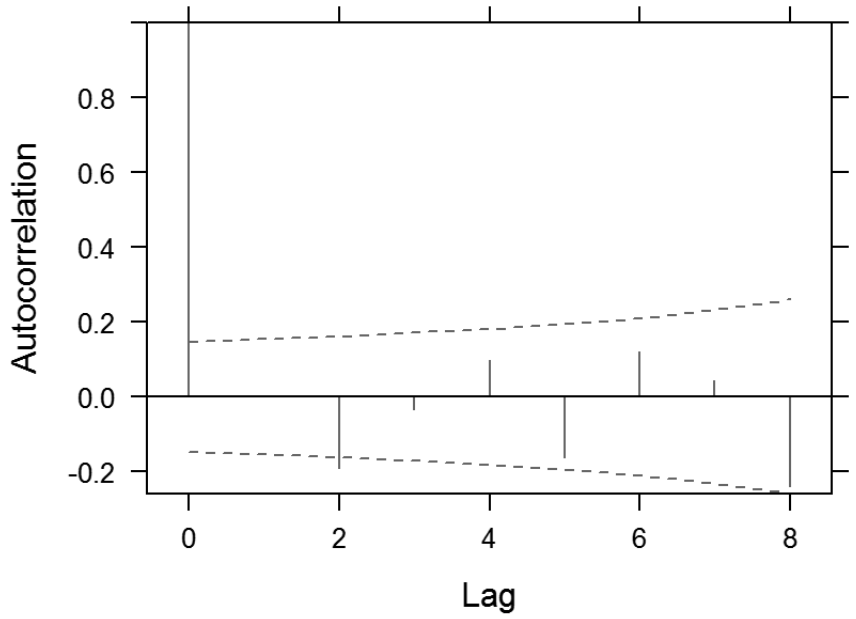

The plot of the empirical autocorrelation function (ACF) shows no evident sign of depedency among the groups' residuals. Lag 2 is barely significant, whereas dependencies at lag 1 seem to be nonexistent. Still, I tested whether the inclusion of correlation structures would improve the model. Of the four structures tested

- corAR1, corCAR1 and ARMA(1,1) could not be fitted, and
- corARMA(p=0, q=2) did not improve the model.

I therefor did not include any correlation structure in the model.

Random effects

After the recent model changes, I extract the random effects anew to investigate whether the model's fixed and random effects structure should be refined further.

```
agrowth.nlme.Asym.var1.RE <- ranef(agrowth.nlme.Asym.var1, augFrame=T)
plot(agrowth.nlme.Asym.var1.RE, form=~medium, layout=c(3,1))
pairs(agrowth.nlme.Asym.var1.RE[1:3])
```

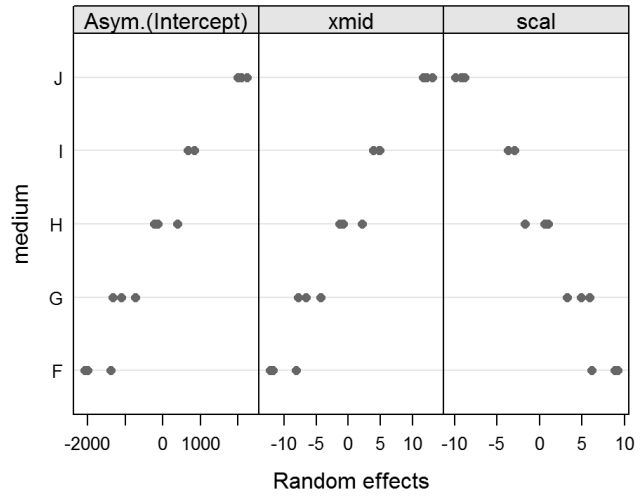

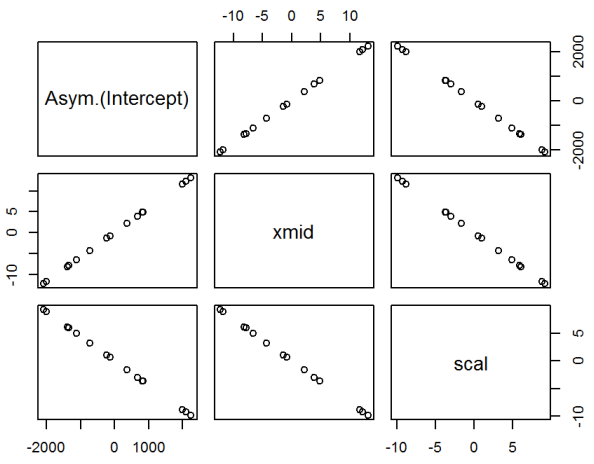

There is a strong positive correlation between Asym and xmid random effects, and a strong negative correlation between scal and the random effects for the other two parameters. Notice that the comparisons between the parameters random effects are done with the intercept value for Asym (Asym estimate for medium F) and not the Asym estimates for each medium type.

It is to be expected that the inflection point of the curve (xmid) comes at successively later timepoints with an increasing carrrying capacity of the system (Asym) (given that the initial population sizes are equal, which they were in this case). That these two parameters are positively correlated is therefore reasonable, and it implies that medium type should be included as a covariate to explain the variation observed in the xmid estimates.

Include medium type to explain variation in xmid estimates

```
agrowth.nlme.AX <- update(agrowth.nlme.Asym.var1, fixed = list(Asym ~ medium, xmid ~
medium, scal ~ 1), start = c(60665, 60665+49163,60665+167370,60665+387486,60665+99110
8, 0, 0, 0, 0, 0, 23))

kable(anova(agrowth.nlme.Asym.var1,agrowth.nlme.AX)[,-1])
```

	Model	df	AIC	BIC	logLik	Test	L.Ratio	p-value
agrowth.nlme.Asym.var1	1	15	4147.624	4195.266	-2058.812		NA	NA
agrowth.nlme.AX	2	19	4112.538	4172.885	-2037.269	1 vs 2	43.08588	0

The model with the additional covariate structure has a significantly better fit, and I thus keep it in the model.

Currently, the model contain random effects estimates for all parameters, which is probably redundant, especially since the variation in Asym and xmid estimates are explained by the differences in medium types. I investigated three other random effects structures in the model: keeping only random effects for Asym, only for scal and only for xmid. They had all lower AIC and BIC measures compared to the model with random effects estimates for all parameters, proving that the random effects structure was over-parameterized. However, all three model performed equally well (have the exact same likelihood measures). This likely indicates a strong correlation between the random effects and possibly also that they all could be removed from the model. I did not find a way to remove all random effect, so I choose the model with random effects for scal.

```
agrowth.nlme.AX.r2 <- update(agrowth.nlme.AX, random=scal ~ 1) # only random effect
for scal
kable(anova(agrowth.nlme.AX, agrowth.nlme.AX.r2)[,-1])
```

	Model	df	AIC	BIC	logLik	Test	L.Ratio	p-value
agrowth.nlme.AX	1	19	4112.538	4172.885	-2037.269		NA	NA
agrowth.nlme.AX.r2	2	14	4102.538	4147.004	-2037.269	1 vs 2	9.6e-06	1

```
agrowth.nlme.r.RE <- ranef(agrowth.nlme.AX.r2, augFrame=T)
plot(agrowth.nlme.r.RE, form=~medium)
```

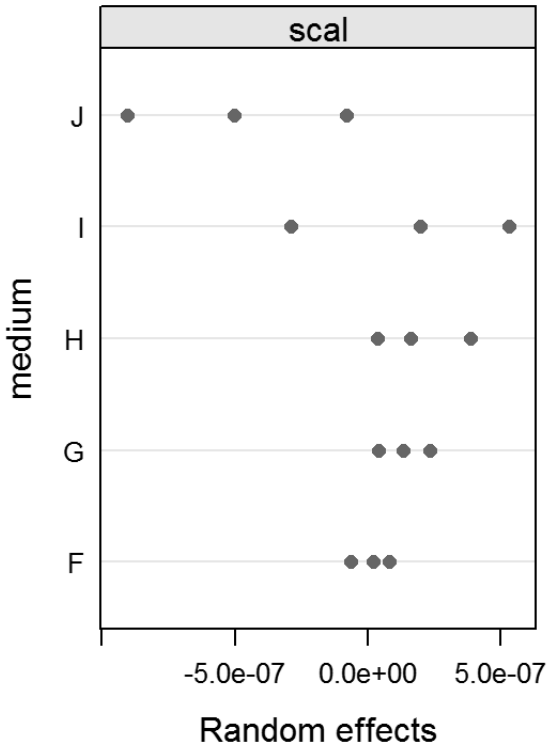

The standard deviation for the scal random effect parameter is very small (see left figure and model output below), and I would therefore assume that it has a minor effect on the model's fixed effects estimates.

The plot on the left shows how the individual scal estimates for each of the 15 cultures deviate from the scal fixed effect. With a quick glance, it seems to suggest that there is a substantial difference in the scal parameter between the medium types. However, the value at which they differ are at the maximum $5.34 \cdot 10^{-7}$, which have no practical significance. Consequenlty, I can conclude that the growth rate parameter of *C. reinhardtii* is equal for all medium types.

The growth model

```
## Nonlinear mixed-effects model fit by maximum likelihood
##   Model: cells ~ SSlogis(hours, Asym, xmid, scal)
##   Data: algaegrowth.grouped
##   Log-likelihood: -2037.269
##   Fixed: list(Asym ~ medium, xmid ~ medium, scal ~ 1)
## Asym.(Intercept)     Asym.mediumG     Asym.mediumH     Asym.mediumI
##     4.959944e+04     4.738626e+04     1.666347e+05     3.906073e+05
##     Asym.mediumJ xmid.(Intercept)     xmid.mediumG     xmid.mediumH
##     1.037023e+06     4.419792e+01     2.489433e+01     4.329865e+01
##     xmid.mediumI     xmid.mediumJ             scal
##     5.421773e+01     7.090857e+01     1.791278e+01
##
## Random effects:
##  Formula: scal ~ 1 | replicate
##                 scal Residual
## StdDev: 0.0008380237 25.26198
##
## Variance function:
##  Structure: Power of variance covariate
##  Formula: ~fitted(.)
##  Parameter estimates:
##    power
## 0.609766
## Number of Observations: 177
## Number of Groups: 15
```

Extracting model coefficients

```
coefficients <- intervals(model, which="fixed")

Scal.coef <- coefficients$fixed[11,]

Asym.coef <- coefficients$fixed[1:5,] # extracting Asym coefficients
Asym.est <- Asym.coef[2:5,]+Asym.coef[1,2] # calculating the estimates
Asym.est <- rbind(Asym.coef[1,], Asym.est)

Xmid.coef <- coefficients$fixed[6:10,] # extracting Xmid coefficients
Xmid.est <- Xmid.coef[2:5,]+Xmid.coef[1,2]
Xmid.est <- rbind(Xmid.coef[1,], Xmid.est)
```

Making curves for plotting

```
logist <- function(x, Asym, xmid, scal) Asym/(1 + exp(-(x-xmid)/scal))

growthfuncF <- logist(1:315, Asym.est[1,2] , Xmid.est[1,2], Scal.coef[2])
growthfuncG <- logist(1:315, Asym.est[2,2] , Xmid.est[2,2], Scal.coef[2])
growthfuncH <- logist(1:315, Asym.est[3,2] , Xmid.est[3,2], Scal.coef[2])
growthfuncI <- logist(1:315, Asym.est[4,2] , Xmid.est[4,2], Scal.coef[2])
growthfuncJ <- logist(1:315, Asym.est[5,2] , Xmid.est[5,2], Scal.coef[2])
```

Code rendering Figure 1.2 (top).

Make a plot function

```
growthplot <- function(rep1, rep2, rep3, name, plotcol){

points(algaegrowth1[1:12,3],rep1, pch=19, col=brewer.pal(9,"Greens")[plotcol], ce
x=0.5)
points(algaegrowth1[1:12,3],rep2, pch=19, col=brewer.pal(9,"Greens")[plotcol], ce
x=0.5)
points(algaegrowth1[1:12,3],rep3, pch=19, col=brewer.pal(9,"Greens")[plotcol], ce
x=0.5)

legend("topleft", legend=c("320 N","160 N","80 N","40 N","20 N"), bty="n", cex=1.2, t
ext.col=rev(brewer.pal(9,"Greens")[4:8]))
}
```

Raw data with fitted model

```
par(family="serif", mar=c(4,6,2,4)) # adjust the graphical parameters

plot(1,1,type="n", ylim=c(0,1250000), yaxt="n", xaxt="n", xlim=c(0,315), xlab="", yla
b="")

growthplot(algaegrowth1[1:12,4],algaegrowth1[13:24,4],algaegrowth1[25:36,4], "F", 4)
points(1:315,growthfuncF, type="l", col=brewer.pal(9,"Greens")[4]) # the growth model

growthplot(algaegrowth1[37:48,4],algaegrowth1[49:60,4],algaegrowth1[61:72,4], "G", 5)
points(1:315,growthfuncG, type="l", col=brewer.pal(9,"Greens")[5])

growthplot(algaegrowth1[73:84,4],algaegrowth1[85:96,4],algaegrowth1[97:108,4], "H",
6)
points(1:315,growthfuncH, type="l", col=brewer.pal(9,"Greens")[6])

growthplot(algaegrowth1[109:120,4],algaegrowth1[121:132,4],algaegrowth1[133:144,4],
"I", 7)
points(1:315,growthfuncI, type="l", col=brewer.pal(9,"Greens")[7])

growthplot(algaegrowth1[145:156,4],algaegrowth1[157:168,4],algaegrowth1[169:180,4],
"J", 8)
points(1:315,growthfuncJ, type="l", col=brewer.pal(9,"Greens")[8])

axis(2, at=seq(0,1250000,200000), labels=format(seq(0,1250000,200000), big.mark=" ",
scientific=FALSE), las=1); mtext(2, text="Cells /ml", line=4, col="black")
axis(1, seq(0,315,48), labels=seq(0,12,2)); mtext(1, text="Days", line=2.5)
```

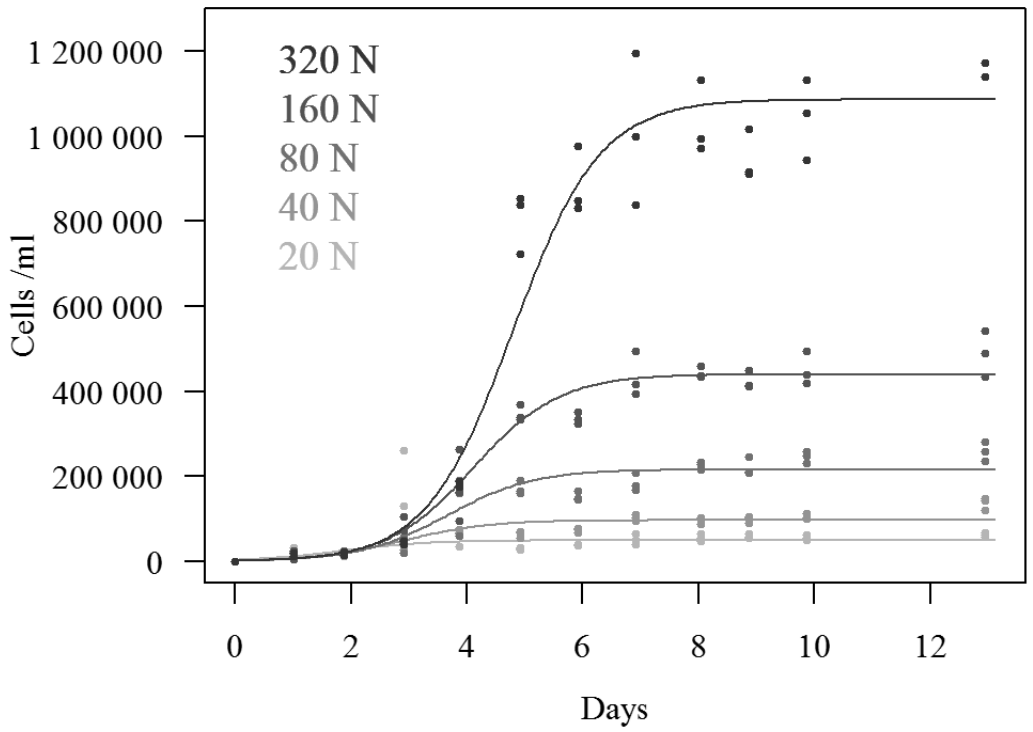

Calculating model parameters

In order to calculate the algal conversion parameter, I fit a linear model to the Asym estimates found above to find the relationship between nutrient concentration and asymptotic algal density.

```
N.conc <- c(20,40,80,160,320)
regression <- lm(Asym.est[,2]~N.conc)
summary(regression)
```

```
##
## Call:
## lm(formula = Asym.est[, 2] ~ N.conc)
##
## Residuals:
##              Asym.mediumG Asym.mediumH Asym.mediumI Asym.mediumJ
##        31627         9790        -9406       -62324        30313
##
## Coefficients:
##             Estimate Std. Error t value Pr(>|t|)
## (Intercept) -51249.6    30245.3  -1.694 0.188750
## N.conc        3461.1      183.1  18.901 0.000323 ***
## ---
## Signif. codes:  0 '***' 0.001 '**' 0.01 '*' 0.05 '.' 0.1 ' ' 1
##
## Residual standard error: 44680 on 3 degrees of freedom
## Multiple R-squared:  0.9917, Adjusted R-squared:  0.9889
## F-statistic: 357.2 on 1 and 3 DF,  p-value: 0.0003233
```

Plot the linear model

```
par(family="serif", mar=c(4,6,2,4))

# Plotting the asym estimates
plot(N.conc, Asym.est[,2], pch=20, ylim=c(0, 1300000), col=brewer.pal(9,"Greens")
[4:8], yaxt="n", ylab="", xlab=expression(paste("Nutrient concentration ",mu,"mol
N/l")), cex=2)

axis(2, at=seq(0,1300000,250000), labels=format(seq(0,1300000,250000),big.mark=" ", s
cientific=FALSE),las=1); mtext(2, text="Asym estimate", line=5)

# Draw the linear model
abline(regression, lty=1)

# and confidence bands
newseq <- seq(0,330)
mpredict <- predict(regression, newdata=data.frame(N.conc=newseq), interval=c("confid
ence"), level=0.95, type="response")
lines(newseq, mpredict[,2], lty=2)
lines(newseq, mpredict[,3], lty=2)
```

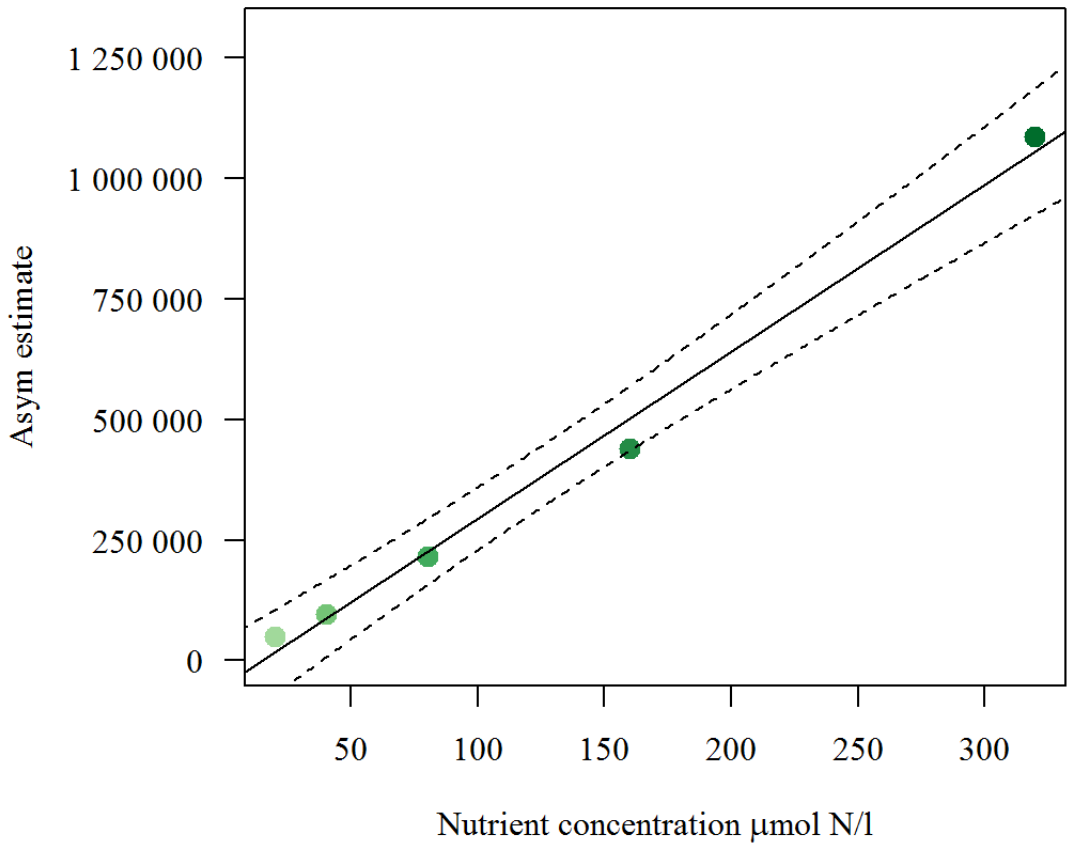

The algal model parameters

Algal conversion factor (10^9 cells/ µmol N), X_c

From the linear model we have that there will be an increase of 3461.1 cells/ml for each µmol N increase per liter, i.e.:

$$3461.1 \frac{cells}{ml} / \frac{\mu molN}{liter}$$

which equals

$$X_c = \underline{0.0034611 \cdot 10^9 \, cells/\mu molN}$$
$$X_c \approx \underline{0.0035 \cdot 10^9 \, cells/\mu molN}$$

Maximum algal per capita reqruitment, B_c

The model's estimate for the growth parameter is:

```
print(Scal.coef)
```

```
##    lower     est.    upper
## 16.44289 17.91278 19.38267
```

This scal parameter is inversely proportional to the population growth rate ($scal = 1/B_c$), and can thus be used to calculate the maximum algal per capita reqruitment (B_c).

$$B_c = \frac{1}{scal} = \frac{1}{17.91} = 0.056\ ind/ind\ per\ hour$$

$$B_c = \frac{1}{17.91} \cdot 24 = \underline{1.34\ ind/ind\ per\ day}$$

95% Confidence interval

$$B_c = \frac{1}{19.38} \cdot 24 - \frac{1}{16.44} \cdot 24 = \underline{1.23 - 1.46\ ind/ind\ per\ day}$$

Maximum nutrient uptake rate, ρ - B_c/X_c

$$\frac{B_c}{X_c} = \frac{1.34}{0.0034611} = \underline{387.2\ \mu molN/10^9\, cells/day}$$

APPENDIX F

Cell counts, fluorescence and distribution of cell sizes

This appendix presents the results for the algal features that were investigated in the algal growth experiment (part 1.2). The results are collated by medium type and comprise the cell counts, the fluorescence and the distribution of cell sizes for each day of the experiment. Beanplots are used to display the distribution of cell sizes. These are plots that draw density curves for groups of numerical data, and it is a visualization method that is available in R by the package *beanplot* written by Peter Kampstra. Several kernel functions are available for plotting the density distribution; here the beanplots are computed using "gaussian".

The fitted growth curves and the values for the xmid parameters (derived in Appendix E) are plotted with the cell counts for each medium type. The xmid parameter designates the x-value for the inflection point of the fitted curve, which equals the time point for the maximum rate of increase. Medium type **F** had an initial nitrate concentration of 20 µmol/l, **G** of 40, **H** of 80, **I** of 160 and **J** of 320 µmol/l. The cell counts for the F-cultures at day three are left out of the plot because of their extreme values (indicated with a star).

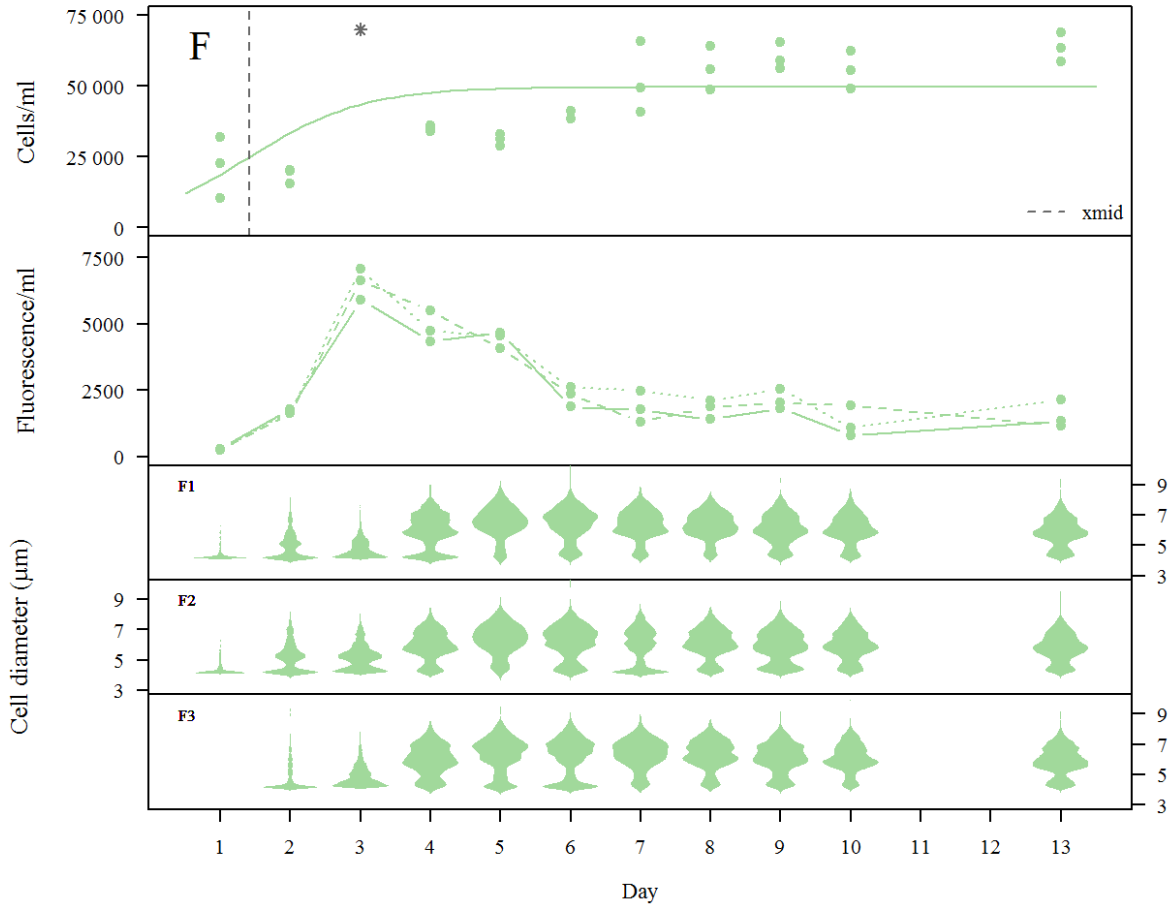

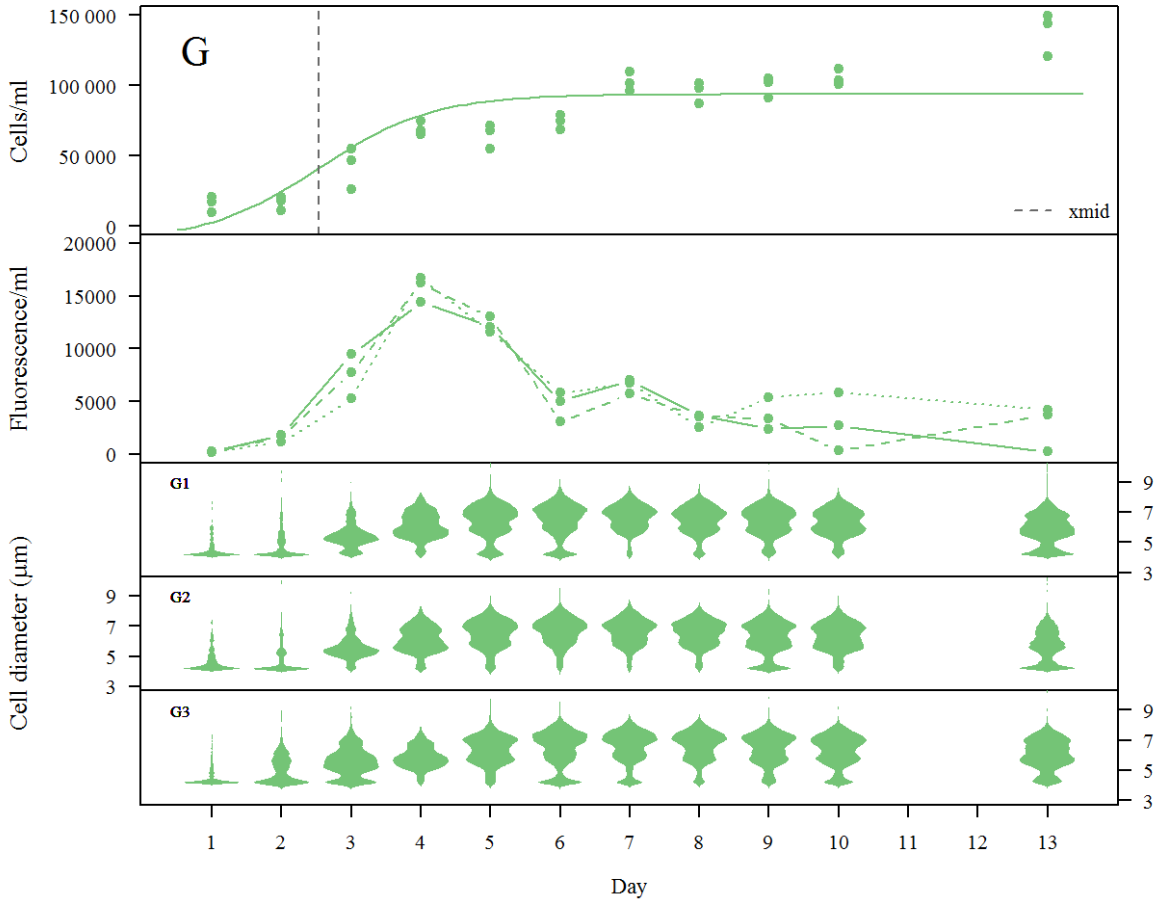
G
Cells/ml
150 000
100 000
50 000
0
xmid
Fluorescence/ml
20000
15000
10000
5000
0
Cell diameter (µm)
G1
G2
G3
9
7
5
3
1
2
3
4
5
6
7
8
9
10
11
12
13
Day

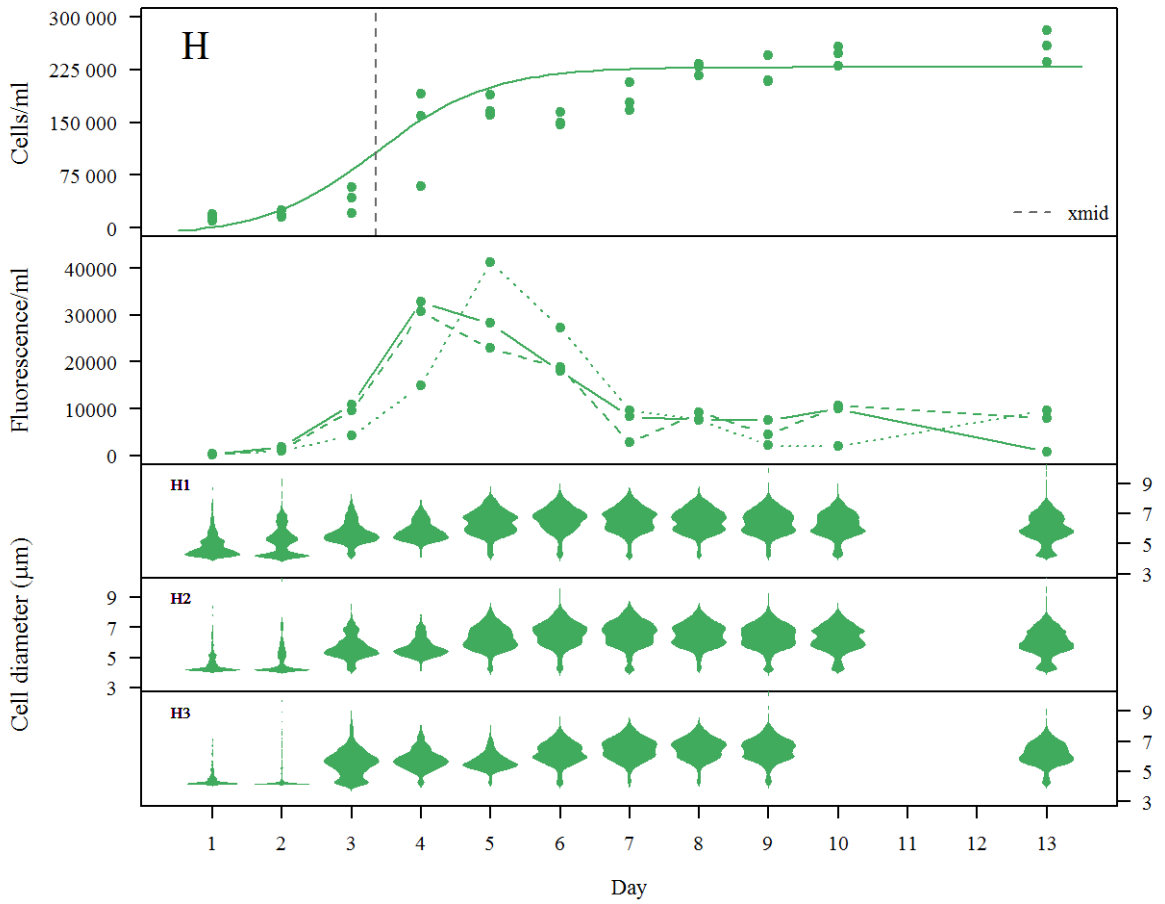
H
Cells/ml
300 000
225 000
150 000
75 000
0
xmid
Fluorescence/ml
40000
30000
20000
10000
0
Cell diameter (µm)
H1
H2
H3
9
7
5
3
1
2
3
4
5
6
7
8
9
10
11
12
13
Day

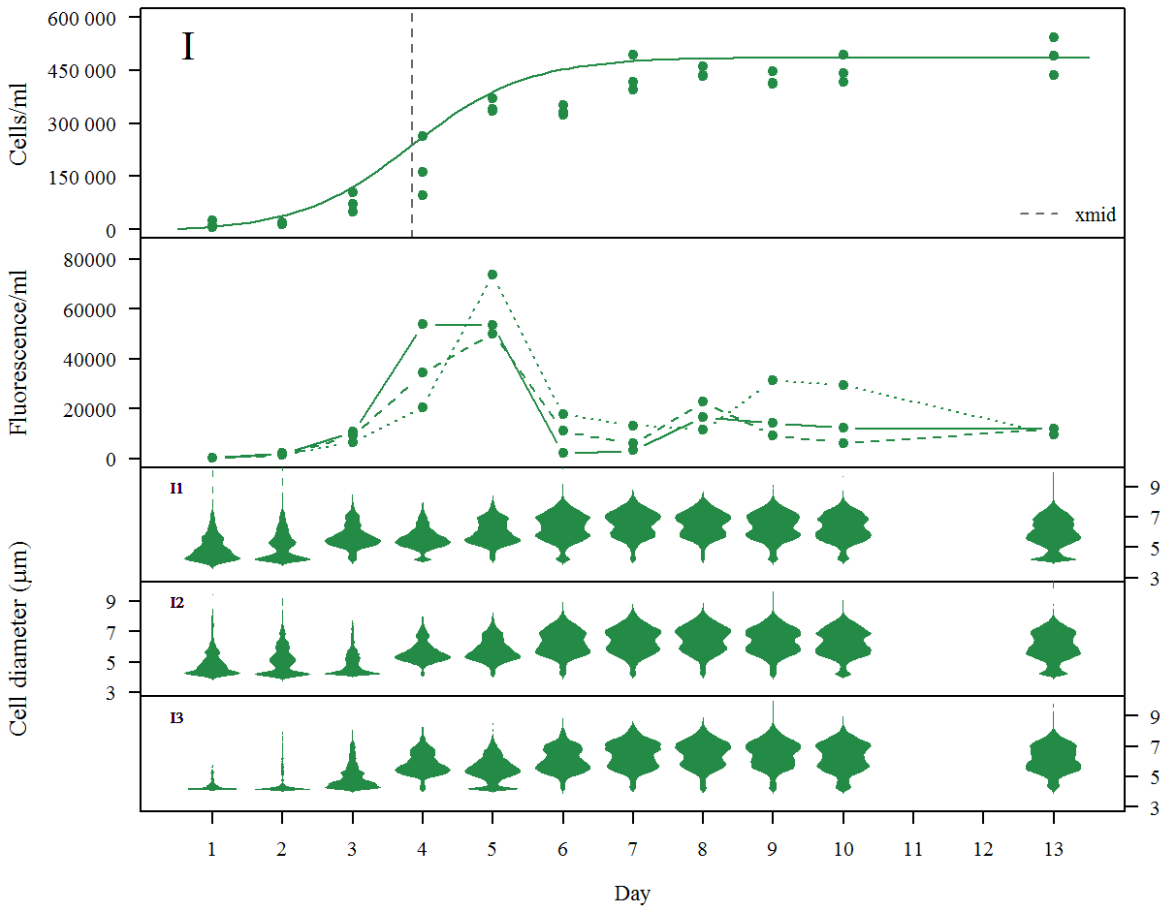
I
Cells/ml
600 000
450 000
300 000
150 000
0
xmid
Fluorescence/ml
80000
60000
40000
20000
0
Cell diameter (µm)
I1
I2
I3
9
7
5
3
1
2
3
4
5
6
7
8
9
10
11
12
13
Day

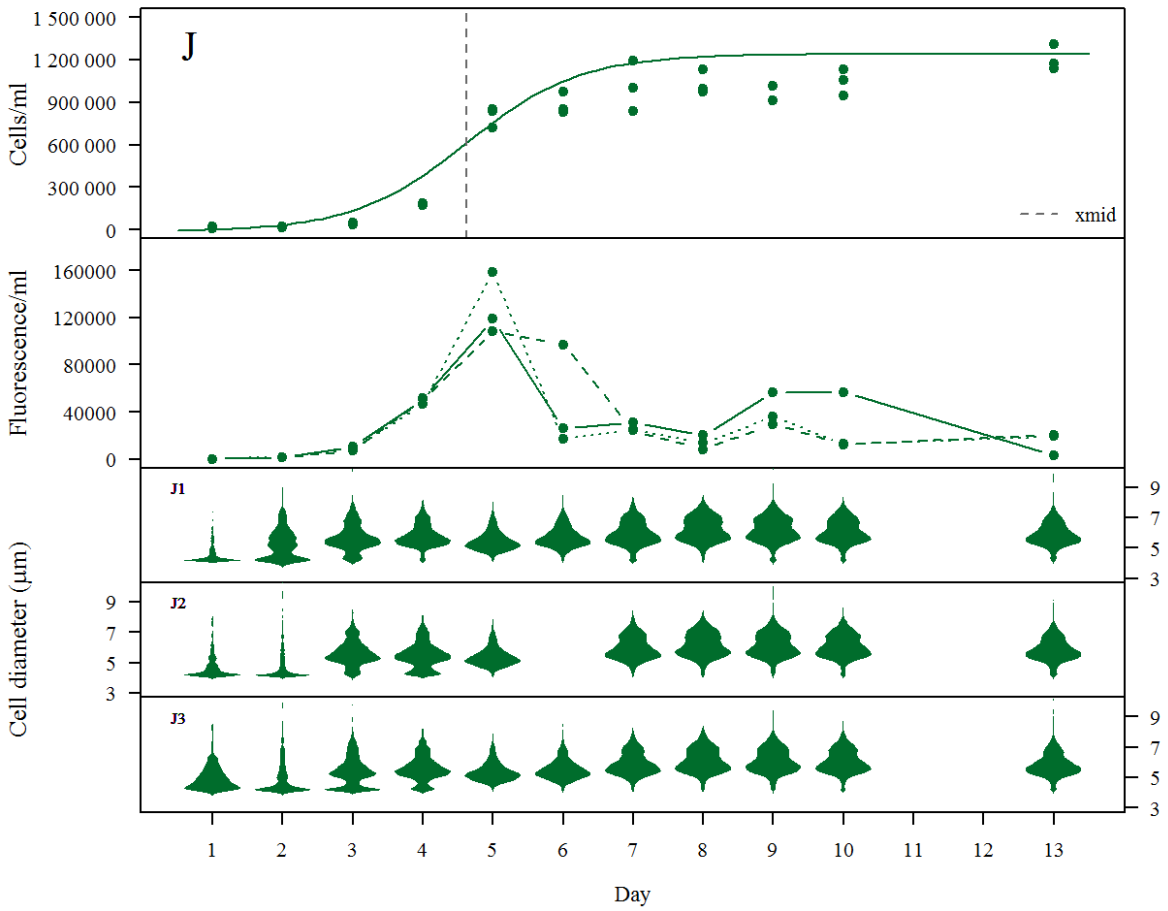
J
Cells/ml
1 500 000
1 200 000
900 000
600 000
300 000
0
xmid
Fluorescence/ml
160000
120000
80000
40000
0
Cell diameter (µm)
J1
J2
J3
9
7
5
3
1
2
3
4
5
6
7
8
9
10
11
12
13
Day

Appendix G

Analysis of the *Chlamydomonas - Brachionus* model of ordinary differential equations

This appendix gives a description of the code used to construct the time series plot, the bifurcation diagrams and the parameter planes in part **2.1**. The exact code that produsedall plots will not be presented because it would demand a lot of space and hardly be informative. Instead I choose to describe the essential parts of the code in a way that hopefully makes the structure of the code comprehensible, while simultaneously illustrating some important aspects of the *Chlamydomonas - Brachionus* model.

All plots produced in part **2.1** rely on the **deSolve** package written by Karline Soetaert, Thomas Petzoldt and R. Woodrow Setzer (2010). This package serves functions for solving ordinary differential equations. The task of solving such equations analytically, that is by methods producing a solution that has a form of an equation, is for most cases practically impossible. For this reason, there has been developed methods that solve differential equations numerically (e.g. the Runge-Kutta family of methods). The deSolve package is written to implement such numerical methods in the R environment.

In contrast to analytical methods, numerical methods produce a solution that is a list of numbers. If the equation describes a system that changes over time, the list of numbers are the values for the state variables for each time step in a sequence of time. In order to produce such a solution the solver require four elements:

- the model equations
- the parameter values of the model
- the initial values for the model's state variables
- the time period the solver is to produce a solution

All plots presented in part **2.1** are produced by different ways of plotting the results obtained from the solver that combine the four elements above. The main purpose of the theoretical analysis of the *Chlamydomonas - Brachionus* model system was to investigate how the predator-prey dynamics would be affected by changes in the experimental parameters D and Ni, i.e. the dilution rate and the nitrate concentration of the supplied medium. So, the key principle behind all plots in part **2.1** is to make alterations to the model's parameter values for D and Ni, while keeping the other three elements above unchanged.

Required package

```
library(deSolve)
```

Colours for plotting

```
col.def <- "#238b45"    # defended algal clone
col.undef <- "#a1d99b"  # undefended algal clone
col.tota <- "#41ab5d"   # both algal clones
col.rot <- "#252525"    # rotifers
```

The parameter values of the model

```
# The experimental parameters
Ni <- 60   # Limiting nutrient in supplied medium (µmol N/ l)
D <- 0.3   # Dilution rate (/day)

# The algal parameters estimated from the algal growth experiment
xc <- 0.0034611    # Algal conversion (10^9 cells/ µmol N)
Bc <- 1.34         # Maximum algal per-capita recruitment (/day)
ro <- 387          # Maximum nutrient uptake rate (µmol N/ 10^9 cells/ day)

# The algal parameters as described in Becks et al. (2010)
p2 <- 1              # prey quality parameter, undefended algae
p1 <- 0.05           # prey quality parameter, defended algae (variable)
                     # Maximum defence = 0, no defence = 1

Kc2 <- 2.20          # (µmol N/l) Half-saturation constant, undefended algae
Kc1 <- 8-(5.8*p1)    # (µmol N/l) Half-saturation constant, defended algae (dependent
on p1)

# The rotifer parameters (as in Becks 2010)
m <- 0.055    # Rotifer mortality (/day)
l <- 0.4      # Rotifer senescence rate (/day)

Qc <- 0.05    # Critical prey density for rotifer clearance (10^6 algal cells/ ml)

Bb <- 1.9     # Maximum rotifer per-capita recruitment (/day)
xb <- 170     # Rotifer conversion (rotifers/ 10^6 algal cells)

Kb <- 0.15    # Rotifer half-saturation constant (10^6 algal cells/ ml)
G <- Bb/xb    # Rotifer grazing parameter: Bb/xb (ml/rotifer/d)

# Collect the parameters in a single object
parameters <- c(Ni,D,m,l,xc,Bc,Kc1,ro,Qc,Bb,xb,Kb,G)
```

Description of the model system

Notice that the object below (becks2) which defines the *Chlamydomonas* - *Brachionus* model is a function of time, the state variables (state2) and parameters.

Recall that the state variables of the model system are:

- N/nt = the concentration of the limiting substrate (µmol/liter)
- C1 = the concentration of defended algal cells (10^6 cells/ml)
- C2 = the concentration of undefended algal cells (10^6 cells/ml)
- B = the concentration of breeding rotifers (individuals/ml)
- S = the concentration of senescent rotifers (individuals/ml)

Since the formulation of the model system is only descriptive, and not coded to do any calculations in itself, the state variables object (state2) and times object (times) do not need to be defined yet.

```
# TWO CLONE MODEL

becks2 <- function(times, state2, parameters) {
with(as.list(c(state2, parameters)), {

  # Derived parameters specific to each time point
  Kcvalues=c(Kc1,Kc2)
  fN <- ro*nt/(Kcvalues+nt)
  Q <- p1*c1+c2
  fB <- G/(Kb+max(Q,Qc))

  # The model equations
  dN <- D*(Ni-nt) - fN[1]*c1 - fN[2]*c2   # Nitrogen
  dC1 <- c1*(xc*fN[1] - p1*(b+s)*fB - D)  # Defended clone
  dC2 <- c2*(xc*fN[2] - p2*(b+s)*fB - D)  # Undefended clone
  dR <- b*(xb*Q*fB - (D + m + l))         # Breeding rotifers
  dS <- l*b - (D+m)*s                     # Senescent rotifers

  return(list(c(dN,dC1,dC2,dR,dS)))
  })
}
```

Solving the two-clone *Chlamydomonas - Brachionus* model system

In the deSolve package, the **ode**-function serves as a wrapper for all the implemented solvers of ordinary differential equations (Soetaert *et al.* 2010). The default solver method is **lsoda**, and is a solver that automatically switch between stiff and non-stiff methods (ibid.).

Notice that the **ode**-function takes four arguments, the four it needs to have specified in order to solve the system of equations. The arguments are as decribed intially. Before the **ode**-function is launched I need to specify the initial values of the state variables and the time period the solver is to produce a solution. Here the solver is set to calculate the values for the state variables for 100 days in increments of 0.2 days.

```
# Initial values for state variables
state2 <- c(nt=Ni, c1=0.0001, c2=0.01, b=0.02, s=0.01)

# Time specification
times <- seq(0, 100, by = 0.2)

# Solving model
TWO <- ode(y = state2, times = times, func = becks2, parms = parameters)
```

```
head(TWO)
```

```
##      time       nt           c1         c2          b          s
## [1,]  0.0 60.00000 0.0001000000 0.01000000 0.02000000 0.01000000
## [2,]  0.2 59.19067 0.0001193867 0.01219011 0.01756227 0.01076139
## [3,]  0.4 58.25204 0.0001424735 0.01485796 0.01549293 0.01129695
## [4,]  0.6 57.15340 0.0001699434 0.01810711 0.01374420 0.01164886
## [5,]  0.8 55.85785 0.0002025898 0.02206249 0.01227629 0.01185286
## [6,]  1.0 54.32080 0.0002413335 0.02687568 0.01105665 0.01193940
```

```
tail(TWO)
```

```
##         time       nt           c1         c2        b        s
## [496,]  99.0 1.842727 4.414961e-07 0.09890701 3.251780 3.664018
## [497,]  99.2 1.842726 4.364788e-07 0.09890705 3.251776 3.664015
## [498,]  99.4 1.842724 4.315185e-07 0.09890710 3.251773 3.664012
## [499,]  99.6 1.842723 4.266146e-07 0.09890715 3.251769 3.664009
## [500,]  99.8 1.842722 4.217664e-07 0.09890719 3.251766 3.664006
## [501,] 100.0 1.842720 4.169732e-07 0.09890725 3.251763 3.664003
```

The solution to this two-clone *Chlamydomonas* - *Brachionus* system is stored in an object named “TWO”. The head() command shows the first six rows of the object and the tail() command shows the last six.

Notice the structure of the data object. The first column (time) shows the sequence of time points that was defined above in order to specify the time period the solver was to produce a solution. It starts at time zero and increase in steps of 0.2 to day 100. Each row then gives the values for the five state variables at each time point. The initial values of the state variables (first row, when time = 0) are as I defined in the state2-object. Row two shows the status of the at time 0.2, row three at time 0.4 and so forth.

The results above indicate that the concentrations of organisms initially increase, in parallel with a decrease in the concentration of nitrate, and then stabilize at the end of the time period. These results are conveniently plotted to depict the development over the 100 days.

Plotting results as time series

```
par(family="serif", mar=c(4, 6, 4, 6), cex=1.2)

# Brachionus (breeding)
plot(TWO[,1], TWO[,5], lwd=2, type = "l", lty = 1, col=col.rot,  ylim=c(0,max(TW
O[,5])), xlim=c(0,max(TWO[,1])), axes=F, ylab="", xlab="")

axis(4, pretty(range(TWO[,5])),lwd=1, lty=1, line=0)
mtext(4, text="Brachionus (ind/ml)", line=2.5, col="black", cex=1.2)

axis(1, pretty(range(-5, max(TWO[,1])+5)), line=-0.5)
mtext("Time (days)",side=1,col="black",line=2, cex=1.2)

par(new=T)

# Chlamydomonas
plot(TWO[,1], TWO[,3], type = "l", lty = 1, lwd=2, col=col.def, axes=F,
ylim=c(0,max(TWO[,3],TWO[,4])), xlim=c(0,max(TWO[,1])), ylab="", xlab="")

lines(TWO[,1], TWO[,4], lwd=2, col=col.undef)

axis(2, pretty(range(0,max(TWO[,3],TWO[,4]))), col="black", lwd=1, line=0)
mtext(2, text=expression(paste("Chlamydomonas (", "10"^"6", "cells/ml)")), line=2.5,
lwd=1, cex=1.2)

legend("topright", legend=c("Undefended algae","Defended algae", "Rotifers", "", past
e("D = ",D), paste("Ni =",Ni, "µmol/L")), lty=1, lwd=2, col=c(col.undef,col.def, co
l.rot, gray.colors(1, alpha=0), gray.colors(1, alpha=0), gray.colors(1, alpha=0)), ce
x=0.8, bty="n")
```

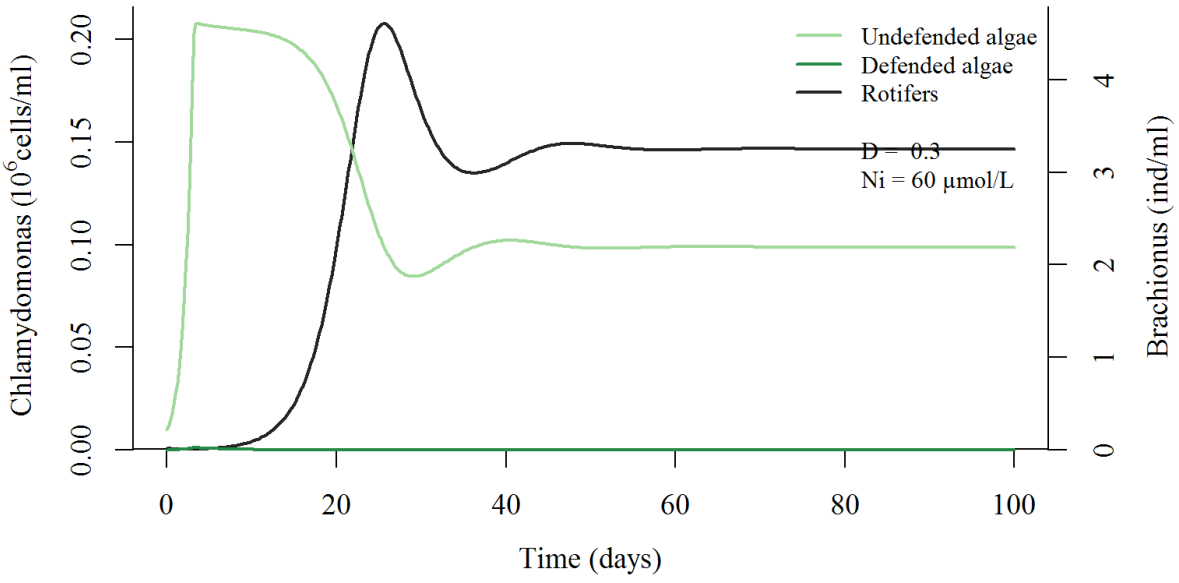

The plot above shows how the concentration of organisms change during the course of time when the dilution rate is 0.3 /day and the nitrate concentration of the supplied medium is 60 µmol/l. After an initial increase, the rotifers and the undefended algal clone stabilize in a stable equilibrium. The results also show that the undefended algal clone outcompete the defended clone (that has a high degree of defence) under these experimental conditions.

Changing the dynamics by increasing the nitrate concentration of the supplied medium (Ni)

To see how the model system behaves when the nitrate concentration is increased to 160 µmol/l, I change the Ni-parameter object and update the other objects that contain this parameter.

```
Ni <- 160

# Update the parameter and the initial state object
parameters <- c(Ni,D,m,l,xc,Bc,Kc1,ro,Qc,Bb,xb,Kb,G)
state2 <- c(nt=Ni, c1=0.0001, c2=0.01, b=0.02, s=0.01)

times <- seq(0, 110, by = 0.2)

# Solving model
TWO <- ode(y = state2, times = times, func = becks2, parms = parameters)
```

For the plotting I run the exact same code as above (code is therefore hidden).

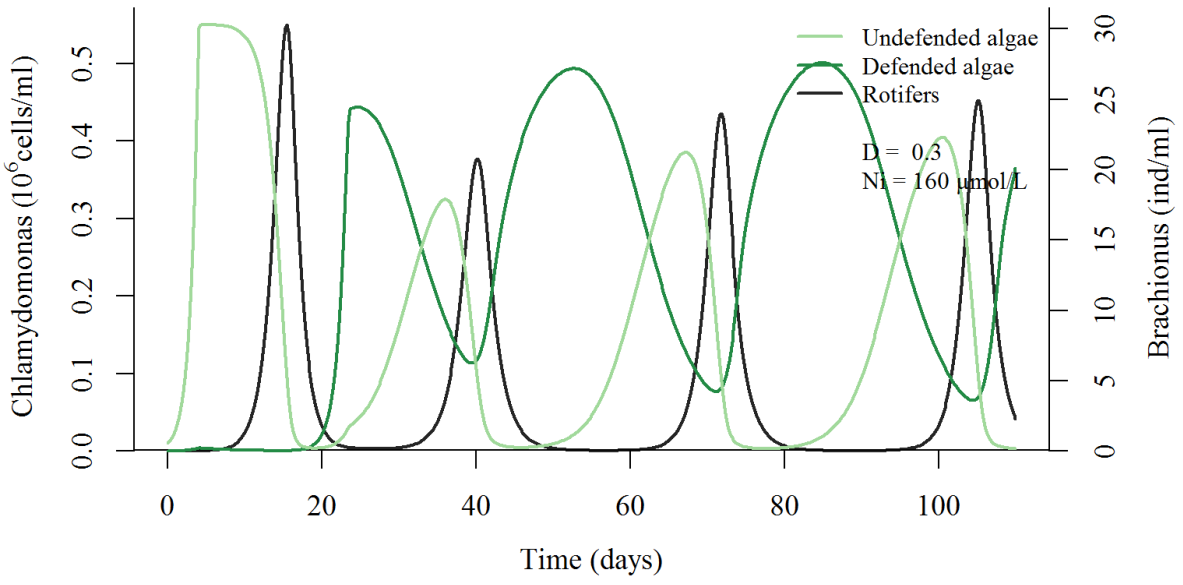

Under these experimental conditions, the model predicts that the system will be in a stable cycle. Additionally it predicts that both algal clones will be present, but with the highest abundances at different timepoints during the course of the development.

Eco-evolutionary dynamics

The change in frequencies of the two algal clones during the population cycles (previous plot) is exactly what is argued to cause the anti-phase eco-evolutionary dynamics observed in the *Chlorella-Brachionus* system of Fussmann *et al.* (2000) and Yoshida *et al.* (2003), and the *Chlamydomonas-Brachionus* system in Becks *et al.* (2010).

The anti-phase pattern of the eco-evolutinary dynamics becomes apparent when the population densities of the two algal clones are added together, as done in the plot below (dashed line). The code producing this plot is basically identical to the code for the plot above, except for the plotting of the algal densities which now were done like this:

plot(TWO[,1], TWO[,3]+TWO[,4], type = "l", lty = 2, lwd=2, col=col.tota, axes=F,
ylim=c(0,max(TWO[,3]+TWO[,4])), xlim=c(0,max(TWO[,1])), ylab="", xlab="")

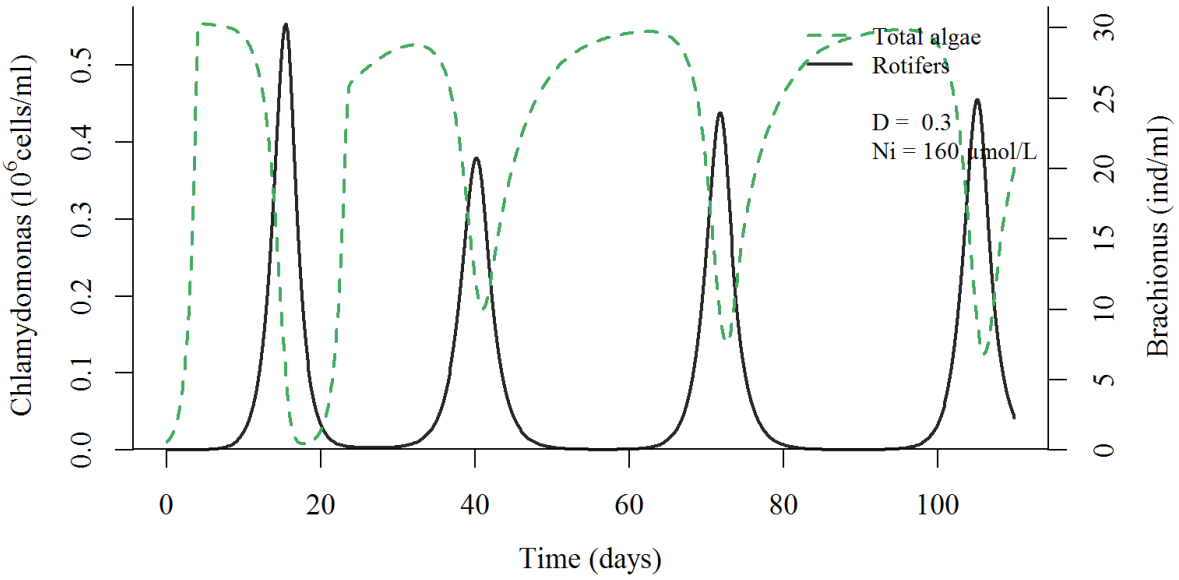

Bifurcation diagram

From the time series plots above it is evident that Ni, the nitrate concentration of the supplied medium, is a structuring factor for the dynamics of the *Chlamydomonas - Brachionus* system. However, it is not very efficient to investigate the effects of changing Ni by the means of time series plots.

A better way of investigating the effects of different Ni values is by making a plot that shows the system's behaviour as a function of the parameter in interest. Such a plot is called a bifurcation diagram (if the qualitative behaviour of the system changes depending on the parameter value).

I am not aware of any R packages that serve built-in functions for constructing bifurcation diagrams. Fortunately, Professor Tom Andersen has made a code that I could use to contruct bifurcation diagrams in R (see next page).

The core part of the code is still the ode()-solver from the deSolve package, and what the code basically does is to run the solver repeatably for a sequence of values for the bifurcation parameter. After each loop of calculation, the minimum and maximum values of the state variables are stored in separate objects, so that in

the end one has lists of how the minimum and maximum levels change depending on the bifurcation parameter.

```
# Adjust the degree of defence for the defended algal clone
# (because this value produce a nice looking diagram)
p1 <- 0.25
Kc1 <- 8-(5.8*p1)

parameters <- c(Ni,D,m,l,xc,Bc,Kc1,ro,Qc,Bb,xb,Kb,G)

# Define the range of the bifurcation parameter
Ni <- seq(0, 800, 20)

# Make "empty" objects that will be filled with data during the loop
c1.min <- 0 * Ni
c1.max <- 0 * Ni
c2.min <- 0 * Ni
c2.max <- 0 * Ni
b.min <- 0 * Ni
b.max <- 0 * Ni

# Define the loop that extracts minimum and maximum values for the concentration of
organisms when the values of Ni range between 0 and 800 µmol/l

for (i in 1:length(Ni)) {
    parameters$Ni <- Ni[i]

    state3 <- c(nt=Ni[i], c1=0.0001, c2=0.01, b=0.02, s=0.01)
    time2 <- seq(0, 200, 0.1)
    X <- as.data.frame(ode(state3, time2, becks2, parameters))

    X <- subset(X, time2 > 100)
    c1.min[i] <- min(X$c1)
    c1.max[i] <- max(X$c1)
    c2.min[i] <- min(X$c2)
    c2.max[i] <- max(X$c2)
    b.min[i] <- min(X$b)
    b.max[i] <- max(X$b)

}
```

Now, with the list of maximum and minimum levels for a range of Ni values calculated, the bifurcation diagram can be drawn.

```
par(family="serif", mar=c(4, 6, 4, 6), cex=1.2)

# Defended algae
plot(c1.max ~ Ni, type = "l", lty = 1, lwd=2, col=col.def, axes=F, ylim=c(0,max(c1.ma
x,c2.max)), xlim=c(0,800), ylab="", xlab="")
lines(c1.min ~ Ni, lty = 1, lwd=2, col=col.def)

# Undefended algae
lines(c2.min ~ Ni, lty = 1, lwd=2, col=col.undef)
lines(c2.max ~ Ni, lty = 1, lwd=2, col=col.undef)

axis(2, pretty(range(c1.min,c1.max), 7), col="black", lwd=1, line= -0.1)
mtext(2, text=expression(paste("Chlamydomonas (", "10"^"6", "cells/ml"))), line=2.5,
lwd=1, cex=1.2)

legend("topleft", legend=c(paste("D =", D),"Undefended algae", "Defended algae", "Rot
ifers"), lty=1, col=c("white",col.undef,col.def,col.rot), lwd=2, cex=0.8, bty="n")

par(new=T)

# Rotifers
plot(b.max ~ Ni, type="l", lty = 1, lwd=2, col=col.rot, ylim=c(0,max(b.max)), xli
m=c(0,800), axes=F, ylab="", xlab="")

lines(b.min ~ Ni, lty = 1, lwd=2, col=col.rot)
axis(4, pretty(range(0,max(b.max))),lwd=1, lty=1)
mtext(4, text="Brachionus (ind/ml)", line=2, col="black", cex=1.2)

axis(1,pretty(range(-5,805), 10), line=-0.2)
mtext("Supplied nitrate, Ni (µmol/liter)",side=1,col="black",line=2, cex=1.2)
```

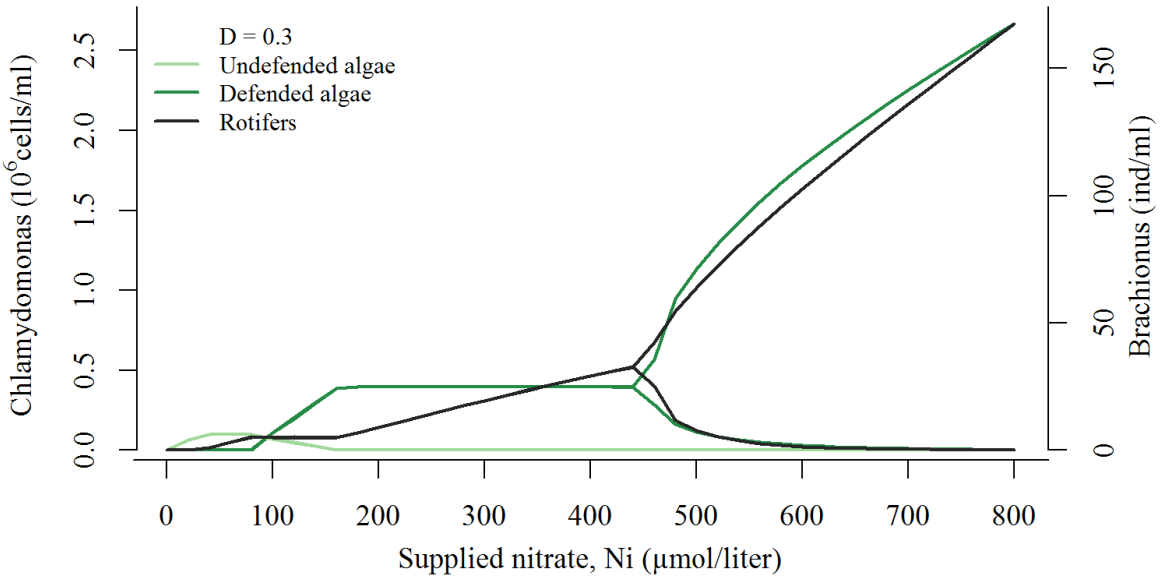

The bifurcation diagram shows that the system is in a stable equilibrium when Ni values are up to about 450 µmol/l, given that D is 0.3 /day and the defended clone has a relative high degree of defence (p1 = 0.25). Ni values above 450 µmol/l are predicted to produce cycles. The plot also shows that the undefended algal clone dominate the system when Ni is low (below 100) and that it is outcompeted by the defended clone at higher Ni values.

Bifurcation diagram with dilution rate as bifurcation parameter

A bifurcation diagram can also be made with the dilution rate (D) as the bifurcation parameter. The necessary alterations of the code (that runs the calculations) are shown below. The code that produce the plot is essentially identical to the one above and is therefore not shown.

```
# Choose a concentration for Ni
Ni <- 200

parameters <- c(Ni,D,m,l,xc,Bc,Kc1,ro,Qc,Bb,xb,Kb,G)

# Define the range of the bifurcation parameter
D <- seq(0, 1.5, 0.04)

# Make "empty" objects that will be filled with data during the loop
c1.min <- 0 * D
c1.max <- 0 * D
c2.min <- 0 * D
c2.max <- 0 * D
b.min <- 0 * D
b.max <- 0 * D

# The loop that extract minimum and maximum values for the concentration of organisms
when the values of D range between 0 and 1.5 per day

for (i in 1:length(D)) {
    parameters$D <- D[i]

    state3 <- c(nt=Ni, c1=0.0001, c2=0.01, b=0.02, s=0.01)
    time2 <- seq(0, 200, 0.1)
    X <- as.data.frame(ode(state3, time2, becks2, parameters))

    X <- subset(X, time2 > 100)
    c1.min[i] <- min(X$c1)
    c1.max[i] <- max(X$c1)
    c2.min[i] <- min(X$c2)
    c2.max[i] <- max(X$c2)
    b.min[i] <- min(X$b)
    b.max[i] <- max(X$b)

}
```

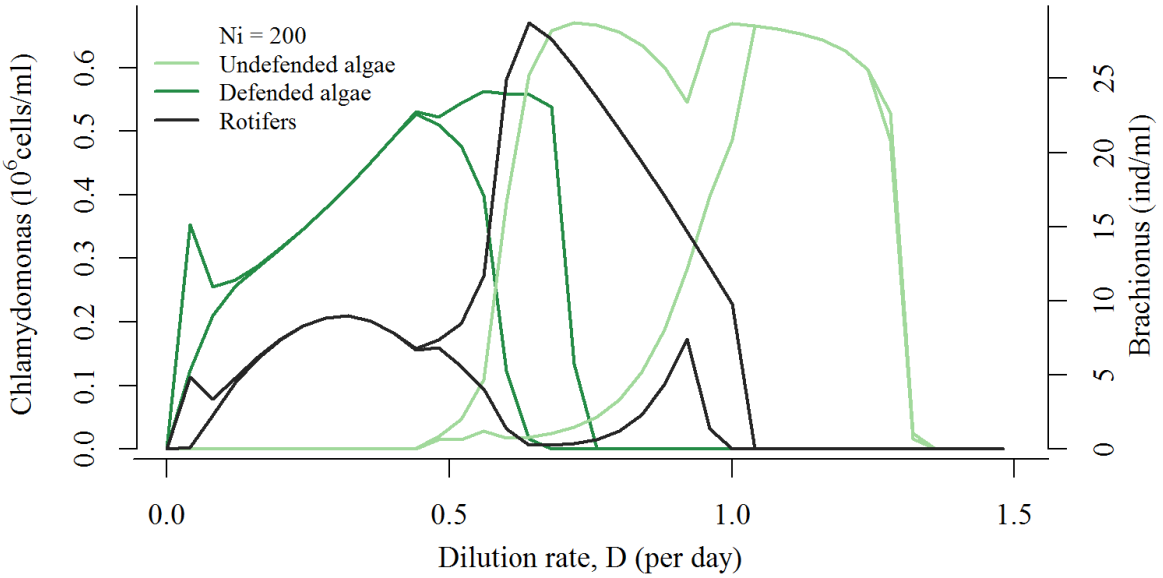

This bifurcation diagram now shows how the behaviour of the system changes for different values of D, when Ni is set to 200 µmol/l. The system expected to oscillate at the lowest dilution rates and with only the defended clone present. For increasing values of D, the system first goes into a state of equilibrium, and then, when D is about 0.5 and higher, the system starts to oscillate. Notice also that there is a shift from a dominance of the defended algal clone to the undefended clone with increasing D. For dilution rates above 1, the rotifers go extinct, followed by extinction of algae at D close to 1.4.

The two bifrucation diagrams indicate that both the Ni and D have a potential to change the qualitative behaviour of the model system. However, how these parameters act in concert is not easily illustrated by bifurcation diagrams. A better tool for investigating this is by contructing a parameter plane.

Construction of a parameter plane

A crucial part of the design of rotifer-algal experiment was to choose values for the experimental parameters Ni and D. In order to do so efficiently, it was beneficial to have an overview of the system's behaviour in a range of combinations of the two parameters. Parameter planes produce such an overview.

The code producing the parameter planes presented in part **2.1** is given below. This code is an extension I made of the code for the bifurcation diagram. Basically, the code now includes an extra loop such that values for the state varibles are calculated for a range of combinations of both Ni and D. In the code below, the loop starts off by setting Ni equal to the first value in the range of Ni values (Ni=0) and then solve the system for the entire sequence of D values specified, one calculation for each D value. When the entire sequence of D values is covered for Ni=0, the same procedure is repeated for the next Ni value, in this case Ni=19, and so it continues until the entire sequence of Ni values also is covered.

As in the bifurcation diagram, the minimum and maximum values of the state variables are extracted after each loop of calculation. However, the minimum and maximum values are in this case used differently. The joint information from the state variables are now used to make a coloured map that describes the dynamical behaviour of the system for the set of parameter combinations. The colour indicates the type of behaviour.

```
# Define colours that describe the type of predator-prey dynamics

# Predator-prey cycles, different colour depending on the amplitude's size
col.cy1 <- "#08519c"; col.cy2 <- "#3182bd" ;col.cy3 <- "#6baed6" ; col.cy4 <- "#bdd7e
7"; col.cy5 <- "#eff3ff"

col.ext.a <- "#e7e1ef"  # algae and rotifers extinct
col.ext.r <- "#fff7bc"  # only rotifers extinct

p1 <- 0.25
Kc1 <- 8-(5.8*p1)

parameters <- c(Ni,D,m,l,xc,Bc,Kc1,ro,Qc,Bb,xb,Kb,G)

# The code

Ni <- seq(0,800,19)
D <- seq(0, 1.5, 0.04)

C2.1range <-  matrix(0,length(D),length(Ni))
C2.2range <-  matrix(0,length(D),length(Ni))
C2.1min <- matrix(0,length(D),length(Ni))
C2.2min <- matrix(0,length(D),length(Ni))
C2.1max <- matrix(0,length(D),length(Ni))
C2.2max <- matrix(0,length(D),length(Ni))
B3.min <- matrix(0,length(D),length(Ni))

par(family="serif", mar=c(4,5,4,4), xpd=TRUE, cex=1.2)

plot(1,1,type="n", ylim=c(0, range(Ni)[2]), xlim=c(0,range(D)[2]),
xlab="Dilution rate, D (per day)", ylab="Supplied nitrate, Ni (µmol/liter)", bty="L")

for (j in 1:length(Ni)){
    parameters$Ni <- Ni[j]

    for (i in 1:length(D)) {
        parameters$D <- D[i]

        X0 <- c(nt=Ni[j], c1=0.0001, c2=0.01, b=0.02, s=0.01)
        time2 <- seq(0, 200, 0.1)
        X <- as.data.frame(ode(X0, time2, becks2, parameters))

        X <- subset(X, time > 100)
        C2.1range[i,j] <- range(X$c1)[2]-range(X$c1)[1]     # defended algae
        C2.2range[i,j] <- range(X$c2)[2]-range(X$c2)[1]     # undefended algae
        C2.1min[i,j] <- min(X$c1)
        C2.2min[i,j] <- min(X$c2)
        C2.1max[i,j] <- max(X$c1)
        C2.2max[i,j] <- max(X$c2)
        B3.min[i,j] <- min(X$b)      # breeding rotifers ind/ml

            if ((C2.1min[i,j] <= 0.000001) & (C2.2min[i,j] <= 0.000001)){
              # less than 5 cells/500ml = algae extinct
```

```
            plotfarge <- col.ext.a

            } else if (B3.min[i,j] <= 0.01){
              # rotifers extinct, algae fixed
            plotfarge <- col.ext.r

            } else if ((C2.1range[i,j] < 0.0001) & (C2.1max[i,j] > C2.2max[i,j])){
              # stable equilibrium (amplitude< 100 cells/ml) and defended dominating
            plotfarge <- col.def

            } else if ((C2.2range[i,j] < 0.0001) & (C2.1max[i,j] < C2.2max[i,j])){
              # stable equilibrium (amplitude<100 cells/ml) and undefended dominating
            plotfarge <- col.undef

            } else if (max(C2.1range[i,j],C2.2range[i,j]) < 0.010){
              # small amplitude 10 000 cells/ml
            plotfarge <- col.cy1

            } else if (max(C2.1range[i,j],C2.2range[i,j]) < 0.1){
              # medium-small amplitude 100 000 cells/ml
            plotfarge <- col.cy2

            } else if (max(C2.1range[i,j],C2.2range[i,j]) < 0.75){
              # medium amplitude 750 000 cells/ml
            plotfarge <- col.cy3

            } else if (max(C2.1range[i,j],C2.2range[i,j]) < 1.25){
              # large amplitude 1 250 000 cells/ml
            plotfarge <- col.cy4

            } else {
            plotfarge <- col.cy5            # max amplitude
            }
        points(D[i],Ni[j], pch=16, col=plotfarge, cex=1.8)
    }
}

legend("topright", bty="n", legend= c(paste("Kc1 =", Kc1), paste("p1=", p1)))

points(c(0.3,0.3), c(50,250), pch=8, lwd=2, cex=1.8, col="#67001f")

### Legend describing the qualitative behaviour of the system

par(family="serif", mar=c(0,5,0,4), cex=1.2)
plot(1,1,type="n", axes=F, ylab="", xlab="")

legend("center", legend=c("Stable equilibrium","Defended dominating", "Undefended dom
inating","", "Cycle amplitude", "< 10 000 cells/ml", "< 100 000 cells/ml", "< 750 000
cells/ml", "< 1 250 000 cells/ml", "> 1 250 000 cells/ml","", "Extinction rotifers",
"Extinction algae and rotifers"), pch=16, bty="n",

col=c("white",col.def, col.undef,"white", "white", col.cy1, col.cy2, col.cy3, col.cy
4, col.cy5,"white",col.ext.r, col.ext.a))
```

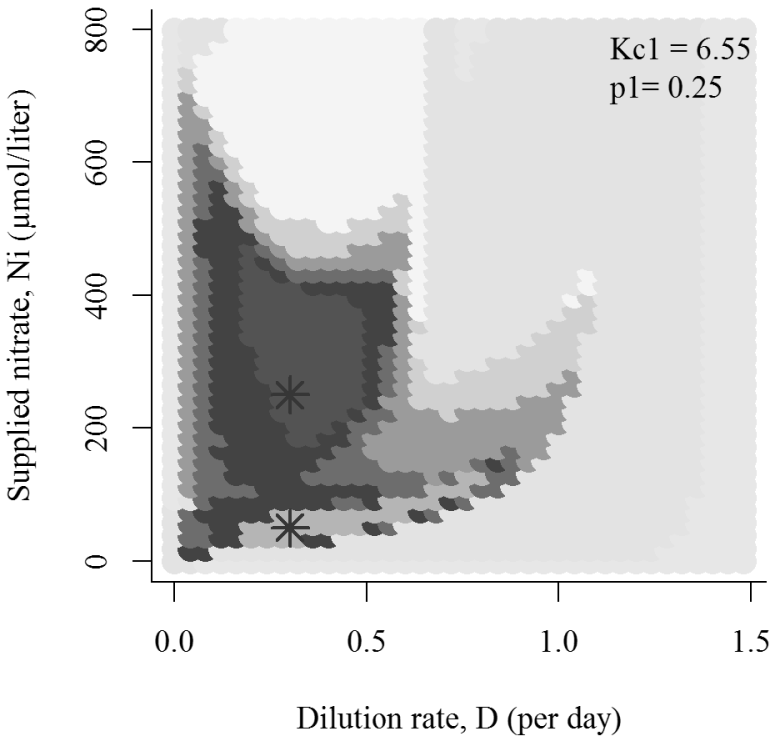

Stable equilibrium
- Defended dominating
- Undefended dominating

Cycle amplitude
- < 10 000 cells/ml
- < 100 000 cells/ml
- < 750 000 cells/ml
- < 1 250 000 cells/ml
- > 1 250 000 cells/ml

- Extinction rotifers
- Extinction algae and rotifers

APPENDIX H

Schematic drawing and pictures of the rotifer-algal continuous cultures

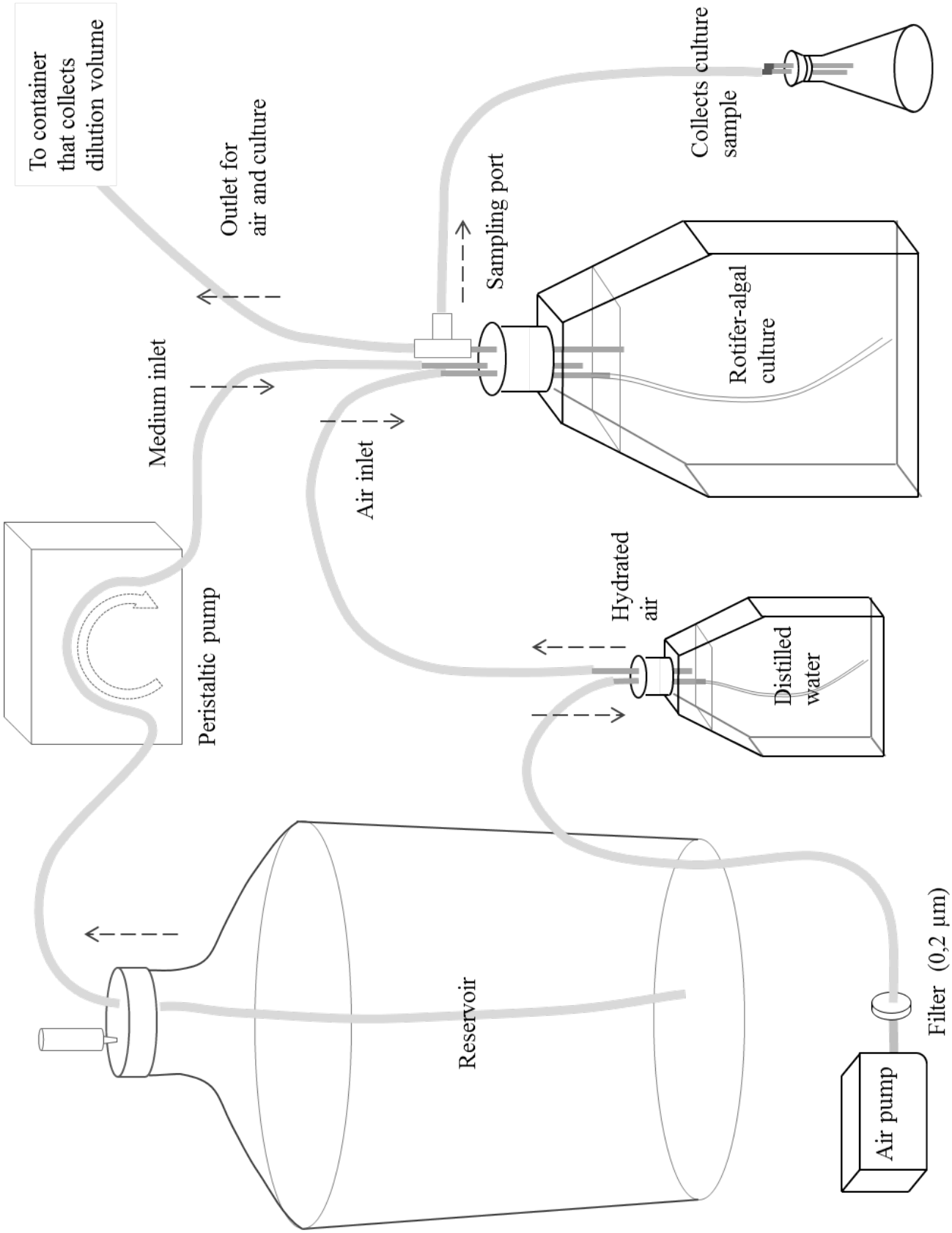

Pictures from day 10

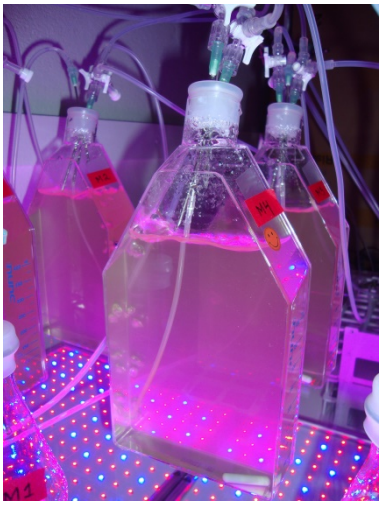

APPENDIX I Experimental conditions

DILUTION RATES

Summary statistics of the measured dilution rates of the continuous cultures.

Sd = standard deviation.

Culture	Range	Mean	Sd
L1	0.27 – 0.30	0.29	0.01
L2	0.26 – 0.30	0.28	0.01
L3	0.25 – 0.28	0.27	0.01
L4	0.25 – 0.27	0.26	0.01
M1	0.27 – 0.31	0.30	0.01
M2	0.28 – 0.30	0.29	0.01
M3	0.28 – 0.31	0.30	0.01
M4	0.26 – 0.30	0.28	0.01

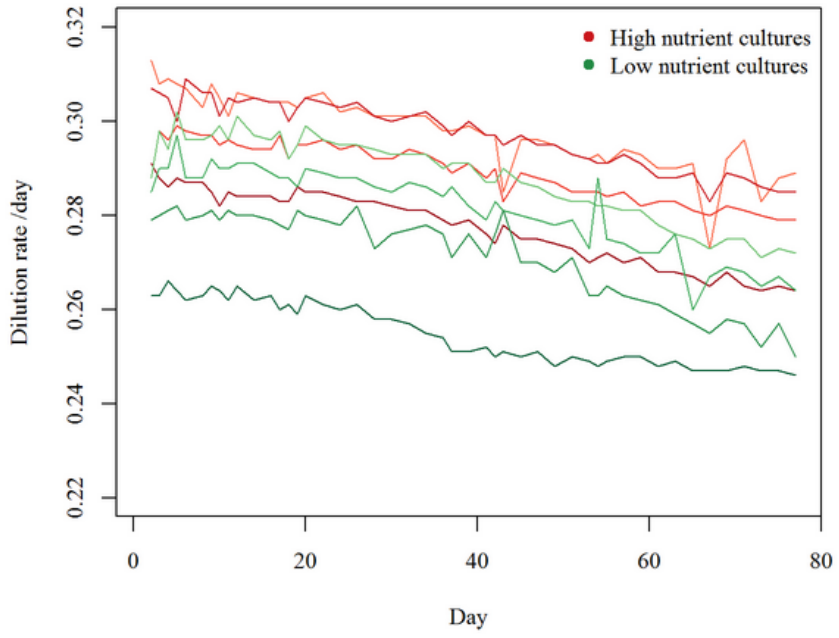

Plot of the cultures' dilution rates during the experimental period. Light-to-dark red curves = M1-to-M4 cultures, and light-to-dark green curves = L1-to-L4 cultures.

TEMPERATURE

Summary statistics of the measured temperatures (°C) of the continuous cultures.

Culture	Range	Mean	Sd
L1	17.7 – 19.3	18.3	0.34
L2	17.6 – 19.9	18.3	0.37
L3	17.8 – 20.0	18.3	0.36
L4	17.7 – 20.2	18.3	0.40
M1	18.0 – 20.0	18.5	0.34
M2	17.9 – 20.7	18.5	0.42
M3	17.9 – 20.1	18.5	0.35
M4	17.9 – 20.5	18.6	0.41

pH

Summary statistics of the measured pH of the continuous cultures.

Culture	Range	Mean	Sd
L1	6.7 – 7.5	7.1	0.18
L2	6.9 – 7.5	7.2	0.16
L3	7.0 – 7.6	7.2	0.16
L4	6.9 – 7.6	7.3	0.16
M1	7.0 – 7.9	7.3	0.20
M2	7.0 – 8.0	7.4	0.22
M3	6.9 – 7.8	7.4	0.21
M4	7.0 – 8.0	7.4	0.18

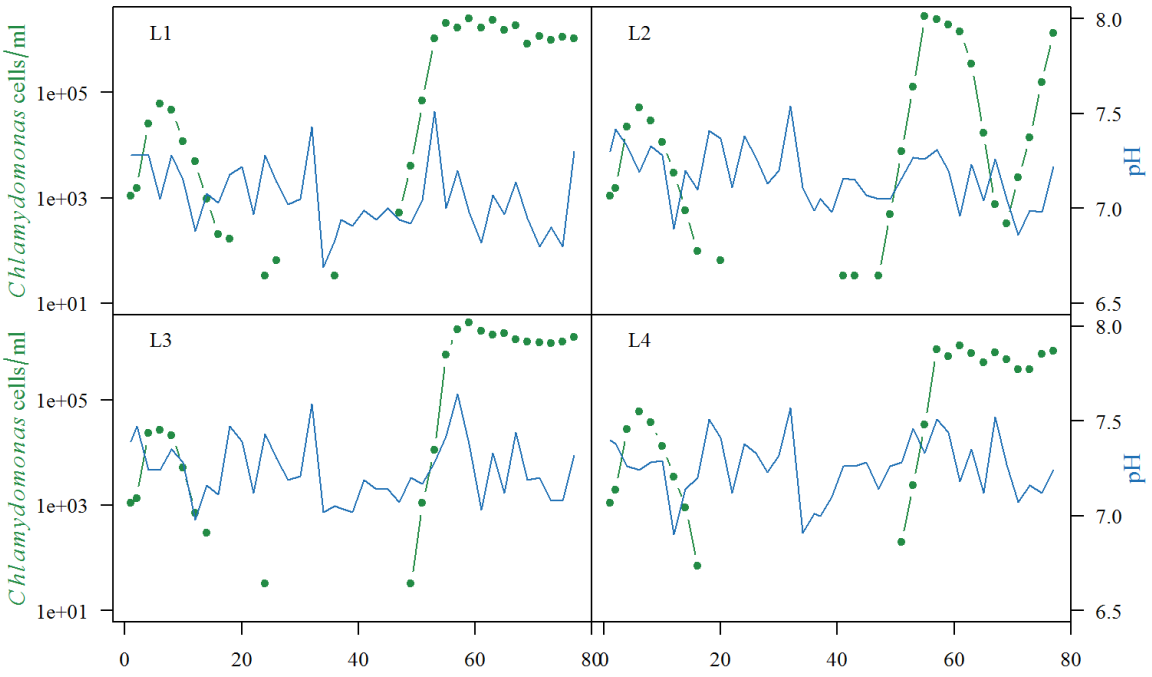

The measured pH-results for the low nutrient cultures plotted together with the estimates for algal densities.

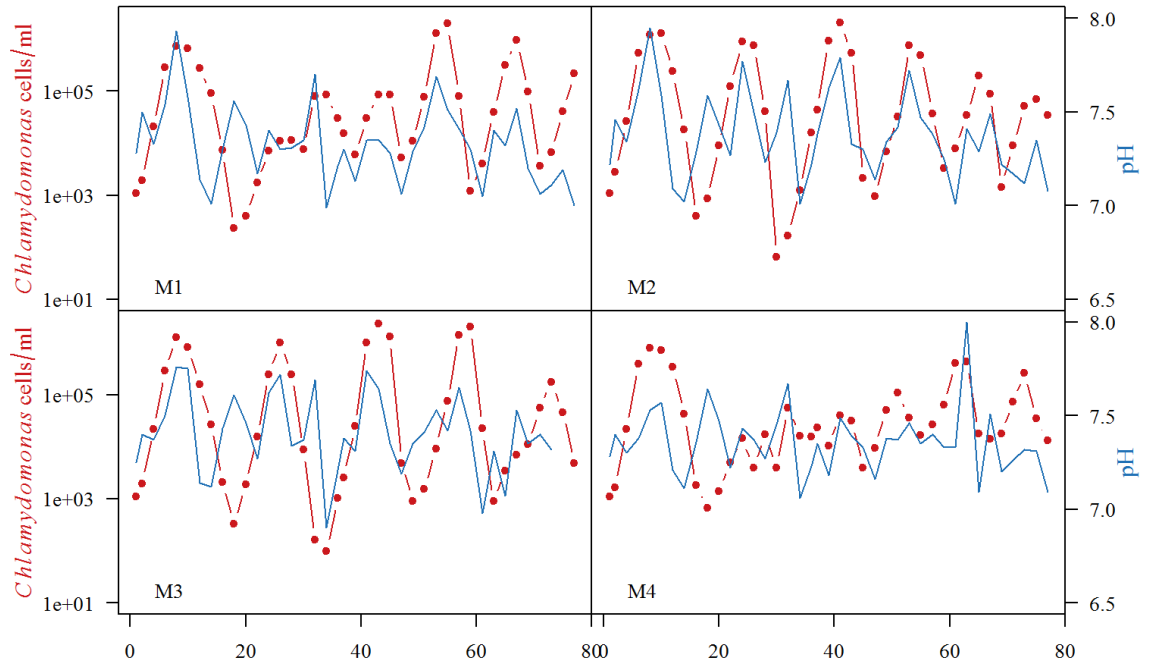

The measured pH-results for the high nutrient cultures plotted together with the estimates for algal densities. There is a positive correlation between pH and algal density.

APPENDIX J Nutrient dynamics

This appendix presents the results for the analyses of dissolved nutrients in the rotifer-algal cultures. The nutrient levels that were measured included nitrate, phosphate and total nitrogen, and they are here compiled together with the estimated population densities of rotifers and algae.

Below are the results for the low nutrient cultures, while the results for the high nutrient cultures are presented on the next two pages. Recall that the nutrient level of the supplied medium for the L-cultures was increased at day 42 (nitrate from 50 to 150 µmol/liter and phosphate from 1.67 to 5 µmol/liter). The results for measured total nitrogen are

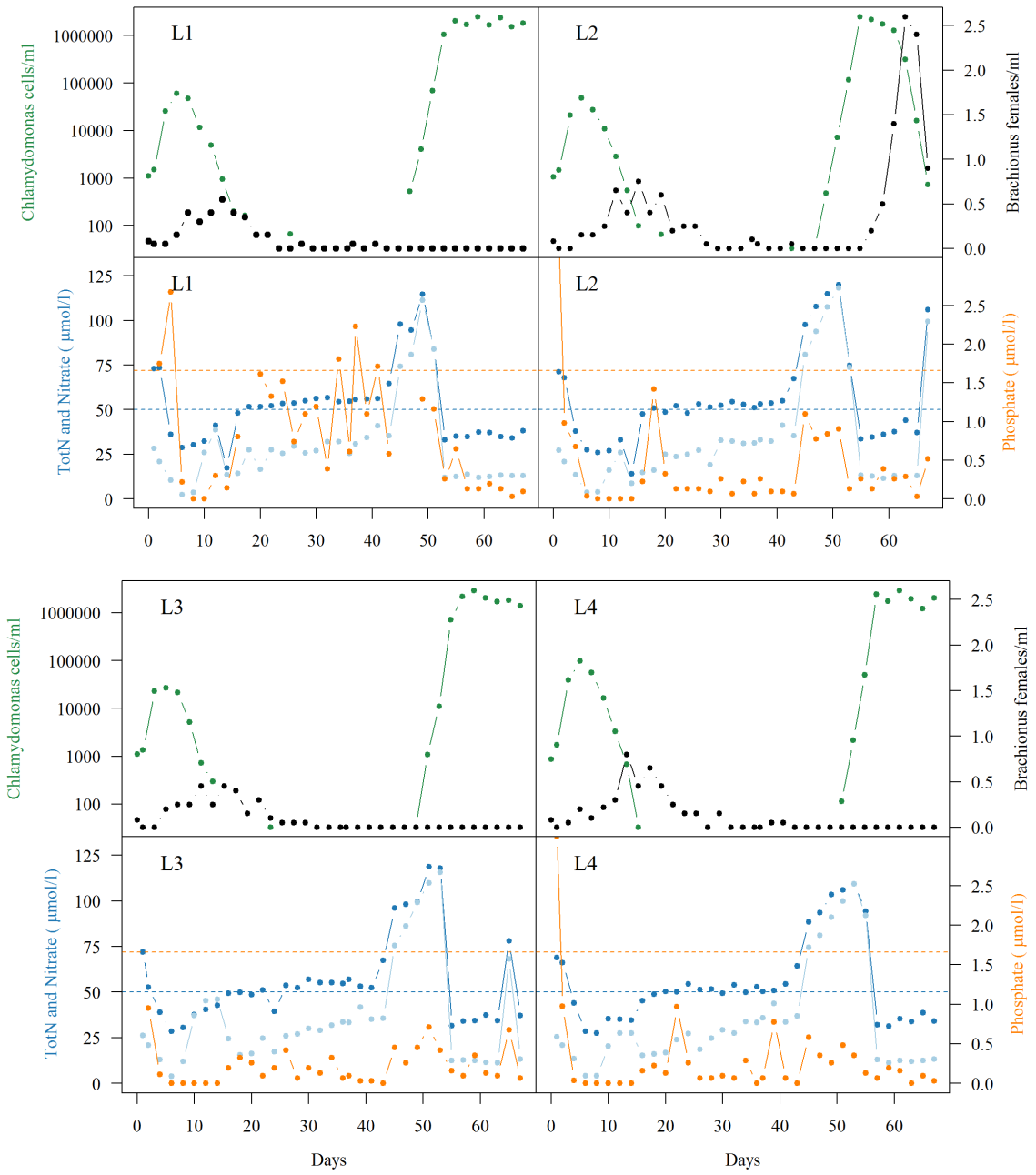

represented in the plots by a dark blue curve and nitrate by a light blue. The horizontal lines in the plots for the nutrient levels are set at the concentration of nitrate and phosphate in the supplied medium (blue for nitrate and orange for phosphate).

For the first 41 days there appears to be a considerable difference in the measured levels of nitrate and total nitrogen, whereas the levels are almost identical for the remaining days in the high nutrient cultures. This is most likely caused by some variability in how the analyses were conducted. The chemical analyses were done in four batches (listed at the end of the appendix), and the marked difference in the results for the measurements of nitrogen species fit the batch grouping.

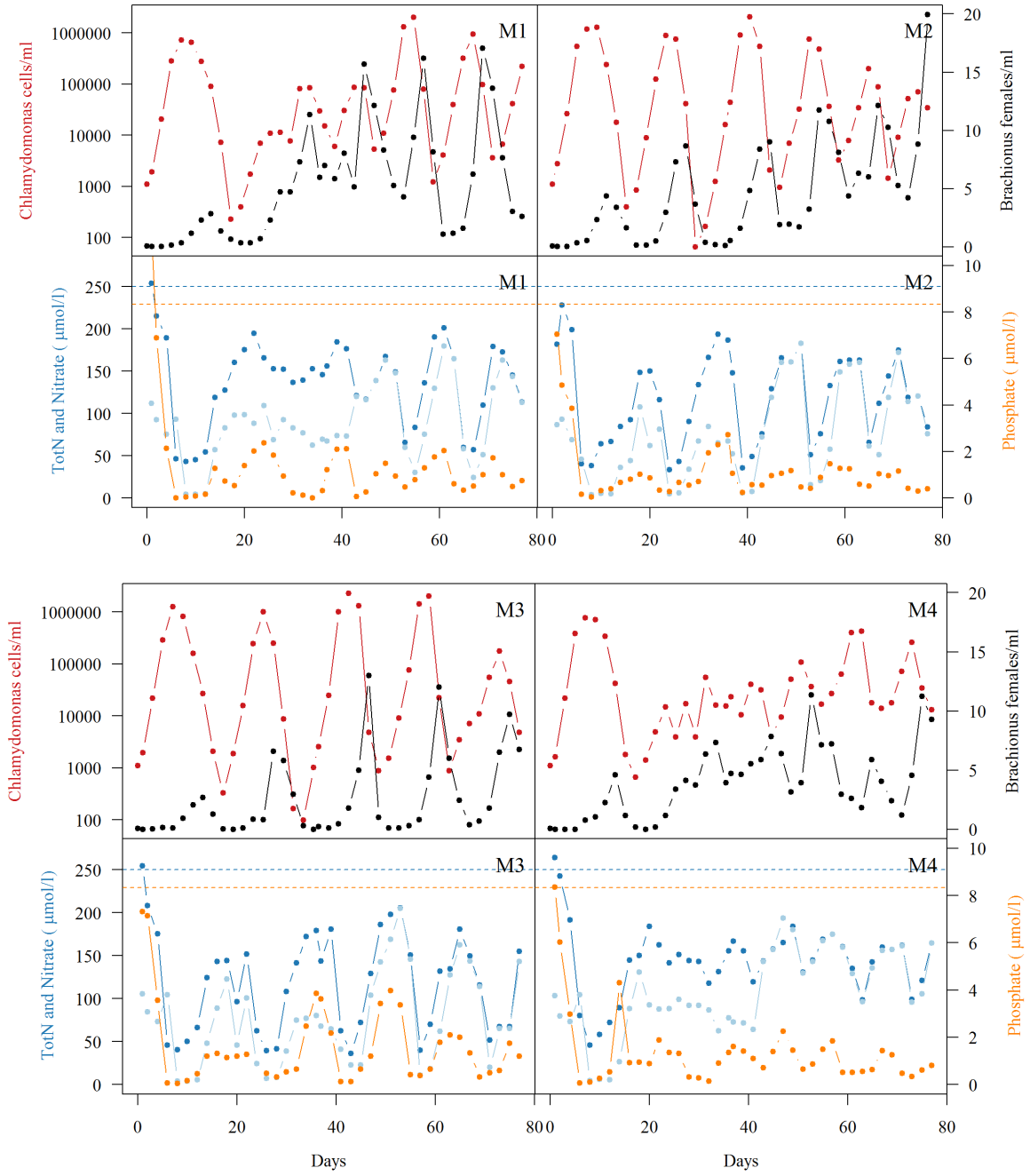

Below is another set of plots for the high nutrient cultures, here with the density of algae drawn together with the measured concentration of phosphorus and total nitrogen.

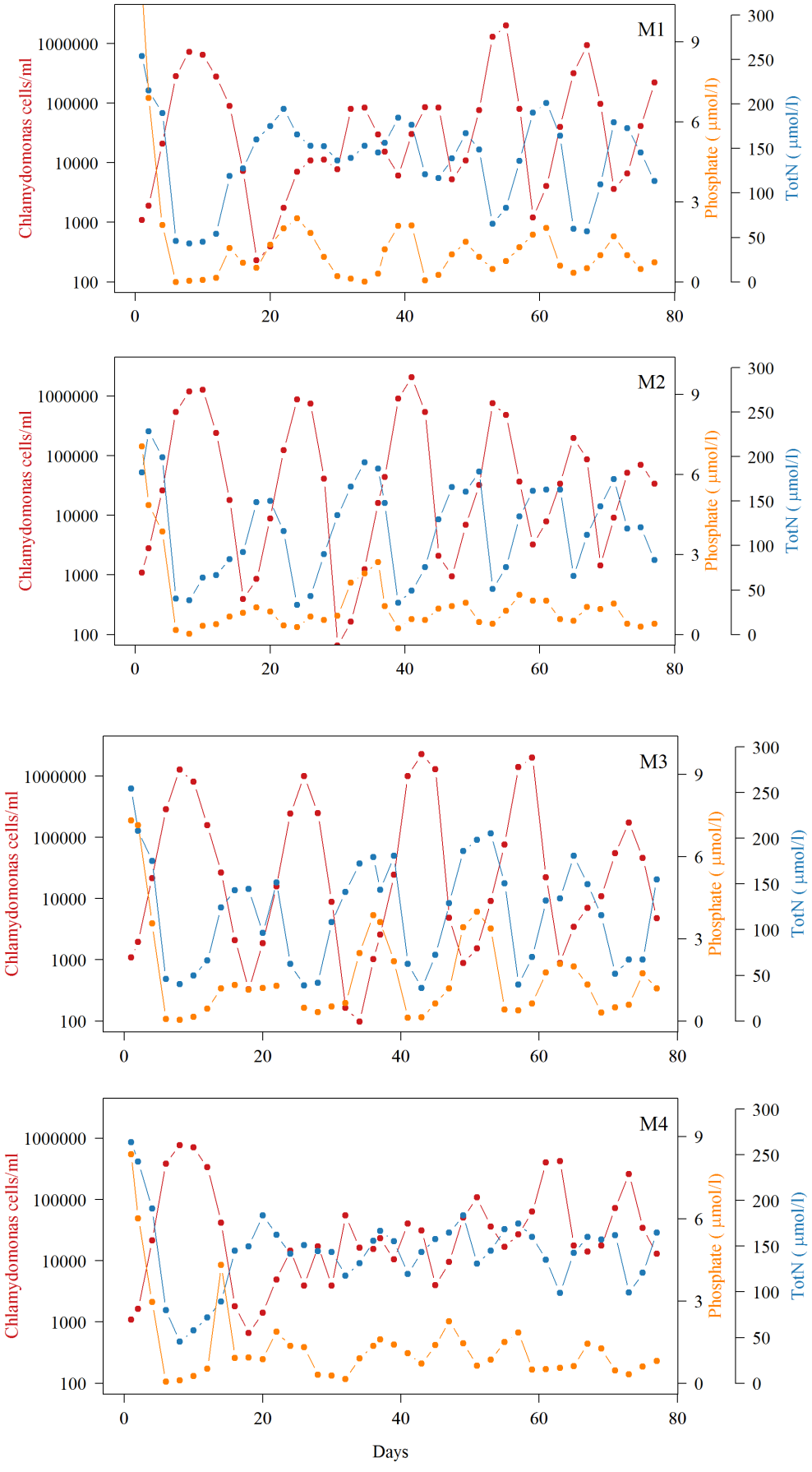

The culture samples were analyzed in the four following batches:

1. L-cultures day 1 – 14 and M-cultures day 1 – 12

2. M-cultures day 14 – 41

3. L-cultures day 16 – 43

4. L-cultures day 45 – 67 and M-cultures day 43 – 77

The nutrient levels for the last 10 days of the L-cultures were not analyzed.

APPENDIX K

Comparison of predicted and observed dynamics

The theoretical model used in the comparison here is essentially identical to the *Chlamydomonas – Brachionus* model presented in part 2.1 with p_1=0.9 (i.e. the model where the defended algal clone has a low degree of defence), except that the initial values for the rotifer and algal concentrations now is set equal to what was the initial concentration of organisms in the continuous cultures.

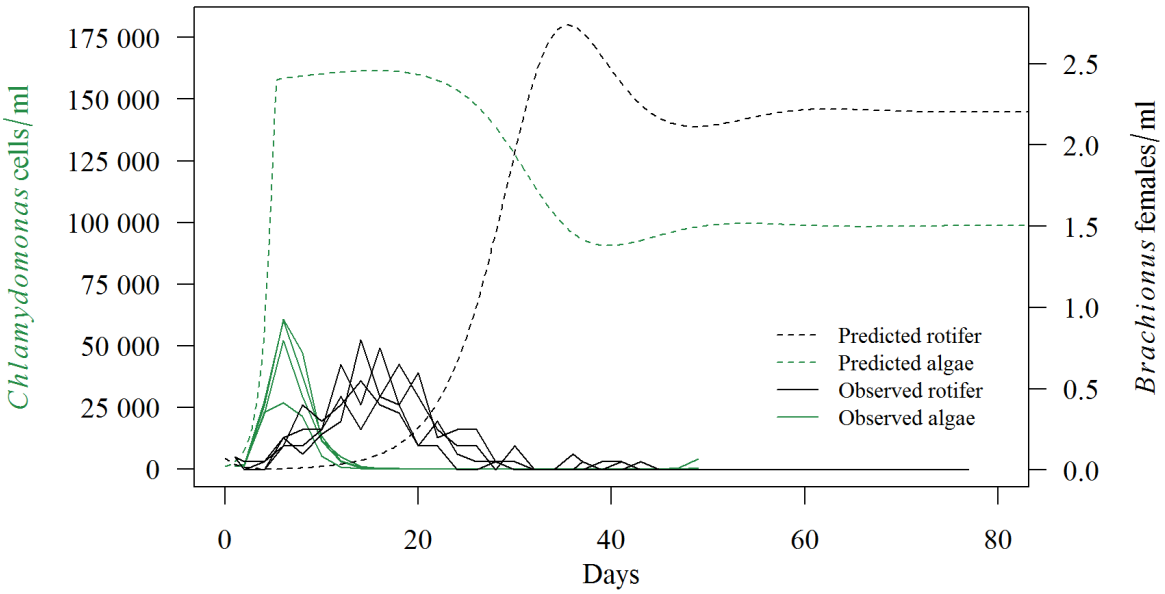

Above are the predicted and observed dynamics for the set of low nutrient cultures (Ni = 50µmol N/l). Only the undefended algal clone is predicted to be present under this low nutrient condition.

The predicted and observed dynamics for the high nutrient cultures are presented on the next page in three separate plots. Rotifer numbers are compared for each of the four replicates in the top plot, algal densities are compared in the middle, and the bottom plot depict the expected and observed concentrations of dissolved nitrogen in the culture medium.

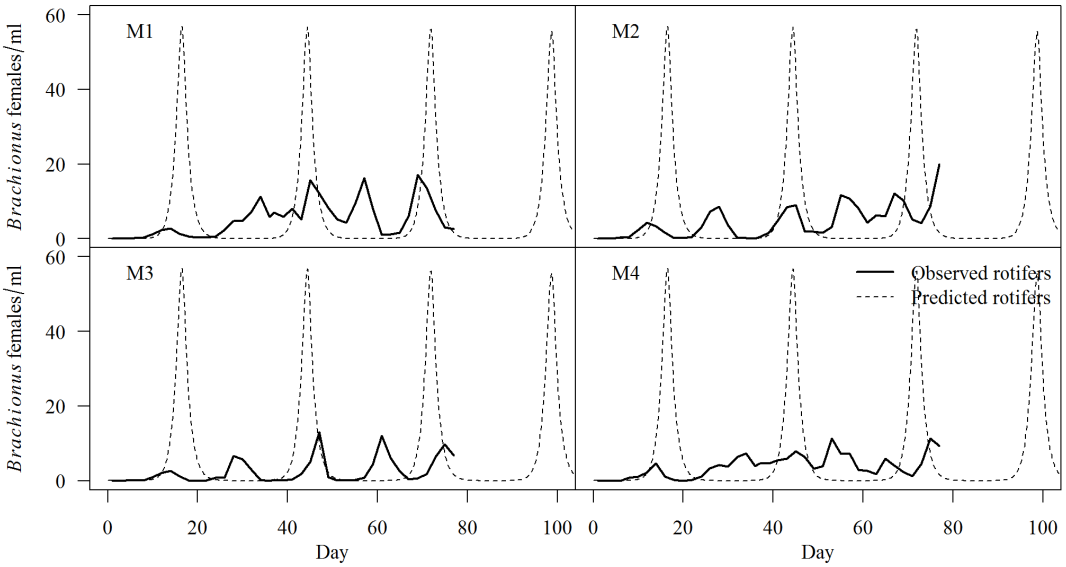
M1
M2
M3
M4
Brachionus females/ml
Observed rotifers
Predicted rotifers
Day

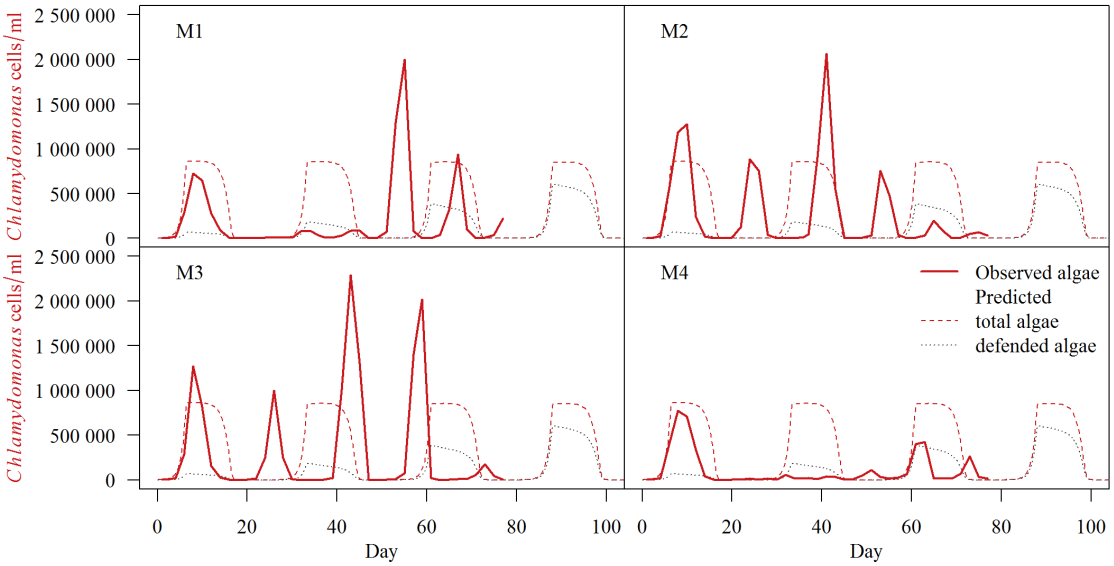
M1
M2
M3
M4
Chlamydomonas cells/ml
Observed algae
Predicted
total algae
defended algae
Day

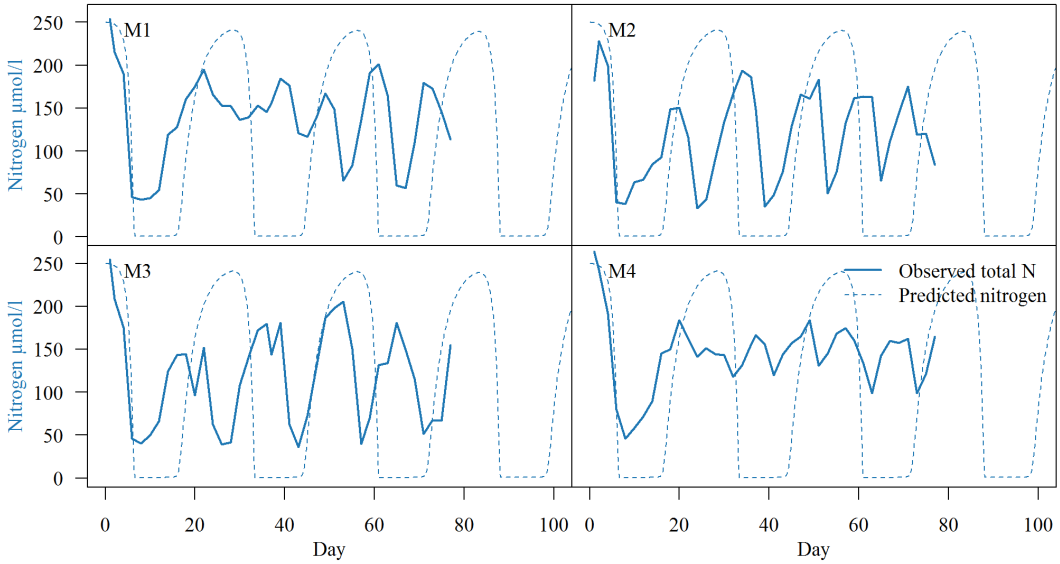
M1
M2
M3
M4
Nitrogen µmol/l
Observed total N
Predicted nitrogen
Day

APPENDIX L Rotifer mortality

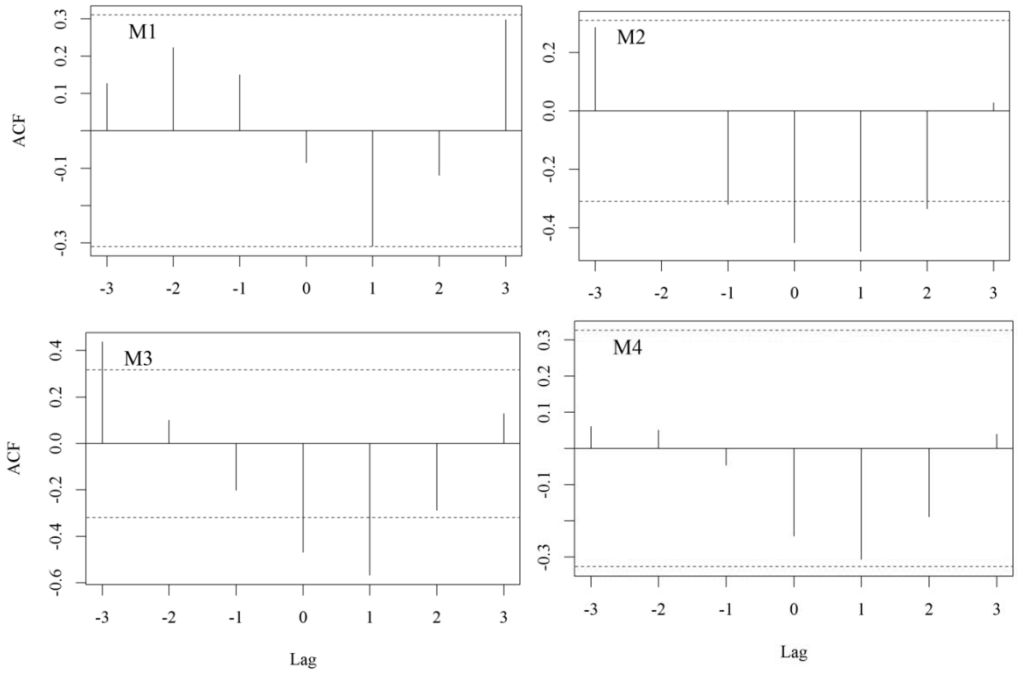

The plots above show the cross-correlation between the time series of algal cell density and fraction of dead female rotifers. Because the cultures were sampled every other day, each time lag represents two days. The horizontal blue lines indicate the significance level (0.05). There is a significant correlation between algal density and fraction of dead females two days later for all cultures except M4.

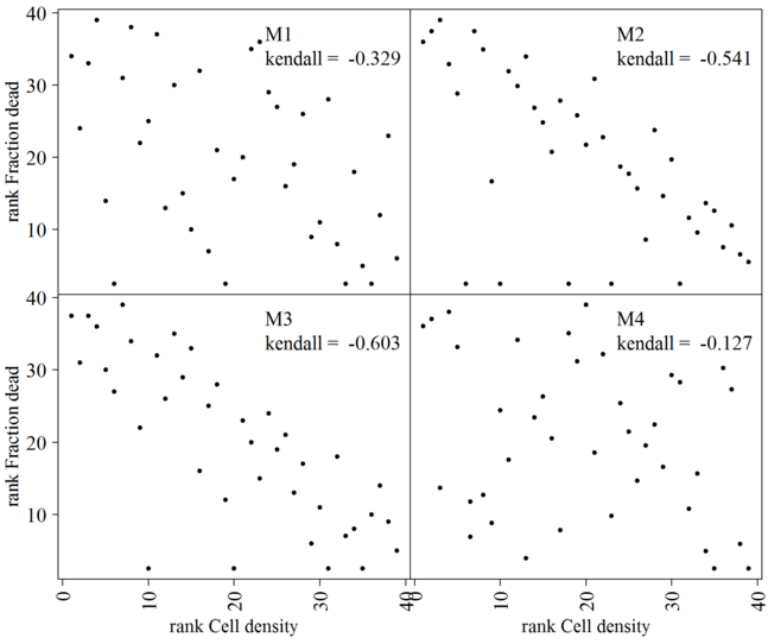

To the left are the ranked cell densities plotted against the ranked fraction of dead rotifer females two days later (lag +1). *Kendall* gives a ranked-based correlation coefficient between the two variables.

APPENDIX M Rotifer growth

ROTIFER MAXIMUM RECRUITMENT

In order to make an estimate of the maximum per capita recruitment, I collected data from four intervals in culture M2 and M3 where the rotifer population was in a phase of exponential growth. The time points that were extracted are indicated as open circles in the plot below.

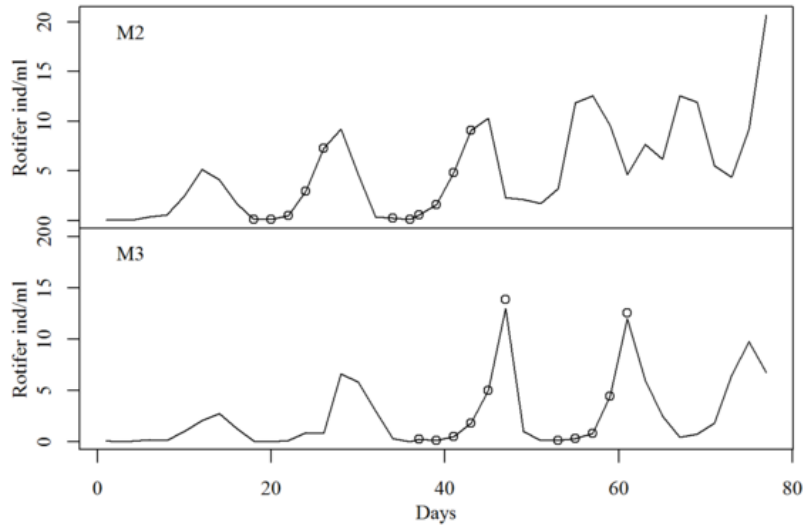

Next, a model for exponential growth was fitted to the group of collected data. A model for exponential growth can be as follows:

$$N_t = N_0 \cdot e^{rt}$$

Where $\mathbf{N_t}$ denotes the population size at time **t**, $\mathbf{N_0}$ the initial population size, **e** is the base of the natural logarithm and **r** denotes the maximum per capita recruitment (maximum net specific growth rate).

The model fit to the data gave an estimate for **r = 0.51** ind/ind per day, i.e.

$$N_t = N_0 \cdot e^{0.51t}$$

The data points and fitted model are plotted in the top figure on the next page.

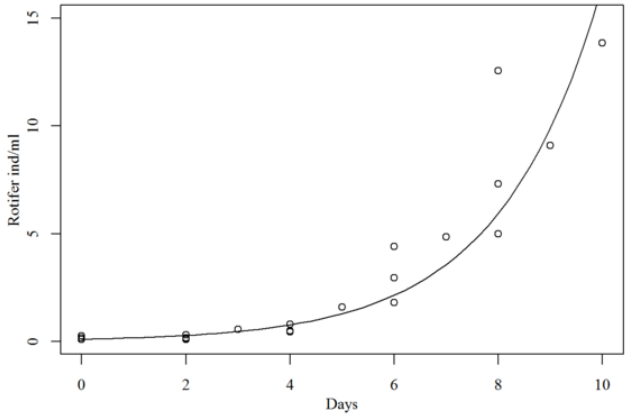

Since the cultures were diluted continuously, the estimate for **r** would be lower than the true maximum growth rate (a substantial part of the recruited rotifers would be lost in the dilution process). The **r** parameter is the difference between the birth and death rates of the population, r = b – d (Gotelli 2008), so since the dilution process imposes a factor that leads to additional loss of individuals from the population, the growth rate would equal r – D = 0.51. As the cultures were diluted at a rate of 0.30 /day, the true maximum per capita recruitment would be close to:

r = 0.51 + 0.30 = **0.81 ind/ ind per day.**

The growth factor **λ** which is used in population models in discrete time equals $\mathbf{e^r}$ (Gotelli 2008), and gives in this case: $\boldsymbol{\lambda = e^{0.81} = 2.24.}$ This value is the ratio of the population size at time N_{t+1} against N_t and is thus a dimensionless number (Gotelli 2008).

CORRELATION PLOTS

On the right are the ranked algal densities plotted against the ranked densities of live rotifers two days later (lag +1). *Kendall* gives a ranked-based correlation coefficient between the two variables. All correlations are significant ($p< 0.02$). Thus there is a positive correlation between algal densities and rotifer densities two days later.

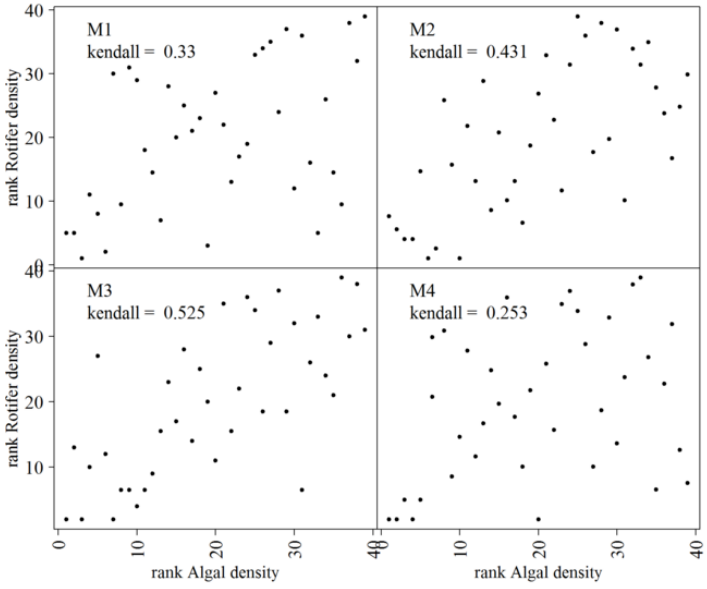

ROTIFER CONVERSION FACTOR

Since the results indicate that there is a considerable correlation between algal cell densities and the rotifer densities two days later, I used the data to make an approximate estimate of the rotifer conversion factor. The estimation is based on data from all four high nutrient cultures, however only the paired data that had algal densities below 60 000 cells/ml were included in the analysis. The high cell densities were left out because they strongly deviated from the linear relationship that was more apparent for the low densities. Thus, the resulting estimate is at best the rotifer conversion factor for relatively low cell densities.

On the right are the algal densities plotted against the rotifer densities two days later, together with the linear model of the association between the two variables. The dashed lines give the 95% confidence interval for the model.

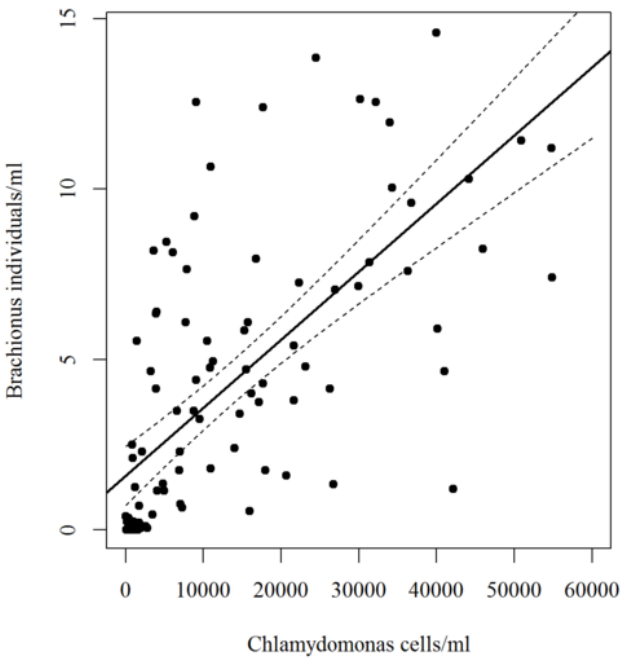

The estimates for the model parameters are as follows:

Intercept = 1.6 (SE = 0.4)

Slope = 0.00020 (SE = 0.00002)

with an R^2 of 0.47.

Thus for each increase in a single cell of *C. reinhardtii*, there is a predicted increase of a 0.00020 *B. calyciflorus*, or equally, with the units used in the rotifer-algal model, the model predicts that for an increase of 10^6 algal cells, there would be an increase of 202 rotifers two days later (Intercept + Slope · 10^6).

The analysis of this data suggests that the rotifer conversion factor is 202 rotifers/10^6 *Chlamydomonas* cells, which is relatively close to estimate used in Becks and colleagues' *Chlamydomonas – Brachionus* model (170 rotifers/10^6 algal cells).

APPENDIX N Images of the high nutrient cultures

The appendix includes different images of the high nutrient cultures. On the first page I have attached some photos of selected palmelloids that emerged in the high nutrient cultures and a photo of *B. calyciflorus* surrounded by some single celled *C. reinhardtii*. The second page includes photos of the high nutrient cultures at two time points with differing degree of palmella formation. Thereafter follows a collection of scan images retrieved from the iCys imaging cytometer. The collection includes one scan image (out of six) from day 34 to day 77. These scan images are the images that were used to estimate cell densities and distribution of cell sizes in the rotifer-algal experiment. Above each image, there is indicated how much of the culture sample that was added to the microplate well.

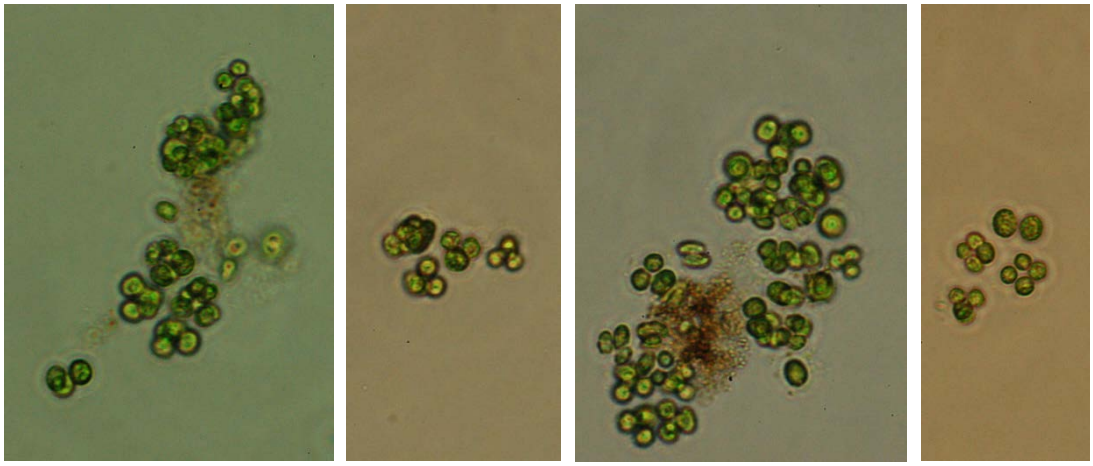

Female *B. calyciflorus* and single celled *C. reinhardtii*.

At high cell densities, the high nutrient *Chlamydomonas – Brachionus* cultures would initially look like the photo on the left (photo from day 11).

When palmelloids began to be prominent in the high nutrient systems, *C. reinhardtii* was found to sediment at the bottom of the culture flask and to attach to the walls (depicted in the photos below).

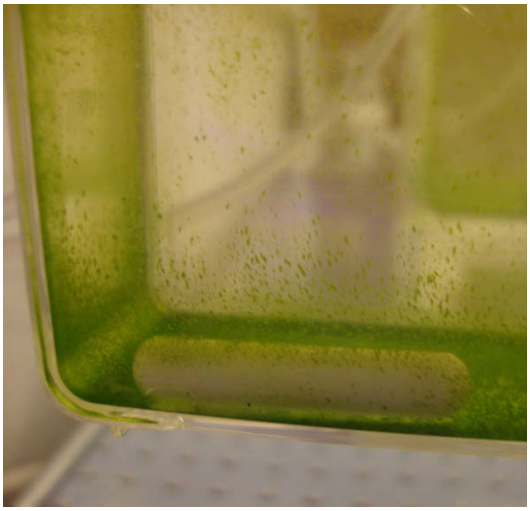

The two cultures below are culture M3 (left) and M2 (right) at day 53. Notice how the rotifer population has cleared the culture medium from algae in M3, while in M2 a substantial amount of algae has settled at the bottom.

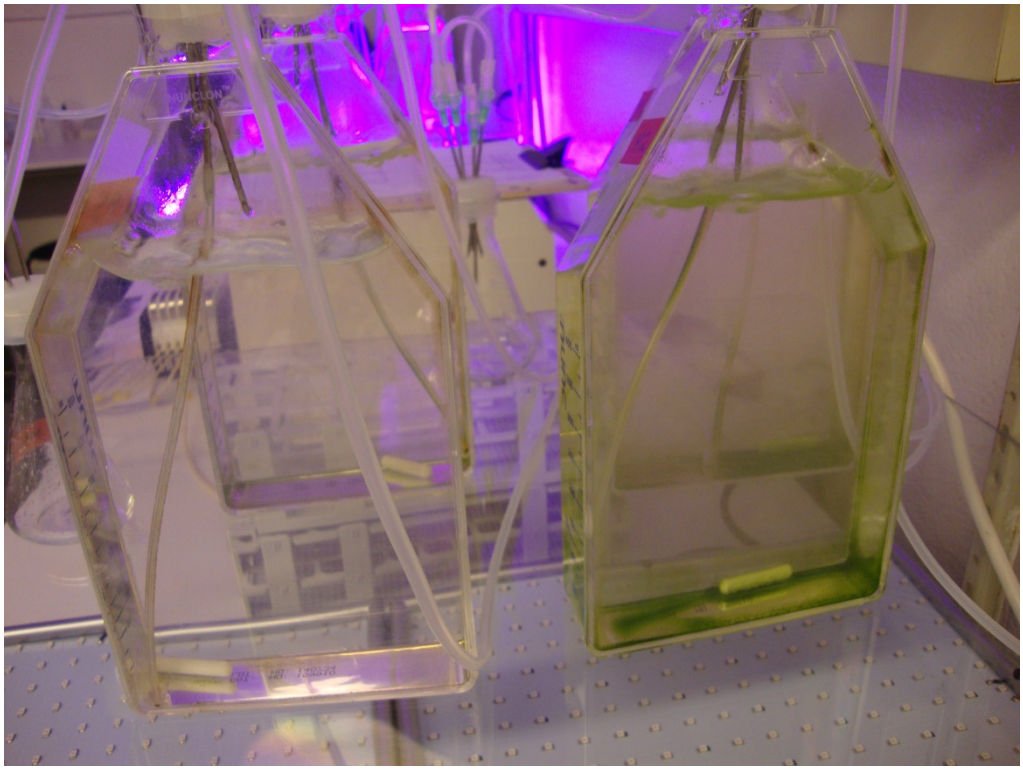

M1

Day 34 (50 µl) - Day 36 (200 µl) - Day 37 (150 µl) - Day 39 (200 µl)

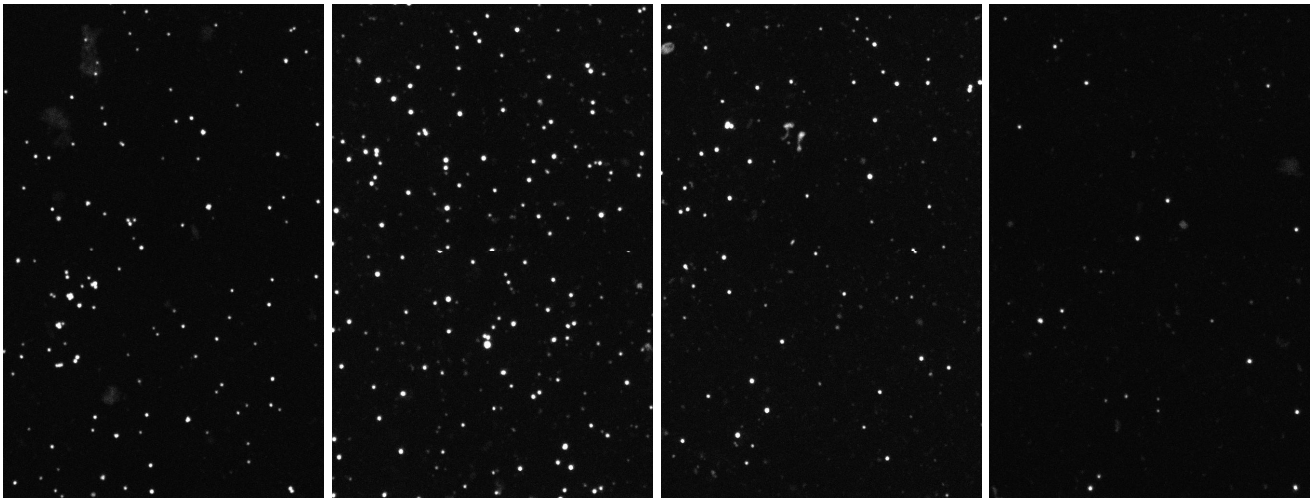

Day 41 (200 µl) - Day 43 (100 µl) - Day 45 (50 µl) - Day 47 (200 µl)

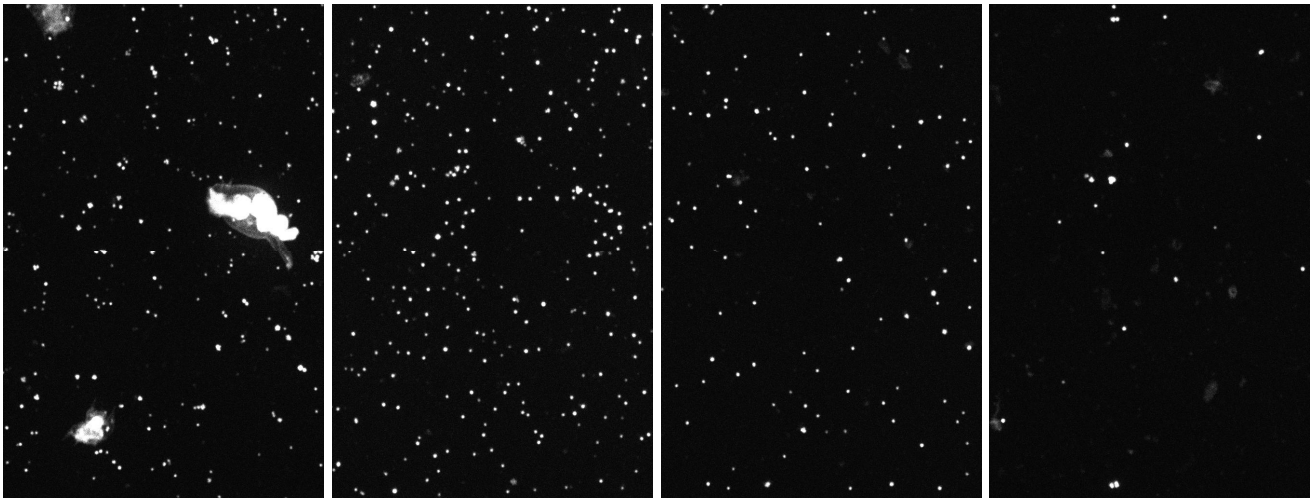

Day 49 (200 µl) - Day 51 (100 µl) - Day 53 (5 µl) - Day 55 (2 µl)

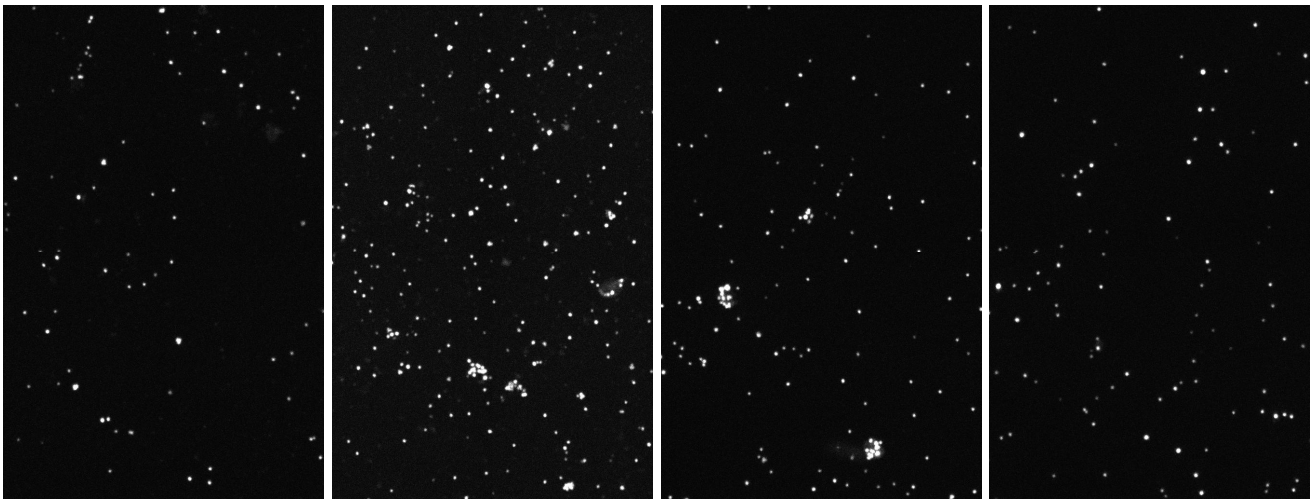

Day 57 (10 µl) - Day 59 (100 µl) - Day 61 (100 µl) - Day 63 (100 µl)

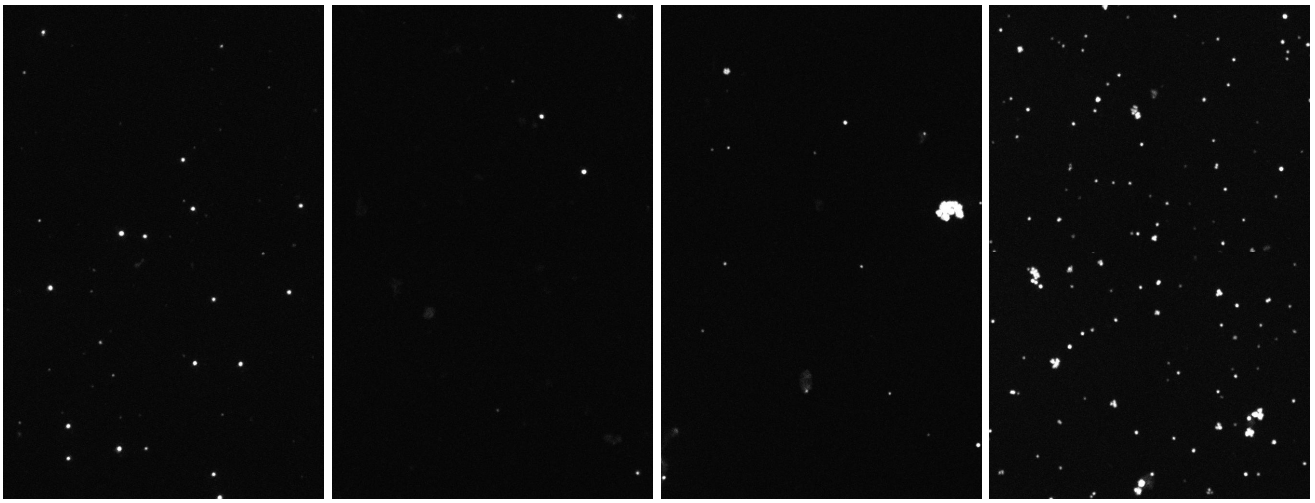

Day 65 (5 µl) - Day 67 (5 µl) - Day 69 (10 µl) - Day 71 (200 µl)

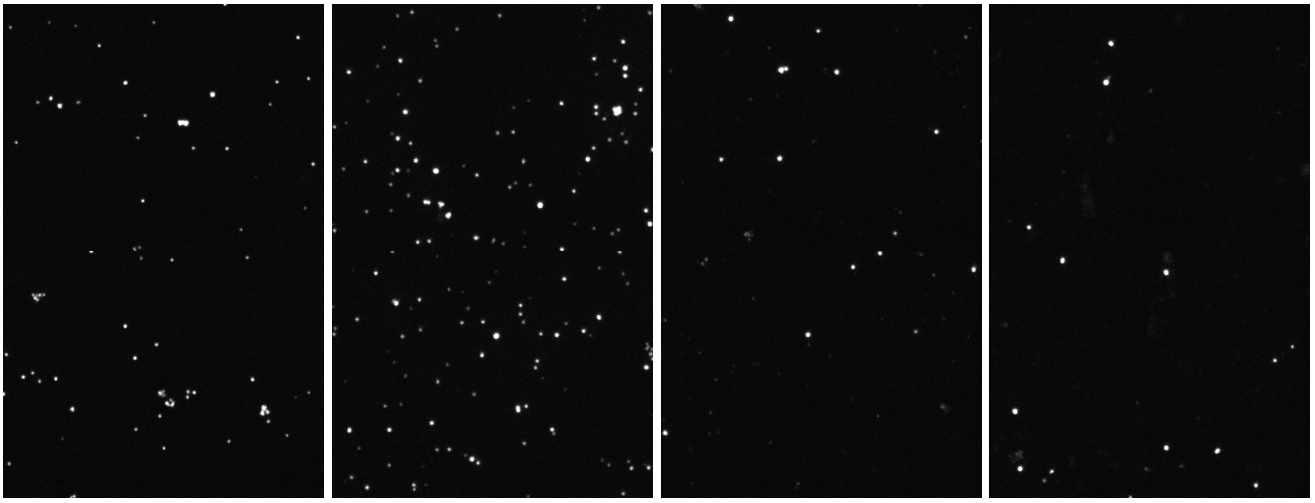

Day 73 (200 µl) - Day 75 (100 µl) - Day 77 (20 µl)

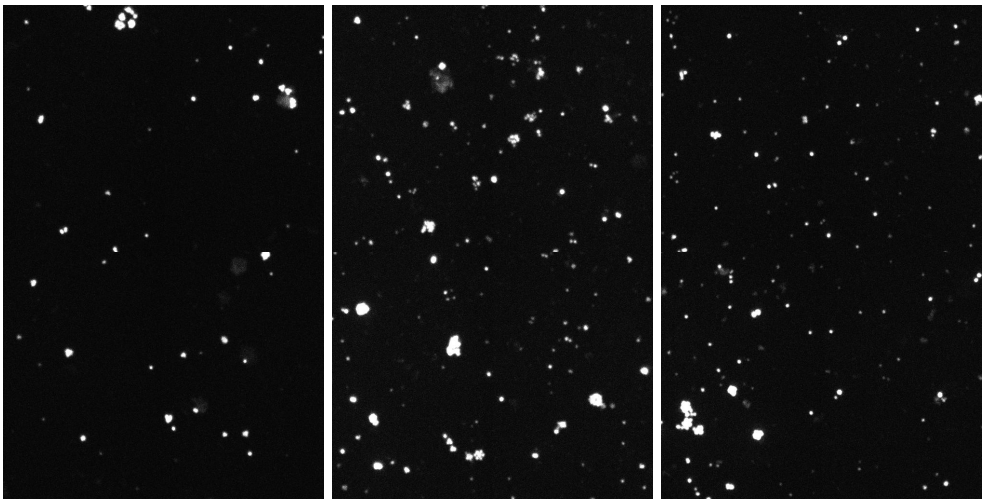

M2

Day 34 (200 µl) - Day 36 (200 µl) - Day 37 (50 µl) - Day 39 (10 µl)

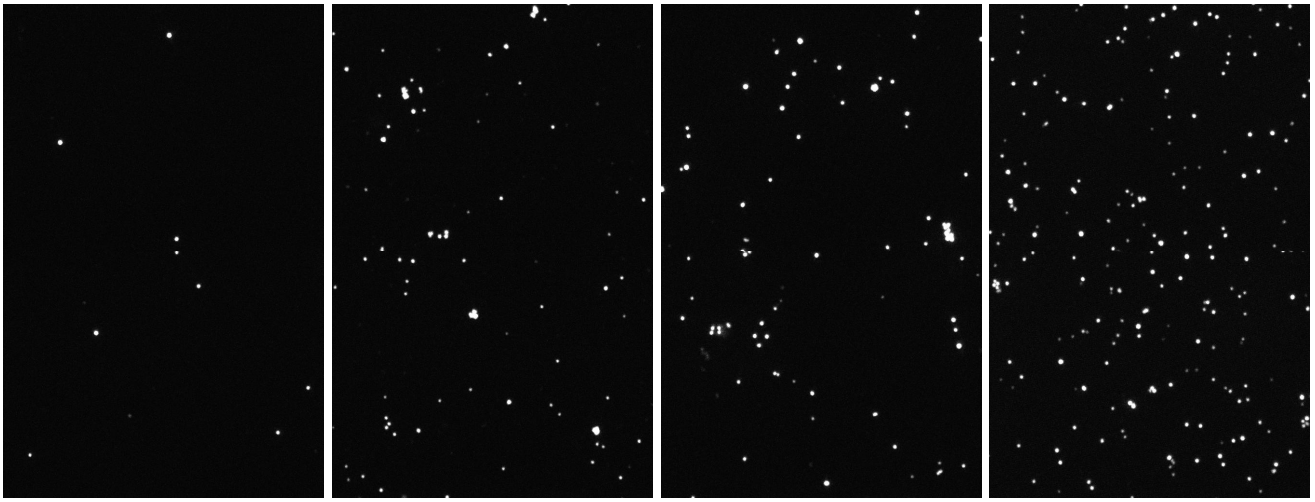

Day 41 (5 µl) - Day 43 (2 µl) - Day 45 (200 µl) - Day 47 (200 µl)

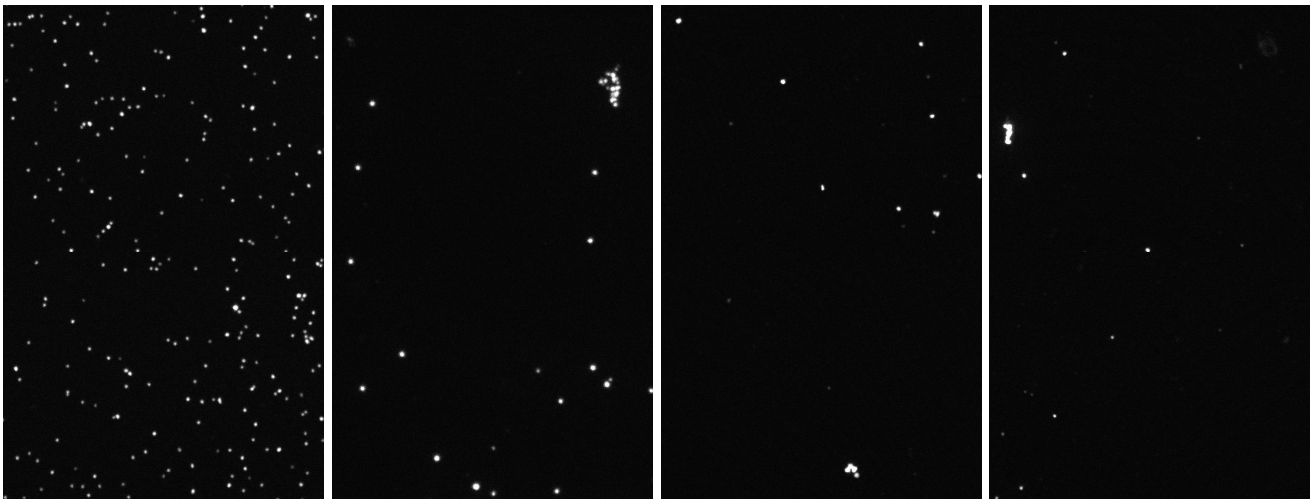

Day 49 (200 µl) - Day 51 (200 µl) - Day 53 (10 µl) - Day 55 (2 µl)

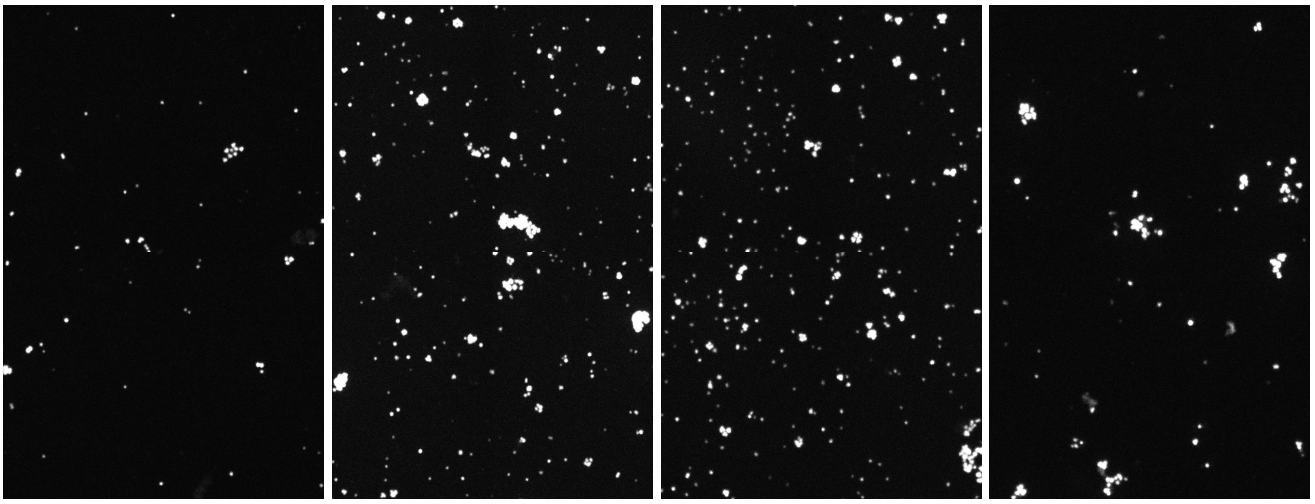

Day 57 (10 µl) - Day 59 (200 µl) - Day 61 (200 µl) - Day 63 (200 µl)

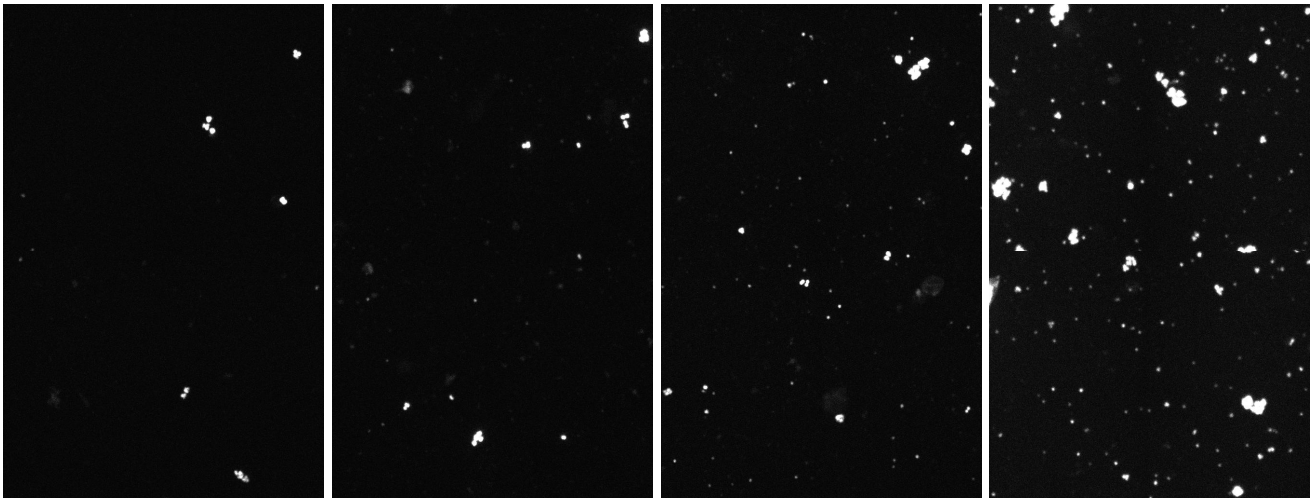

Day 65 (10 µl) - Day 67 (10 µl) - Day 69 (100 µl) - Day 71 (200 µl)

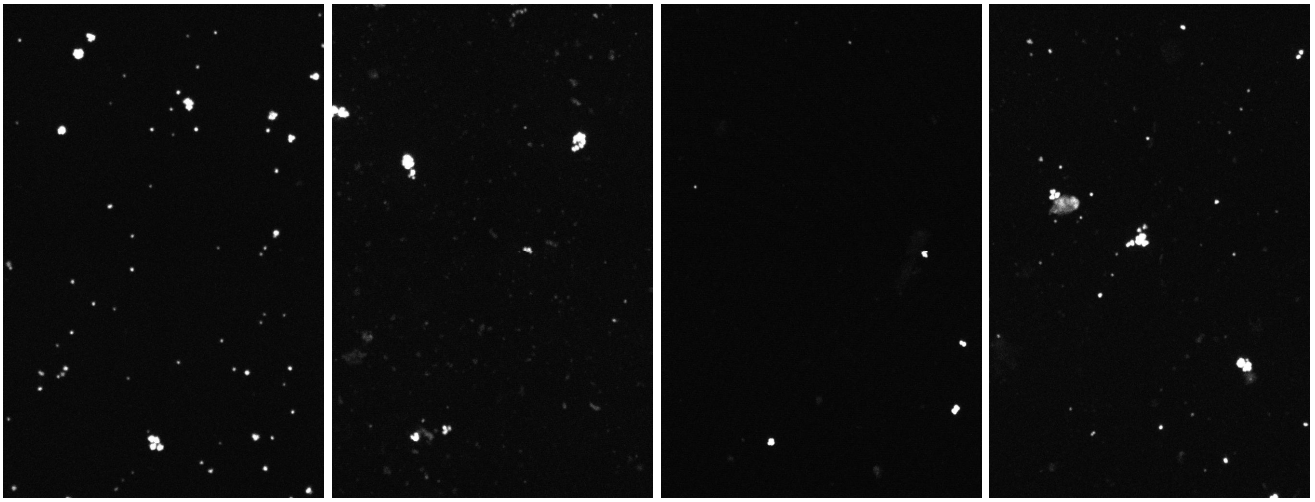

Day 73 (100 µl) - Day 75 (50 µl) - Day 77 (50 µl)

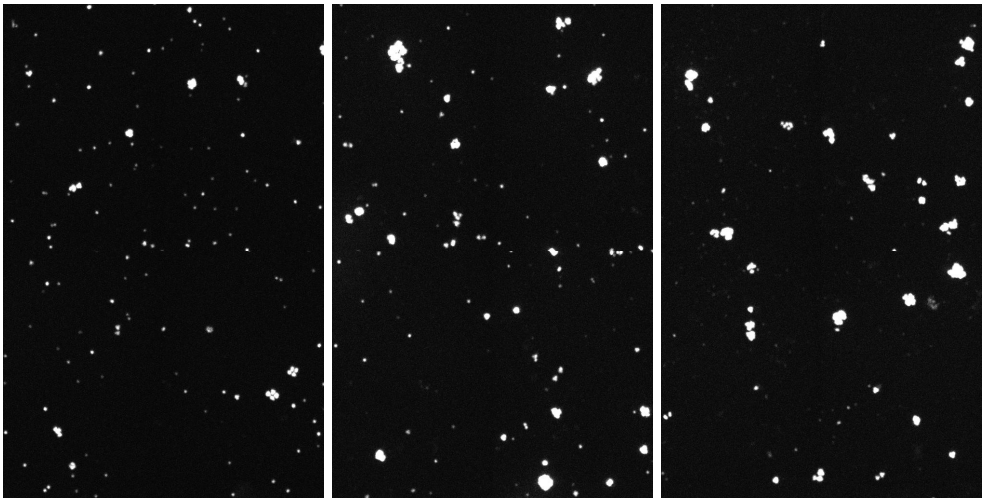

M3

Day 34 (200 µl) - Day 36 (200 µl) - Day 37 (200 µl) - Day 39 (200 µl)

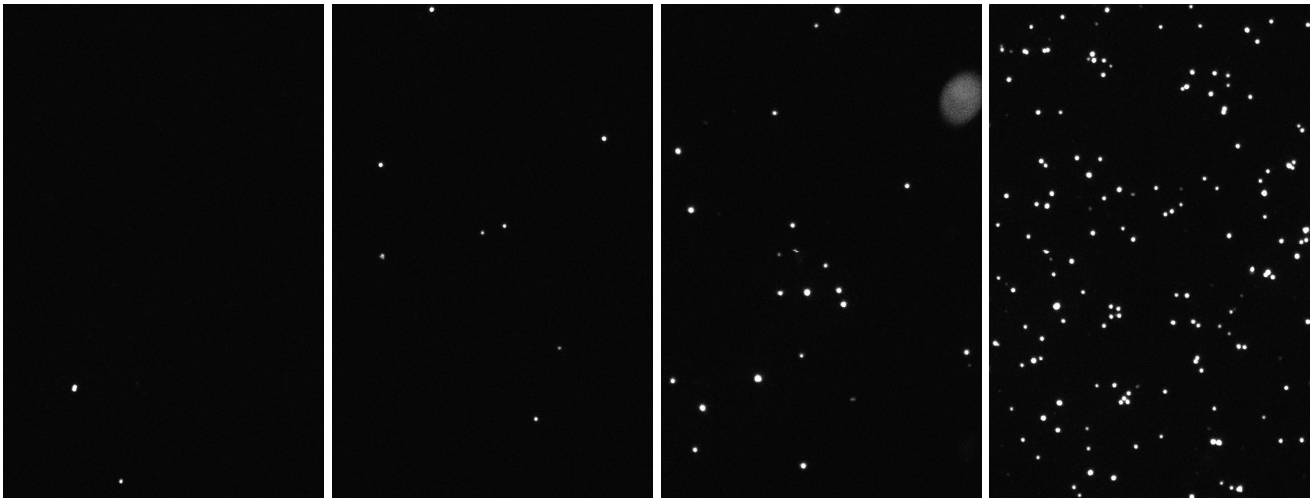

Day 41 (20 µl) - Day 43 (5 µl) - Day 45 (2 µl) - Day 47 (200 µl)

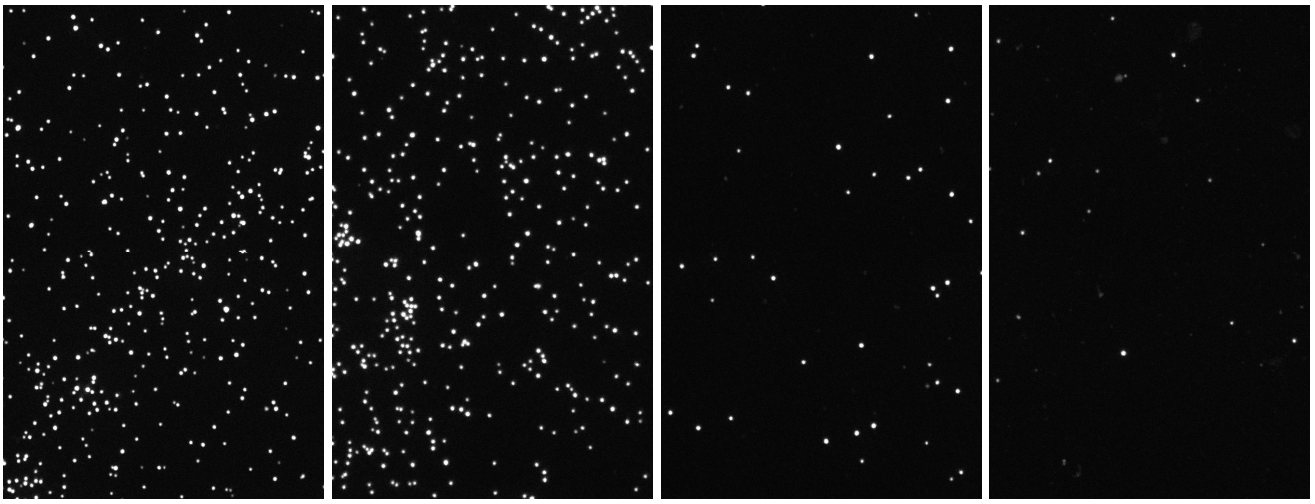

Day 49 (200 µl) - Day 51 (200 µl) - Day 53 (200 µl) - Day 55 (5 µl)

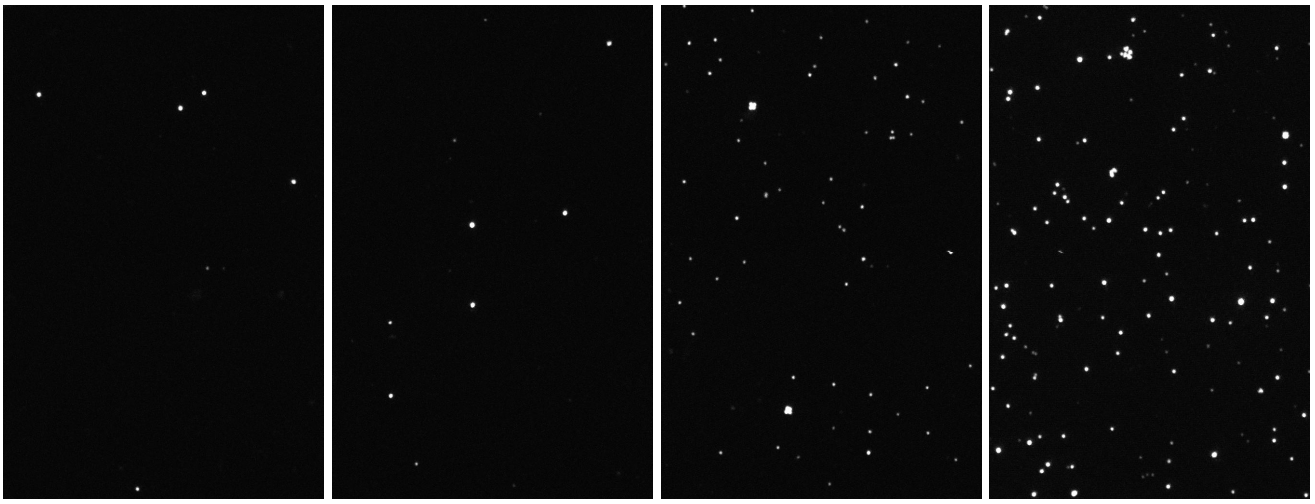

Day 57 (5 µl) - Day 59 (2 µl) - Day 61 (5 µl) - Day 63 (200 µl)

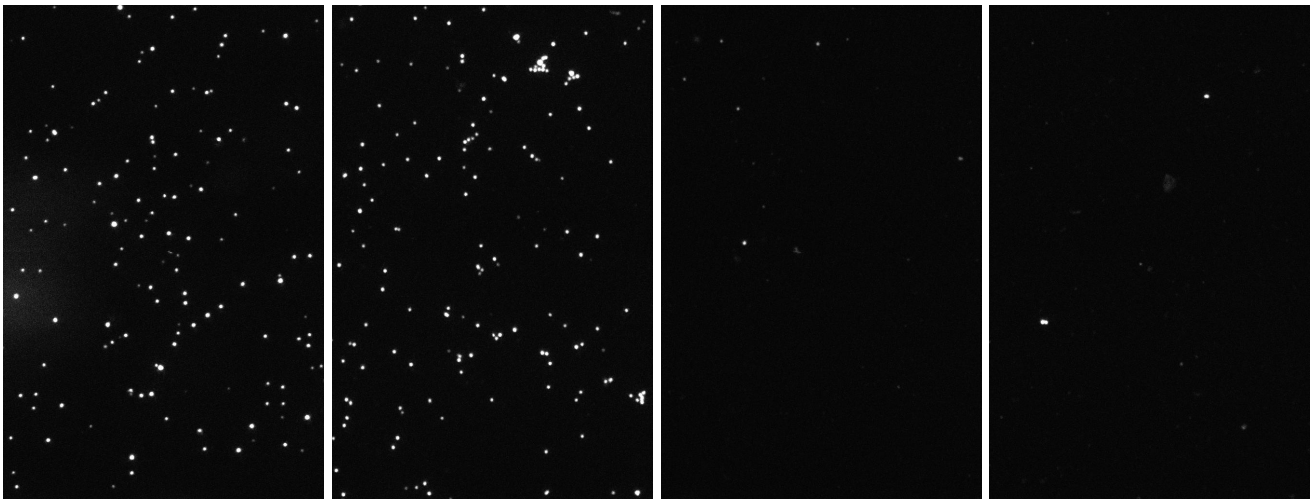

Day 65 (200 µl) - Day 67 (200 µl) - Day 69 (100 µl) - Day 71 (20 µl)

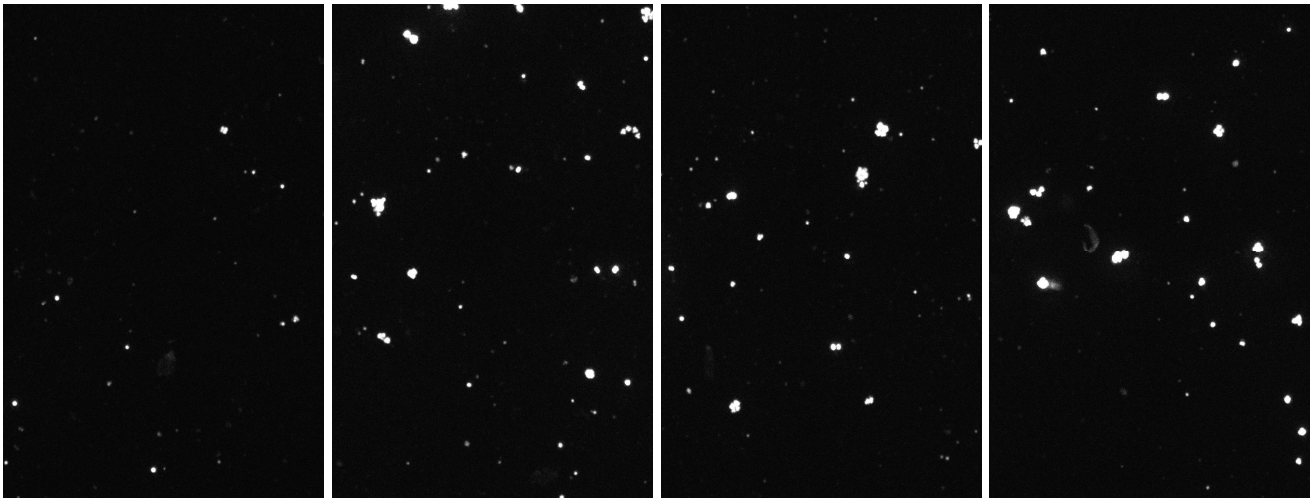

Day 73 (10 µl) - Day 75 (5 µl) - Day 77 (200 µl)

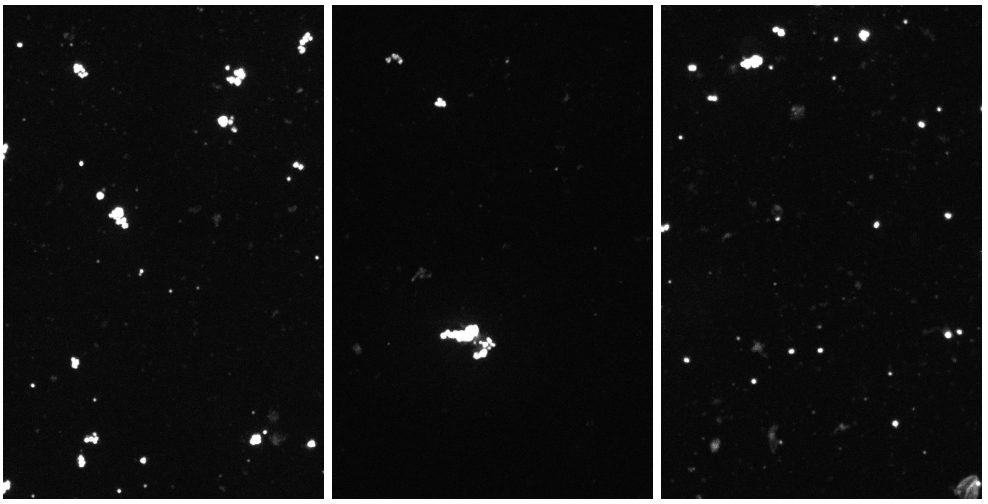

M4

Day 34 (150 µl) - Day 36 (200 µl) - Day 37 (200 µl) - Day 39 (200 µl)

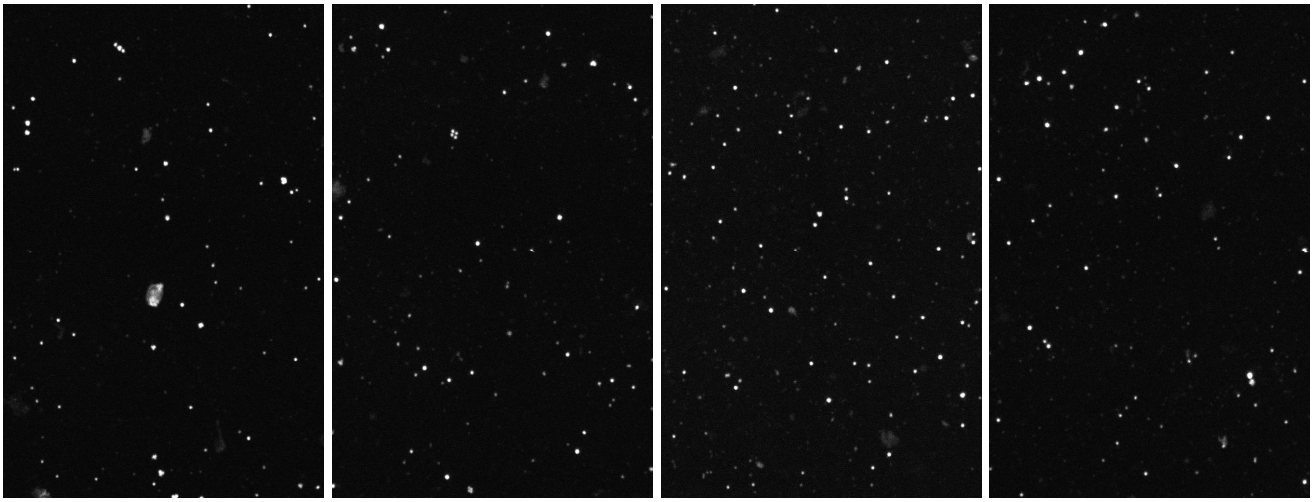

Day 41 (200 µl) - Day 43 (200 µl) - Day 45 (200 µl) - Day 47 (200 µl)

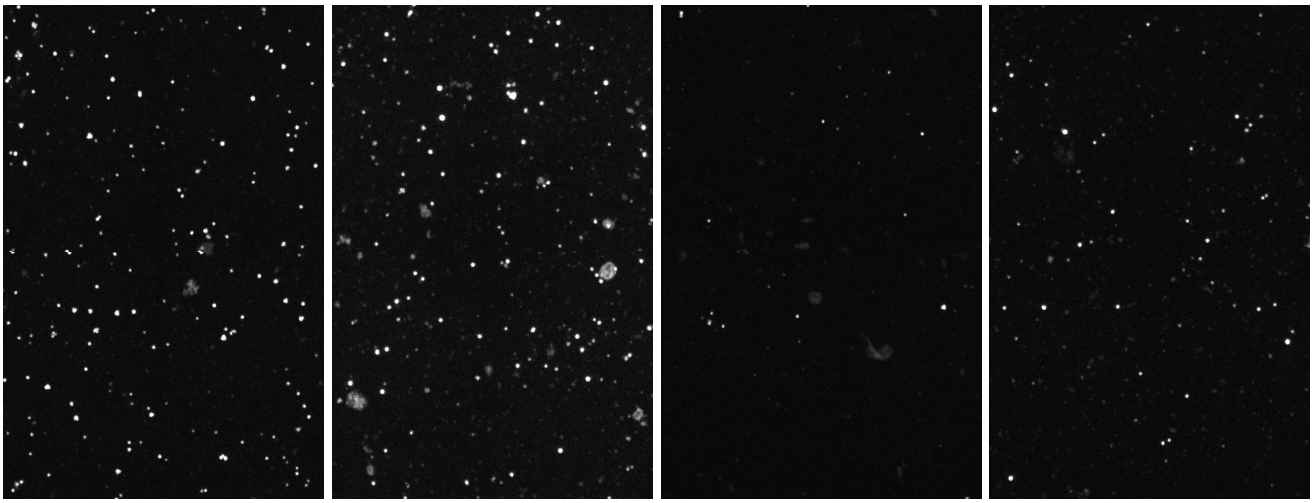

Day 49 (100 µl) - Day 51 (50 µl) - Day 53 (100 µl) - Day 55 (100 µl)

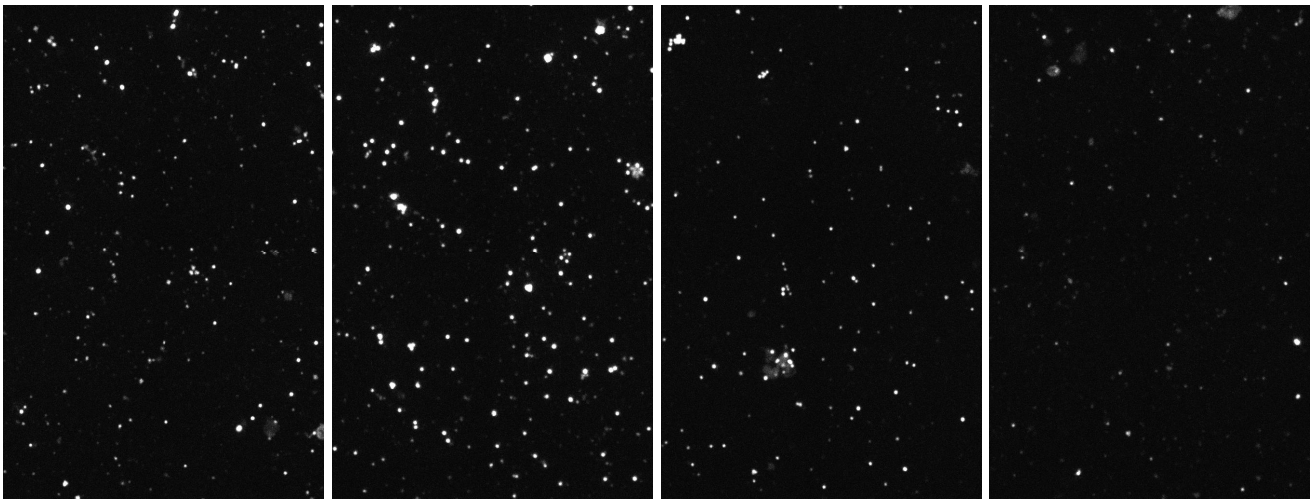

Day 57 (150 µl) - Day 59 (50 µl) - Day 61 (2 µl) - Day 63 (5 µl)

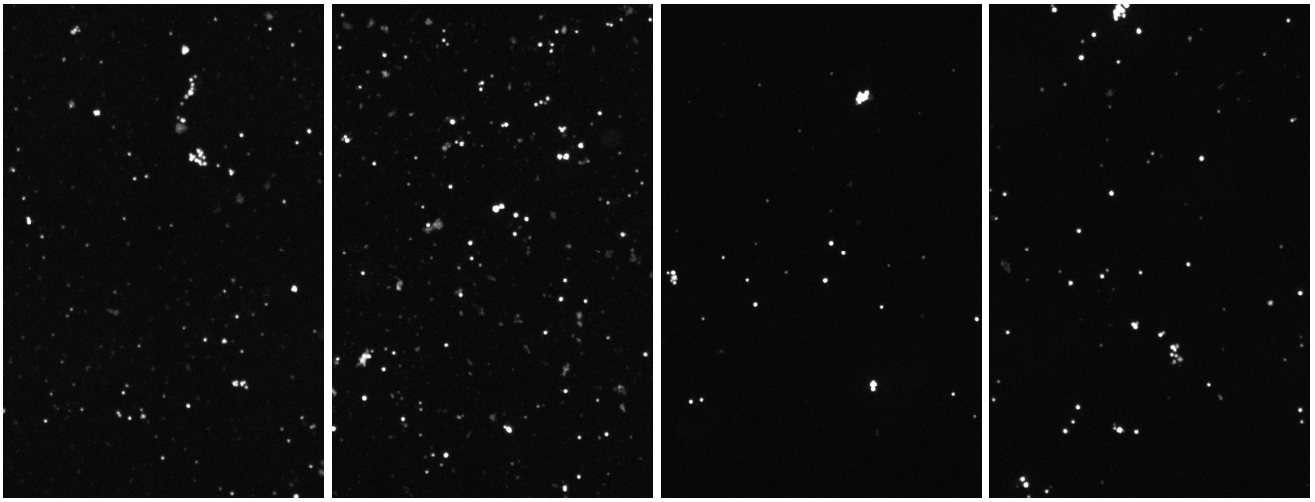

Day 65 (5 µl) - Day 67 (200 µl) - Day 69 (200 µl) - Day 71 (50 µl)

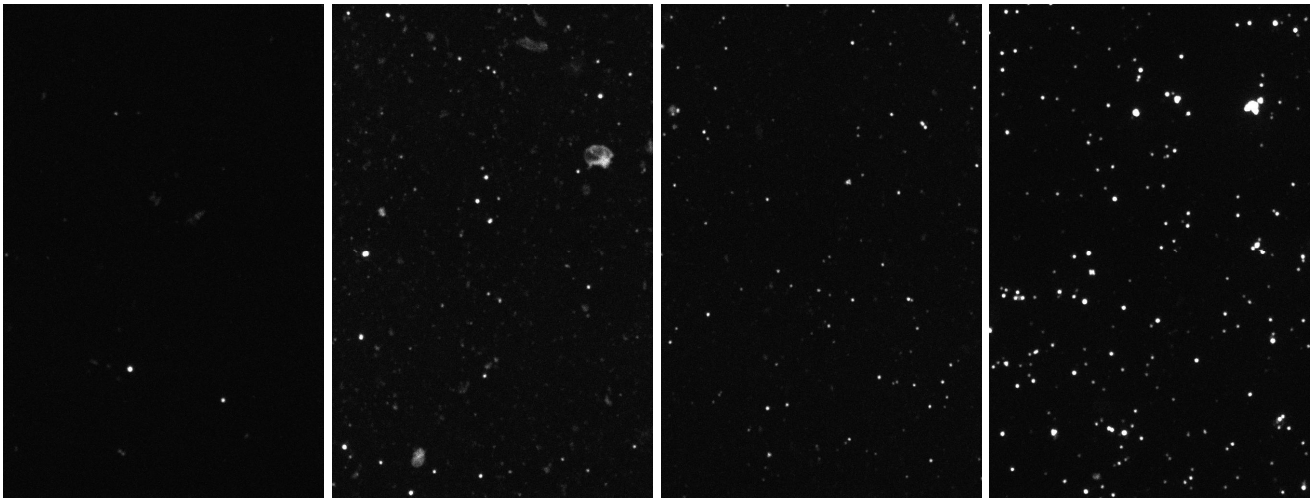

Day 73 (20 µl) - Day 75 (50 µl) - Day 77 (200 µl)

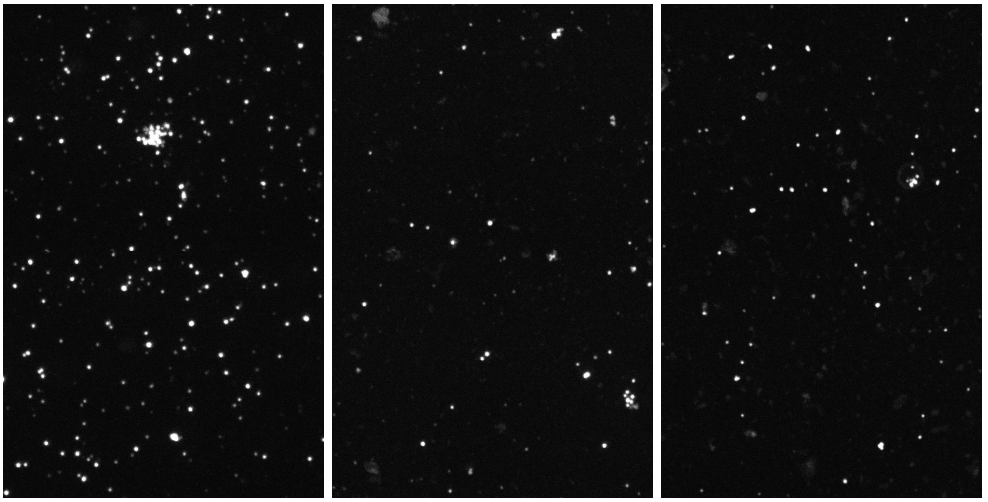

APPENDIX O Size distributions of the algal populations

The plots on the first page show the estimated median and interquartile range of cell diameters for *C. reinhardtii* in the rotifer-algal continuous cultures, while the plots on the second page summarizes the raw data of cell sizes as it was obtained by the iCys imaging cytometer. The imaging cytometer produce estimates of the area of each cell or cell aggregate in the scan field (based on fluorescence). Estimates of cell diameters were calculated from the recorded cell areas, assuming a circular shape of the cell (or cell aggregate).

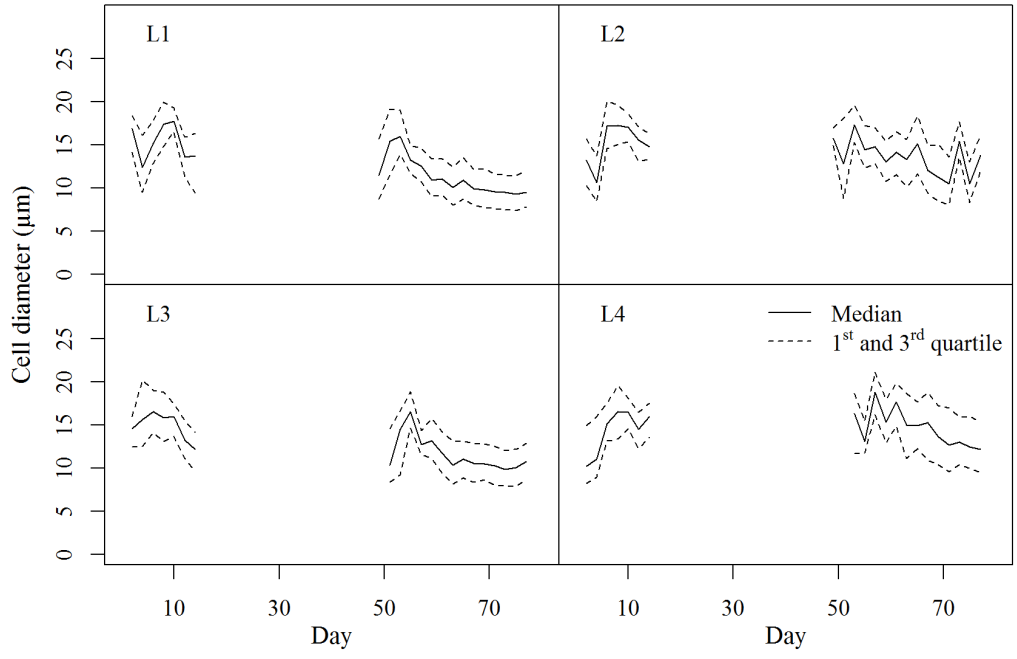

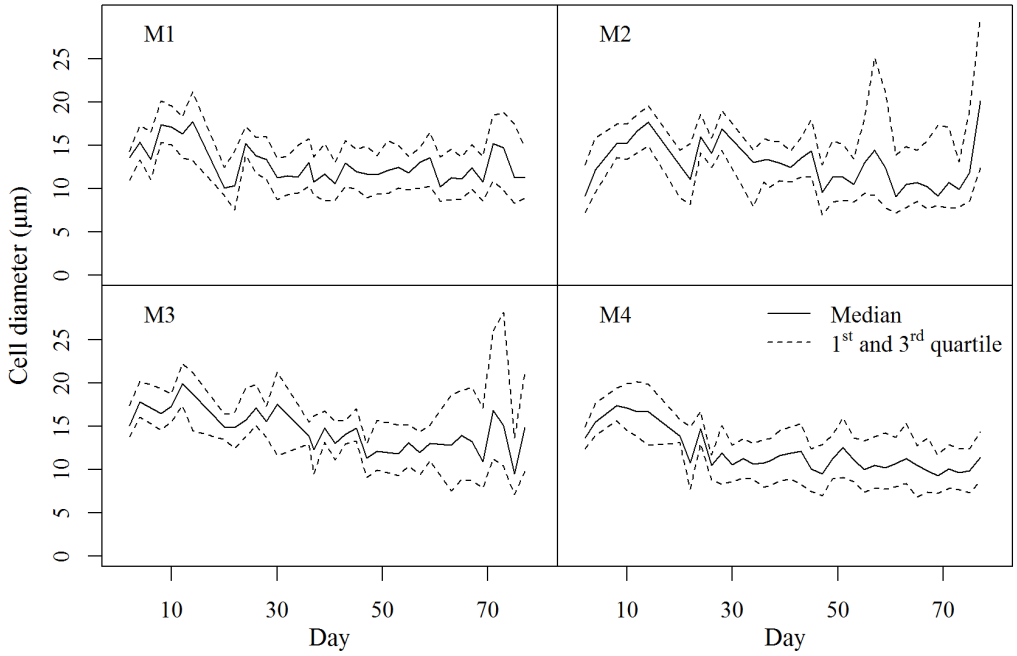

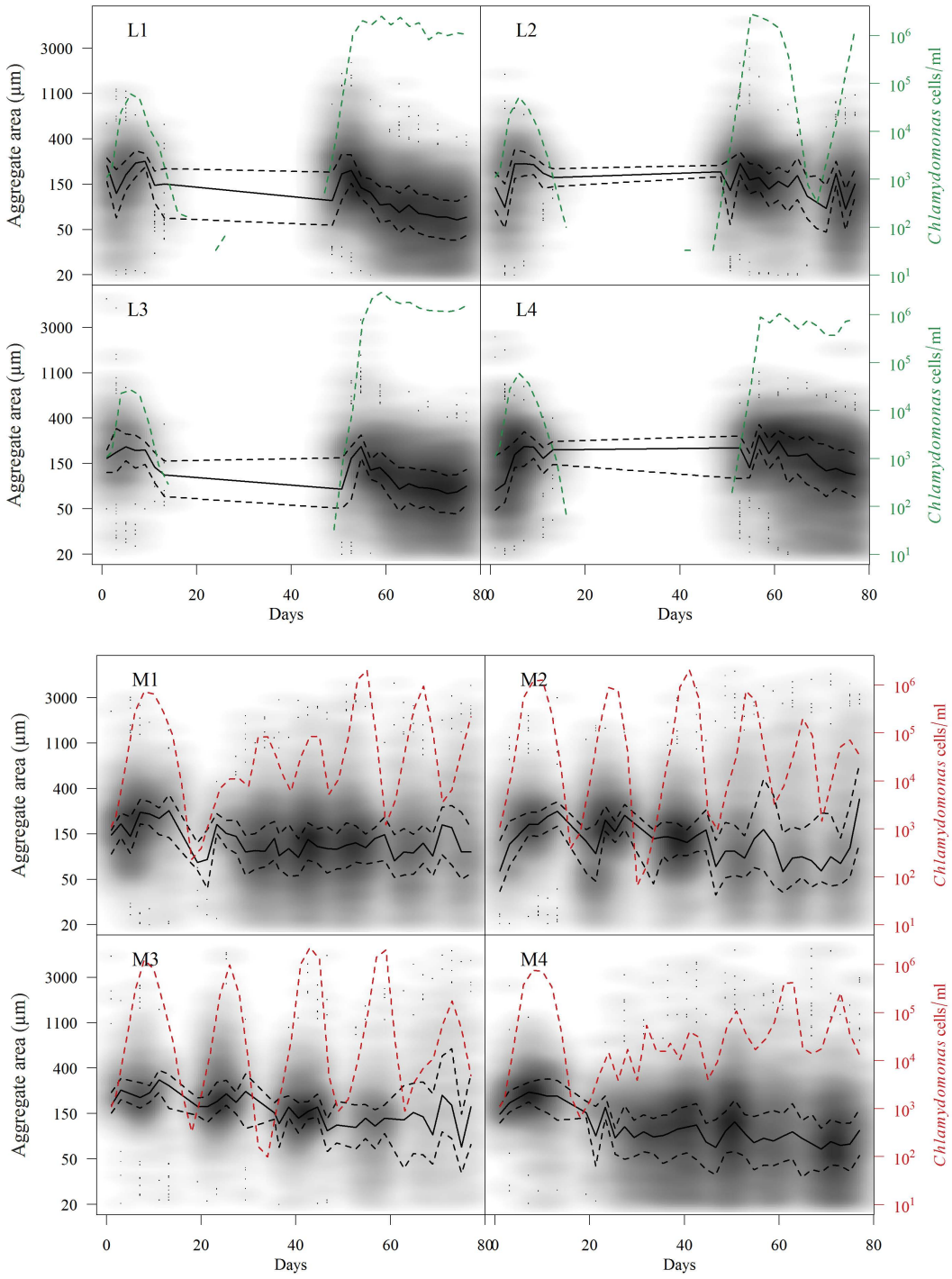

The plots above are smoothed scatter plots of the recorded cell or cell aggregate area of *C. reinhardtii*. The dark fields in the plots represent the areas that were recorded by the imaging cytometer (the darker the field, the more observations). The median and interquartile ranges of the recorded areas are added to the plots (black lines), in addition to the estimates of cell densities (green or red dashed lines). Notice that the gaps in the smoothed scatter plots coincide with low algal densities in the cultures. Thus, the gaps occur because there were few (or no) cells present to obtain data on cell or cell aggregate sizes.

References appendixes

Becks, L., S. P. Ellner, L. E. Jones & N. G. Hairston (2010). Reduction of adaptive genetic diversity radically alters eco-evolutionary community dynamics. *Ecology Letters*, **13**(8): 989-997.

Felpeto, A. B. & N. G. Hairston (2013). Indirect bottom-up control of consumer–resource dynamics: Resource-driven algal quality alters grazer numerical response. *Limnology and Oceanography*, **58**(3): 827-838.

Fussmann, G. F., S. P. Ellner, K. W. Shertzer & N. G. Hairston Jr. (2000). Crossing the hopf bifurcation in a live predator-prey system. *Science*, **260**: 1358-1360.

Gotelli, N. J. (2008). *A Primer of Ecology*. Sinauer Associates, Sunderland, Massachusettes, p. 291.

Guillard, R. R. L. & C. J. Lorenzen (1972). Yellow-green algae with chlorophyllide c. *Journal of Phycology*, **8**(1): 10-14.

Pinheiro, J. C. & D. M. Bates (2000). *Mixed-effects models in S and S-PLUS*. Springer-Verlag, New York, p. 537.

Soetaert, K., T. Petzoldt & R. W. Setzer (2010). Solving differential equations in R: package deSolve. *Journal of Statistical Software*, **33**(9): 1-25.

Yoshida, T., L. E. Jones, S. P. Ellner, G. F. Fussmann & N. G. Hairston (2003). Rapid evolution drives ecological dynamics in a predator-prey system. *Nature*, **424**(6946): 303-306.